Carbon dioxide losses from terrestrial organic matter resulting from photodegradation and microbial respiration

A thesis

submitted in fulfilment

of the requirements for the degree

of

Doctor of Philosophy

at

The University of Waikato

by

Susanna Rutledge-Jonker

THE UNIVERSITY OF
WAIKATO
Te Whare Wānanga o Waikato

The University of Waikato

2010

Abstract

Losses of soil organic matter (SOM) can lead to a decrease in soil quality, cause an increase in CO_2 emissions, thereby contributing to a rise in atmospheric CO_2 concentration, which in turn can affect the global climate.

Microbial decomposition of SOM to CO_2 is one of the main processes by which SOM is lost. Breakdown of organic matter (OM) by solar irradiance (called "photodegradation") can also contribute to decomposition, especially in dry ecosystems. Photodegradation has been studied in the field by measuring the mass loss of litter, but its contribution to CO_2 losses has not previously been determined at spatial and temporal scales appropriate for ecosystems.

The main aim of this research was to examine the magnitude and drivers of the CO_2 efflux from terrestrial organic matter resulting from both microbial decomposition and photodegradation.

Carbon dioxide fluxes were measured at a bare peatland in New Zealand using eddy covariance (EC) and a closed chamber. The EC system measured the total CO_2 flux, whereas the chamber only measured the biological component of the CO_2 flux. The abiotic irradiance-induced component of the CO_2 flux was obtained by subtracting the chamber flux from the EC flux, and by comparing day-and night-time EC measurements made under similar temperature and moisture conditions. Analogous comparisons were made using field data from a grassland site in California during the dry summer period when plants had senesced. To confirm that solar irradiance contributed to CO_2 effluxes from terrestrial OM, short incubations of OM in a small transparent flow-through chamber system (referred to as the "container") were conducted. The container was also used to study the controls of photodegradation including the effects of irradiance intensity, wavelength and substrate species.

On hot summer days, irradiance-induced CO_2 fluxes accounted for up to 58% and 90% of the total mid-day CO_2 flux at the peatland and grassland, respectively. Annual CO_2 production at the peatland was estimated to be 269 g C m^{-2}, of which 20% was due to photodegradation. At the grassland during the dry

season (~3 months), approximately 27 g C m^{-2} was lost as CO_2, of which 60% was due to photodegradation.

Irradiance-induced CO_2 fluxes measured both in the field and in the container showed a very strong relationship with the intensity of solar irradiance. Higher fluxes were observed at greater temperatures, but temperature effects could not be separated from irradiance effects. Field data suggested that the dose response coefficient (=moles of CO_2 produced per unit of energy of incoming solar irradiance) did not differ between wet and dry conditions at the peatland. Per unit of energy, peat produced more CO_2 than grass litter in both the field and the container. Container measurements indicated the irradiance in the UV wavelength band was responsible for 14 % of the total irradiance-induced CO_2 flux. Per unit of energy, approximately 5 times as much CO_2 was produced in the field compared to the container fluxes. The causes for this difference are not known, and this observation highlighted the importance of conducting ecosystem-scale field experiments in addition to small-scale controlled experiments.

The rate of CO_2 loss at the peatland resulting from microbial respiration was primarily controlled by the position of the water table, which in turn determined the thickness of the aerated peat layer. Greatest losses were observed in summer, when the water table was low and peat temperatures relatively high. Simple models previously applied in northern hemisphere peatlands predicted up to 86% of the variation in the observed daily averaged CO_2 fluxes based on peat temperature and depth to water table. The models were less successful at explaining the within-day variation of the CO_2 flux. To explain the complex variation in CO_2 fluxes at the within-day time scale, or if modelling is intended to increase understanding of the underlying processes of soil respiration, mechanistic models describing both CO_2 production at various depths and diffusion of CO_2 to the peat surface might be more appropriate.

Carbon dioxide losses due to abiotic processes like photodegradation have generally been ignored in ecosystem-scale carbon exchange studies and models. The results of this study strongly suggest that this process should not be ignored for a variety of ecosystems where OM is exposed to high levels of solar

irradiance for extended periods of time. The role of photodegradation in assisting microbial decomposition of complex OM is also poorly understood.

To obtain reliable estimates of carbon cycling component fluxes, the contribution of photodegradation to OM decomposition and CO_2 losses should be quantified across a wide range of other ecosystems and the process should be incorporated into global carbon cycling models.

Preface

"Thus, the task is, not so much to see
what no one has yet seen; but to think
what nobody has yet thought, about
that which everybody sees."
Erwin Schrödinger, physicist, 1887-1961

At the beginning of this research in April 2005, I started with the overall aim to advance the understanding of the controls of microbial respiration by doing a large scale field experiment. By choosing a bare peat mine as a study site – a simple ecosystem – I regarded it as given that microbial respiration could be quantified quite straightforwardly, by measuring the CO_2 efflux from the peat.

However, especially in summer under hot and dry conditions, I measured unexpectedly high CO_2 effluxes using the eddy covariance technique. These high fluxes occurred during the day, but not at night. Also, I was unable to confirm these large effluxes using chamber measurements. My first inclination was to doubt the eddy covariance measurements because of the complex nature of this technique. I corresponded with experts in eddy covariance across the world, some of whom had found similarly high CO_2 effluxes that could not be explained. The extremely large density correction caused by the high heat exchange from the surface to the air during summer days was considered the most likely culprit of the incorrect CO_2 efflux readings, although no-one could satisfactorily explain why.

Daniel J. Boorstin (historian, 1914 – 2004) once said: "The greatest obstacle to discovery is not ignorance - it is the illusion of knowledge." Whereas I – and many others along with me – had implicitly assumed to know that the only process contributing to the CO_2 efflux from organic matter was microbial respiration, this turned out not to be the case. I spent considerable time examining and questioning the data in great detail, before I concluded that the premise my analyses were based on (namely that the sole process responsible

for to the CO_2 efflux was microbial respiration) could not be correct for my study site.

Once I recognised this, I realised my data held substantial evidence for an additional abiotic process that was contributing considerably to the measured CO_2 losses from the peatland: the organic matter of the peat was directly broken down by solar radiation through a process called photodegradation. Photodegradation had not previously been recognised as a potentially large contributor to ecosystem-scale CO_2 emissions from terrestrial ecosystems. My findings, combined with those based on data obtained in a seasonally dry grassland, suggested that photodegradation could be important in a wide range of ecosystems where terrestrial organic matter is exposed. Until now, the process has been ignored in ecosystem scale carbon exchange studies.

To some, the findings of my research might seem self evident, and maybe they are. I suppose that the interpretation of data depends strongly on the background and knowledge of the one who does the interpreting. Whereas for a researcher in the field of photodegradation my results might be “less than surprising”, I know that most researchers in the field of terrestrial ecosystem CO_2 exchange are not aware of the existence of irradiance-induced CO_2 fluxes. I agree with Paul Crutzen (atmospheric chemist, born 1933) when he said that “great ideas often lie within combinations of fields of studies”, so let my contribution to science be the bringing together of two fields by informing researchers in the area of ecosystem CO_2 exchange about the potentially large contribution that photodegradation can make to CO_2 losses from ecosystems.

Although my original research proposal consisted of proper research questions and hypotheses, this is not the way the results will be presented. My journey has been one of discovery, and as such some of the field results will not be presented as if hypotheses were tested. Also, I would like to point out that, if the goal of my research had been to detect and quantify the CO_2 flux resulting from photodegradation, I would have set up the experiment differently. I have not conducted the perfect study on ecosystem-scale irradiance-induced CO_2 losses, yet imperfect studies, when correctly interpreted, can still substantially advance science (altered from Weiss, 1993)

It has been very exiting to travel along the road of discovery of this previously unrecognised pathway of CO_2 losses from terrestrial ecosystem. As always in science, this discovery led to more questions then answers. This thesis does not aim to answer all questions that arose from my findings. Instead, it sheds light on some aspects, and highlights where further work is needed.

I can say that now, at the end of the journey, the overall aim of this research has only changed slightly. Instead of the magnitude and controls of soil respiration of peat, it now focuses on the magnitude and controls of CO_2 losses: losses that can be the result of biotic and abiotic processes.

Acknowledgements

Although a PhD is a very personal endeavour and one that requires many hours working in solitude, it is also true that no PhD can be accomplished without substantial help. Thus I take great pleasure in being able to acknowledge all the people and organisations that supported me during my journey.

First I would like thank Dr Dave Campbell, my first supervisor. It was thanks to Dave's encouragement, support, and enthusiasm that I first embarked down this road. I originally met Dave when I worked with Dr Joost Nieveen, who was a post-doc at Landcare Research. At the time Joost was working with Dave studying CO_2 exchange above pastures using eddy covariance systems. I came to New Zealand to work with Joost on an internship for my Master's degree. When it happened that I came back to New Zealand, Dave and I discussed the possibility of undertaking a novel study that would help understand the controls of nutrients on microbial activity at ecosystem scales.

Although no one had really done it this way before, that did not deter us. Dave provided me with start-up funding, equipment, and support while we searched for more stable, long-term funding. At the time I had limited experience with the EC equipment, so Dave also spent considerable time to teach me the ropes. This included setting up a trial system to try to work out the kinks, as we were applying the EC system in an untested environment, i.e. bare peat soils. His support continued throughout the PhD as he was always there to help work through the technical details and to confirm that they were actually important, even if obscure!

I also greatly appreciated that Dave always made time for me despite his incredibly busy schedule as department chair. He always gave his undivided attention to my project when we had our meetings. His kind and uplifting words at the times things didn't seem to work out were also much appreciated. Dave was consistently a patient and thorough editor who provided valuable feedback and guidance. Somehow he managed to keep that up for the entire duration of my thesis, including delivering his final set of comments late Sunday night before

heading out of town the weekend before I submitted my thesis. Thank you Dave!!!

Second I would like to thank Dr Louis Schipper, my other first supervisor. Louis gave me the confidence from the start that I had what it took to do a PhD. His belief in my abilities helped overcome the doubts that I held in my own mind as to whether I should undertake this journey. Louis is also a fountain of ideas – which he distributes widely and shares freely with all who will listen! – and was instrumental in helping develop the original research hypotheses for my thesis.

Throughout my time as a PhD student, Louis provided a guiding and steady hand. He was constantly engaged and enthusiastic about my ideas, offered encouragement, and provided valuable insights. He often dropped by my office just to see how I was doing. Probably little did he know how important that was to keeping me going. He was particularly good at keeping my spirits up when things did not go smoothly – which felt like all the time at some points – but he was always there to help me through it and see the bigger picture.

Louis also delivered in another important way: he managed to help me with financial support when money from other sources ran low.

Thank you, Louis, for guidance, support, encouragement, intellectual stimulation and everything else that you've done for me.

Dave and Louis also worked well as a team at making sure that I had opportunities beyond my research to grow and develop as a scientist. They encouraged me to seek additional training and provided co-funding to attend two EC workshops, one in Belgium and the other in Australia. They also provided the chance to gain teaching experience by asking me to help them with their courses in Weather & Climate and Soils.

They were 100% behind me as we worked through the 62 or so drafts of our manuscript, first for Nature and then eventually for Global Change Biology. Possibly not the easiest way to learn how to write paper, and I can't say it was always fun, but definitely a very worthwhile learning experience. It's exciting to think about how close we actually came to publishing in Nature!

I want to thank a number of organisations that provided the funding that made my PhD possible. My main funding came from a University of Waikato Doctoral Scholarship. I would to thank the University and the funding committee for having the confidence in me for such an award. I would especially like to thank Dr. Cam Nelson, whose strong support helped me secure this funding.

Manaaki Whenua Landcare Research provided financial support during the start-up phases of my project from the Soil Services Programme (FRST C09X0705). Landcare Research also provided office space and computer facilities during the initial stages of my dissertation. Landcare Research's Wetlands Research Programme (FRST C09X0508) also provided access to equipment and vehicles for use during my field work.

DairyNZ provided funds in the final stage of my research.

I want to thank everyone who provided support for me to carry out my experiments. A very big thanks goes to Gamman Mining for allowing access onto the peat mine in the Hauraki Plains and for delaying restoration activities that allowed us to carry out the research. In particular, I'd like to thank Russell Gamman, Paul Gamman and Danny Bowers for their practical help with the field work, especially when the site was too wet to drive our utes onto the peat for site maintenance.

I received technical and field support during this project from Craig Burgess, Matt Evans and Craig Hosking. Thanks guys for all the trips to the field site and for your help in maintaining and troubleshooting the equipment.

Over the years many others have accompanied me to the field to sample peat, collect chamber data and maintain and fix the eddy covariance gear. Thank you, Chris McKinnon, Steve Cook, Jacinta Parenzee, Paul Mudge, Yvonne Tay, Sören Warneke, Maria Winterfeld, Louise Fisk, Örjan Berglund, Tarnia Hodges, Corrine Watts, Danny Thornburrow, Claire, Janine and Elsa, for all your help. Thanks to Daniel for only coming once… I didn't need *that* kind of help.

Louise Fisk, thank you for your help in the lab with the nutrient experiment, the results of which unfortunately didn't make it into the thesis.

Thank you for your time and effort spent making part of the measurements with the transparent container for Chapter 5. Your measurements might form the beginning of an exciting research field.

Thanks to Paul Mudge and Tehani Kuske for their help in collecting some additional data from the Scott Farm research site that I needed to complete my research.

I would also like to thank a number of other people for their contributions to this project:

- Paul Mudge for all the interesting discussions and commiserations with Matlab programming, flux corrections, eddy covariance gear malfunctions and all the other bits that make EC research so “interesting.” I enjoyed it that we worked on similar research, as you shared both my understanding of the topic as well as appreciated the challenges and frustrations of trying to undertake this kind of research;
- Örjan Berglund for visiting us from Sweden, and working alongside me for 6 months. It was great to have you here to bounce ideas around, and your hands-on, can-do attitude was inspirational;
- Gert-Jan Steeneveld and Arjan van Dijk, my friends from Wageningen, for your ideas and opinions when I contacted you with thorny issues;
- Stephen Newcombe, our in-house glass blower, for helping with the construction of the transparent container;
- Merilyn, Annie, Michael, Ben and Jonathan from the Chemistry department for assisting in characterising Torehape peat;
- Janet Bornman for an enlightening meeting with Louis and me. At the time, we knew nothing about this process or photochemistry in general, and our meeting can best be described as ‘Effects of UV Radiation - 101’;
- Joseph Lane for a very insightful and helpful discussion that introduced me to the basics of photochemistry;
- Judi McWirther and Ray Littler helped me with statistical support. It took me a little while to learn how to communicate with a statistician, but we

got there in the end. A challenging process because, as Ray puts it: 'you can leave it to a statistician to complicate your point of view' ;-).

- Sydney Wright for her help over the years with departmental and administrative matters.

I would like to thank Dr Dennis Baldocchi at the University of California, Berkeley. Thank you for sharing our enthusiasm about my findings and for providing data that helped strengthen our publication. Our discussions at the Belgium workshop helped me realise that I was not the only one to have recorded unexpectedly large fluxes. This spurred me to keep looking for an explanation and eventually led to my findings about photodegradation.

Finally I owe special thanks to a number of people for providing on-going and substantial support.

Thanks firstly to Christian Fritz, Brendan Roddy, Debra Stokes, Natalie Miedema, Paul Mudge, Sören Warneke, and Yvonne Tay. I really appreciated our discussions, your advice and your camaraderie throughout my dissertation. You helped make my path a little brighter and a little lighter.

To Jacinta Parenzee: Thank you!!! For your friendship, patience, listening ear and down-to-earth, common sense - advice whenever I needed it. Our regular lunch-time meanderings around the lakes greatly benefited my mental health over the past several years! *Merci*!

To Graham and Ruth: thanks so much to both of you for your friendship and support over the years. Your house was a refuge for Daniel and me, a place where we knew that we could go to rest, recover and reenergise ourselves. Thanks as well to Graham for his scientific counsel, encyclopaedic knowledge of, well, just about everything, and wonderful dinners. Thanks to Ruth for always reminding us to enjoy ourselves and to get the most out of life.

To my Kiwi family: Angela, Daniel, and Christina! And to Louis, for leading a double life! What would I have done without all of you? Certainly played fewer games, eaten less food, had less good times, found fewer treasures, looted and

pillaged less, laughed less and been even more boring than I already was as a PhD student. What else can I say: you're great!

Pap, mam, Joris, Rosalie en Nielz: mijn stevige basis zo ver van hier. Dankjulliewel voor de steun die jullie me gaven, of het nu in daden, woorden of onvoorwaardelijk vertrouwen was dat ik het allemaal tot een goed einde zou brengen. Het is gelukt.

And then there is my family: Daniel and our poesjes Bugs and Daffy. Daniel, thank you for your interest in my research, understanding when nobody understood, patience when things went slow, and oo-ing and aah-ing about yet another exciting and colourful graph! Your support, encouragement and your listening ear along the way have been invaluable. It has been a long road, but we made it. You might be the one person in this world who is even more relieved than I am about finishing this project!

The people behind the project. Photos by Susanna Rutledge, Daniel Rutledge, David Campbell and Sören Warneke.

Table of Content

Abstract i
Preface v
Acknowledgements ix
Table of Content xv
List of symbols and abbreviations xxi
Chapter 1 Introduction 1
1.1 Background 1
1.2 Aims and objectives of research 2
1.3 Thesis outline 3
Chapter 2 Literature review 5
2.1 Purpose and structure of this literature review 5
2.2 Soil carbon and respiration 5
2.3 Carbon stored in peat 7
2.3.1. Peatlands of the world 7
2.3.2. Peat mines of the world 9
2.4 Terminology related to carbon cycling 9
2.4.1. Decomposition 9
2.4.2. Carbon exchange between ecosystems and the atmosphere 10
2.4.3. Partitioning soil respiration 12
2.5 Methods 14
2.5.1. Methods to measure CO_2 fluxes from soil 14
2.5.2. Methods to measure decomposition 22
2.6 Microbial respiration within bare peatlands 23
2.6.1. Controls of microbial respiration 24
2.6.2. Rates of respiration from bare peat 29
2.6.3. Models of respiration 31
2.7 Photodegradation 34
2.7.1. Methods to measure photodegradation 36
2.7.2. Mechanisms whereby solar irradiance affects decomposition 39
2.7.3. Rates of photodegradation 43

2.7.4. Controls of photodegradation 47
2.8 Summary 56
Chapter 3 Site description and methods 59
3.1 Approaches to measure radiation-induced CO_2 flux 59
3.2 Site description 61
3.3 Field study 65
3.3.1. Eddy covariance 65
3.3.2. Chamber measurements 67
3.3.3. Additional measurements 68
3.4 Container study 69
3.4.1. Experimental design 69
3.4.2. Additional measurements 70
3.4.3. Measurement dates and location 71
3.4.4. Flux calculation 71
3.4.5. Experiment A: Radiation and temperature 73
3.4.6. Experiment B: Wavelength 73
3.4.7. Experiment C: Different substrates 75
3.4.8. Experiment D: Availability of oxygen 75
3.4.9. Test without peat 76
3.5 Additional data 77
3.5.1. CO_2 flux data from Californian grassland 77
3.5.2. UV irradiance at Torehape 80
3.5.3. Differential scanning calorimetry 80
Chapter 4 Can ecosystem CO_2 exchange research ignore photodegradation? 81
4.1 Introduction 81
4.2 Study sites and methods 82
4.2.1. Study sites and measurements 82
4.2.2. Data analysis 83
4.3 Results 85
4.3.1. Two-fold evidence of irradiance-induced CO_2 production 85
4.3.2. Average contribution of photodegradation to the total CO_2 flux 89
4.4 Discussion 92

4.4.1. Size of total and irradiance-induced flux 92
4.4.2. Potential implications for other ecosystems 94
4.4.3. Implications for measurements and modelling 95
4.4.4. Methodological considerations 99
4.5 Summary 101
Chapter 5 Controls of photodegradation 105
5.1 Introduction 105
5.2 Methods 108
5.2.1. Measurements 108
5.2.2. Data analysis 109
5.3 Results 110
5.3.1. Photodegradation in the field 110
5.3.2. Photodegradation in the container experiment 119
5.3.3. Differential scanning calorimetry to identify thermal decomposition 129
5.4 Discussion 130
5.4.1. Pathways of abiotic CO_2 production 130
5.4.2. Control by moisture 133
5.4.3. Control by wavelength 134
5.4.4. Control by temperature 135
5.4.5. Control by radiation and co-varying factors 135
5.4.6. Influence of substrate 140
5.4.7. Control by oxygen availability 142
5.4.8. Methodological considerations 143
5.5 Summary 145
Chapter 6 Controls of microbial respiration of peat 147
6.1 Introduction 147
6.2 Methods 151
6.2.1. Study site and conditions 151
6.2.2. Measurements 151
6.2.3. Data analysis 152
6.3 Results 155

6.3.1. Temperature, rainfall, moisture and soil respiration throughout the measurement period 155
6.3.2. Controls of temperature, DWT and VMC – monthly averages 158
6.3.3. Controls of temperature, DWT and VMC – daily averages 159
6.3.4. Controls of temperature – within-day timescale 165
6.3.5. Short-term effects of rainfall and moisture on CO_2 efflux – within-day time scale 173
6.3.6. Modelling CO_2 flux at the within-day time scale 177
6.4 Discussion 180
6.4.1. Monthly respiration rates 181
6.4.2. Control of the CO_2 efflux by DWT, moisture content and rain 182
6.4.3. Control of the CO_2 efflux by temperature 186
6.4.4. Interactive control of peat respiration by temperature and DWT 191
6.4.5. Modelling respiration from peat 193
6.5 Summary 195
Chapter 7 Summary and conclusions 197
7.1 Introduction and review of thesis objectives 197
7.2 Magnitude of CO_2 efflux resulting from microbial decomposition and photodegradation 198
7.3 Mechanisms of irradiance-induced CO_2 production 199
7.4 Controls of irradiance-induced CO_2 production 200
7.5 Controls of microbial respiration at the peatland 201
7.6 A new conceptual model 202
7.7 Recommendations for further research 203
7.7.1. Small scale studies 204
7.7.2. Field studies 205
7.7.3. Modelling 206
References 209
Appendix A Global Change Biology paper 239
Appendix B Timing error 249
B.1 Introduction 249

B.2 Timing error at the peatland 251
B.2.1 Aim 251
B.2.2 Methods: Estimation of effect of timing error 251
B.2.3 Results and discussion 254
B.3 Summary 260
Appendix C Estimates of UV irradiance at the peatland 263
Appendix D Density term 267
D.1 Introduction 267
D.1.1 Background to the WPL term 267
D.1.2 Potential error propagation 268
D.1.3 Field validation WPL term 269
D.1.4 Sensor separation and the WPL term 270
D.2 WPL term at the peatland and grassland 272
D.2.1 Size of the WPL term 272
D.2.2 Potential error propagation tested at the peatland 274
D.2.3 Effect of sensor separation tested at the grassland 284
Appendix E Negative CO_2 fluxes observed in the container 287
E.1 Background and aim 287
E.2 Methods 287
E.3 Results 288
E.4 Discussion 291
E.4.1 Shade runs 291
E.4.2 Sun runs 292
E.4.3 Length of run chosen for analysis 292
E.4.4 Further work 293
E.5 Conclusion 293
Appendix F Spatial representativeness of CO_2 efflux measurements 295
F.1 Background and aim 295
F.2 Methods 295
F.2.1 Survey chamber measurements 295
F.2.2 Analysis 297
F.3 Results and discussion 297

F.3.1 Depth to water table 298
F.3.2 Peat temperature 300
F.3.3 CO_2 flux 300
F.4 Conclusion 303

List of symbols and abbreviations

AD	Abiotic degradation
AR	Autotrophic respiration
AR_a	Above-ground autotrophic respiration
AR_b	Below-ground autotrophic respiration
BREB	Bowen ratio/energy balance method
C	Carbon
CH	Chamber
CO	Carbon monoxide
CO_2	Carbon dioxide
DIC	Dissolved inorganic carbon
DOC	Dissolved organic carbon
DSC	Differential scanning calorimetry
DWT	Depth to water table
EC	Eddy covariance
ER	Ecosystem respiration
GPP	Gross primary production
H	Sensible heat flux
HR	Heterotrophic respiration
IRGA	Infrared gas analyzer
$K\downarrow$	Shortwave incoming irradiance
LT	Lloyd and Taylor equation for soil respiration
LE	Latent heat flux
NEE	Net ecosystem exchange
NEP	Net ecosystem production
NPP	Net primary production
OM	Organic matter
Q_{10}	Proportional increase of a respiration for a 10^{o}C increase (-)
PAR	Photosynthetically active radiation
PD	Photodegradation

RH	Relative humidity
SE	Standard error
SOC	Soil organic carbon
SOM	Soil organic matter
SR	Soil respiration
SZA	Solar zenith angle
T	Temperature
UV-A	Ultraviolet radiation (320-400 nm)
UV-B	Ultraviolet radiation (280-320 nm)
VMC	Volumetric moisture content
WPL	Webb, Pearman and Leuning term for density corrections of turbulent flux measurements

Chapter 1 Introduction

1.1 Background

Organic matter (OM) in soil increases the soil's capacity to hold water, provides nutrients needed for plant growth and improves soil structure (Luo and Zhou, 2006; McLaren and Cameron, 1996). Additionally, soils form the largest terrestrial storage pool of carbon (Amundson, 2001; Janzen, 2004).

Microbial decomposition is the process by which bacteria and fungi in the soil break down organic matter, thereby producing CO_2 (Luo and Zhou, 2006; Swift et al., 1979). This soil respiration is the main process by which soil organic carbon is released back into the atmosphere. Because of the role of soil respiration in the global carbon cycle and because of the effect of atmospheric CO_2 on global climate, scientific interest in the controls of soil respiration rates has increased over the last few decades. For example, there is evidence for positive feedback between global temperature and respiration rates, whereby an increase in temperature (due to a rise in concentration of greenhouse gases like CO_2) leads to an increase in microbial activity and thereby respiration rates. This in turn could lead to a further release of CO_2 to the atmosphere (Davidson and Janssens, 2006; Friedlingstein et al., 2006; Jones et al., 2003; Kirschbaum, 2004; Raich and Schlesinger, 1992; Rustad et al., 2001) and a decrease in the magnitude of the carbon pool in soils.

Improving our understanding of the response of rates of CO_2 losses from soils to changing environmental conditions or management practices is crucial if we are to predict the stability of soil organic carbon and the atmospheric CO_2 concentration in the future.

Uncertainty still exists about what controls losses of CO_2 through heterotrophic respiration by microbes (Jones et al., 2003; Trumbore, 2006). Controls of microbial respiration are usually studied using small plots in the field, or using laboratory incubations of soil. Field studies are generally conducted in vegetated ecosystems where the response of microbial respiration to changing environmental conditions is confounded by plant responses to these changing

conditions (e.g. Bahn et al., 2008; Tang et al., 2005). For this reason studies of microbial respiration at ecosystem scales are rare.

Recent studies have shown that the direct breakdown of organic matter by solar irradiance (i.e. photodegradation) can also contribute substantially to decomposition, especially in dry ecosystems (Austin and Vivanco, 2006; Brandt et al., 2007; Day et al., 2007; Gallo et al., 2009; Throop and Archer, 2009). Two small incubation studies have confirmed that photodegradation produces CO_2 (Anesio et al., 1999; Brandt et al., 2009). However, no estimates of the magnitude of this irradiance-induced CO_2 flux, or its controls, have been reported in field studies in the literature. Furthermore, studies have not partitioned CO_2 losses in the field into the contributions of microbial respiration and photodegradation.

1.2 Aims and objectives of research

The original aim for this study was to determine how soil moisture, soil temperature and ultimately nutrient availability controlled soil respiration rates resulting from microbial decomposition of organic matter at a bare (mined) peatland. The bare peatland was chosen to avoid the confounding effects of plants. It was assumed that soil respiration could be quantified by measuring CO_2 losses from peat.

However, the discovery of photodegradation shifted the focus of the thesis somewhat and the overall aim of the thesis was re-formulated as “to advance the understanding of the controls of CO_2 losses from terrestrial organic matter at large scales”. A substantial part of this thesis was re-directed to investigate the magnitude and controls of irradiance-induced CO_2 losses. The objectives of this research were to:

1) quantify the contribution of photodegradation to the total CO_2 flux from a bare peatland in New Zealand and an annual grassland in California
2) investigate the controls of CO_2 flux caused by photodegradation
3) examine the controls on microbial respiration rates at the bare peatland without the confounding effects of plants.

For the detection of photodegradation in the field, data from a field site in California were re-analysed in addition to the data from the peatland in New Zealand. For the microbial work (objective 3), only the respiration at the peatland was studied.

1.3 Thesis outline

The thesis is organised as follows.

Chapter 2 reviews the existing literature, discussing both CO_2 effluxes from photodegradation and microbial respiration. Because the process of terrestrial photodegradation is poorly understood compared to biological soil respiration, the emphasis in the literature review is on photodegradation.

Chapter 3 describes the field sites and the methods that were used for the field studies and the small scale incubation experiments.

Chapters 4-6 present the results of this thesis, and discuss the findings in the context of previous published research. Chapter 4 describes the field measurements that demonstrated that substantial portions of the measured CO_2 effluxes from a peatland and an annual grassland were irradiance-induced.

Chapter 5 expands on the findings in the field, and reports results of small-scale incubation experiments designed to confirm the field observations of photodegradation. This chapter also aims to determine some of the controls on the rates of production of CO_2 through photodegradation as measured in the field and the incubation study. Challenges encountered with the newly designed chamber setup for measuring irradiance-induced CO_2 losses are discussed.

Chapter 6 describes the findings regarding microbial respiration. This chapter focuses on the magnitude and controls of CO_2 fluxes resulting from microbial respiration at the peatland in the absence of plants examined at different time scales.

Chapter 7 contains a summary of the findings, the main conclusions and recommendations for future research.

Some of the findings of Chapter 4 and 5 are part of a paper that has been accepted for publication:

> Rutledge, S., Campbell, D.I., Baldocchi, D. and Schipper, L.A., 2010. Photodegradation leads to increased CO_2 losses from terrestrial organic matter. Global Change Biology: "Accepted Article"; doi: 10.1111/j.1365-2486.2009.02149.x

This paper can be found in Appendix A.

The remaining five appendices (B – F) deal with methodological issues.

Chapter 2 Literature review

2.1 Purpose and structure of this literature review

This chapter will review knowledge on the processes leading to CO_2 losses from terrestrial organic matter. It will focus on two processes that contribute to the total CO_2 efflux. The main process is biological: respiration resulting from microbial decomposition of soil organic matter (SOM). A second potential contributor to CO_2 losses from soil and litter is the abiotic process of photodegradation.

After explaining why SOM and CO_2 losses are of importance and presenting a short introduction of peatlands and peat mines worldwide, an overview will follow of the terminology commonly used in studies on ecosystem exchange of CO_2 (Section 2.4). The following section (Section 2.5) describes the methodologies most commonly used for measuring CO_2 fluxes. Section 2.6 describes the process of microbial respiration in bare peatlands, the main controls and a summary of respiration rates measured by other studies. As much as possible, the review focuses on studies examining respiration rates from bare peatlands, as these are the most comparable to the study site used for this thesis.

Section 2.7 focuses on photodegradation in terrestrial ecosystems. Because very little is known about terrestrial photodegradation, and no studies have presented data on photodegradation from peat or soil, this review encompasses all studies focussing on photodegradation of terrestrial litter.

2.2 Soil carbon and respiration

Carbon is an essential compound for all organisms on Earth and it cycles between the atmosphere, biosphere, hydrosphere and soil systems. In the terrestrial part of the carbon cycle (Figure 2.1), carbon from the atmosphere (CO_2) is sequestered into biomass by autotrophs (plants) through the process of photosynthesis. When plants die, some fraction of their organic matter accumulates in the soil. In the soil, organic matter enhances soil quality by increasing water holding capacity, supplying nutrients for plant growth,

maintaining soil fertility through its cation exchange capacity and improving soil structure and stability (Luo and Zhou, 2006; McLaren and Cameron, 1996). About half of the total mass of organic matter in or on top of soils is carbon (Blanco-Canqui and Lal, 2004; Luo and Zhou, 2006). This carbon makes its way back to the atmosphere primarily as CO_2, mostly through the process of respiration as a result of microbial decomposition of organic matter (Figure 2.1).

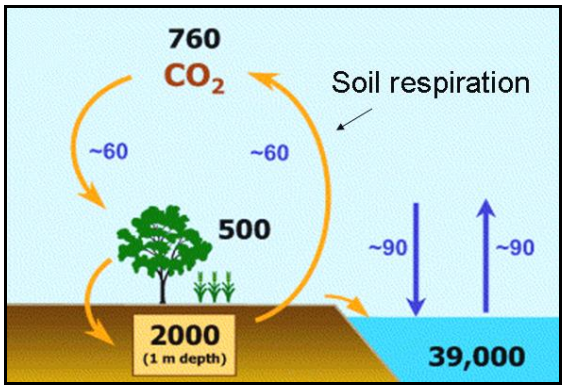

Figure 2.1 The global carbon cycle. All C stocks are in units of Pg C, and flows are in Pg C per year (Pg = 10^{15} g). Reprinted from Janzen (2004) with permission from Elsevier.

There is strong evidence that the rising CO_2 concentration in the atmosphere over the last century is largely responsible for the globally rising temperatures (IPCC, 2007). Because of CO_2's role as a greenhouse gas, scientists' interest in the processes and controls of carbon cycling has increased drastically over the last decades. Soil carbon forms the largest reservoir of carbon in terrestrial ecosystems (1500-2000 Pg; Amundson, 2001; Janzen, 2004; Figure 2.1) and soil respiration represents the largest flux of carbon from soils to the atmosphere. Because changes in the mineralisation of SOM can have large implications for soil quality and the CO_2 concentration in the atmosphere on a global scale, increasing our understanding of the response of carbon cycling in terrestrial ecosystems to changing environmental conditions is of utmost importance.

2.3 Carbon stored in peat

2.3.1. Peatlands of the world

A peatland can be described as “an area with or without vegetation with a naturally accumulated peat layer at the surface” (Joosten and Clarke, 2002). Peat accumulates in an ecosystem when its carbon balance is positive, which means that more carbon is fixed in plants than is decomposed. Peat accumulation is the result of limited decomposition of plant material usually caused by low oxygen availability as a result of inundation by water (Clymo, 1984; Davidson and Janssens, 2006; Joosten and Clarke, 2002; Laiho, 2006).

There is a lack of globally consistent data on the area and carbon stores in peatlands (Bridgham et al., 2007; Clymo, 1984; Fuchsman, 1980; Joosten and Clarke, 2002; Krankina et al., 2008). This large uncertainty is caused by inadequate data for many regions of the world (Bridgham et al., 2007; Lappalainen, 1996), and by differences in definitions between different countries and scientific disciplines, for example about the minimum thickness of peat in a peatland (Joosten, 2004; Joosten and Clarke, 2002; Lappalainen, 1996; Oleszczuk et al., 2008). Peatlands are estimated to cover about $4 \cdot 10^6$ km^2 (Joosten and Clarke, 2002; Lappalainen, 1996; Maltby and Immirzi, 1993; Table 2.1), which represents approximately 3% of the total land surface of the Earth. Most of these peatlands can be found in the boreal and sub-arctic regions in the Northern hemisphere where wet and cold conditions facilitate peat formation (Gorham, 1991; Joosten and Clarke, 2002; Maltby and Proctor, 1996) with an estimated area of $3.46 \cdot 10^6$ km^2 (Gorham, 1991).

Table 2.1 Estimates of the global area of peatlands in 10^3 km^2.

	Agriculture + Forestry							
	Agriculture			Forestry		Sum drained	Unaltered	*Total*
	Crops	Pasture	*Tot*		*Tot*			
Bridgham et al. (2007)								3440
Lappalainen (1996)								3985
Joosten and Clarke (2002)			250	150	400	>490	>3140	4000
Armentano and Menges (1986)	82	55		94		260	3269	3492
Armentano and Verhoeven (1988) in Maltby and Immirzi (1993)			137	92	250			
Maltby and Proctor (1996)					300			4000
Maltby and Immirzi (1993)			93	118				3880-4080

Peatlands are more important for the global carbon cycle than their surface area would suggest because of their high organic carbon content (Lappalainen, 1996). Peatlands store a large proportion of the terrestrial carbon with estimates ranging between 234 and 528 Pg of carbon (Table 2.2). This large carbon pool contains between 16–33% of the total soil carbon pool (Gorham, 1991; Lappalainen, 1996; Maltby and Immirzi, 1993).

Table 2.2 Estimates of the global pool of soil carbon held in peatlands.

Reference	Store of carbon (Gt/Pg/10^{15} g.)
Immirzi et al. (1992) in Charman (2002)	329 – 528
Gorham (1991)	455*
Armentano and Menges (1986)	276**
Sjörs (1981) in Marikainen and Lappalainen (1996)	300*
Maltby and Immirzi (1993)	462 – 525
Lappalainen (1996)	234 – 252
Bridgham (2007)	462 (± 50%)
Turunen et al. (2002)	270-370***

* in peatlands boreal and subarctic regions alone

**assuming that peat layer is 1m thick, which is thought to be too shallow (Maltby and Immirzi, 1993)

*** in mires in boreal and subarctic regions alone

2.3.2. Peat mines of the world

Human activities in the non-tropical world alone have led to an area loss of pristine mires of over 16% (Joosten and Clarke, 2002). Around 10% of peatlands around the world are currently drained, and used mostly for agriculture and forestry (Table 2.1; Joosten and Clarke, 2002). A small part of peatlands (approximately $50 \cdot 10^3$ km^2, Joosten and Clarke, 2002) are used for peat extraction, with the mined peat being used for energy generation, domestic heating, as organic fertiliser and humus in agriculture and as growing medium in horticulture (Joosten and Clarke, 2002). These days, most of the peat used for energy production (almost 90%) is produced in the Russian Federation, Belarus, Sweden, Finland and Ireland (Strack, 2008). Canada and Germany account for more than half the production of horticultural peat (Strack, 2008).

2.4 Terminology related to carbon cycling

This section will present the terms and abbreviations that are commonly used in carbon cycling studies and that will be used throughout this study.

2.4.1. Decomposition

The term "carbon turnover" will be used synonymous with carbon cycling which includes mineralisation and the transformation of carbon from one pool (or reservoir) to another pool. Decomposition is the overall process by which a substrate is transformed into organic compounds and CO_2 (Shibu et al., 2006) and in this thesis the terms "degradation" and "breakdown" will be used to indicate the same. The main resulting products of decomposition are recalcitrant organic matter, CO_2 and dissolved organic and inorganic carbon (DOC and DIC) that can leach from the soil (Figure 2.2). Leaching is the loss of incompletely decomposed organic compounds or inorganic compounds from the decomposing substrate, due to the actions of water (altered from Berg and McClaugherty, 2008). The conversion of organic C to the inorganic compounds CO_2 and DIC is called mineralisation. Because decomposition rates are often determined by measuring mass loss of soil or litter over time, decomposition is sometimes also defined as "mass loss from organic matter" or "CO_2 release plus leaching of

compounds" (adapted from Berg and McClaugherty, 2008; Figure 2.2). Fragmentation is "a reduction in particle size of the organic resource" (Swift et al., 1979). This fragmentation can be brought about by abiotic factors such as freezing and thawing, or wetting and drying cycles (Berg and McClaugherty, 2008) or by soil animals breaking down large pieces of SOM or litter (Lavelle and Martin, 1992; Luo and Zhou, 2006; Wolters, 2000).

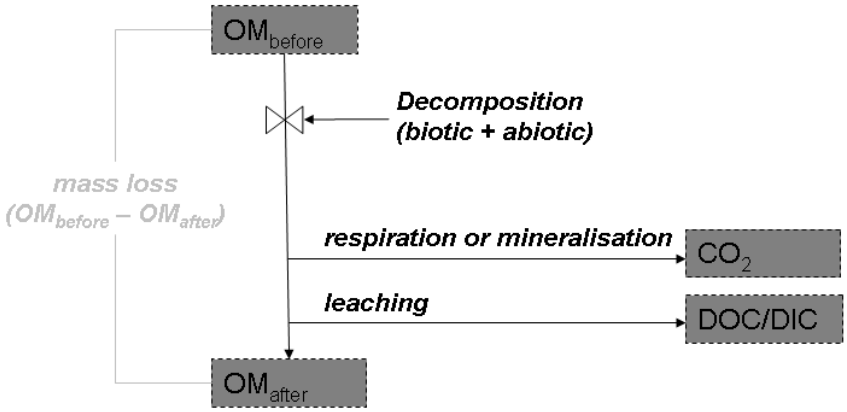

Figure 2.2 Diagram showing processes (bold lettering) and begin and end products (in grey boxes) of decomposition.

2.4.2. Carbon exchange between ecosystems and the atmosphere

The terminology used in studies of the carbon exchange between the Earth's vegetated surface and the atmosphere is illustrated in Figure 2.3. Gross primary production (GPP) is the carbon fixed by plants through photosynthesis. Part of this carbon is respired by the plant both above- and below ground (autotrophic respiration, AR = AR_a +AR_b), and the remaining net production of organic matter by plants is called net primary production (NPP = GPP – AR). HR is heterotrophic respiration, defined as "the production of CO_2 from the decomposition of organic matter by microbial and fungal organisms" (Schimel and Manning, 2003) and takes place in the litter layer and soil. Net ecosystem production (NEP) equals NPP – HR. NEP also equals GPP – ER, where ER is ecosystem respiration. ER is the sum of autotrophic and heterotrophic respiration (ER = AR + HR).

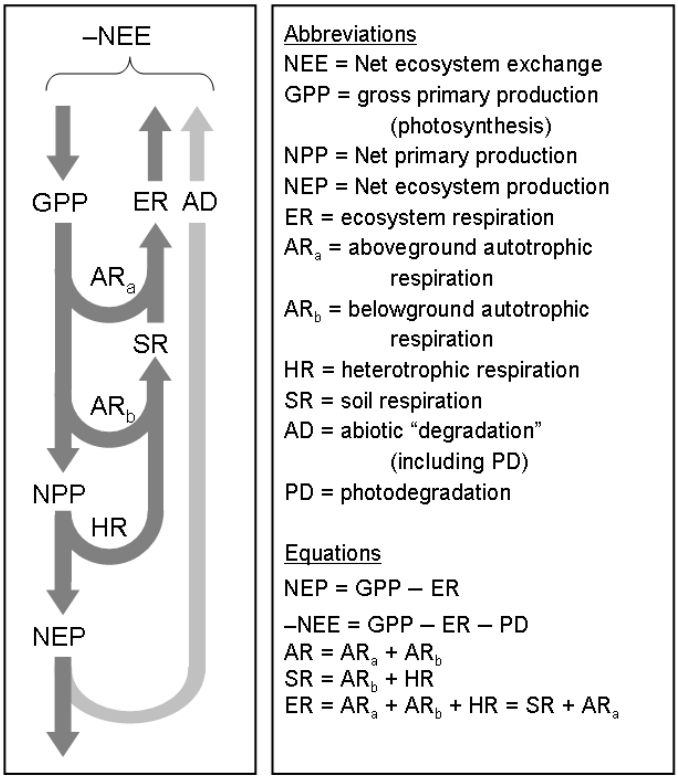

Figure 2.3 Diagram summarising the terms commonly used in describing fluxes of CO_2 in ecosystem studies. The figure was adapted from Luyssaert et al. (2007) and is based on definitions given by Chapin et al. (2006).

Chapin et al. (2006) defined net ecosystem exchange (NEE) as "the net CO_2 flux from the ecosystem to the atmosphere (or net CO_2 uptake)". NEE is defined by atmospheric scientists, and uptake of CO_2 by an ecosystem is defined as negative, and losses of CO_2 to the atmosphere are positive. In contrast, NEP is used by ecologists and is of opposite sign compared to NEE: i.e. NEP is defined as positive when the ecosystem acts as a sink, and as negative when carbon is lost from the ecosystem (Chapin et al., 2006).

The biotic process of respiration is considered the main pathway for carbon moving from terrestrial ecosystems back to the atmosphere (e.g. Aerts, 1997; Ryan and Law, 2005) and the measured CO_2 efflux from soils is usually considered to be equal to soil respiration (Bridgham and Richardson, 1992; Raich and Schlesinger, 1992).

Likewise, measured CO_2 effluxes from an ecosystem are usually considered to be the result of biotic processes (respiration by living organisms, ER) only. However, both *biotic* and *abiotic* processes may contribute to CO_2

losses from ecosystems. Abiotic processes can contribute to the CO_2 loss from ecosystems ("the non-respiratory CO_2 losses"; Luyssaert et al. 2007) through processes like fire (Chapin et al., 2006; Randerson et al., 2002), the breakdown of OM by solar radiation ("photodegradation", Brandt et al., 2009), and the dissolution and precipitation processes of carbonates in soils or parent material (Emmerich, 2003; Kowalski et al., 2008; Mielnick et al., 2005; Serrano-Ortiz et al., 2010). NEE is the exchange of CO_2 resulting from gross primary production, ecosystem respiration and abiotic (non-respiratory) CO_2 losses (see Figure 2.3):

$$-NEE = GPP - ER - AD \qquad \textbf{Equation 2.1}$$

where AD are the CO_2 losses caused by abiotic processes. However, in studies on carbon cycling, the net CO_2 flux measured above the vegetation (NEE) is often assumed to be equal to –NEP which does not include the non-respiratory CO_2 losses:

$$-NEE \approx NEP = GPP - ER \qquad \textbf{Equation 2.2}$$

This common assumption that abiotic CO_2 losses can be ignored is usually made in ecosystem-scale carbon cycling studies (Serrano-Ortiz et al., 2010) without being acknowledged (e.g. Baldocchi, 2008a; Desai et al., 2008; Luyssaert et al., 2009; Ma et al., 2007; Strack et al., 2008).

2.4.3. Partitioning soil respiration

In ecosystems without plants, soil respiration equals heterotrophic respiration (HR): the production of CO_2 by microbes. Soil mesofauna (for example earthworms and nematodes) also contribute to the heterotrophic respiration, but this forms only a very small part of the total CO_2 respired by heterotrophic organisms (references in Kuzyakov, 2006). In vegetated ecosystems, below-ground autotrophic respiration (AR_b) from roots and root-associated respiration from mycorrhizae (root-infecting fungi, Luo and Zhou, 2006) and microbes in rhizosphere (the zone directly next to the root surface, Luo and Zhou, 2006) also contribute to the total soil respiration ($RS = AR_b + HR$).

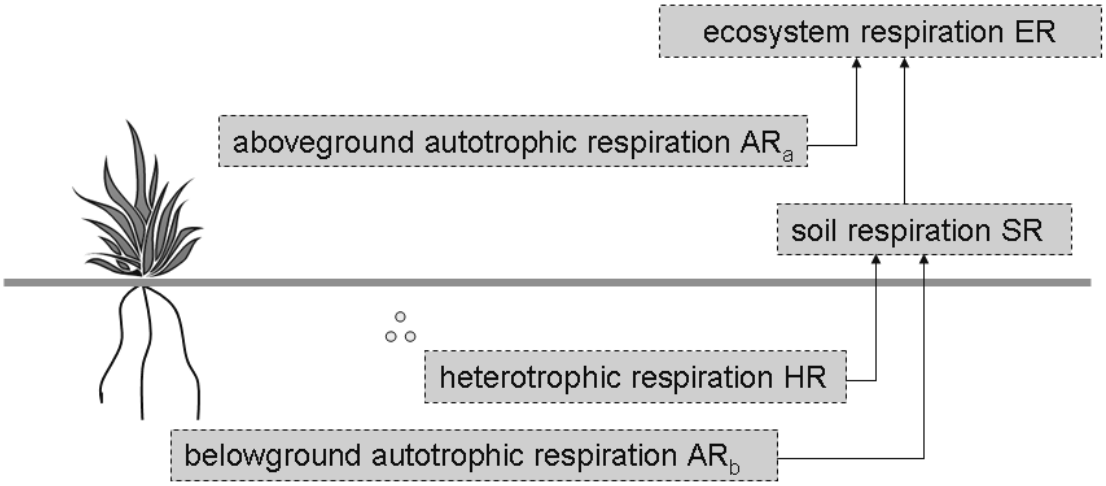

Figure 2.4 Components of soil and ecosystem respiration. See also Figure 2.3.

In this thesis, respiration from rhizosphere and mycorrhizae is combined with the root respiration in the term 'belowground autotrophic respiration' or 'root-associated' respiration (see also Hanson (2000), Bond-Lamberty et al. (2004) and references therein), because for this thesis it is only important to distinguish between bare soil and plant+soil respiration. Even though this definition is used regularly in the science community (e.g. Ryan and Law, 2005), one could reason this is not correct. The reader is referred to the review by Kuzyakov (2006), and following papers (Högberg et al., 2006; Kuzyakov, 2006a) for a detailed discussion on the proper terminology of root, rhizosphere and mycorrhizae respiration.

In ecosystem carbon dynamics studies, the components of SR (i.e. HR and AR_b) are often not measured individually, which means that measured values of SR need to be partitioned into autotrophic respiration by plants (AR_b) and heterotrophic respiration by microbes (HR). Reviews on methods of partitioning of soil respiration into AR_b and HR are provided by Hanson et al. (2000), Kuzyakov (2006), Subke (2006) and Bond-Lamberty et al. (2004). Root-associated respiration normally accounts for approximately 30-80% of the total soil respiration (Davidson et al., 2006b; Hanson et al., 2000). We need to keep this in mind when comparing studies on soil respiration in the presence and absence of plants. Soil respiration measurements in this thesis do not include root-associated respiration.

2.5 Methods

Soil respiration rates are determined by measuring CO_2 evolution from soils, either in the field or in the lab. In Section 2.5.1, three different methods will be discussed.

Rates of OM decomposition are often quantified by measuring mass loss of soil and/or litter. Although the current study focuses on soil respiration only, the results are compared to other studies that measure decomposition rates using mass loss. For this reason the most common method for measuring decomposition, the litter bag method, is discussed in Section 2.5.2.

2.5.1. Methods to measure CO_2 fluxes from soil

The three methods for measuring soil respiration discussed here operate on very different spatial and temporal scales: evolution of CO_2 from soil in jars in the lab, chambers and the soil CO_2 gradient method on plot scales in the field and eddy covariance (EC) at ecosystem scales. As Denmead and Raupach (1993) point out, different methods should often be considered as complementary rather than alternatives. Each method has its own benefits and drawbacks which will be discussed below. After describing the three different methods, an overview will be given of studies that have compared fluxes measured by chamber and EC technique.

Laboratory studies: CO_2 evolution in jars

When measuring soil respiration in the lab, small quantities of soil are placed in jars. Jars are sealed with a lid with a septum in it, which allows gas samples to be taken from the headspace. The microbial respiration rates can be determined by monitoring the increase of CO_2 concentration in the jars over time by sampling at regular time intervals. Care must be taken not to let the CO_2 concentration reach values above 10,000 ppm (Reichstein et al., 2000), because above this threshold CO_2 is found to inhibit microbial activity. Air from the headspace can be analysed for CO_2 using an infrared gas analyser or gas chromatograph.

Lab studies offer the possibility of doing highly controlled and replicated experiments where different treatments can be compared. However, it is often unclear how representative the results are for situations in the field.

Plot scale: Chamber

At plot scale in the field, soil respiration is traditionally measured using a chamber system. Chamber systems can be divided into two groups: static and dynamic chamber systems. Static systems, whereby CO_2 evolution into an enclosed volume is measured either by trapping the CO_2 using a alkali trap or by taking regular air samples over time which are analysed for CO_2 later in the lab, are less common than dynamic chamber systems. In closed dynamic chamber systems air circulates between the chamber and the infrared gas analyser (IRGA) to determine the change in CO_2 concentration over time. These systems are also referred to as flow-through non-steady state (FT-NSS, Livingston and Hutchinson, 1995).

Before making measurements, collars must be inserted into the soil. These collars ensure a good seal between the chamber and soil and avoid any disturbances to the soil caused by placing the chambers (Norman et al., 1992). To make a measurement, the chamber is placed on the collar and the CO_2 concentration is monitored by circulating air between the chamber volume and the gas analyser. Individual measurements are commonly several minutes long. Afterwards, the CO_2 flux can be calculated by fitting a regression equation to the data points describing the CO_2 evolution with time.

Chamber studies allow for replicated treatment studies in the field. Operation of a chamber system is relatively straightforward, especially when a commercially available soil respiration system is used which includes both hardware and software.

A drawback of the chamber technique is the limited spatial extent compared to the spatial variability of the CO_2 efflux from the soil (Law et al., 2001; Rayment and Jarvis, 2000). As Savage and Davidson (2003) point out, the most effective way to characterise soil respiration over time and space with soil chambers is to combine data from a manually operated chamber with that of an

automated system. The manual system allows one to measure at several points within the area of interest, and has great spatial distribution but poor temporal distribution, whereas an automated system operates at one point only but has a high degree of temporal distribution. Obtaining spatial readings using a portable chamber can be very labour-intensive.

Soil respiration is the result of two processes: CO_2 production within the soil profile and transport of CO_2 from soil to the soil-atmosphere interface (Fang and Moncrieff, 1999; Luo and Zhou, 2006). Transport of CO_2 from the soil to the soil-atmosphere interface occurs as a result of both concentration gradients (diffusive flow) and pressure gradients (mass flow; Luo and Zhou, 2006). When measuring soil respiration, care needs to be taken not to modify the conditions that control production and transport of CO_2 (Luo and Zhou, 2006).

The main challenges of the closed dynamic chamber technique when measuring CO_2 produced by microbes in the soil are the following (see review by Davidson et al., 2002):

- Pressure effects. Ideally, pressure conditions in the chamber headspace and outside the chamber are the same. However, especially under windy or gusty conditions, pressure fluctuations between the chamber headspace and the ambient atmosphere may occur (Livingston and Hutchinson, 1995; Xu et al., 2006), often leading to overestimation of the flux (Bain et al., 2005). These issues should be dealt with through chamber design (Hutchinson and Livingston, 2001; Xu et al., 2006) such as correct venting design.
- Inhibition of CO_2 efflux caused by a build-up of CO_2 in the chamber. The increase of CO_2 concentration in the chamber leads to a decrease in the CO_2 gradient between soil and atmosphere, thereby possibly suppressing the diffusion of CO_2 into the chamber. One can avoid underestimating the flux by using an exponential fit to the data instead of a linear fit (Kroon et al., 2008), and by changing the duration of measurements to suit the conditions (i.e. at high respiration rates shorter measurements suffice; Davidson et al., 2002).

- Non-steady state CO_2 efflux. After periods of relative drought, rainfall or irrigation can lead to a large increase of measured CO_2 flux caused by CO_2- rich soil air being displaced by water infiltrating the soil (soil degassing). During these periods, measurements might accurately reflect the CO_2 efflux from the soil, but this efflux is not equal to CO_2 production in the soil because CO_2 production and transport are not in equilibrium (Chen et al., 2008; Liu et al., 2002).

To obtain a reliable estimate of the average CO_2 flux over a large area, chamber measurements should be made at several locations in the area of interest (for example the footprint of an EC tower) because of the usually large spatial heterogeneity of soil respiration (Savage and Davidson, 2003).

Plot scale: Soil CO_2 gradient

CO_2 effluxes from soil to the atmosphere can also be estimated by measuring the change in CO_2 concentration in soil air with depth (Fierer et al., 2005a; Jassal et al., 2005; Luo and Zhou, 2006). This can either be done by sampling soil air at different depths and analysing it using one gas analyser (also called the 'gas well method' described by Luo and Zhou (2006), see for example Fierer et al. (2005a), Fang and Moncrieff (1996) and Hamada and Tanaka (2001)), or by installing multiple sensors that determine the CO_2 concentration at various depths in the soil profile simultaneously (see e.g. Hirano et al. (2003), Jassal et al. (2005), Tang et al. (2003) and references therein). Using the CO_2 concentration determined at various depths, fluxes of CO_2 can be calculated using flux gradient theory, based on Fick's law of diffusion which states that the flux is proportional to the gradient in the CO_2 concentration (Fierer et al., 2005a; Luo and Zhou, 2006). This method assumes that diffusion is mostly responsible for the transport of CO_2 from the soil to the soil surface (and not mass flow), and relies heavily on the correct estimation of diffusivity of CO_2 in soil (Luo and Zhou, 2006). Soil CO_2 probes will not take into account any CO_2 produced from litter at the soil surface. Still, good agreement between estimates of CO_2 flux based on soil CO_2 gradient

and chamber measurement has been observed at an annual grassland in California (Tang et al., 2003).

Ecosystem scale: Eddy covariance

There are several micrometeorological methods that can be used to measure gaseous exchange of CO_2 between ecosystems and the atmosphere at large scales: the eddy covariance (EC), Bowen ratio/energy balance (BREB), aerodynamic, eddy accumulation and surface renewal methods (Luo and Zhou, 2006).

Micrometeorological methods are very powerful because they do not disturb the source area or its microclimate (Shurpali et al., 1995), they integrate over large areas and operate rapidly and continuously, thereby allowing the study of environmental effects on the rate of exchange of CO_2 between the surface and the atmosphere (Baldocchi, 2003; Denmead, 1983; Denmead and Raupach, 1993). Especially the eddy covariance technique has emerged in recent decades as an alternative way to assess carbon exchange between the atmosphere and the land surface. The use of the EC technique is widespread with the largest international network, FLUXNET (http://www.fluxnet.ornl.gov/fluxnet/index.cfm; Baldocchi et al., 2001), currently comprising over 500 EC towers (Baldocchi, 2008a; Baldocchi, 2008b).

Despite being widely used, there are several drawbacks of the EC technique. To acquire reliable data from EC systems requires a high level of technical understanding of both the instrumentation and associated data processing software. EC systems are expensive and require regular maintenance. Even with a perfect set-up, many corrections need to be applied to the raw data to obtain fluxes: Corrections for the spatial separation between sensors and the limited frequency response of the sensors (Massman, 2000; Moore, 1986); for the humidity dependence of the acoustically sensed temperature (Schotanus et al., 1983); coordinate rotation (Finnigan et al., 2003; Lee et al., 2004; McMillen, 1986) and for changes in air density (WPL correction describes by Webb et al. (1980), Leuning (2004) and Leuning (2007)). When applying the EC technique, measurements have to be made under certain atmospheric conditions so that

many of the terms in the budget equation that are difficult to measure can be ignored (Aubinet et al., 2000). Under those conditions, only two terms of the equation have to be measured to determine the source or sink of CO_2 at the land's surface: the turbulent flux in the vertical direction which is measured by the EC system, plus the rate of change in storage of CO_2 below the sensor height (Aubinet et al., 2000; Kowalski and Serrano-Ortiz, 2007). Only when the assumptions that the EC technique is based on are not violated, can one expect to get reliable results using EC. For example, horizontal homogeneity is assumed so that advection and flux divergence can be ignored. However, when the upwind area is not homogeneous and this assumption is violated, the advection terms in the budget equations cannot be assumed zero (Laubach and Teichmann, 1999). Also, the EC technique assumes stationary conditions. When non-stationarity occurs, for example when atmospheric changes take place – like large scale changes of air mass associated with passage of frontal zones and the evening and morning transitions in stability (Moncrieff et al., 2004) – the equations that underlie the EC technique are not valid. One of the main challenges the EC community is currently facing is obtaining reliable measurement of night-time CO_2 fluxes. Massman and Lee (2002) describe the challenges during night-time measurements as "a co-occurrence of all eddy covariance limitations" and give a comprehensive outline of these weaknesses. One of the main challenges faced at night is that low wind speeds and stable atmospheric conditions lead to CO_2 transport by advection (Aubinet et al., 2005; Aubinet et al., 2000; Feigenwinter et al., 2004), which cannot be measured using eddy covariance. This leads to an underestimation of night-time respiration fluxes (Aubinet et al., 2005; van Gorsel et al., 2008). Traditionally, this problem is dealt with by discarding data obtained under conditions of low levels of turbulence (using the 'u* filter'; Gu et al., 2005; Hutyra et al., 2008; Wohlfahrt et al., 2005), However, this is not ideal, and research into this area is ongoing (Gu et al., 2005; van Gorsel et al., 2009; van Gorsel et al., 2008; Van Gorsel et al., 2007).

In addition to discarding data when turbulence levels are low, data are also discarded when wind is blowing from behind the tower (flow distortion; Geissbühler et al., 2000; Wyngaard, 1990) when the flux does not originate from

the desired source area ('the footprint'; Horst and Weil, 1992; Schmid, 2002; Schuepp et al., 1990) or when sensors were malfunctioning, for example because of a power outage or wet sensors during and after rain (Heusinkveld et al., 2008). Normally, after flux computations and filtering out bad data, around 65 % of the data remain (Falge et al., 2001a), but this percentage can be as low as 40% (Moffat et al., 2007). For carbon budget studies, the gaps in the data need to be filled using gap-filling techniques (Falge et al., 2001a; Falge et al., 2001b; Foken et al., 2004; Moffat et al., 2007). In contrast, when trying to answer questions on processes and controls (e.g. the response of CO_2 flux from soil to changing soil temperature conditions), gap-filling should be avoided (Foken et al., 2004).

Only when eddy covariance systems are set up above surfaces that have no active autotrophs that fix CO_2 (GPP = 0), do they give a direct measurement of soil respiration. This could be either above bare soil surfaces (Billesbach et al., 2004; Dugas, 1993; Ham and Heilman, 2003; Leuning et al., 1982; Ono et al., 2007), or above ecosystems at times when plants have senesced. However, most EC systems are set up in vegetated environments and EC provides only indirect measurements of soil respiration (Luo and Zhou, 2006). This is because EC measures the net ecosystem exchange of CO_2 (NEE) and not the respiration directly. NEE is the sum of many processes as outlined in Section 2.4.2 and Figure 2.3. During the day, NEE is the sum of photosynthesis (GPP) and ecosystem respiration (ER) and non-respiratory CO_2 losses, while at night, NEE equals ecosystem respiration plus non-respiratory CO_2 losses. To obtain estimates of ER from NEE measurements, it is generally assumed that the non-respiratory CO_2 losses are negligible so that the night-time values of [–NEE] equal ER. It is common practice to fit a regression model to these night-time measurements (for example using soil temperature) and this model of ER is then used to model ER during the day (Desai et al., 2008; Falge et al., 2002; Reichstein et al., 2005a). Another approach to estimate daytime ER is extrapolating the relationship between daytime NEE and solar irradiance to night-time conditions (when irradiance = 0, see e.g. Falge et al., 2002; Gilmanov et al., 2007; Suyker and Verma, 2001; Wohlfahrt et al., 2005; Xu and Baldocchi, 2004).

Comparison studies between chambers and eddy covariance

Because the conclusions drawn in Chapter 4 rely heavily on the comparison of CO_2 fluxes obtained using a chamber with CO_2 fluxes obtained using the eddy covariance technique, a brief overview of studies will be given that focuses on comparing the chamber and eddy covariance methods.

In ecosystems without plants, the measured CO_2 flux is the result of only heterotrophic respiration (HR) and abiotic decomposition (AD), and CO_2 fluxes measurement by EC (NEE_{EC}) and chamber (NEE_{CH}) are assumed to be comparable during the day and night. Only in a few instances have CO_2 fluxes from micrometeorological methods and chamber systems been compared above bare surfaces. Kabwe et al. (2005) measured NEE above a uranium mine in Canada and found that NEE_{EC} flux was 12 % smaller than NEE_{CH}. Dugas (1993) found good agreement between BREB and a chamber with the average fluxes for BREB and chamber over four days differing by less than 10%. Ham and Heilman (2003) also found only a small difference between EC and a chamber system. They measured for 7 days over a parking lot where only very small CO_2 fluxes were expected and CO_2 fluxes of the two systems were generally within 0.26 µmol CO_2 m^{-2} s^{-1}.

In vegetated ecosystems, night-time measurements from chamber and EC can be compared if respiration by above-ground biomass is taken into account as well. Studies comparing night-time EC and chamber measurements of CO_2 losses show mixed results. Some studies demonstrated that reasonable agreement could be reached between the two measurement techniques (e.g. Laine et al., 2006; Tang et al., 2008) whereas other studies detected discrepancies (Baldocchi, 2003; Loescher et al., 2006). When measurements from the two methods did not agree, it was usually the EC values that were lower than the chamber values. The underestimation of EC fluxes compared to chamber fluxes can be quite substantial, for example 35% (Goulden et al., 1996), 32% (Kominami et al., 2003), 27% (Lavigne et al., 1997), 41%(Subke and Tenhunen, 2004) or 50% (Bolstad et al., 2004; Law et al., 1999). One of the several possible causes (Davidson et al., 2002; Drewitt et al., 2002; Goulden et al., 1996; Lavigne et al., 1997; Wohlfahrt et al., 2005) often mentioned for this observed difference

was the underestimation of EC fluxes caused by stable atmospheric conditions (Drewitt et al., 2002; Goulden et al., 1996; Lavigne et al., 1997).

2.5.2. Methods to measure decomposition

In this study soil respiration rates will at times be compared to decomposition rates measured in other studies. One of the most commonly used methods to measure decomposition rates is mass loss in litter bags (Kurz-Besson et al., 2005). When using litter bags to determine decomposition, bags made with a suitable mesh size are filled with litter and either buried in the soil or laid on the soil. At regular sampling times, some of the bags are collected and analysed for remaining mass. Decomposition rates are calculated based on the decrease of the dry mass over time (Karberg et al., 2008).

The litter-bag method has a number of drawbacks: the bag might affect the micro-climate and thereby decomposition rates, parts of the litter might be fragmented and carried out of the bag by soil fauna or fall through the mesh. Or, if the mesh is too fine, part of the soil macro fauna might be excluded (Karberg et al., 2008). The duration of the experiment must be decided beforehand based on expected, but unknown, decomposition rates (Kurz-Besson et al., 2005). Despite these limitations, the use of the litter bag method is widespread because it is inexpensive and easy.

When comparing soil respiration rates with mass loss rates, one needs to keep in mind that mass loss = respiration of CO_2 + leaching of DIC and DOC and other mineralised compounds (e.g. NO_3). This means that if leaching is not negligible, mass loss will not be equal to measured respiration (e.g. Cotrufo et al., 2008).

2.6 Microbial respiration within bare peatlands

The body of literature on soil respiration and microbial respiration of soil organic matter is very large[1] and a multitude of review papers and textbooks are available on these topics (Davidson and Janssens, 2006; Hibbard et al., 2005; Kirschbaum, 2000; Luo and Zhou, 2006; Pendall et al., 2004; Raich and Potter, 1995; Rustad et al., 2001; Ryan and Law, 2005). This section is by no means a comprehensive review of microbial respiration: its main purpose is to provide a very broad overview of existing knowledge and principles. Because this thesis examines microbial respiration at a bare peatland, this review will aim to focus on studies into respiration of drained peatlands, and where possible, peat mines.

Microbial respiration has been shown to be affected by many factors: substrate availability (and therefore carbon inputs from vegetation; Bahn et al., 2008; J. Curiel et al., 2007; Janssens et al., 2001; Raich and Tufekciogul, 2000; Ryan and Law, 2005; Tang et al., 2005), oxygen availability (Davidson and Janssens, 2006; Glatzel et al., 2004; Moore and Dalva, 1997; Waddington et al., 2001), moisture content (Gaumont-Guay et al., 2006; Orchard and Cook, 1983), nutrient availability (Bridgham and Richardson, 2003; Manning et al., 2008), temperature (Davidson et al., 2006a; Kirschbaum, 2006; Lloyd and Taylor, 1994; Reichstein et al., 2005c), substrate quality (Berg and McClaugherty, 2008; Hogg et al., 1992; Luo and Zhou, 2006; Swift et al., 1979), pH (Aciego Pietri and Brookes, 2008; Laiho, 2006), depth (Davidson et al., 2006b; Salomé et al., 2010) and microbial community composition (Balser and Wixon, 2009; Moorhead and Sinsabaugh, 2006; Steinweg et al., 2008; van der Wal et al., 2006). However, the main controls of microbial respiration in peat are temperature, soil moisture content and substrate quality (Davidson et al., 2006b; Jauhiainen et al., 2005; Moore et al., 1998). In this review, emphasis is put on the control of temperature and moisture on microbial respiration rates, because this is the focus of Chapter 6.

[1] A search on the ISI Web of Science website using keyword “soil respiration” resulted in 2,285 papers (12 Apr 2010)

2.6.1. Controls of microbial respiration

Temperature

The temperature sensitivity of soil respiration has recently received substantial attention because of its importance in determining how soil carbon stocks might change in response to global warming (Davidson and Janssens, 2006; Kirschbaum, 2006). The rate of microbial decomposition (and thus respiration), like that of any biochemical process, tends to increase with increasing temperature. Many studies have confirmed that CO_2 production from soils increased with increasing temperature, also in peatlands (Blodau et al., 2007; Dorrepaal et al., 2009; Hogg et al., 1992; Maljanen et al., 2002; Moore and Dalva, 1993; Petrone et al., 2003; Silvola et al., 1996; Updegraff et al., 2004; Waddington and Warner, 2001).

Increasing temperatures not only enhance microbial activity, but also cause an increase in the diffusion rates of gases (O_2 and CO_2) and solutes, which further increases microbial activity (Davidson et al., 2006a).

Temperature sensitivity is often expressed in terms of the Q_{10} value: the factor by which the rate of decomposition increases with a 10°C increase in temperature (Davidson et al., 2006a; Fierer et al., 2005b; Luo and Zhou, 2006). This value is expected to be around 2, i.e. a doubling of respiration rate is expected when temperature increases by 10°C. Several researchers have shown that the temperature sensitivity (Q_{10}) of decomposition rates decreased with increasing temperature (Dalias et al., 2001; Kirschbaum, 1995; Lloyd and Taylor, 1994; Xiang and Freeman, 2009). Davidson and others (Davidson et al., 1998; Davidson et al., 2006a) suggested that if temperature sensitivity is much larger than 2, there are other drivers confounding the temperature response. When using time series of *in situ* measurements to determine the temperature sensitivity, factors like root respiration (Boone et al., 1998; Schindlbacher et al., 2008), co-varying substrate supply (for example seasonal growth dynamics; Gu et al., 2004; Moyano et al., 2007; Reichstein et al., 2005a) and moisture conditions (Davidson et al., 1998; Reichstein et al., 2002) can confound the sensitivity of soil respiration to changes in temperature (Kirschbaum, 2000). Similarly in laboratory

incubations, changes in substrate availability can vary over time if depletion of labile OM occurs (e.g. Reichstein et al., 2000; Rey and Jarvis, 2006).

Moisture and oxygen availability

Pores in soils are either filled with air or water (Luo and Zhou, 2006). The air-filled pores allow diffusion of oxygen from the atmosphere to the reaction microsites, enabling aerobic decomposition by microbes (Davidson et al., 2000). Diffusion of CO_2 through the air-filled pores is the main process transporting the produced CO_2 from the microbial microsites to the soil surface. The water films in pores allow microbial mobility, diffusion of carbon substrate to the microbes, and diffusion of extracellular enzymes produced by the microbes to break down OM (Davidson et al., 2006a; Davidson et al., 2000; Luo and Zhou, 2006).

When the moisture content exceeds optimal levels, microbial activity – and thus soil respiration – may be inhibited (Davidson and Janssens, 2006; Davidson et al., 2000; Fang and Moncrieff, 1999) because the diffusion rate of oxygen is much lower in water than in air (Luo and Zhou, 2006). Low oxygen levels form the main limiting factor for microbial decomposition in water-logged ecosystems like wetlands (Clymo, 1984; Davidson and Janssens, 2006; Joosten and Clarke, 2002). Under those conditions, aerobic microbial activity is suppressed and often only anaerobic respiration takes place, generally resulting in much lower CO_2 production rates than respiration under aerobic conditions (Davidson and Janssens, 2006; Glatzel et al., 2004; Moore and Dalva, 1997; Waddington et al., 2001 and references therein). As a result, respiration rates measured in peatlands under waterlogged conditions are generally less than rates observed when (part of) the peat column is above the water table (Glatzel et al., 2006; McNeil and Waddington, 2003; Waddington et al., 2002) . For example, a comparison of CO_2 effluxes during three summer months from two abandoned mined peatlands for a wet and a dry summer showed the that decomposition in wetter peat was inhibited by as much as 73%, even when the average water table was only approximately 62 mm shallower during the wet summer compared to the dry summer (Waddington et al., 2002). Spatial differences in CO_2 efflux within a single wetland have also been explained by

differences in water table depth and moisture content, with wet locations releasing less CO_2 than moderately dry locations (Glatzel et al., 2006; McNeil and Waddington, 2003). Many studies examining the effect of drainage of peatlands have observed a large increase in CO_2 efflux as a result of water table drawdown because of an increase in the thickness of the aerated layer (Freeman et al., 1993; Jauhiainen et al., 2005; Laiho, 2006; Moore and Dalva, 1993; Moore and Knowles, 1989; Silvola et al., 1996).

When the moisture content is below optimal levels, diffusion of substrate through soil water to the micro sites is inhibited, leading to low substrate supply to the microbes (Davidson and Janssens, 2006; Luo and Zhou, 2006), thereby limiting decomposition. Lowered soil moisture can also cause direct physiological changes in microbes (Luo and Zhou, 2006; Schimel et al., 2007). For example during drought, low moisture conditions can inhibit metabolic activity of soil microorganisms (Fang and Moncrieff, 1999) and induce cell dehydration, dormancy (Luo and Zhou, 2006) or death. Dormancy can lead to substantial decreases in respiration (Luo and Zhou, 2006; Schimel et al., 2007). Incubation studies of peat have confirmed that low moisture contents can indeed inhibit CO_2 production potential from peat (e.g. Glatzel et al., 2006; Waddington et al., 2001). Field measurements on mineral soils during periods of drought confirm that soil respiration was generally limited compared to respiration during wetter seasons (e.g. Mudge, 2009; Reichstein et al., 2002; Xu and Baldocchi, 2004) . In contrast, these limiting effects of low moisture levels on soil respiration are not commonly observed in the field in peat soils. The main difference between peat soils and mineral soils is that mineral soils tend to contain more organic matter in the top horizon compared to lower horizons (Jobbagy and Jackson, 2000), and most of the CO_2 is produced in the upper layers of the soil (Davidson et al., 2006b; Hirano et al., 2003) which are most affected by drought. In contrast, peatlands have very high levels of organic matter throughout the peat profile. The total CO_2 efflux measured at the peat surface is the sum of all CO_2 produced throughout the peat profile (Davidson et al., 2006b; Graf et al., 2008). Because low moisture levels at the peat surface are commonly accompanied by low water tables leading to a deeper layer of peat being aerated, measured CO_2 effluxes

tend to increase rather than decrease when the surface peat dries out because a deeper layer of peat is contributing to the total CO_2 flux measured between the surface peat and the atmosphere.

Filling pore spaces with water as a result of rainfall might lead to increases or decreases in CO_2 fluxes between the soil surface and atmosphere, even when production remains constant (Ryan and Law, 2005). Rainfall can displace air with high concentrations of stored CO_2 (i.e. mass flow instead of diffusion) resulting in a peak in the measured CO_2 flux (Eriksen and Jensen, 2001; Luo and Zhou, 2006; Reicosky et al., 1999; Ryan and Law, 2005). Alternatively, water from rainfall can also result in a decrease in CO_2 flux (Buchmann et al., 1997; Hirano et al., 2003) because the diffusivity of CO_2 in water is about 10,000 times smaller than in air (Fang and Moncrieff, 1999).

Substrate quality

Soil organic matter (SOM) is a mixture of assorted materials, some of which are still recognisable as plant or animals parts, and some of which are altered to the degree that the origin of the OM cannot be distinguished (humus; Amundson, 2001; Luo and Zhou, 2006). These constituents vary in age, chemical composition and 'substrate quality' (Trumbore, 2006). The terms 'substrate quality', 'decomposability', 'recalcitrance' and 'stability' (Leinweber et al., 2008) are all used to describe how decomposable OM is by microbial populations.

Soluble and non-soluble carbohydrates are most labile (= most easily degradable) and these substrates are therefore decomposed by microbes in the early stages of decomposition (Luo and Zhou, 2006; Swift et al., 1979). This pool with fast turnover times is generally small compared to the other pools (Berg, 2000; Trumbore, 2006). Hemicellulose and α-cellulose are degraded at a slower rate, and lignin, humic acids and phenolic compounds are typically the compounds to display the slowest decomposition rates (Berg and McClaugherty, 2008; Luo and Zhou, 2006; Swift et al., 1979). Most of the carbon stored in soils resides in what is called the 'slow or recalcitrant pool' with long turnover times (Trumbore, 2006). Decomposition of this hummified carbon is slow because microbes obtain little energy from it (Fontaine et al., 2003).

'Litter quality' or 'recalcitrance' as such cannot be easily determined and they are often approximated by a range of different metrics (Bosatta and Ågren, 1999), for example initial nitrogen concentration (e.g. Berg et al., 1982; Parton and Silver, 2007), C/N ratio (e.g. Webster et al., 2009), lignin concentration (e.g. Melillo and Aber, 1982; Taylor et al., 1989).

At any given moment, the slow pool contributes only a small amount of carbon to the total CO_2 flux (Trumbore, 2000), and it is this large recalcitrant pool which is most important for the storage of carbon in soil (Trumbore, 2006). Generally, if plants are not available to add labile OM to the OM pool, decomposition rates decrease over time as the concentration of easily decomposable compounds decreases, and the more recalcitrant OM, with low decomposition rates, remains (Berg, 2000; Berg and McClaugherty, 2008; Swift et al., 1979).

In peatlands, CO_2 production has been found to be negatively correlated to the Von Post humification index (Glatzel et al., 2004; Glatzel et al., 2006). The Von Post index of peat is determined by a qualitative squeeze test in the field which classes the peat in different stages of humification (and references therein Andriesse, 1988; Klavins et al., 2008). Larger values for the humification index indicate a higher degree of decomposition.

The Von Post humification index tends to increase with depth (Glatzel et al., 2006; Waddington et al., 2002) and substrate quality of peat has often been assumed to decrease with depth (Glatzel et al., 2006; Waddington et al., 2001). Incubation of peat from different depths revealed that CO_2 production potential decreased with depth, even when incubated under common temperature and moisture content (Glatzel et al., 2006; Hogg et al., 1992; Waddington et al., 2001). However, this trend is not always observed (Stewart and Wheatly, 1990). Likely causes for this decrease of decomposability with depth are the lower input of labile organic compounds from living plant tissue (Waddington et al., 2002) and the relative accumulation of recalcitrant compounds like lignin, phenolic compounds and humic substances after the labile compounds have been decomposed over time (Hogg et al., 1992 and references therein). The temperature sensitivity of decomposition rates has been hypothesized to

increase with decreased organic matter quality (Hartley and Ineson, 2008; Knorr et al., 2005), as would be expected from kinetic theory (Bosatta and Ågren, 1999; Davidson and Janssens, 2006). This would mean, for example, that decomposition of relatively stable OM in deeper soil layers might be more sensitive to changes in temperature than more labile OM in the surface layers (Fierer et al., 2003; Jin et al., 2008; but see Reichstein et al., 2005b). However, no consensus has been reached and the difference in temperature sensitivity between labile and recalcitrant OM is still a topic of debate (Conant et al., 2008; Davidson and Janssens, 2006; Fang et al., 2005; Fierer et al., 2005b; Fontaine et al., 2007; Giardina and Ryan, 2000; Liski et al., 1999; Reichstein et al., 2005c; Wetterstedt et al., 2009).

2.6.2. Rates of respiration from bare peat

Table 2.3 lists a number of studies examining respiration rates from bare peatlands in the Northern Hemisphere. Many of these studies only measured respiration rates during summer. Average soil respiration rates ranged from 0.17 to 7.2 g C m^{-2} d^{-1}, with the majority of the measured rates being less than 3.5 g C m^{-2} d^{-1} (Table 2.3). These values fall in the lower half of the range of values reported by Roehm (2005), who reported a global average of 7.2 g C m^{-2} d^{-1} and 4.8 g C m^{-2} d^{-1} for vegetated peatland ecosystems in temperate and boreal areas, respectively.

Table 2.3 Summary of mean soil respiration from bare peat soils.

Reference	Site	Vegetation	Location	Depth of peat (m)	Measurement method	Time span of measurements	DWT (mm)	*T* at 5 cm (°C)	Peat respiration (g C $m^{-2}d^{-1}$)
Berglund (1989) as cited in Nykänen et al. (1995)	Cultivated peat soil	n/a	Southern Sweden	n/a	n/a	n/a	n/a	n/a	1.2
Maljanen et al. (2002)	Bare organic soil	0% cover	Finland	0.2	Opaque static chambers	Mean during summer	-800	n/a	7.2
McNeil and Waddington (2003)	Abandoned (>30 yrs) cut-over peatland	some	Canada	Up to 4	Opaque chamber	Mean over 3 summer months	-254	14.2	0.91
Nykänen et al. (1996)	3 peat mining areas	0% cover	Finland	n/a	Static chamber	Mean over two years	~-600	n/a	0.66
Nykänen et al. (1995)	Drained fen (>60 yr), used for agriculture	0% cover	Finland	1.4	Closed chamber	Mean over two years	-200 to -1170	n/a	1.12
Tuittila et al. (1999)	Abandoned cut-away peatland	0% cover	Finland	1	Closed chamber	May – Nov for 3 years	-380	n/a	1.5
Sundh et al. (2000)	8 sites in 6 drained peatlands	some	Sweden	n/a	Syringe from chamber	Jun-Sep 1995	n/a	n/a	0.39 / 0.54/ 0.48 /0.17/ 0.39/ 0.30 / 0.76/ 0.35
Waddington and Warner (2001)	Abandoned cutover peatland 7	5 % cover	Canada	1.7	Closed chamber	May-Aug '98	-351	16.6	3.49
	Cutover and abandoned peatland	0% cover	Canada	n/a	Closed chamber	May-Aug '98			3.49
Waddington et al. (2002)	Cutover and abandoned peatland	5%	Canada	1.8	Closed chamber	May-Aug '98	-306	14.7	3.19
	Cutover and abandoned peatland	5 % cover	Canada	1.7	Closed chamber	May-Aug '99	-305	15.8 (at 10cm)	1.01
	Cutover and abandoned peatland	5%	Canada	1.8	Closed chamber	May-Aug '99 (wet)	-351	15.7 (at 10 cm)	0.79
Waddington et al. (2003)	Cutover peatland	n/a	Canada	n/a	EC	Mean May-Oct 2001	n/a	15.1	2.49-3.49
Waddington and McNeil (2002)	Abandoned peat mine invaded	some	Canada	n/a	Closed chamber	Mean between May – Oct 2001	-527	10.3	2.2

n/a = not available

2.6.3. Models of respiration

Many different models have been developed to explain the temporal variation of CO_2 efflux from soils. Whereas some studies have ventured into the development of mechanistic models which aim to represent the processes of the decomposition process (e.g. those listed in Shibu et al. (2006) like RothC (Coleman and Jenkinson, 2008; Jenkinson et al., 1990) and CENTURY (Parton et al., 2001; Parton et al., 1987)), the majority of respiration models are based on empirical regression analyses which describe the effect of temperature and moisture on the CO_2 efflux (Fang and Moncrieff, 2001; Kirschbaum, 2000; Richardson et al., 2006a; Tuomi et al., 2008).

Models for temperature

The simplest model used for predicting respiration as a function of temperature is the linear model (Raich and Potter, 1995; Rochette et al., 1991; Wofsy et al., 1993):

$$HR = a + bT \qquad \textbf{Equation 2.3}$$

where HR is the CO_2 efflux (µmol CO_2 m^{-2} s^{-1}) of microbial origin (heterotrophic respiration), *T* the peat temperature (°C) and *a* and *b* are fitted parameters.

However, most studies use some sort of exponential equation based on kinetics to model the effect of temperature on respiration rates. One of the simplest, but very commonly used models that describes the response of respiration to temperature is the exponential model, first proposed by Van 't Hoff (1884) to describe the response of chemical reactions to changes in temperature:

$$HR = \alpha e^{\beta T} \qquad \textbf{Equation 2.4}$$

where α is the soil respiration rate at 0°C and β is the temperature sensitivity parameter (°C^{-1}). The temperature sensitivity is often expressed in terms of the Q_{10} value: the factor which the rate of decomposition will increase

by over a 10°C increase in temperature (Fierer et al., 2005b; Luo and Zhou, 2006). The Q_{10} can be calculated using the above regression using $Q_{10} = e^{10 \cdot \beta}$.

Based on the exponential model of Van 't Hoff (1884), Arrhenius (1889) presented a model to describe how the reaction rate for biochemical processes (like microbial respiration) depends on temperature as follows:

$$k = Ae^{\frac{-E_a}{RT}} \qquad \textbf{(Equation 2.5)}$$

where k is the reaction rate constant (mol m^{-3} s^{-1}) , A is a frequency or pre-exponential factor (the theoretical reaction rate constant in the absence of activation energy (Davidson and Janssens (2006); mol m^{-3} s^{-1}), E_a is the required activation energy (i.e. the minimum energy required for a specific chemical reaction to occur (Luo and Zhou, 2006) in J mol^{-1}), R is the gas constant (8.314 J mol^{-1} K^{-1}) and T is the temperature in Kelvin. Davidson and Janssens (2006) describe the term $e^{\frac{-E_a}{RT}}$ as "the fraction of molecules present with energies equal or in excess of the required activation energy". The Arrhenius model (in contrast to the Van 't Hoff model) correctly describes the decrease in Q_{10} with increasing temperature (Davidson and Janssens, 2006), which has been confirmed by some experiments (Dalias et al., 2001; Kirschbaum, 1995; Tjoelker et al., 2001; Xiang and Freeman, 2009). Also, the model predicts that substrates that are more recalcitrant (i.e. with higher activation energies) are predicted to have higher sensitivities to temperature changes (Bosatta and Ågren, 1999; Davidson and Janssens, 2006; but see discussion in Section 2.6.1 about the controversy surrounding this topic).

Lloyd and Taylor (1994) compared the performance of several respiration models using data collected at 15 sites over a range of ecosystems. They found that the assumption made by the Arrhenius model, that the activation energy is constant with temperature, was incorrect. In the same study, they found that the Arrhenius equation resulted in a biased distribution of the residuals, meaning that it systematically underestimated respiration rates at low temperatures and overestimated respiration rates at high temperatures (Lloyd and Taylor, 1994). In

response to these inadequacies in the model described by Arrhenius, Lloyd and Taylor (1994) developed a modified Arrhenius function which is now one of the most commonly used models for soil respiration. This model allows the effective activation energy to vary according to temperature, with higher temperatures leading to lower effective activation energies. The general form of the Lloyd and Taylor (referred to as LT hereafter) equation can be written as (Luo and Zhou, 2006)

$$R = R_{\text{ref}} e^{E_0\left(\frac{1}{T_{\text{ref}} - T_0} - \frac{1}{T - T_0}\right)} \qquad \textbf{(Equation 2.6)}$$

where R_{ref} is the respiration rate at a reference temperature, E_0 is an empirical coefficient related to the activation energy (K), T_{ref} is the reference temperature, T_0 is the lowest temperature at which respiration can occur (Luo and Zhou, 2006). Regression analysis can be used to determine R_{ref}, E_0 and T_0.

In models describing ecosystems CO_2 exchange, both the simple exponential model and the Lloyd and Taylor model are very commonly used to model soil respiration rates, for example to aid partitioning of the daytime net ecosystem exchange into respiration and photosynthesis (e.g. Falge et al., 2002; Lasslop et al., 2009).

Models for moisture conditions

Various models incorporating moisture can be found in the literature using gravimetric moisture content, volumetric moisture content, water filled pore space, depth to water table, matrix potential, and percentage of water holding capacity (Davidson et al., 2000; Luo and Zhou, 2006). In addition, different kinds of equations are used as well (Davidson et al., 2000; Luo and Zhou, 2006; Richardson et al., 2006a): for example linear (Waddington and Warner, 2001), exponential (Silvola et al., 1996) and quadratic. In contrast to general consensus around the approach for modelling the effect of temperature on respiration rates, there is no consensus about the best way to model the effect of moisture and models tend to vary from study to study (Davidson et al., 2000; Luo and Zhou, 2006).

2.7 Photodegradation

In mesic ecosystems (i.e. systems with intermediate moisture conditions, neither humid nor dry), litter decomposition is controlled mostly by moisture, temperature and substrate quality and mass loss can be predicted reasonably well using decomposition models that predict mass loss using these drivers (Meentemeyer, 1978; Parton and Silver, 2007; Raich and Schlesinger, 1992). However, these commonly used decomposition models assume that microbial decomposition is the sole contributor to mass loss and they are unable to predict the high rates of mass loss measured in arid and semi-arid ecosystems (Parton and Silver, 2007; Vanderbilt et al., 2008).

Several studies on mass loss in arid regions have concluded that the measured mass loss could not be sufficiently explained by temperature, moisture and substrate quality (e.g. Meentemeyer, 1978; Montana et al., 1988; Parton and Silver, 2007; Whitford et al., 1981). In central New Mexico, Vanderbilt (2008) found that neither precipitation nor litter quality were major controls of litter decomposition in a 10-year decomposition study in four different arid and semi-arid ecosystems. Although shading and watering litter bags in the Chihuahuan Desert decreased temperature and increased the moisture content and the number of microarthropods, treatments had no effect on mass loss (Mackay et al., 1986). Even after applying biocides to eliminate all organisms, mass loss was still detected on semi-arid sites in Colorado, New Mexico and Argentina when litter was exposed to sunlight (Austin and Vivanco, 2006; Mackay et al., 1986; Vossbrinck et al., 1979), but not when litter was buried 5 cm beneath the soil surface (Moorhead and Reynolds, 1989). Contrary to expectations, Schaefer (1985) found that, in New Mexico, substrates with the highest lignin content were the fastest to decompose (see also Figure 1 in Moorhead and Callaghan, 1994). This is contrary to established understanding, which is that lignin is typically most recalcitrant to microbial decomposition and slowest to decompose (Berg, 2000; Berg and McClaugherty, 2008; Swift et al., 1979). As part of a large cross-site comparison study of decomposition rates, Parton and Silver (2007) found unexpected high rates of decomposition of leaf litter in arid ecosystems. Mass loss during the later stages of decomposition equalled those of humid

ecosystems, there was no indication of nitrogen immobilisation (indicative of microbial decomposition; Swift et al., 1979), and the high decomposition rates found in leaves were not found in roots that were not exposed to solar radiation.

The results of all these studies suggest that decomposition in drylands might be controlled by different drivers than decomposition in mesic ecosystems and that mechanisms responsible for decomposition in dry regions might be very different from those in mesic regions.

Pauli (1964) was possibly the first to suggest that photochemical processes, brought about by the high levels of solar irradiance in most arid and semi-arid regions, might contribute to the degradation of organic material. Since then, manipulative studies have been conducted that tested hypotheses regarding the breakdown of organic matter by solar irradiance.

This degradation by sunlight, or *photodegradation*, is a large area of research, but studies have mostly focussed on photodegradation of OM in aquatic ecosystems (Moran and Zepp, 1997; Osburn and Morris, 2003; Zepp, 2003; Zepp et al., 2007), and of materials and substances like wood (Derbyshire et al., 1997; George et al., 2005), paper (Kelly and Williams, 1981; Moorhead and Reynolds, 1989), plastics (Andrady et al., 2007; Fernando et al., 2009; Torikai and Hasegawa, 1999), paint (Christensen et al., 1999; Smith et al., 2001) and pesticides (Katagi, 2004; Pirisi et al., 1996). Very little is known about photodegradation of organic matter in terrestrial ecosystems and studies in this area of research have only recently been conducted (e.g. Austin and Vivanco, 2006; Brandt et al., 2009; Brandt et al., 2007; Day et al., 2007; Gallo et al., 2009; Gallo et al., 2006; Smith et al., 2010; Throop and Archer, 2009)

This section reports on the current state of knowledge on photodegradation of organic matter in terrestrial ecosystems. Several studies have reported that solar irradiance can control decomposition *indirectly*: they found that solar irradiance (especially that in the UV-B wavelength bands) applied during plant growth affected subsequent decomposition (e.g. Duguay and Klironomos, 2000; Gehrke et al., 1995; Newsham et al., 1999; Pancotto et al., 2003; Rozema et al., 1997b; Verhoef et al., 2000). However, the current review will only focus on the mechanisms whereby solar irradiance *directly* contributes

to or inhibits decomposition, which are summarised in Section 2.7.2. Methods that are used to measure photodegradation are described in Section 2.7.1. The measured rates of photodegradation are summarised in Section 2.7.3 and the controls of photodegradation are discussed in Section 2.7.4. Studies measuring both mass loss and CO_2 emissions are discussed; however emphasis is put on the studies focussing on CO_2 losses.

For other review papers on photodegradation the reader is referred to Moorhead and Callaghan (1994), Liu (2004), Throop and Archer (2009) and Smith et al. (2009).

2.7.1. Methods to measure photodegradation

Supplementation and exclusion studies

Manipulative experiments on the effect of irradiance on decomposition can be divided based on the approach that is taken to establish different treatments with respect to radiation: irradiance is either (partly) blocked in *exclusion* studies or added in *supplementation* studies.

In exclusion studies, rates of decomposition of litter under filters that exclude or attenuate parts of the solar spectrum ("block treatment", e.g. using a Mylar-D film, DuPont Co., Wilmington, DE, USA) are compared to decomposition rates under filters that are transparent for radiation of all wavelengths ("pass treatment", e.g. using an Aclar film, Aclar Fluoropolymer Film type 22A, Honeywell, Pottsville, PA, USA).

In supplementation studies, lamps are used to irradiate litter with different levels of radiation of chosen wavelengths. Often, litter is irradiated with UV-A and/or UV-B, with or without a background level of solar radiation.

There are many methodological challenges and issues with both exclusion and supplementation approaches, which are laid out clearly by Rozema et al. (1997d) and a review paper by Flint et al. (2003). One of the main issues with supplementation studies is the distribution of radiation along wavelengths when using lamps to irradiate organic matter. Ratios of wavelengths emitted by UV lamps used in supplementation studies (often used without background solar radiation) do not match the spectral irradiance of the sun (Caldwell and Flint,

1995). For example, UV lamps typically emit insufficient photosynthetically active radiation (PAR, irradiance with wavelengths between 400 and 700 nm, approximately equal to the wavelengths visible to the eye) compared to the solar spectrum (Rozema et al., 1997d). An unrealistic balance in UV-B, UV-A and PAR might lead to overestimation of the UV effects, as is shown in studies on plant damage by UV-B irradiance (Caldwell and Flint, 1997; Rozema et al., 1997d). Also, when comparing results of supplementation and exclusion studies, we have to keep in mind that in supplementation studies, the difference in irradiance intensity between treatments is usually smaller than for exclusion studies (Day et al., 2007).

Photodegradation determined using mass loss, CO_2 production and litter quality

Most studies focusing on photodegradation determine the effect of irradiance on mass loss of litter as a measure of decomposition. The most common method of measuring mass loss is by using litter bags (see Section 2.5.2). One of the additional challenges when using litter bags in high-radiation environments is that the mesh of the litter bags can degrade under the influence of irradiance (Vossbrinck et al., 1979) or block as much as 50% of the irradiance (e.g. Brandt et al., 2007; Pancotto et al., 2005). Different setups have been developed to avoid or minimize blocking the radiation before it reaches the litter: litter envelopes made of filter plastics (Day et al., 2007), specialized boxes (Austin and Vivanco, 2006), open top microcosms or litter rings (Gallo et al., 2006; Gehrke et al., 1995; Henry et al., 2008).

A few studies have measured CO_2 evolution from litter as a result of photodegradation (Anesio et al., 1999; Brandt et al., 2009; Cory et al., 2008; Duguay and Klironomos, 2000; Gehrke et al., 1995). This is usually done by irradiating litter in jars and measuring the CO_2 build-up in the jar over set intervals of at least 24 hours.

No studies so far have been able to detect both changes in mass loss and changes in CO_2 emissions as a result of photodegradation. Gehrke et al. (1995) measured neither a change in CO_2 emissions nor a change in mass loss when

exposing litter to UV-B over 62 days. Despite the fact that Duguay and Klironomos (2000) found that litter exposed to extra UV-B emitted 85% less CO_2 than litter in a control treatment, they did not measure a matching difference in mass loss between treatments. Brandt et al. (2009) also found a highly significant effect of exposure to solar radiation on CO_2 flux, but were not able to detect mass loss at all in any of the treatments. These results might indicate that the studies measuring both mass loss and CO_2 production resulting from photodegradation up till now have been too short (maximum study period was 10 weeks) to detect significant differences in mass loss. Consequently, for short-term studies, it might be more appropriate to estimate rates of photodegradation by measuring CO_2 production rather than mass loss.

In addition to mass loss, some studies have also measured the change in litter chemistry as a result of exposure to irradiance. This includes, for example, changes in lignin, holocellulose, hemicellulose, cell solubles, total organic C, total N, C:N ratio, fats and lipids (e.g. Brandt et al., 2007; Day et al., 2007; Gallo et al., 2006; Gehrke et al., 1995; Pancotto et al., 2003; Pancotto et al., 2005; Rozema et al., 1997b).

Studies under sterile conditions

To study the process of photochemical mineralisation separately from the other mechanisms through which solar irradiance can affect decomposition rates (see Section 2.7.2), some experiments have been conducted under sterile conditions (Anesio et al., 1999; Austin and Vivanco, 2006; Brandt et al., 2009). This is achieved by killing the microbes in the litter through application of biocides (Austin and Vivanco, 2006) or chemicals (Vossbrinck et al., 1979), autoclaving (Anesio et al., 1999; Smith et al., 2010), or microwaving (Smith et al., 2010). However, it is very challenging to conduct long-term studies in the absence of microbes because bacteria and fungi from outside the treated area will quickly re-colonise the treated litter. To prevent this, repeated treatments to eradicate microbes are necessary throughout the duration of a study (Austin and Vivanco, 2006; Smith et al., 2010).

2.7.2. Mechanisms whereby solar irradiance affects decomposition

Four mechanisms have been suggested that could affect the carbon losses from litter (or soil organic matter) under the direct influence of solar irradiance. Two of those are abiotic processes: photochemical mineralisation and leaching, while the other two involve microbes: biological facilitation and microbial inhibition. The four mechanisms will be discussed in the following sections and are summarised in Figure 2.5.

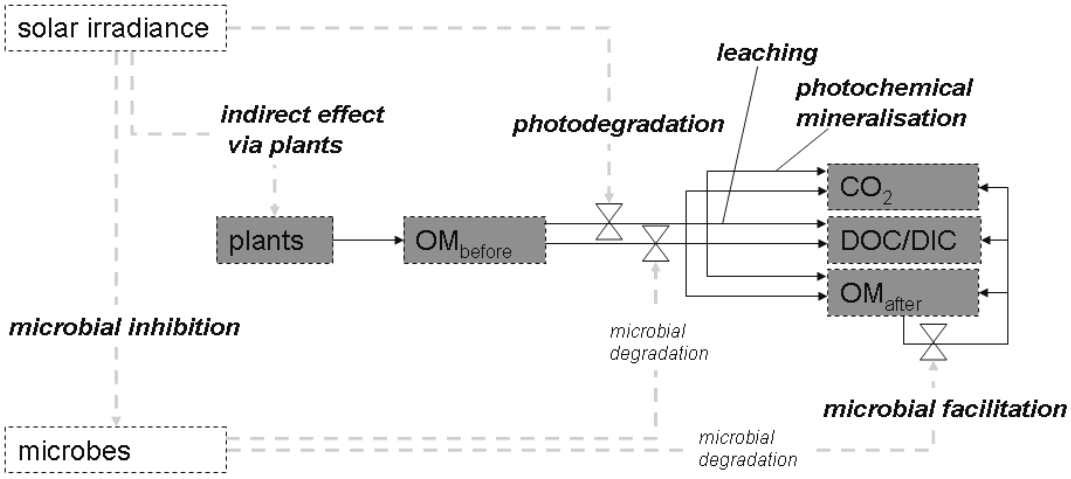

Figure 2.5 Diagram showing mechanisms by which solar irradiance can affect organic matter decomposition. Mechanisms are explained in Section 2.7.2 and subsections.

The energy contained in one photon is inversely proportional to the wavelength of the radiation: the shorter the wavelength, the more energy is held per photon (Anslyn and Dougherty, 2006; Atkins and de Paula, 2005; Klán and Wirz, 2009). Photons in the UV and visible region of the solar spectrum have enough energy per photon to break typical covalent bonds in organic molecules (Anslyn and Dougherty, 2006; Moorhead and Callaghan, 1994). Moorhead and Callaghan (1994) describe how by breaking of organic molecules, free radicals are formed which react with oxygen to form a peroxy radical after which a large number of reactions can happen involving these radicals. A large range of possible photoproducts can be formed (Moorhead and Callaghan, 1994).

Photochemical mineralisation to CO_2

One of the photoproducts of the photodegradation process is CO_2, with several studies confirming that irradiation can lead to the release of CO_2 from terrestrial organic matter (Anesio et al., 1999; Brandt et al., 2009; Cory et al., 2008; Gehrke et al., 1995). Other direct gaseous losses of carbon from litter can include carbon monoxide (Kisselle et al., 2002; Schade et al., 1999; Tarr et al., 1995; Yonemura et al., 1999) and methane (CH_4, Vigano et al., 2008). CO_2 emissions resulting from the photochemical oxidation of organic matter of litter in air were first measured by Anesio et al. (1999) under laboratory conditions. They irradiated sterile leaves with UV-A and UV-B radiation from lamps, thereby proving that UV radiation could directly cause CO_2 emissions in the absence of microbial organisms. Only recently, CO_2 evolution from litter has also been measured under ambient conditions of solar irradiance in Minnesota under sterile conditions in a jar (Brandt et al., 2009).

Leaching of DOC

UV radiation can cause changes in chemical composition of organic matter (Gehrke et al., 1995) through the breakdown of macromolecules into smaller molecules (Moorhead and Callaghan, 1994). This transformation of organic matter could affect litter solubility. Although this process has mostly been studied in aquatic systems (e.g. Denward and Tranvik, 1998; Vähätalo et al., 1998), a few studies have focused on leaching from terrestrial plant litter resulting from photodegradation with contradictory conclusions. Although Vossbrinck (1979) hypothesized that the large mass loss measured in the early stages of decomposition of sterile grass leaf litter on a shortgrass prairie was probably due to leaching, this had not been confirmed by measurements. Generally, no clear change in dissolved organic matter was observed after irradiation of OM with UV radiation (Brandt et al., 2009; Gallo et al., 2006; Gehrke et al., 1995). Brandt et al. (2009) hypothesised this was caused by the generally low contribution of leaching to mass loss in arid ecosystems and by the asynchronous nature of photodegradation and leaching: leaching can only occur during infrequent wet period when photodegradation is limited by cloud cover.

If leaching was a large contributing pathway for mass loss through photodegradation, we would expect the measured mass loss to be larger following infrequent rainfall events. However, apart from a few exceptions (Newsham et al., 1997; Vossbrinck et al., 1979), mass loss in dry ecosystems has usually been found to be linear with time (e.g. Parton and Silver, 2007). This might indicate that even though leaching might be a possible pathway for mass loss as a result of photodegradation (Gallo et al., 2006), it is probably not a major one.

Biological facilitation and priming

The change in chemical composition of the OM caused by photochemical transformation (called "phototransformation" by Zepp et al. (2007)) has been hypothesized to enhance microbial decomposition by increasing substrate availability (e.g. Gallo et al., 2009; Henry et al., 2008). Especially lignin and other phenolics, which are typically recalcitrant to microbial degradation, have been found to absorb strongly in the UV range of the spectrum (Day et al., 2007), possibly making them preferentially susceptible to photodegradation. Breakdown of lignin or other molecules with high aromaticity by radiation can make litter more labile (Day et al., 2007; Gallo et al., 2006; Henry et al., 2008) and therefore easier to decompose by microbes. This way, UV radiation can facilitate microbial decomposition (Brandt et al., 2009; Henry et al., 2008). Lignin is also known to protect a large fraction of cellulose in so-called lignocellulose complexes (Adair et al., 2008; Rozema et al., 1997b and references therein), which means that breakdown of lignin can increase the bioavailability of cellulose for microbes, thereby enhancing microbial decomposition (Henry et al., 2008). Similary, Day et al. (2007) hypothesised that if lignin in cell walls is broken down, fats and lipids from the cell could be released, and those compounds could then be available to microbes.

Several studies have confirmed that microbial decomposition was accelerated by radiation through the process of biological facilitation (Day et al., 2007; Gallo et al., 2009; Gallo et al., 2006; Henry et al., 2008), whereas others

were unable to find supporting evidence (Austin and Vivanco, 2006; Brandt et al., 2009).

Microbial inhibition

Investigation of the mechanism of microbial facilitation is difficult, because solar irradiance can also directly affect microbial activity. Terrestrial microbes are poorly protected from solar irradiance and many studies have shown that decomposer organisms are negatively affected by UV irradiation, either in activity, abundance or both, thereby reducing the contribution of microbial decomposition to total decomposition (e.g. Duguay and Klironomos, 2000; Pancotto et al., 2003).

Many studies have found negative effects of exposure to UV on the number of fungi (Austin and Vivanco, 2006; Brandt et al., 2009; Gehrke et al., 1995; Pancotto et al., 2003) and bacteria (Austin and Vivanco, 2006; Brandt et al., 2009). Negative effects of UV radiation on the number of microarthropods have also been found, for example in mites and Collembola (Convey et al., 2002; Verhoef et al., 2000). Not all microorganisms are equally susceptible to the negative effects of UV-B irradiance (Gehrke et al., 1995; Newsham et al., 1997). Duguay and Klironomos (2000) concluded that the five fungi species they compared differed in their tolerance to UV-B radiation, when they found that competition between different species altered as a result of exposure to increased UV-B. Moody et al. (2001) also found significant changes in the fungal community structure, with some species increasing and others decreasing. Verhoef et al. (2000) found that microarthropods like Collembola were also differentially sensitive to exposure to UV radiation. Pigmentation has been put forward as a possible explanation for more tolerant fungal species, whereby pigments might provide protection against UV-B (Verhoef et al., 2000). However, studies into this potential control are not conclusive (Duguay and Klironomos, 2000). Even though some species of micro-organisms seem less susceptible to detrimental effect of UV-B radiation, and their number might increase during exposure to radiation (Moody et al., 2001; Newsham et al., 1997), the general

trend seems to be that exposure to UV irradiance lowers the abundance of bacteria and fungi.

2.7.3. Rates of photodegradation

Overview of photodegradation rates

As explained in Section 2.7.2, solar irradiance can affect decomposition in two opposite directions: it can increase decomposition rates by increasing photochemical degradation and microbial facilitation (and to a lesser extent increase solubility and therefore leaching), and it can decrease rates of decomposition by decreasing microbial abundance and activity. This multitude of mechanisms through which irradiance can affect decomposition rates makes it hard to measure the contribution of the individual mechanisms to the total loss of mass or CO_2 and to predict what the net effect of exposure to irradiance will be. This is illustrated by the wide range of responses of mass loss and CO_2 emissions from organic matter exposed to (sun) light under non-sterile conditions (Table 2.4), with studies reporting

- an increase in the rate of mass loss (Austin and Vivanco, 2006; Brandt et al., 2007; Cory et al., 2008; Day et al., 2007; Gallo et al., 2009; Henry et al., 2008; Rozema et al., 1997b) and CO_2 loss (Anesio et al., 1999; Brandt et al., 2009) in response to exposure of OM to irradiance
- no significant response of mass loss (Gallo et al., 2006; Moody et al., 2001; Newsham et al., 1997; Pancotto et al., 2005; Verhoef et al., 2000) and CO_2 loss (Gehrke et al., 1995) in response to exposure of OM to irradiance, and
- a decrease in the rate of mass loss (Moody et al., 2001; Pancotto et al., 2003) and CO_2 loss (Duguay and Klironomos, 2000) in response to exposure of OM to irradiance

Table 2.4 Overview of photodegradation studies reporting a stimulating, nil or inhibiting response of mass loss of OM and CO_2 production from OM to exposure to irradiance.

	Mass loss studies			CO_2 studies		
	stimulating	nil	inhibiting	stimulating	nil	inhibiting
Exclusion studies						
Exclude UV-B	+33% Aus +14-22% Day +11% Pan05		-14-20% Pan03	+31% Bra09		
Exclude UV-AB	+0 – 25% Bra07	Bra07		+49% Bra09		
Exclude all	+60% Aus +46-100% Gal09 +27-46 % Hen	Hen		+94% Bra09		
Supplementation studies						
Add UV-B	+2 - 10% Roz +500% Smi (dry)	Ver New Geh Geh Moo01	n/a Moo01 -22% Dug -23% Smi (wet)	+31% Ane	Geh	-85% Dug
Add UV-AB		Gal06 New Ver		+46% Ane +90% Bra09 +89% Bra09		

Ane = (Anesio et al., 1999), Aus = (Austin and Vivanco, 2006), Bra07 = (Brandt et al., 2007), Bra09 = (Brandt et al., 2009), Day = (Day et al., 2007), Dug = (Duguay and Klironomos, 2000), Gal06 = (Gallo et al., 2006), Gal09 = (Gallo et al., 2009), Geh = (Gehrke et al., 1995), Hen = (Henry et al., 2008), Moo01 = (Moody et al., 2001), New = (Newsham et al., 1997), Pan03 = (Pancotto et al., 2003), Pan05 = (Pancotto et al., 2005), Roz = (Rozema et al., 1997b), Smi = (Smith et al., 2010), Ver = (Verhoef et al., 2000), n/a = not available

Rates of photodegradation in studies without microbes

To elucidate the effect of radiation through direct photochemical mineralisation only, a small number of experiments have been conducted in the absence of microbes (Anesio et al., 1999; Austin and Vivanco, 2006; Brandt et al., 2009) thereby making sure microbial inhibition and microbial facilitation are not taking place. All studies found that decomposition rates increased under higher irradiance levels, either through increase of mass loss (33 - 60% increase, Austin and Vivanco, 2006) or CO_2 emissions (31 - 90% increase, Anesio et al., 1999; Brandt et al., 2009). The size of response depended largely on which parts of the solar spectrum were blocked.

Rates of photodegradation in studies with microbes

Under more realistic non-sterile conditions (when microbes are present in the substrate) it is hypothesised that the extent to which the positive effect of irradiance (through photodegradation leading to photochemical mineralization and microbial facilitation) can offset the negative effect of irradiance (through

microbial inhibition) depends on the level of microbial activity. Pancotto et al. (2005), for example, suggested that litter quality might affect the relative role of the three mechanisms. When litter quality is low and is limiting microbial activity, the decrease in microbial activity caused by solar irradiance might be insignificant, and a net positive effect of solar irradiance on decomposition rates is expected. The same might hold under dry conditions when moisture is already limiting microbial activity (Day et al., 2007). Under these conditions, the abiotic process of photochemical degradation might dominate and a net increase in decomposition rates is most likely to be observed. This could possibly explain why both Austin and Vivanco (2006) and Brandt et al. (2009) found that sterilising litter did not influence the positive effect of irradiance on decomposition rates: the experiments were either conducted with oven-dried litter (Brandt et al., 2009) or outside in a desert environment (Austin and Vivanco, 2006) when levels of microbial decomposition were already low.

Under moist conditions, the dominant effect of irradiance might shift from photochemical degradation to microbial inhibition (Smith et al., 2010). Possibly the study that sheds most light on the relative importance of the various irradiation-induced processes, is the study by Smith et al. (2010), which will be discussed in more detail in Section 2.7.4,

Issues when comparing studies

When comparing the results of studies into the effect of irradiance on decomposition rates, we find a wide range of mass loss and CO_2 emission rates (Table 2.4). It is likely that at least part of the differences between the results of these studies can be explained by the differences in experimental design and methodology among studies. These differences include:

- differences in irradiance intensity, either intentional or unintentional. Different studies expose substrate to different levels of irradiation, filters might not be equally transparent between and within experiments, e.g. for PAR (Flint et al., 2003) and different containers to hold the substrate will affect irradiation levels differently.

- different wavelengths manipulations between studies (block UV-A; block UV-A and UV-B; block all radiation)
- different temperature and moisture conditions under which the experiment is undertaken. For example, some experiments are conducted in a laboratory setting, where others are conducted in the field. Temperature might inadvertently be different between different irradiance treatments.
- a wide variety of substrates are used with different litter qualities
- differences in duration of studies, ranging from 1 day to 36 months
- difference in levels of microbial activity: some studies are conducted under (near) sterile conditions, where others are not.
- different exposed area to mass ratios of the substrate

The different results obtained by different studies are associated with the drivers that control the effect of radiation on decomposition. In Section 2.7.4, the state of knowledge on each of these possible controls is summarised

Extrapolation of irradiance-induced CO_2 production to field scale

To estimate the contribution of irradiation-induced decomposition to total CO_2 losses and carbon budgets at ecosystem scales, one would ideally conduct experiments under natural field conditions (Smith et al., 2010). However, these experiments have not been conducted yet. Although some of the studies report on the absolute values of the CO_2 flux measured from irradiated litter in jars (e.g. $1.5 \cdot 10^{-3}$ µmol CO_2 m^{-2} s^{-1} in Anesio et al. (1999) and $3.8 \cdot 10^{-3}$ µmol CO_2 m^{-2} s^{-1} in Brandt et al. (2009)), quantitative extrapolation to larger scales is not often attempted. Such an extrapolation is challenging, because conditions at the litter surface in the field must accurately be known, and the conditions in the lab must be comparable to field conditions (for example with regards to temperature, moisture and irradiance intensity). Furthermore, there must be confidence that decomposition rates measured in the lab agree with rates found in the field, which is not often the case (e.g. Smith et al., 2010). Also, we have to take into account that in the field not all litter and

SOM is exposed (because of shading leaf litter and soil by plants) and that cloud cover will attenuate the radiation conditions (Smith et al., 2010). Only Brandt et al. (2009) extrapolated their results from jar-level to field level. They measured an average response of 0.6 mg CO_2-C MJ^{-1} due to photodegradation and by assuming a linear relationship with irradiance this would be 20 mg CO_2-C m^{-2} d^{-1}. Correcting for litter coverage of approximately 25% and shading, they estimate that photodegradation caused a CO_2 loss of 1 g C m^{-2} y^{-1} (= 25% of total mass loss).

2.7.4. Controls of photodegradation

Irradiance levels

It is often assumed that there will be a linear relationship between response of decomposition and (UV) dose (Flint et al., 2003), but this dose-response relationship has received little attention so far in the literature. Although the dependency of photodegradation on light intensity has been shown directly for aquatic ecosystems in the lab (e.g. Kieber et al., 1990) and indirectly in the field (for example by comparing field experiments in different locations with different doses of UV exposure), only one study has directly examined the dependency of photodegradation of litter on light intensity by using three levels of UV-B irradiation instead of the commonly used two (Smith et al., 2010). The effect of UV-B radiation depended on moisture treatment (further discussed later), but within moisture treatments the response of decomposition appeared to be more or less linear with irradiance (Figure 2.6).

Brandt et al. (2009) came to the same conclusion after comparing CO_2 flux data from two experiments 12 days apart. Mean solar radiation levels were different (28 vs. 20 MJ m^{-2} d^{-1}) during the two experiments, and resulted in different levels of CO_2 emissions (expressed in µmol CO_2 m^2 s^{-1}). However, when expressing fluxes per unit energy (µmol CO_2 MJ^{-1}), the fluxes were approximately the same between experiments and averaged around 50 µmol CO_2 MJ^{-1}. This finding supported the hypothesis of a linear relationship between CO_2 efflux and irradiance levels.

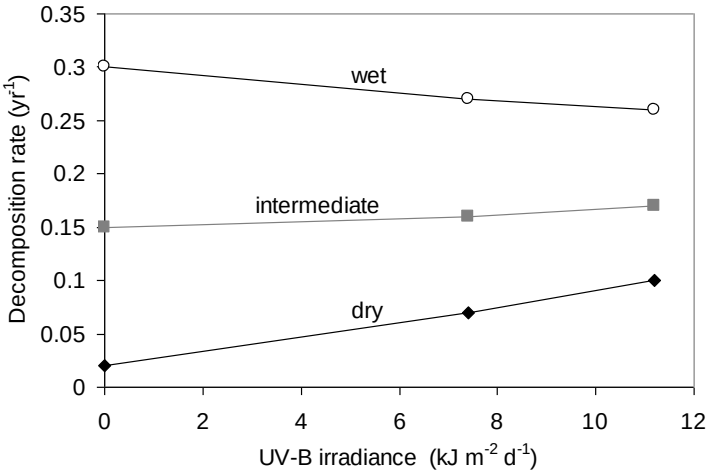

Figure 2.6 Effect of different UV-B irradiance levels and different moisture contents on decomposition rates determined over 6 months. 0, 7.4 and 11.2 kJ m^{-2} d^{-1} represent nil, ambient and elevated UV-B levels. Different precipitation regimes were established by rewetting the litter and soil beneath to 60% water holding capacity every 24, 12 or 4 days for dry, intermediate and wet treatments, respectively. Data from Smith et al. (2010).

Among studies examining the irradiance-induced production of carbon monoxide, data suggested both a linear (Yonemura et al., 1999), and non-linear (Schade et al., 1999) response of CO production to irradiance. The non-linear response suggested that OM is not as sensitive for photodegradation at low levels compared to higher levels of irradiance.

Exposure

The penetration depth of UV light is in the order of micrometers for soils (Moorhead and Callaghan, 1994), wood (Williams, 2005) and leaves (e.g. Day et al., 1992; DeLucia et al., 1992), and a few millimetres for peat (Searles et al., 2001). This shallow penetration depth means that solar irradiance can only affect the litter and SOM at the very surface of the substrate.

Four studies have confirmed that rates of photochemical mineralisation depend on the exposed area of organic matter, or specific leaf area (exposed leaf area per unit mass) for litters (Anesio et al., 1999; Brandt et al., 2009; Gallo et al., 2009; Henry et al., 2008).

Because Brandt et al. (2009) observed no difference in CO_2 emissions between different litters of different species but with equal specific leaf area, even though the chemical composition of the leaves differed substantially, they

speculated that leaf morphology, rather than litter chemistry, was possibly the main driver if photodegradation rates among different litters found in other studies. Gallo et al. (2009) also identified specific leaf area as the most important control in explaining the difference in rates of mass loss for leaves of three species. Anesio et al. (1999) measured 4 different litters and found that the leaves that tended to curl during exposure to UV radiation had the lowest CO_2 emission (on a mass basis), because the surface area perpendicular to the source of radiation was smaller compared to the non-curling leaves. When expressed per unit of exposed area, the CO_2 production was the same for the different litters.

As Henry et al. (2008) point out, the contribution of photodegradation to total decomposition must be integrated over the whole contributing layer (litter + soil), and the amount of shading by vegetation and litter is therefore important. Two manipulative studies on shading and self-shading have been conducted.

Henry et al. (2008) examined the effect of self-shading by litter by covering their litter samples with litter layers of different depths. Their findings were somewhat inconclusive: even though on a percentage mass basis, mass loss between different levels of shading was not different (suggesting that photochemical mineralisation was not an important contributor to overall mass loss), the lignin content only decreased significantly for litter shaded by the thinnest two litter layers, which would imply photodegradation was contributing substantially to lignin breakdown, but only when shading was minimal. Brandt et al. (2009) more conclusively confirmed the importance of specific leaf area on irradiance-induced CO_2 flux by manipulating litter density of sterile litter, and found no difference in CO_2 flux between litters of different densities when fluxes were expressed per unit area.

Of course, most ecosystems are vegetated and much of the litter and SOM are not exposed to sunlight because solar irradiance is intercepted by the canopy or litter above. Most exposure of litter in deciduous forests is expected during the leafless period of the year (Newsham et al., 1997), when irradiance intensities would be lowest. In contrast, in arid ecosystems up to 75% of solar

irradiance reaches the soil surface (Gallo et al., 2006) because the low biomass density limits light interception by the canopy in these ecosystems.

Although it is conceivable that solar irradiance could photodegrade live plant material in addition to dead OM, studies examining the photoproduction of carbon monoxide (CO) found much smaller amounts of CO (≈ 10 times less) produced from live leaves than from dead leaves upon irradiation (Tarr et al., 1995; Yonemura et al., 1999). These results suggested that live plant material is less susceptible to photodegradation than senesced material.

Wavelength

Most energy received at the Earth's surface is in the region of visible light (400 – 700 nm) and this radiation is also called photosynthetically active radiation or PAR. UV-radiation is partitioned into three wavelength bands: UV-C (100-280 nm), UV-B (280 – 320 nm) and UV-A (320 – 400 nm) (Blumthaler and Webb, 2003; Madronich, 1993). UV-C is completely absorbed by the atmosphere and does not reach the Earth's surface (Blumthaler and Webb, 2003; Madronich et al., 1998; Smith et al., 2009). Only a small part of the total energy received from the sun is in the UV range: typically UV makes up around 7-9 % of total energy received at the Earth's surface (Brandt et al., 2009; Madronich, 1993), of which the majority is contained in the UV-A range.

Even though the energy contained in the UV wavelengths is small, the effects of UV irradiance on biological organisms and organic material are disproportionally large. Because the energy per photon is inversely proportional to the wavelength (Klán and Wirz, 2009), photons in the UV region of the spectrum are the photons with the highest energy per photon to reach the Earth's surface. The energy contained in photons in the visible and UV bands of the solar spectrum range between approximately 40 and 140 kcal/mol photons (Anslyn and Dougherty, 2006), which coincides with the range of bond dissociation energies for bonds typically found in organic molecules (Anslyn and Dougherty, 2006; Klán and Wirz, 2009).

Originally, studies into the direct effects of solar irradiance on decomposition focussed mainly on exposure to (increased) UV-B radiation,

because UV-B had been identified to be important in affecting plants (Bornman and Teramura, 1993; Kakani et al., 2003) and decomposition of OM under water (e.g. Bertilsson and Tranvik, 2000; Osburn and Morris, 2003). However, more recently, several studies have established that irradiance of longer wavelengths (i.e. UV-A and PAR) are also contributing to degradation of both terrestrial (Table 2.5) and aquatic OM (Wetzel, 2003). For example, Brandt et al. (2009) found that UV-B, UV-A and PAR accounted for 31%, 15% and 48 % of the CO_2 production respectively (with the remaining 6% also occurring in the control that was not irradiated). Austin and Vivanco (2006) found that whereas attenuation of UV-B reduced mass loss by 33% compared to the control, additional blocking of the rest of the solar spectrum reduced mass loss by a further 27%. A contribution of 35 and 16% to the CO_2 flux was attributed to UV-B and UV-A respectively by Anesio et al. (1999). Within the PAR range of the solar spectrum (2009) found that the shorter wavelengths (wavelengths 400 – 500 nm) contributed most to photochemical mineralisation to CO_2 (39% for wavelengths between 400 and 500 nm vs. 2% for wavelengths between 500 and 700 nm).

Table 2.5 Contribution of different wavelength to total decomposition of OM.

Study	Measured	Microbial status	Experimental approach	Biological	UV-B	UV-A	PAR
Brandt et al. 2009 (Figure 5)	CO_2	non-sterile + sterile (averaged)	exclusion	6%	31%	15%	48%
Austin and Vivanco 2006	Mass	non-sterile	exclusion	40%	33%	27%*	
Anesio et al. 1999	CO_2	sterile	supplementation	23%	31%	46%	n/a
Newsham et al. 1997	Mass	non-sterile	supplementation	100%	0%	0%	n/a
Verhoef et al. 2000	mass	non-sterile	supplementation	100%	0%	0%	n/a

* UV-A and PAR together

Temperature

No manipulative studies have been conducted whereby the effect of temperature on photodegradation of OM has been explicitly examined. In exclusion studies, where treatments consist of preventing part of the solar radiation spectrum from reaching the substrate, researchers often attempt to minimize the difference in temperature between the pass and block treatments, but naturally the litter that receives more visible light will be warmer if temperature is not controlled. Even though Austin and Vivanco (2006) for example attributed the difference in mass loss between the "full sun" and "blocked total" treatment fully to the difference in irradiation, they also found that surface soil temperatures in summer were significantly higher in the irradiated plots compared to the shaded plots (Austin and Vivanco, 2006, supplementary information). This suggests that the extra mass loss might be controlled by increased temperature combined with higher irradiation, whereby photons might be more effective in breaking bonds at higher temperatures.

Oxygen availability

Little is known about the process by which CO_2 forms from organic matter through photochemical mineralisation or where the oxygen atoms in the produced CO_2 originate from. It is known that photodegradation of organic polymers occurs especially if atmospheric oxygen is present (Wayne and Wayne, 1996). Also, comparison of the isotopic signatures of emitted CO_2 from irradiated litter and of atmospheric O_2 suggested that the oxygen in the emitted CO_2 most likely originated from the atmosphere, and not from the decomposed litter (Cory et al., 2008). The high rates of irradiance-induced conversion of organic matter into DIC in aquatic systems (e.g. Anesio et al., 1999) seem to suggest that, even though oxygen concentrations in water is much lower than in air, the photo-oxidation of immersed OM does not seem to be limited by the low availability of oxygen.

Moisture

As described in Section 2.7.3, the relative importance of mechanisms by which irradiance affects decomposition might be influenced by the moisture status of the substrate. Under wet conditions when microbial activity is high, the dominant effect of irradiation on decomposition dynamics might shift from photodegradation to microbial inhibition, whereas under dry conditions microbial activity is limited and the positive effect of irradiance on decomposition through photodegradation might be larger than the negative effect on the decomposer organisms (Brandt et al., 2007; Gallo et al., 2009; Gallo et al., 2006; Smith et al., 2010). The largest increases in decomposition rates due to exposure to solar irradiance have indeed been found in dry ecosystems (e.g. Austin and Vivanco, 2006; Day et al., 2007) whereas the net effect of UV radiation in ecosystems with higher moisture availability is often low or negative (Moody et al., 2001; Newsham et al., 1997; Verhoef et al., 2000).
However, moisture conditions of soil and litter are often correlated with the degree of exposure of dead OM to solar radiation and microbial activity. Drylands typically contain more standing dead material than mesic ecosystems and microbial activity is often limited by low moisture availability (Throop and Archer, 2009). Comparatively, the small or negative effect of UV radiation on decomposition rates in ecosystems with high moisture availability are often attributed to the higher microbial activity in wet ecosystems (Gallo et al., 2006) or higher degree of plant cover shading litter from irradiance (Brandt et al., 2007). These correlated factors (moisture availability, exposure and microbial activity) are hard to separate in field experiments (Moorhead and Callaghan, 1994) without explicit manipulative studies.

Very little is known about the potential direct effect of moisture availability on the processes of photodegradation and photochemical mineralization. The most insightful studies so far are the studies by Brandt et al. (2007) and Smith et al. (2010), who manipulated both the moisture status and level of microbial activity in litter. Smith et al. (2010) were able to demonstrate the expected control of moisture status on the effect of exposure to UV irradiance under normal levels of microbial activity: a positive effect under dry

conditions, and a negative effect under moist conditions (Table 2.6 and Figure 2.6). However, for the reduced-microbial activity treatment they were unable to show the positive effect of irradiance on mass loss which would be expected if microbial inhibition was zero and photodegradation continued to take place under wet conditions (Table 2.6). Because microbial activity under wet conditions was found to be reduced but not stopped, and microbial inhibition might have occurred, they could not draw any conclusions about the degree to which photodegradation was taking place under wet conditions. Brandt et al. (2007)

In a short 72-hour experiment Anesio et al. (1999) compared production rates of CO_2 and dissolved inorganic carbon (DIC) from sterile macrophyte leaves incubated in air and water, respectively. They found that the loss of carbon as DIC in water was larger than a loss of carbon as CO_2 in air under the same irradiation conditions (both expressed in µg C/mg dry mass/hr). This, in addition to a multitude of experiments that have shown photodegradation of OM to DIC in aquatic systems when substrate was submerged in water (e.g. Bertilsson and Tranvik, 2000; Osburn and Morris, 2003) provide evidence in situations where OM is immersed in water (or possibly when OM has a film of water around it, for example in saturated soil), photochemical mineralisation can still take place.

Table 2.6 Effect of UV-B irradiance on mass loss as reported by Smith et al. (2010).

	dry	moist	wet
Normal microbial activity	+	0	–
Reduced microbial activity	+	0*	0*

* a positive effect was expected but not observed

Litter chemistry

The degree to which litter chemistry determines the rates of photodegradation has been examined using two approaches: (1) by simultaneously measuring mass loss or CO_2 emissions from litters of different species, and (2) by determining the extent to which degradation of different compounds of OM is affected by exposure to irradiance.

Several studies have examined the effect of exposure of litter to irradiation on litter chemistry by measuring changes in concentration of for

example lignin, holocellulose, hemicellulose and cell solubles (e.g. Austin and Ballaré, 2010; Gallo et al., 2006; Gehrke et al., 1995; Rozema et al., 1997a). It has been hypothesized that UV-B absorbing compounds like lignin and other poly-aromatic compounds are most susceptible to photochemical degradation (Austin and Ballaré, 2010; Gallo et al., 2009; Henry et al., 2008) and photodegradation has been shown on several occasions to preferentially break down lignin (Austin and Ballaré, 2010; Day et al., 2007; Gehrke et al., 1995; Henry et al., 2008; Moorhead and Callaghan, 1994; Rozema et al., 1997a). However, others found no effect of irradiance on lignin content (Brandt et al., 2007; Pancotto et al., 2003) or instead found that other compounds were mostly responsible for the mass loss by photodegradation (Brandt et al., 2007; Schade et al., 1999). If polyphenolic compounds like lignin are indeed most susceptible to photodegradation, one might expect irradiation-induced mass loss to be higher for litter with high contents of polyphenolics compared to litter with a lower content of polyphenolics (Gallo et al., 2009). Even though some experiments have shown more mass loss in litters with high lignin contents (Austin and Ballaré, 2010; Schaefer et al., 1985), this is not always found (Brandt et al., 2009). Anesio et al. (1999), Brandt et al. (2009), and Gallo et al. (2009) suggested that, possibly, differences in specific leaf area are more important in controlling the rate of photodegradation than differences in litter quality. Another possible explanation for the lack of agreement between different studies on the control of lignin on rates of photodegradation could be that microbial decomposition, which takes place simultaneously with photodegradation in varying degrees in different studies, confounded the signal, because polyphenolic compounds are most recalcitrant to breakdown by microbes.

Time

If decomposition of litter is brought about totally through microbial degradation, rate of mass loss tends to decrease with time (see Section 2.6.1). This slow-down with time can be explained by the depletion of labile substrate in the earlier stages, which causes decomposition rates to decrease when more and more recalcitrant substrate is left (Berg, 2000; Berg and McClaugherty, 2008;

Swift et al., 1979). Typically, mass loss brought about by microbial decomposition can be described by an asymptotic decay relationship with time (e.g. Adair et al., 2008) and is often described as first order kinetics, whereby the rate of decomposition is proportional to the mass of the remaining litter (Parshotam, 1996; Shibu et al., 2006).

In contrast, rates of decomposition brought about by photodegradation depend on the exposed surface area of the litter (Anesio et al., 1999; Brandt et al., 2009; Gallo et al., 2009). This means that in ecosystems where photodegradation dominates the decomposition process, decay rates are not expected to decrease with time as long as the surface area stays the same (Brandt et al., 2009). This could explain why decomposition rates of litter observed in arid regions do not taper off after a few years in the same way rates in mesic systems do (Montana et al., 1988; Parton and Silver, 2007).

2.8 Summary

In this review of the literature, two different processes that cause CO_2 losses from terrestrial organic matter have been discussed: microbial respiration and photodegradation.

Most of the previous research has focused on microbial respiration as the main process responsible for decomposition of organic matter. However, there is still uncertainty about the controls of microbial respiration in situ, including substantial debate about the control by temperature and moisture. Few studies have examined these controls at ecosystems scales in the absence of the confounding effects of plants.

In addition to microbial decomposition, a few studies have shown that photodegradation contributed to OM decomposition, especially in exposed arid and semi-arid ecosystems. Photodegradation of litter has only been measured on a few occasions in dry ecosystems, and the susceptibility of OM other than litter (e.g. soil organic matter) has never been examined. Furthermore, no studies to date have investigated to contribution of photodegradation to CO_2 exchange at field scales. There is great need for determining the magnitude of irradiance-induced CO_2 losses within a range of ecosystems.

Studies of photodegradation are often performed using litter bags, and sometimes use lamps to provide (additional) UV-B irradiance. The implications of the results of these studies are hard to interpret, because litter bags block part of the incoming radiation, and the spectral distribution of solar radiation cannot be accurately simulated by lamps. To obtain reliable estimates of the magnitude of photodegradation and to disentangle the main controls of photodegradation, studies under natural field conditions are necessary. New methods need to be developed to measure the rates of photodegradation at high time resolution both in the field and the laboratory.

Evidence exists that heterotrophic respiration and photodegradation are controlled by similar regulators (e.g. solar irradiance, temperature, moisture and substrate chemistry), but they seem to operate differently on the two processes. Whereas reasonable understanding has been gained about the main controls of heterotrophic respiration, the controls on photodegradation and resulting CO_2 losses are poorly understood and untested at field scales.

The process of photodegradation and its controls need to be incorporated into conceptual and numerical models to improve predictions of the response of OM decomposition and CO_2 losses to changing environmental conditions and to increase our understanding of the terrestrial carbon cycle.

These areas of research requiring more attention form the basis for the objectives of the current study (Section 1.2).

.

Chapter 3 Site description and methods

This chapter describes the study site and methods used in this research to measure CO_2 effluxes from OM and the potential drivers. Section 3.1 describes the approaches used to measure radiation-induced CO_2 flux. Section 3.2 describes the bare peatland field site at Torehape. Section 3.3 describes the field measurements made at the bare peatland using the eddy covariance (EC) and chamber systems. Section 3.4 details the closed chamber system designed to do small scale measurement of irradiance-induced CO_2 flux. Section 3.5 describes three additional data sets used in this research.

3.1 Approaches to measure radiation-induced CO_2 flux

If we assume that photodegradation is the only abiotic process producing CO_2 (in addition to biotic processes), the net CO_2 flux from an ecosystem during the day is

$$-NEE = GPP - ER - PD \qquad \textbf{Equation 3.1}$$

where NEE is net ecosystem exchange (= total CO_2 flux), GPP is gross primary production (photosynthesis by plants), ER is ecosystem respiration and PD is the irradiance-induced CO_2 flux. In this situation, ecosystem respiration ER is the sum of autotrophic (AR) and heterotrophic respiration (HR) so that

$$-NEE = GPP - (AR + HR) - PD \qquad \textbf{Equation 3.2}$$

In an ecosystem devoid of living vegetation, i.e. GPP = 0 and AR = 0, this equation can be simplified such that total CO_2 efflux during the day is the sum of only two components:

$$-NEE = -HR - PD \qquad \textbf{Equation 3.3}$$

By re-arranging terms, we can determine photodegradation by subtracting heterotrophic respiration from net ecosystem exchange:

$$PD = NEE - HR \qquad \textbf{Equation 3.4}$$

In systems without living vegetation, measurements of radiation-induced CO_2 losses (PD) can be made in two ways. In situations where microbial respiration is not taking place (HR = 0, for example in sterilised organic matter), the total CO_2 flux can be assumed to be of abiotic origin. This method has been applied in small scale studies using sterile soils in jars (e.g. Anesio et al., 1999; Brandt et al., 2009). However it is not applicable in natural field situations because it is very challenging to completely stop microbial activity.

In a field situation, one can infer irradiance-induced CO_2 fluxes by combining results from two methods: one that measures the total CO_2 flux (HR + PD = NEE) and one that measures only the biological component of the CO_2 flux (HR). The difference between the two fluxes then is an estimate of the irradiance-induced flux (Equation 3.4).

The most common method to measure total net CO_2 flux (NEE) from an ecosystem is eddy covariance (EC). Again, this net CO_2 flux equals total CO_2 loss only at times when photosynthesis is zero (i.e. when there are no active autotrophs).

There are two approaches to determine the biological component (HR) of the CO_2 flux by itself. The first approach directly estimates HR by using measurements from either an opaque chamber (which blocks incoming solar radiation so that PD = 0) or from probes which sample the profile of CO_2 concentrations in the soil air with depth. The second approach is indirect. It estimates the biological component of CO_2 flux first by measuring the total flux at night when radiation is zero such that PD = 0. The values obtained are then used to model the total daytime biological flux (HR).

In summary, three approaches can be used to estimate the irradiance-induced component of the CO_2 flux for an ecosystem without living plants:

1) PD = NEE

   where HR = 0 due to sterile conditions (i.e. lab experiments)

2) PD = NEE – HR_D

   HR_D is directly measurement by opaque chamber or soil probes

3) PD = NEE – HR_M

   HR_M is indirectly determined via modelling based on night-time EC fluxes

This study used all three approaches.

3.2 Site description

Measurements of CO_2 fluxes were made at Torehape peat mine, southeast of Auckland in the Hauraki Plains of the North Island of New Zealand (37.31799°S, 175.45465°E, and 5 m elevation; Figure 3.1).

Figure 3.1 Aerial photo of the study site at Torehape peat mine. (Photo taken by Terralink International Limited, supplied by Dr. Beverly Clarkson). The yellow star indicates the approximate location of the eddy covariance system.

From the old peat bog (> 6000 years), the top metre of peat had been removed for horticultural peat (Sorrell et al., 2004), after which 4 to 5 m of peat remained (Clarkson and Fergie, 2002). Measurements started directly after mining had finished. Dominant vegetation before mining at Torehape was *Sporadanthus ferrugineus* over a lower storey of *Empodisma minus,* and groundcover *Sphagnum cristatum* (Schipper et al., 2002). The mined study site was completely devoid of plants apart from some regenerating vegetation in the ditches. In winter, when part of the site was under water algae formed in some of the puddles of standing water. Dry bulk density of the peat (0-15 cm) was 135 kg m^{-3} and organic matter content was 92%, measured by loss on ignition (Blakemore et al., 1987).

The site was drained to make mining activities possible with drains approximately 40 m apart. Lanes of bare peat were 900 m long. The EC and chamber systems were set up in the middle of the lane which bordered vegetated lanes to the north and bare peat to the south. The site was flat with upwind fetch parallel to the drains greater than 400 m.

Maximum half-hourly values for shortwave incoming radiation varied between 1100 Wm^{-2} in summer and 460 Wm^{-2} in winter (Figure 3.2a). Mean annual temperature at a nearby climate station (Thames, 37.15858°S, 175.55137°E, 3 m elevation, 9.0 km from study site) was 15.2 °C (Figure 3.2b) and average rainfall 1150 mm per year (1970 - 2000, NIWA, 2007) (Figure 3.2c).

During the experiment water table depth varied from 450 mm during summer to 50 mm during winter (Figure 3.2c). In winter, part of the site was under water (Figure 3.3 a). Between June 2005 and July 2007 – the period during which eddy covariance data were available – volumetric moisture content at 45 mm depth ranged from 0.49 m^3 m^{-3} during summer to 0.68 m^3 m^{-3} during winter (Figure 3.2d). Although the peat at 45 mm depth remained relatively moist during dry periods in summer, the surface peat dried out considerably and formed a dry crust over the surface. Surface conditions of the peat were therefore much drier than the VMC at 45 mm depth implied (see loose top layer of peat in Figure 3.3b). The measurements of low values for VMC after mid

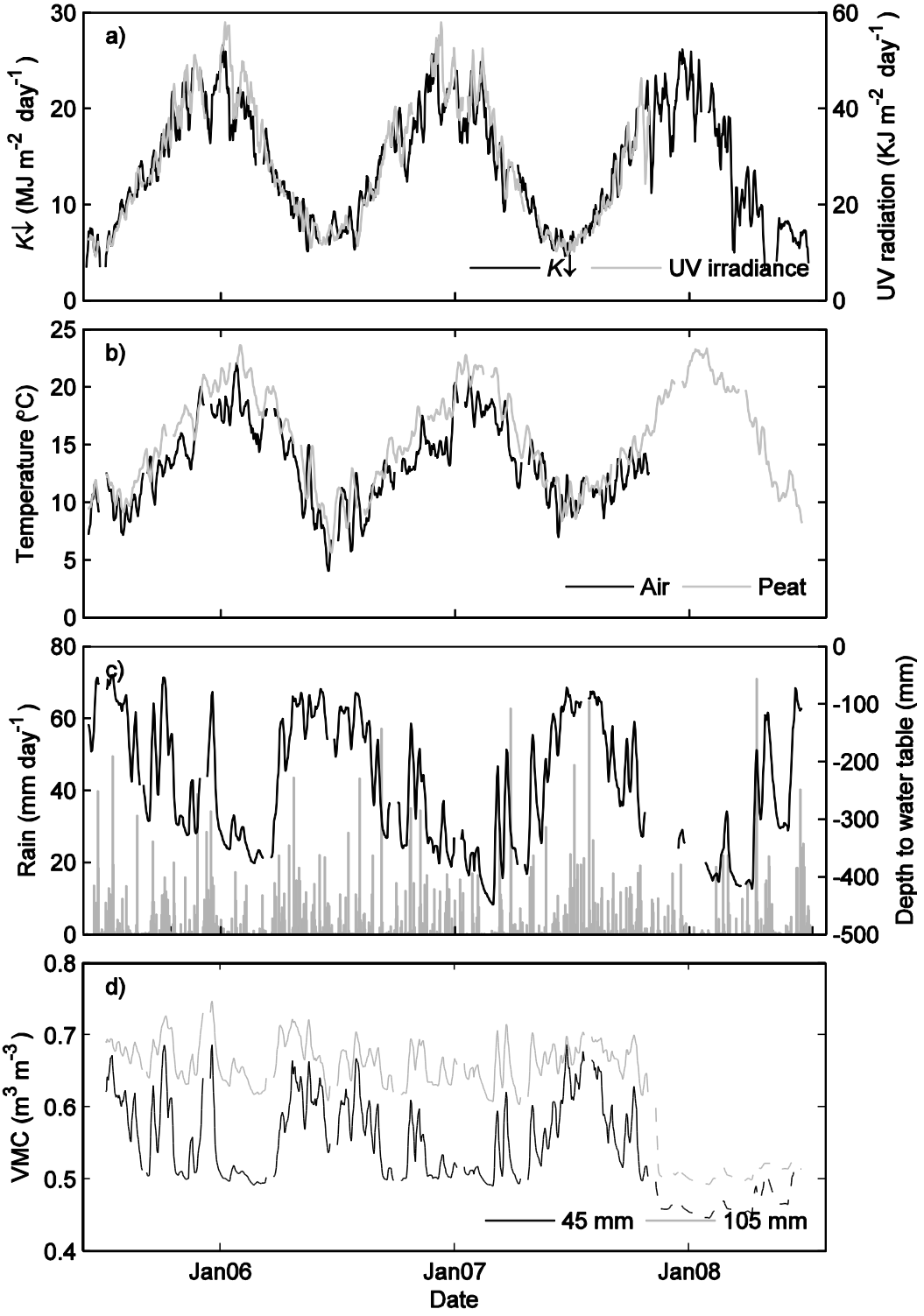

Figure 3.2 Annual trends of (a) shortwave incoming radiation (*K*↓) and estimated UV radiation, (b) air temperature and peat temperature at 50 mm depth, (c) rainfall and depth to water table, (d) and volumetric moisture content at 45 and 105 mm depth. VMC data not used for analysis are shown as dashed lines. All displayed values (except the half-hourly rainfall) are running means calculated using a moving window of 7 days.

Figure 3.3 Torehape peat mine in a) winter (6 June 2007) and b) summer (17 Feb 2006).

November 2007 (dashed lines in Figure 3.2d) were considered unreliable and will be further discussed in Section 6.3.1.

Because the only autotrophs at the study site were some plants in the ditches and algae in puddles during winter, CO_2 exchanges as a result of photosynthesis and autotrophic respiration were expected to be negligible. The measured CO_2 fluxes were assumed to be the results of microbial respiration and possible abiotic processes only (see Chapter 4).

3.3 Field study

3.3.1. Eddy covariance

Instrumentation

Fluxes of sensible heat, water vapour and CO_2 were measured using the eddy covariance (EC) technique, which utilises high-frequency measurements of the vertical component of the wind speed, temperature and concentrations of H_2O and CO_2 to determine the exchange of heat, water and CO_2 between the surface and atmosphere (Baldocchi et al., 2001). Details of the EC setup and data manipulation are given below.

EC instruments were mounted 1.5 m above the peat surface on 3 June 2005. The relatively low mounting height was chosen to avoid measuring any fluxes originating from the neighbouring vegetated lanes. Sensors were pointed towards the west, which was the prevailing wind direction. On 14 March 2007 the sensors were moved up to 2.5 m. Measurements with the EC system were made until 31 July 2007 (Figure 3.4).

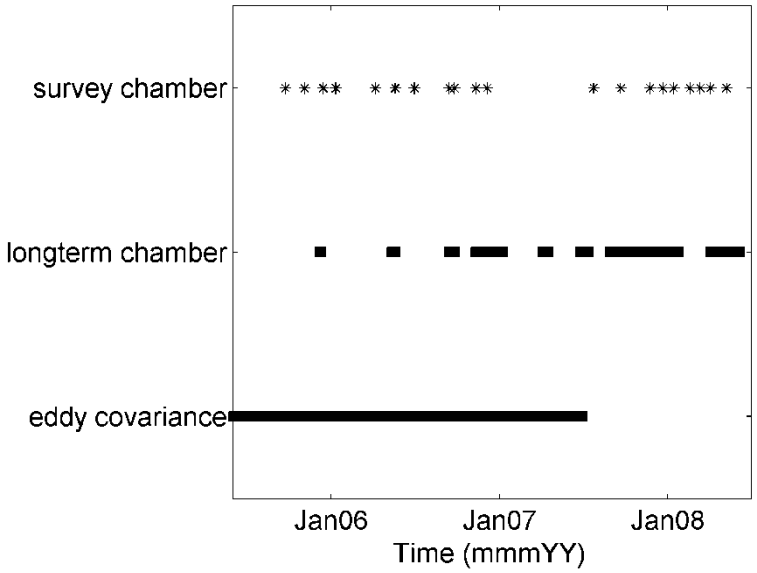

Figure 3.4 Data availability from chamber systems and the eddy covariance system.

The open path EC system consisted of a sonic anemometer (CSAT-3, Campbell Scientific Inc., Logan, UT, USA) and an open path infrared H_2O/CO_2 gas analyser (LI-7500, LI-COR Inc., Lincoln, NE, USA) sampling at 10 Hz. Calibration of the LI-7500 was carried out every 6 months using oxygen free nitrogen gas to set the CO_2 and H_2O zero and CO_2 in air (368.0 ppm ± 0.1 ppm) to set the CO_2 span. The H_2O span was set using a dew point generator (LI-610, LI-COR Inc., Lincoln, NE, USA) set to a dew point of 10°C. Both zero and span settings were very stable over the course of the experiment.

A CR23x datalogger sampled the mV signals of the sonic anemometer and the LI-7500, converted into appropriate units and calculated half-hourly raw fluxes. These raw fluxes were stored to the datalogger's internal memory and downloaded via automated telemetry on a daily basis using a cellular modem (Wavecom WMOD2B GSM).

Flux processing

Half-hourly raw fluxes were calculated online by the CR23X datalogger. Post-processing was done using a modified and improved version of a Matlab software program (Nieveen et al., 2005). Data processing occurred in the following order: 1) 2D coordinate rotation (McMillen, 1986); 2) corrections for sonic temperature (Schotanus et al., 1983); 3) high frequency loss (Moore, 1986); and 4) addition of the density (or WPL) term (Webb et al., 1980), with the order of 3 & 4 following the recommendations by Massman (2004a). Fluxes were also calculated using the planar fit method (Wilczak et al., 2001) instead of the classic 2D rotation but this had minimal effect on the size of the fluxes. For the rest of this study the fluxes rotated using the 2D rotation will be used.

After completion of the measurements it was discovered that the LI-7500 had a timing error in the embedded software of about 1 scan. Therefore the signals of the gas analyser and sonic anemometer were not aligned properly in time, resulting in an underestimation of the covariance between vertical wind speed and CO_2 concentration and the resulting raw (i.e. before corrections) CO_2 flux (see Appendix B). LI-COR indicated that the size of the underestimation of fluxes of CO_2 and H_2O caused by this timing error was affected by wind speed

and installation height, where largest errors were expected above a short crop at high wind speeds (McDermitt, 2003). Because high frequency data were not available to recalculate the CO_2 fluxes with the correct timing delay, the size of the underestimation of the before-WPL CO_2 fluxes (i.e. CO_2 fluxes before addition of the density term (Webb et al., 1980) but after applying the other corrections described above) was approximated using an empirical relationship. This relationship was established using data obtained after the peatland experiment using the same EC system at a dairy farm nearby. By then, the system had been upgraded to store high frequency data so a detailed study into the size and controls of the timing error was possible. The relationships between the size of the underestimation of the before-WPL CO_2 flux, wind speed and the CO_2 flux itself explained 75 and 77% of the observed variation for the low (1.5 m) and high (2.5 m) installation respectively. Average underestimation of the CO_2 flux before addition of the WPL term was 16% and 12% for the low and high measurement height, respectively. CO_2 fluxes were recalculated to account for the timing error by adding the estimation of the missed flux using the regression equation to the before-WPL fluxes, after which a recalculated WPL term was added. For more information on this extra correction, see Appendix B.

Eddy covariance CO_2 flux data were only used when footprint analyses (Schuepp et al., 1990) showed that 80% or more of the flux originated from the bare peat. Also, data were discarded when wind direction was from behind the tower to avoid possible flow distortion. Data were discarded also when rainfall or dew caused unreliable readings from the LI-7500 and when the friction velocity was < 0.2 m s^{-1}. The threshold was chosen conservatively to ensure that only the highest quality data were used for analysis. Because of these strict filter criteria 89% of the data points were discarded, leaving ~ 4000 data points for analysis. No gapfilling of missing data was applied.

3.3.2. Chamber measurements

Repeated chamber measurements were made using an automated soil CO_2 flux system (LI-8100, LI-COR Inc., Lincoln, NE, USA). A long-term chamber (LI8100 -101, collars 200 mm in diameter) was used to measure the temporal

variation of the respiration fluxes from one collar installed within 7 m from the EC system. Measurements were made every 15 minutes. A survey chamber (LI8100 -102, collars 100 mm) was used to sample the spatial variation of the peat surface CO_2 flux (See Appendix F). Between June 2005 and July 2007 data from the long-term chamber were available for 100 days. Soil temperature measurements were made adjacent to the chamber at a depth of 30 mm using an 8100-201 soil temperature probe connected to the LI-8100.

3.3.3. Additional measurements

Table 3.1 lists all additional variables measured at the peatland, the instruments used and the height or depth of deployment. In addition to these quantities, the albedo was determined during summer using a 4-component net radiation sensor (NR01, Hukseflux, Delft, The Netherlands) between 7 Nov 2007 and 14 Jan 2008.

Table 3.1 List of additional variables measured and instrumentation used.

Variable	Sensor	Manufacturer	Height/depth
Temperature + humidity	HMP45	Vaisala, Helsinki, Finland	1.5/2.4m
Shortwave incoming radiation (400 – 1100 nm)	SP Lite pyranometer	Kipp & Zonen,Delft, The Netherlands	2.4 m
Precipitation	Tipping bucket rain gauge, Model TB3/0.2/P	Hydrological services P/L Liverpool, NSW Australia	0 m
Peat temperature	Thermistors*	Local	-50 and -100 mm
Peat temperature**	Thermistors*	Local	-20,-40, -80 -160, -320, -400 and -500 mm
Shallow peat temperature	Four junction averaging thermocouple	Campbell Scientific Inc., Logan, UT, USA	-5 mm
Volumetric moisture content	CS615 water content reflectometer***	Campbell Scientific Inc., Logan, UT, USA	-50 and -100 mm
Depth to water table	Pressure transducer type SS3	Instrument Services and Developments, Rangiora, NZ	-1500 mm

* Equivalent to the 107B Campbell Scientific thermistors, **data available from 10 Nov 2006 onwards, *** calibration for peat was conducted before installation

3.4 Container study

3.4.1. Experimental design

After the field study a controlled set of experiments was conducted to investigate the process of photodegradation further. To determine the immediate response of the CO_2 production from organic substrates to exposure to solar irradiance, a closed chamber system was constructed that included a small transparent container holding the substrate connected to an infra red gas analyser which contained a built-in pump (LI-8100, LI-COR Inc., Lincoln, NE, USA; see Figure 3.5). In this setup, the container was part of a flow-through, non-steady-state system (FT-NSS, Livingston and Hutchinson, 1995) in which changes of CO_2 concentrations could be detected continuously. To distinguish between the chambers used in the field and the small purpose-built chamber system, the latter will be referred to as the 'container' from now on.

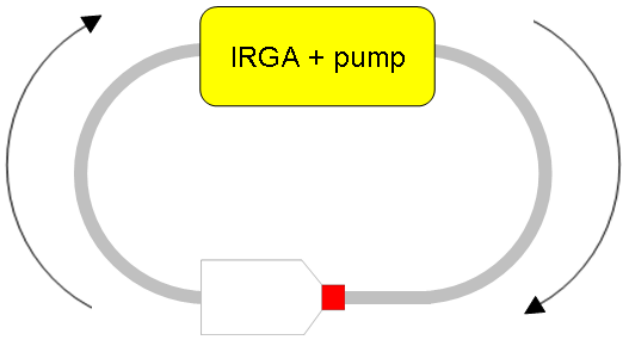

Figure 3.5 Set-up of container experiments. Drawing not to scale. IRGA = Infrared Gas Analyser.

The container was a polystyrene culture flask (Greiner Bio-One Inc., Longwood, FL, USA, volume 270 ml, area 80 cm^2) that housed the substrates (Figure 3.6). This container was chosen for its low volume: area ratio, which facilitated the detection of low CO_2 effluxes from the substrate.

To obtain optimal transmittance of solar irradiance (UV-B, UV-A and visible parts of the solar spectrum) through the top of the container to the substrate, the polystyrene top (transmittance for UV-B = 0.31) was replaced with quartz (plate 3.175 mm thick, GM Associates Inc., Oakland, CA, USA). Transmittance of the quartz was 0.91, 0.93, and 0.93 for visible (400 – 700 nm),

UV-A (320 – 400 nm) and UV-B (280 – 320 nm) irradiance respectively. The quartz top was glued on using silicone and left to cure more than 24 hours before the first experiment.

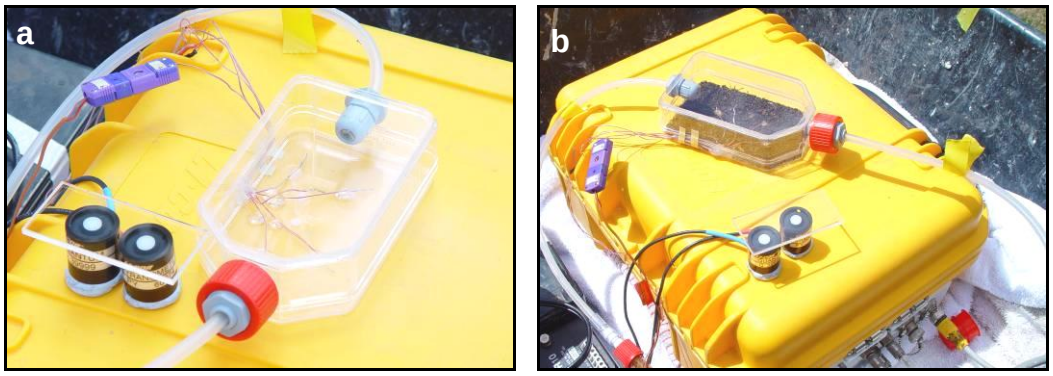

Figure 3.6 Setup of container experiments. a) Empty container showing averaging thermocouple to determine peat temperature. The pyranometer and quantum sensors sit to the left of the container. b) Container filled with a thin layer of peat.

For all experiments, surface peat (top 10 cm) was used that was collected at Torehape on 15 October 2008. Within 5 days of collection, the peat was passed through a 1 cm sieve, and stored at 4°C until use. To limit microbial activity in the organic substrate, all substrates were air dried during the three days before the experiments. In general, the container was filled using as little substrate as possible (approximately 4 grams) while covering the complete surface area of the container. Dry mass equivalent was determined after the experiment by oven-drying the substrates for 3 days at 70°C.

Measurements were made by alternately shading and exposing the container to the sun. Each run of sun or shade lasted for 140 or 200 seconds. CO_2 concentration data were measured and logged every second during the runs.

3.4.2. Additional measurements

Incident solar irradiance ($K\downarrow$) was measured using a LI-200 pyranometer (wavelengths 400-1100 nm, LI-COR Inc., Lincoln, NE, USA) and photosynthetically active radiation was measured using a LI-190 quantum sensor (wavelengths 400-700 nm, LI-COR Inc., Lincoln, NE, USA). The sensors were sat beside the container (Figure 3.6) at the same angle to the sun as the container. An averaging thermocouple (locally made) was used to measure the temperature of the thin

layer of peat ("peat temperature", see Figure 3.6a). An additional thermocouple measured the air temperature in the container ("container temperature") above the peat. The latter temperature was used for flux calculation (see section 3.4.4).

3.4.3. Measurement dates and location

Measurements were made during two time periods: between 3 and 5 February 2009 (3 days, Experiment A described below) and between 29 March and 23 April 2009 (9 days, Experiments B, C and D described below) (Table 3.2). During all measurements from March onwards, the container and solar irradiance sensors were tilted towards the sun to ensure solar radiation was entering the container through the quartz top. This way, blocking of irradiance by the polystyrene sides of the container was minimised.

Table 3.2. Overview of dates of measurements. All measurements were carried out in 2009.

Experiment A	Experiment B (wavelength)	Experiment C (substrate)	Experiment D (oxygen)
3 Feb	29 Mar	2 Apr	3 Apr
4 Feb	30 Mar	22 Apr	6 Apr
5 Feb	1 Apr	23 Apr	17 Apr

All measurements were collected at a sport field bordering the University of Waikato campus in Hamilton, 175.336 °E, 37.862 °S, 50 m elevation. The nearest tall buildings were a few hundred metres away.

3.4.4. Flux calculation

CO_2 fluxes were calculated using the LI8100 software (FV8100, LI-COR Inc., Lincoln, NE, USA). In these calculations an incorrect value for the chamber temperature was used because the use of a custom-made chamber made it impossible to read the chamber temperature with the LI-8100. Instead, fluxes were corrected afterwards using the container temperature measured by the thermocouple using

$$F_{c\_corrected} = \frac{F_c(T_0 + 273.15)}{(T_{correct} + 273.15)} \qquad \textbf{Equation 3.4}$$

where $F_{c\_corrected}$ is the CO_2 flux corrected for the real temperature in the container, F_c is the CO_2 flux calculated by the LI-8100 software using the incorrect chamber temperature, T_0 is the incorrect chamber temperature used for flux calculation in °C and $T_{correct}$ is the real temperature in the container measured by the thermocouple in °C.

To determine the CO_2 flux both exponential and linear regressions were fitted to the CO_2 concentration over time. Both the exponential fit and linear fit data were examined, and because CO_2 build-up in the container was not considered an issue (see Section 2.5.1), the linear fit was preferred because it produced less scatter in the data. Because of the fast response of the flux to changes in temperature and irradiance conditions (see an example in Figure 3.7), fluxes could be calculated using the first 66 seconds of CO_2 concentration data, of which the first 6 seconds were discarded to allow for travel time of air from container to the infra-red gas analyser. The shorter run length was preferred because it ensured temperatures between sun and shade runs overlapped better, which allowed direct comparison between fluxes for sun and shade runs of approximately equal mean temperature. To ensure stable conditions during runs (mostly with regards to fluctuations in irradiance caused by clouds drifting over) fluxes for very short periods (20 seconds) were also calculated in Matlab (The Mathworks Inc., Version 7.3.0.267, R2006b) using linear regression.

Data were only used for analysis if the standard deviation of measured $K\downarrow$ values during the run (1 value per second) was less than 50 Wm^{-2}. Fluxes of CO_2 were calculated on an area basis (µmol CO_2 m^{-2} s^{-1}).

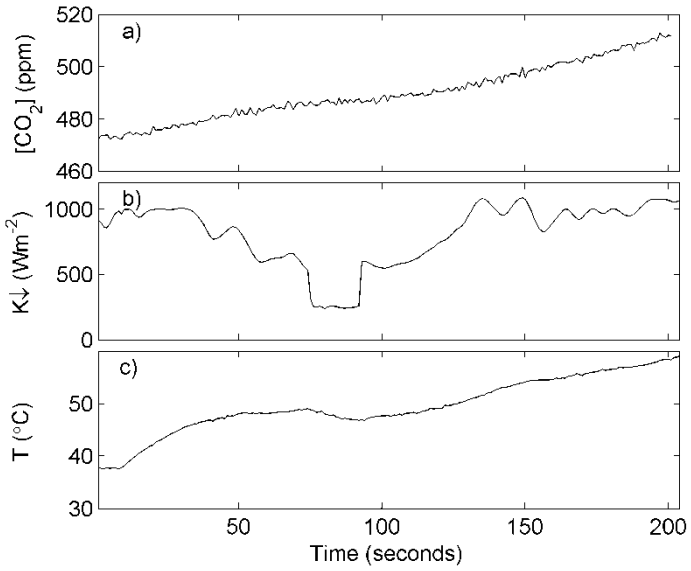

Figure 3.7 Example data from one experimental run. a) CO_2 concentration. b) incident solar irradiance. c) peat temperature. Data show that both peat temperature and increase in CO_2 concentration responded almost immediately to changing irradiance condition caused by passing clouds.

3.4.5. Experiment A: Radiation and temperature

The first experiment was set up to verify the existence of photodegradation of peat, as suggested by the findings in the field (see Chapter 4). In this case the aim was to mimic the field conditions as closely as possible. Measurements were carried out in summer (3-5 Feb 2009) when the zenith angle was low and no additional filters were used.

3.4.6. Experiment B: Wavelength

To determine how much visible (400 – 700 nm), UV-A (320 – 400 nm) and UV-B (280 – 320 nm) irradiance contributed to the measured CO_2 efflux from additional filters were used to block UV-B and UV-A + UV-B. Absorbance of many different materials was determined using a Cary 100 UV-Vis spectrophotometer (Varian Inc, Palo Alto, CA, USA). Transmittance was calculated from absorbance using the following equation:

$$T = 10^{-a} \qquad \textbf{Equation 3.5}$$

where T = transmittance (-)

a = absorbance (-)

Quartz, soda glass and Plexiglas were found to be most suitable to filter out the different wavelengths. Soda glass is transparent to visible light, mostly transparent for UV-A but blocks UV-B (–UVB treatment). Plexiglas is transparent to visible light, but blocks UV-A and UV-B (–UVAB treatment). A sheet of quartz was used to mimic 'ambient' or field conditions, with highest transmittance for all wavelengths (control). The extra layer of quartz ensured that comparable levels of PAR reaching the peat during all treatments as recommended by Flint et al. (2003). The transmittance curves are shown in Figure 3.8, see also Table 3.3.

Table 3.3 Average transmittance of different treatments.

Treatment	Experiment	Top of container	Filter	Total transmittance		
				UV-B	UV-A	PAR
Sun	A,C,D	quartz	-	0.91	0.93	0.93
Control	B	quartz	quartz	0.84	0.87	0.88
– UVB	B	quartz	soda glass	0.03	0.72	0.85
– UVAB	B	quartz	plexiglass	0.08	0.33	0.87
Dark	A,B,C,D	quartz	aluminium foil	0	0	0

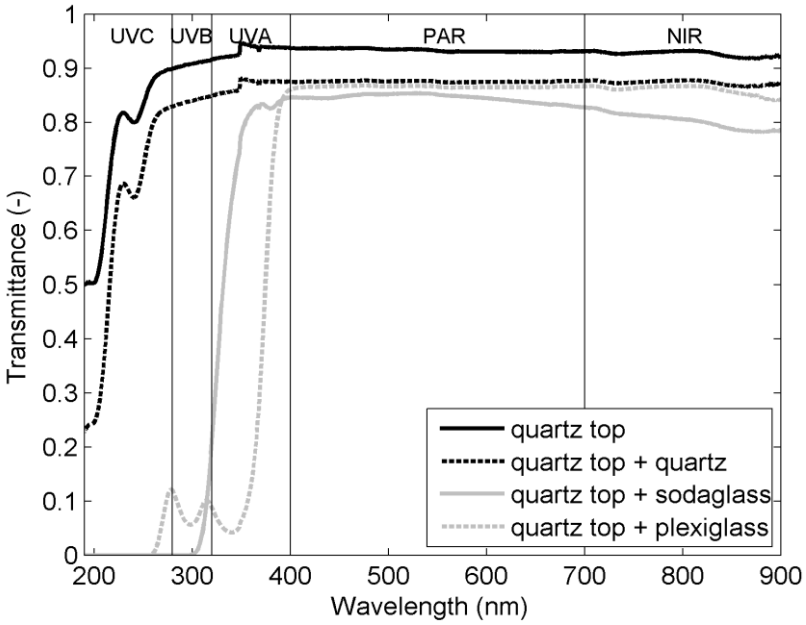

Figure 3.8 Measured transmittance of materials used as filters.

3.4.7. Experiment C: Different substrates

To determine whether different substrates would respond differently to exposure to solar radiation, grass and maize leaves were exposed in addition to the peat. Dead, dry grass mostly consisting of perennial ryegrass (*Lolium perene*) was collected from a sport field nearby the University on 5 Feb 2009. Senesced maize leaves (*Zea mays*) were collected from a cropped field close to Hamilton in the second half of March 2009.

3.4.8. Experiment D: Availability of oxygen

To determine whether atmospheric oxygen is needed to decompose OM to CO_2 through photodegradation, measurements were made of the CO_2 efflux from exposed peat in the absence of oxygen. A system was set up to flush the measurement system with nitrogen (N_2) gas, which was used to expel all oxygen from the air lines. A diagram of the altered setup is shown in Figure 3.9. Both hose clamps were open and nitrogen was forced from a gas cylinder under pressure into the air line. The pump of the IRGA was turned off during flushing.

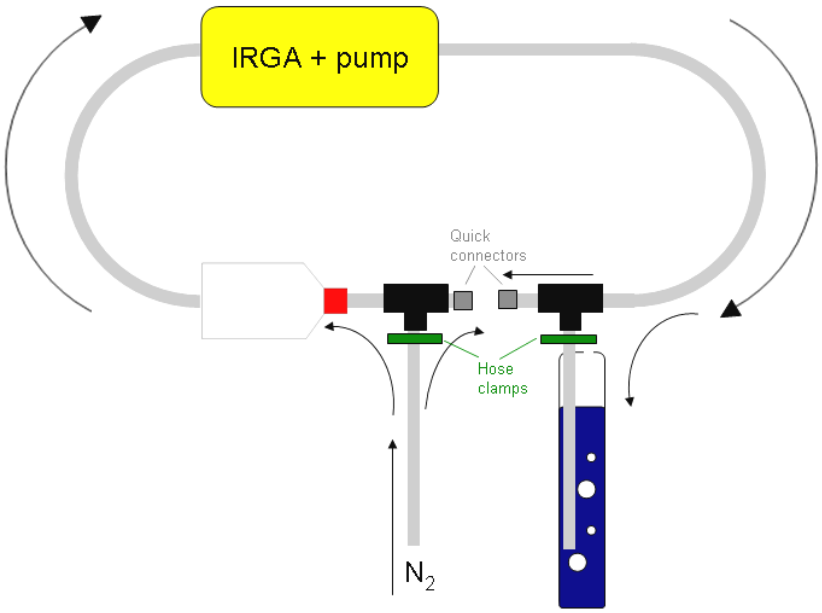

Figure 3.9 Setup for experiment D: expelling oxygen from the lines by flushing with nitrogen. Drawing not to scale.

Nitrogen gas was oozing out of the lines at the three openings: two exits that were later to be joined using quick-connectors and one exit in water. For 3 minutes nitrogen was left to enter the system with all exits open (as in drawing), after which the exits at the quick connectors were closed. After another 5 minutes, the quick connectors were connected up, and all excess nitrogen bubbled out of the water. The system was left to flush for an additional 10 minutes. After that, the nitrogen bottle was closed off, the hose clamps were closed, the pump of the IRGA was turned on and the system was ready for measurements.

3.4.9. Test without peat

Test runs (n = 14), where the empty container was exposed to and shaded from sunlight, confirmed that uptake or release of CO_2 by the container materials in response to exposure to irradiance was negligible (0.0159 and 0.0055 µmol CO_2 m^{-2} s^{-1} for sun and shade runs respectively) and not significantly different from zero (p = 0.15 and 0.65 for sun and shade runs respectively, Figure 3.10).

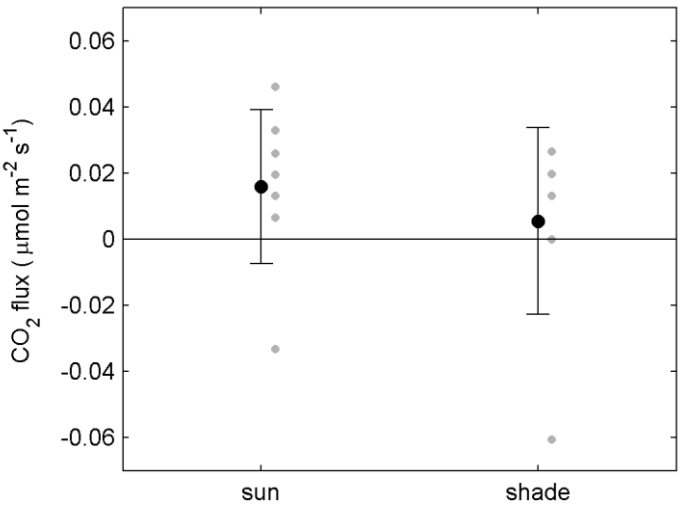

Figure 3.10 CO_2 flux from empty transparent container alternatively exposed to and shaded from solar irradiance during experiment A). Individual measurements are shown as grey points, means are shown as black points and error bars are the 95% confidence intervals (n = 7).

3.5 Additional data

3.5.1. CO_2 flux data from Californian grassland

Data source

CO_2 flux data collected using eddy covariance and soil CO_2 probes were used from two companion sites in California. All data were made available by Dr. Dennis Baldocchi and were collected and processed by his team at the Department of Environmental Science, Policy and Management, Ecosystems Science Division at the University of California, in Berkeley. Dr. Siyan Ma, Dr. Rodrigo Vargas, Dr. Jianwu Tang and Mr. Ted Hehn provided field assistance and computed the fluxes.

Site information

The eddy covariance measurements were made at an annual grassland site (Vaira Ranch, part of the AmeriFlux network) located in the lower foothills of the Sierra Nevada, near Ione, CA (38.4133°N, 120.9508°W, 129 m elevation). The soil is an Exchequer very rocky silt loam (Lithic xerorthents). The bulk density of the surface layer (0-30 cm) is 1.43 ± 0.10 g cm^{-3} (Baldocchi et al., 2004). The site is relatively flat and upwind fetch exceeded 200 m, which was found to be sufficient (Xu and Baldocchi, 2004). Species composition include *Brachypodium distachyon*, *Hypochaeris glabra, Trifolium dubium, Trifolium hirtum, Dichelostemma volubile* and *Erodium botrys* (Xu and Baldocchi, 2004).

The measurements of soil CO_2 flux using a below-ground CO_2 flux gradient system were collected at a companion site (Tonzi Ranch) located 2 km from the grassland site (38.4311°N, 120.966°W, 177 m elevation). This site is composed of oak/grass savanna. The soil is an Auburn very rocky silt loam (Lithic haploxerepts) and has a bulk density at the surface layer (0-30 cm) of 1.64 ± 0.11 g cm^{-3} (Baldocchi et al., 2004). Species of annual herbs and exotic grasses in the understory include *Brachypodium distachyon*, *Hypochaeris glabra*, *Bromus madritensis* and *Cynosurus echinatus* (Baldocchi et al., 2006).

The climate of the region can be described as Mediterranean, with hot and dry summers and cool and wet winters. Mean annual temperature at a

nearby climate station was 16.3 °C and average rainfall was 559 mm per year (1959-1977) (Baldocchi et al., 2004). During summer rainfall was virtually zero and the grass senesces. Figure 3.11 shows photographs of the grass taken at the beginning and end of the dry seasons of 2008 and 2009.

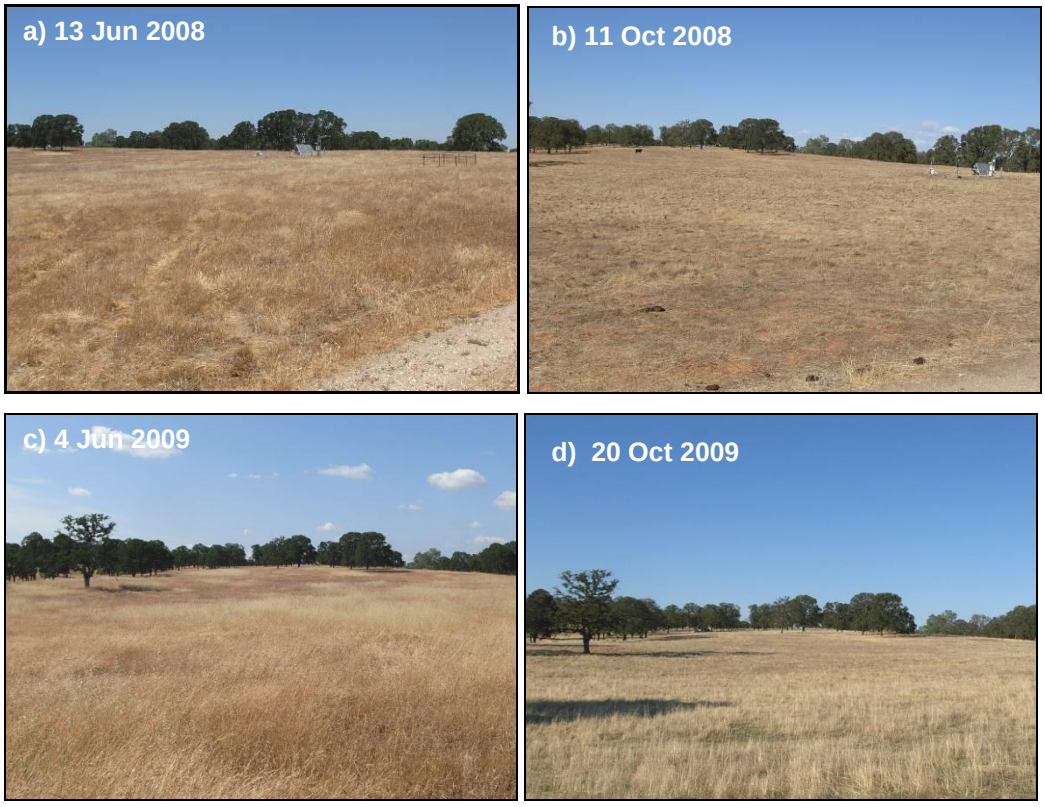

Figure 3.11 Vaira annual grassland at the beginning and end of the dry season for 2008 (a and b) and 2009 (c and d). Photos by Youngryel Ryu.

Instrumentation eddy covariance system and flux processing

The fluxes of CO_2 were measured over the grassland with the eddy covariance technique. The eddy covariance system was mounted at 2.0 m above the ground. It consisted of a 3-dimensional sonic anemometer (Model 1352, Gill Instruments Ltd, Lymington, England) and an open-path fast response infrared gas analyzer (IRGA, LI-7500). The raw data from each 30-min period were recorded at the rate of 10 Hz into separate files on a laptop computer. Standard micrometeorological software was used to compute flux covariances from the raw data. Computation procedures included spike removal, coordinate rotation,

application of standard gas laws, and correction for air density fluctuations (Webb et al., 1980). More detailed information for each procedure can be found in Xu and Baldocchi (2004) and Baldocchi et al. (2004). To select data when photosynthesis was zero during the dry season, eddy covariance CO_2 flux data were only used when the soil volumetric moisture content at 50 mm was < 0.038 m^3 m^{-3}. Data were also discarded when collected during rainfall, and 7 days thereafter.

CO_2 soil probe measurements

Measurements of soil respiration were collected at the oak/grass savanna site using a below-ground CO_2 flux gradient system (Tang et al., 2003). Soil CO_2 concentrations were measured at depths of 0.02, 0.08, 0.16 and 0.24 m, away from trees. Tree roots had negligible influence on the measurements, based on transect measurements of soil respiration using a manual chamber system (Tang and Baldocchi, 2005). CO_2 concentrations in the soil air were measured by solid-state infrared gas analyzers (GMT 222 and GMT 221, Vaisala CarboCap sensors). Soil respiration efflux rates were computed using flux-gradient theory. For a detailed description of the measurement and flux calculation see Baldocchi et al. (2006) and Tang et al. (2003).

Additional measurements

A 4-component net radiometer (CNR1, Kipp & Zonen, Delft, The Netherlands) mounted at 2.5m measured incident solar irradiance ($K\downarrow$, wavelengths between 310 and 2800 nm) and upward longwave radiation. Surface temperature was calculated from the upward longwave radiation signal using

$$T = \left(\frac{L\uparrow}{\varepsilon\sigma} \right)^{1/4} \qquad \textbf{Equation 3.6}$$

Where $L\uparrow$ is outgoing longwave radiation, ε is the emissivity of the surface (ε=0.98), σ = the Stefan Bolzmann constant ($5.67 \cdot 10^8$ $WK^{-4}m^{-2}$).

Soil volumetric water content was measured with a frequency-domain reflectometer probe (ML2x, Delta-T Devices, Burwell, Cambridge U.K.) at a depth of 50 mm.

3.5.2. UV irradiance at Torehape

UV irradiance levels for the peatland site in New Zealand were estimated using data supplied by National Institute of Water and Atmospheric Research (NIWA, Shiona et al., 2006). The calculated clear sky UV irradiation was used from the nearest station at Paeroa (37.378°S, 175.664°E, 4 m elevation, 19 km from the field site. This clear sky UV irradiation was adjusted for clouds following eq. 5 in Bodeker et al. (1996) using measured shortwave irradiance data from the peatland in combination with the calculated clear sky broadband radiation from NIWA. See Appendix C for more details on the procedure followed.

3.5.3. Differential scanning calorimetry

Differential scanning calorimetry was used to investigate whether thermal decomposition of peat occurred between 20 and 60 °C. Using this technique, the required energy input to heat up a small sample of peat in a pan was measured and compared to the energy input required to heat up an empty reference pan. Five samples (between 5 and 10 mg each) were analysed of both vacuum-dried and wet peat in standard pans using a DSC 6 Thermal Analysis System (Perkin Elmer, Norwalk, Connecticut, U.S.A.). Heating took place at 10°C per minute.

Chapter 4 Can ecosystem CO_2 exchange research ignore photodegradation?

4.1 Introduction

Studies into the carbon cycling of ecosystems commonly use eddy covariance (EC) to measure net CO_2 fluxes between the Earth's surface and the atmosphere. Net CO_2 flux is the sum of many processes of both uptake and release of CO_2, as discussed in Section 2.4.2. Usually, CO_2 emissions from ecosystems are assumed to result from biological processes alone, i.e. respiration by plants and microbes. There are also non-respiratory processes such as the weathering of carbonate rocks, fire or photodegradation that can contribute to CO_2 losses (Chapin et al., 2006; see Section 2.4.2). The dissolution and precipitation processes of carbonates in soils or parent material were identified as substantial contributors to CO_2 losses in some carbonate-rich ecosystems (Emmerich, 2003; Kowalski et al., 2008; Mielnick et al., 2005; Serrano-Ortiz et al., 2010). Also, fire can be an important process by which carbon is returned to the atmosphere (Beringer et al., 2007; Harden et al., 2000). However, most CO_2 exchange studies have ignored those non-respiratory processes.

Photodegradation is the abiotic process whereby solar radiation directly breaks down the compounds of dead organic matter. Although this process has received much attention in aquatic ecosystems, research into photodegradation in terrestrial ecosystems is relatively new and has mostly focussed on mass loss of exposed litter. Two small scale studies have confirmed that exposure of litter to radiation can directly result in CO_2 production even in the absence of microbial activity (Anesio et al., 1999; Brandt et al., 2009). These findings suggest that photodegradation might be another non-respiratory process that could contribute to the CO_2 efflux from ecosystems. However, no studies to date have examined whether CO_2 loss caused by photodegradation can be detected at large scales, or what the potential contribution of photodegradation could be to the total CO_2 losses of an ecosystem.

The objectives of this chapter are to 1) show that CO_2 produced through photodegradation is detectable at large scales; and 2) give an estimate of the contribution of photodegradation to the total CO_2 loss for a bare peatland and a grassland. This chapter does not aim to explicitly explore the drivers of photodegradation, which will be discussed in the next chapter. Some of the findings presented in this chapter are part of a paper that has been accepted for publication by Global Change Biology (Rutledge et al., 2010).

4.2 Study sites and methods

4.2.1. Study sites and measurements

Field measurements of CO_2 flux made in two ecosystems form the basis of this chapter: a bare peatland and a seasonally dry grassland (see Sections 3.2 and 3.5.1 for site descriptions). Both ecosystems had dead organic matter (OM) at the surface exposed to high ambient levels of solar irradiance when microbial activity was low due to water limitation. For the grassland data were only used when collected during the dry period when the grass was dead.

A combination of methods was used to test the potential influence of incident solar irradiance on the CO_2 flux (See Section 3.1). Refer to Sections 3.3 and 3.5.1 for an overview of the methods. In short, EC was used to measure the total CO_2 flux, whereas an opaque chamber (which blocks out radiation during the measurements), soil CO_2 probes (which measure CO_2 produced belowground only) and night-time EC measurements were used to isolate the CO_2 efflux of biological origin. The difference between the total flux and the biological flux provides an estimate of the irradiance-induced flux (Section 3.1). Refer to Table 4.1 for a summary of field site information and the methods used.

Table 4.1 Summary of field site information and methods used. See Section 3.1, 3.3 and 3.5.1 for more information.

Ecosystem	Bare peatland	Annual grassland
Country	New Zealand	California, USA
Method total CO_2 flux	Eddy covariance	Eddy covariance
Method biological CO_2 flux	Opaque chamber/ night-time EC	Soil CO_2 probes/ night-time EC
Vegetation	No plants (some algae in ponds when wet in winter)	Annual grasses which completely senesces during the dry season
Data used	All seasons	Only the dry season when grass was dead

4.2.2. Data analysis

Estimation of cumulative CO_2 losses

To calculate total yearly CO_2 losses from the peatland, a model was constructed using lookup tables of EC fluxes defined by bins of volumetric moisture content (VMC) at 50 mm depth (3 bins with equal number of data points: VMC < 0.50 m^3 m^{-3}, 0.50 m^3 m^{-3}< VMC < 0.56 m^3 m^{-3} and VMC > 0.56 m^3 m^{-3}), incident solar irradiance (bins of 100 W m^{-2}) and soil temperature at 5 mm depth (bins of 2°C). Each bin required a minimum of five data points to make an average.

To estimate the irradiance-induced part of the flux for each half hour, the difference was taken between the total CO_2 flux from the lookup table, and the estimated dark (night-time) CO_2 flux at the same temperature and in the same moisture bin. Night-time CO_2 fluxes were estimated using two different regression equations of CO_2 flux as a function of soil temperature for each soil moisture class. As a conservative estimate of the night-time flux, a linear regression between soil temperature and measured flux was used (R^2 = 0.64, 0.45, 0.24 for dry, medium and wet soil moisture class respectively). As a second estimate of night-time flux, the Lloyd and Taylor equation was fitted (Lloyd & Taylor 1994; R^2 = 0.76, 0.71, 0.02 for dry, medium and wet soil moisture classes respectively). By combining the daytime value for the CO_2 flux from the lookup table with the two estimates for night-time flux and summing the differences

over the year, two estimates were calculated for annual contribution of photodegradation to the total CO_2 flux.

For the grassland site, a very similar but slightly simpler method was used to estimate the cumulative contribution of irradiance-induced CO_2 flux to the total CO_2 flux during the dry season. A lookup table of EC fluxes, defined by bins of incident solar irradiance (bins of 100 W m^{-2}) and surface temperature (bins of 2°C), was made using the data from the dry season. In contrast to the peatland site, soil moisture was not used to develop lookup tables because the values of soil VMC were very low with a very narrow range during the senescent period ($0.03 < VMC < 0.04$ m^3m^{-3}); therefore no effect of moisture was expected. Night-time CO_2 fluxes were estimated using the median value of all night-time EC measurements during the dry period, because night-time EC flux showed no clear trend with surface temperature (data not shown). An estimate for the cumulative contribution of photodegradation to the total CO_2 flux during the dry season was calculated by subtracting the estimated night-time flux from the daytime value for the CO_2 flux from the lookup table and summing all half-hourly values for the dry season.

An alternative approach for calculating the irradiance-induced part of the CO_2 flux for the grassland was to calculate the contribution on a 'typical' or average day. The mean diurnal variation was calculated for the EC and probe fluxes resulting in 48 half-hourly values for an average day (Figure 4.5b and c). The sum of these 48 values was used as an estimate of the mean daily total (EC) and biological (probe) flux. The irradiance-induced portion of the flux was calculated by subtracting the probe flux from the total flux. This 'typical day approach' was not attempted for the peatland because the conditions throughout the year varied substantially and chamber measurements were not available for all times of the year.

Statistics

A multiple regression analysis was carried out to test whether solar irradiance explained a statistically significant proportion of variation in abiotic flux (here defined as "the CO_2 flux measured using EC minus CO_2 flux measured

using chamber or soil probes") in addition to the variation explained by soil temperature and soil moisture. The RAR1 procedure in GenStat (Version 11.1.0.1535) was used where fitted terms were: a constant, soil temperature, soil moisture content and solar irradiance. The analysis used REML (residual maximum likelihood) to model correlated regression errors for contiguous blocks of observations (i.e. within observation days).

To test whether the differences between CO_2 fluxes measured by EC and those measured by chamber or soil probes were significantly different from zero at different levels of solar irradiance a one-sample t-test was used (95% significance level, Matlab, Version 7.3.0.267, R2006b). Prior to testing, flux differences were binned by incoming solar irradiance (bin width 150 W m^{-2}) and averaged daily by bin to avoid issues with correlated data within observation days.

4.3 Results

4.3.1. Two-fold evidence of irradiance-induced CO_2 production

In this section, two lines of evidence will be presented that the production of CO_2 from OM was in part due to degradation by solar irradiance. For the first, daytime EC fluxes will be compared to daytime chamber or probe data. For the second, day- and night-time EC data will be compared.

Comparison between eddy covariance and chamber or probes

To examine the contribution of incident solar irradiance ($K\downarrow$) to the total CO_2 fluxes, fluxes measured by chamber (chamber fluxes) and soil probes (probe fluxes) were compared to fluxes measured by EC (EC fluxes) for different levels of solar irradiance. Direct comparison of these fluxes was only made when fluxes were measured less than 15 minutes apart.

At night ($K\downarrow$ = 0 W m^{-2}), EC fluxes agreed well with chamber and probe fluxes (Figure 4.1). However, during the day ($K\downarrow$ > 0 W m^{-2}) there was a large discrepancy between EC fluxes and fluxes measured by chamber and soil probes. This discrepancy increased with increasing incident solar irradiance (Figure 4.1 c and d). At the peatland, the average difference between EC and chamber fluxes

at high irradiances ($K\downarrow$ around 1000 W m^{-2}), was almost 2 µmol m^{-2} s^{-1} (Figure 4.1b). The EC flux was approximately 2.5 times larger than the chamber flux in those instances. At the grassland, the average difference between EC and probe fluxes at high irradiances was 1.1 µmol m^{-2} s^{-1} (Figure 4.1d). The EC flux was 12.5 times larger than the probe flux in those instances, because the probe fluxes were extremely low.

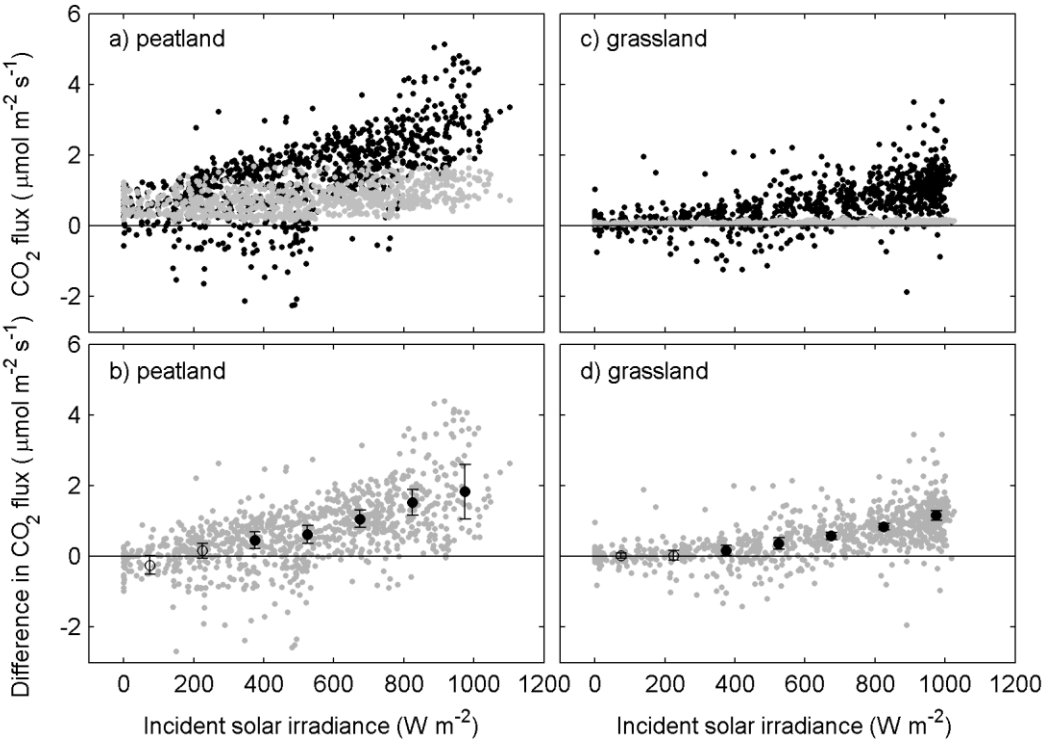

Figure 4.1 Illustration of the effect of irradiance on CO_2 fluxes measured at the peatland (panels a and b) and the grassland (panels c and d). Fluxes were measured by eddy covariance (black points, panel a and c), opaque chamber (for peatland, grey points in panel a) and soil CO_2 probes (for grassland, grey points in panel c). Grey points in panels b and d are the difference in flux between total CO_2 flux (from EC) and biological CO_2 flux (from chamber or probes). Positive values depict instances where the EC system measured larger CO_2 fluxes than the chamber or probes. Large circles in panels b and d are bin averages with error bars showing 95% confidence intervals. For the open circles, the difference between the total and biological CO_2 flux were not statistically different from zero (one sample t-test at a 95% significance level). For the filled symbols, the difference was statistically different from zero. Figure was reprinted from (Rutledge et al., 2010) with permission from John Wiley and Sons.

Incoming solar irradiance and soil temperature are very strongly correlated (Figure 4.2) and separation of these potential drivers is needed to determine whether temperature or irradiance caused the discrepancy between EC fluxes and chamber or probes fluxes. Multiple regression analyses confirmed

that for both sites the effect of solar irradiance explained a significant proportion of variation in the discrepancy between the EC CO_2 fluxes and chamber or soil CO_2 fluxes in addition to the variation explained by temperature of the peat (for the peatland) or surface (for grassland) and soil moisture (P<0.001, Table 4.2).

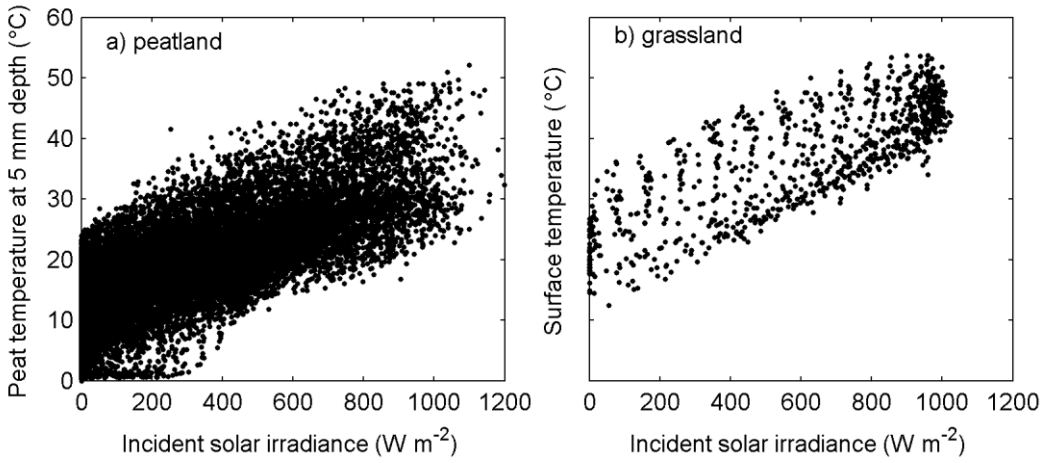

Figure 4.2 Correlation between solar irradiance and soil temperature at the a) peatland and b) grassland. Correlation coefficients were 0.76 and 0.80 for the peatland and grassland, respectively.

Table 4.2 Estimates of parameters of multiple regression analyses on peatland and grassland data Multiple regression equation with abiotic flux (here defined as "the CO_2 flux measured using eddy covariance minus the CO_2 flux measured using chamber or soil probes") as dependent variable and temperature, soil moisture content and solar irradiance as independent variables. The percentage of the variance that was explained by the total regression was 27.0% and 24.7% for the peatland and grassland regressions, respectively. The number of observations is represented by *n*.

Parameter	Estimate coefficient	Standard error	*t*-statistic	P value
Peatland (n= 908)				
Constant	-1.2	1.43	-0.82	0.415
Soil temperature	0.042	0.013	3.3	0.001
Soil moisture content	-0.20	2.5	-0.08	0.937
Solar irradiance	0.0019	0.00020	9.2	<0.001
Grassland (n = 885)				
Constant	-0.48	0.64	-0.76	0.448
Surface temperature	0.025	0.00603	4.2	<.001
Soil moisture content	-7.1	20	-0.35	0.728
Solar irradiance	0.00065	0.00015	4.3	<0.001

Comparison between day- and night-time eddy covariance

The second approach to determine the irradiance-induced portion of the total CO_2 flux was to compare day- and night-time EC fluxes in the same temperature ranges (Figure 4.3). This approach allowed visual separation of the controls of temperature and solar irradiance on CO_2 fluxes. This comparison showed that solar irradiance had a direct effect on CO_2 fluxes measured by EC: at both sites, CO_2 fluxes increased with increasing radiation when comparing fluxes measured at equal temperatures (Figure 4.3 a and b).

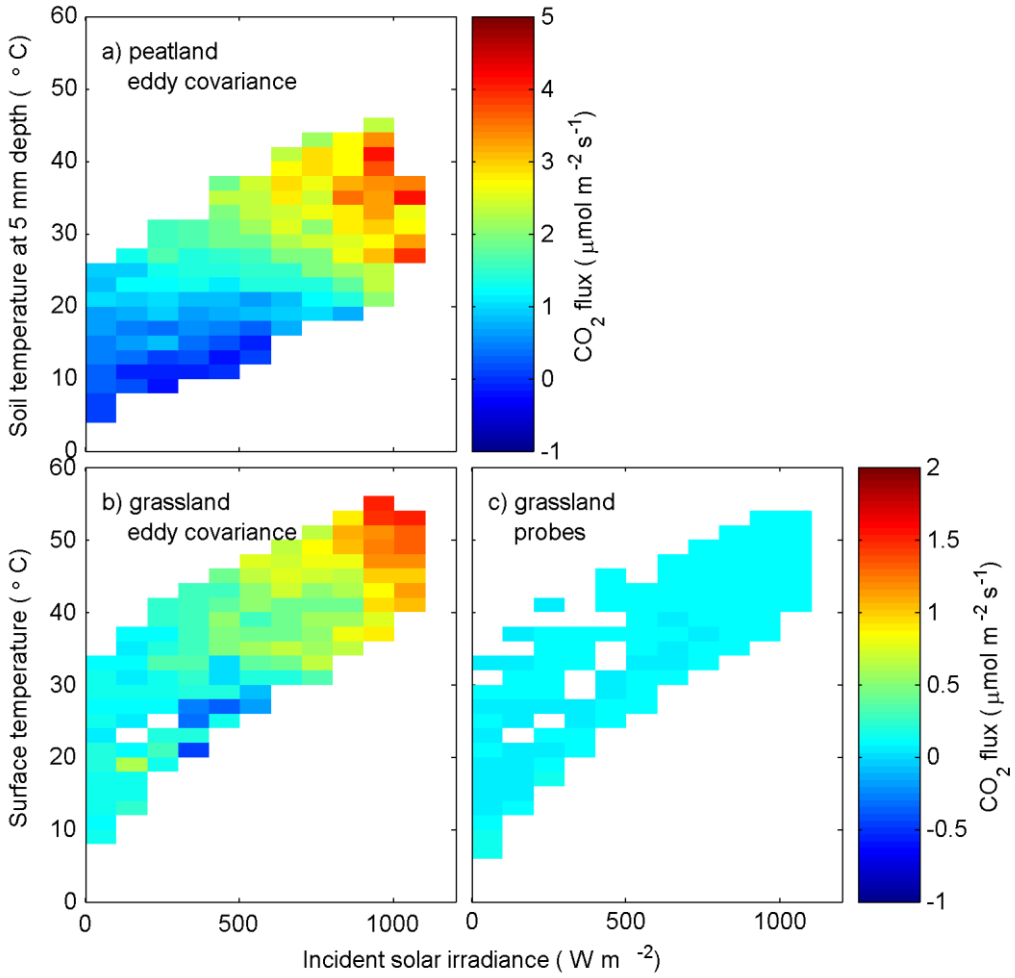

Figure 4.3 Effect of irradiance on CO_2 fluxes from the peatland (panel a) and the annual grassland (panels b and c) measured by eddy covariance (panels a and b) and soil CO_2 probes (panel c). CO_2 fluxes were averaged across intervals defined by incident solar irradiance (bin width 100 W m^{-2}) and temperature (bin width 2 °C). Note that the scales on the colour axes are different between the two sites. Panels a and b were reprinted from (Rutledge et al., 2010) with permission from John Wiley and Sons.

The probe data (Figure 4.3c) collected at the grassland did not show any increase in CO_2 flux with incoming solar irradiance like the EC data. Controls of CO_2 fluxes from peat measured by the chamber cannot be separated into radiation and temperature effects because the chamber closes during a measurement and blocks all solar irradiance, which means that the peat in the chamber is not exposed to the ambient irradiance levels during the measurements.

At the peatland, the effect of irradiance on the CO_2 flux was most pronounced when the surface peat was dry, but could also be observed when the peat was moist (Figure 4.4).

4.3.2. Average contribution of photodegradation to the total CO_2 flux

Using the lookup tables, the calculated yearly losses of CO_2 for June 2005 – May 2007 at the peatland averaged 269 g C m^{-2} y^{-1}. Using the linear regression to estimate the night-time flux, the contribution of photodegradation to the total flux was estimated to be 66 g C m^{-2} y^{-1} (25% of the total CO_2 flux). When using the Lloyd and Taylor equation, 34 g C m^{-2} y^{-1} (13% of the total CO_2 flux) was estimated to be a result of photodegradation. The average of these two results was approximately 50 g C m^{-2} y^{-1} (19% of total CO_2), or 0.14 g C m^{-2} d^{-1}.

For the grassland, the contribution of photodegradation could only be estimated for the dry season when no uptake of CO_2 by photosynthesis occurred. During the entire 2007 dry season, the CO_2 loss from the grassland was estimated to be 27 g C m^{-2} (or 0.314 g C m^{-2} d^{-1}), of which approximately 16 g C m^{-2} (or 0.186 g C m^{-2} d^{-1}) was irradiation-induced, equalling almost 60% of the total dry season CO_2 flux.

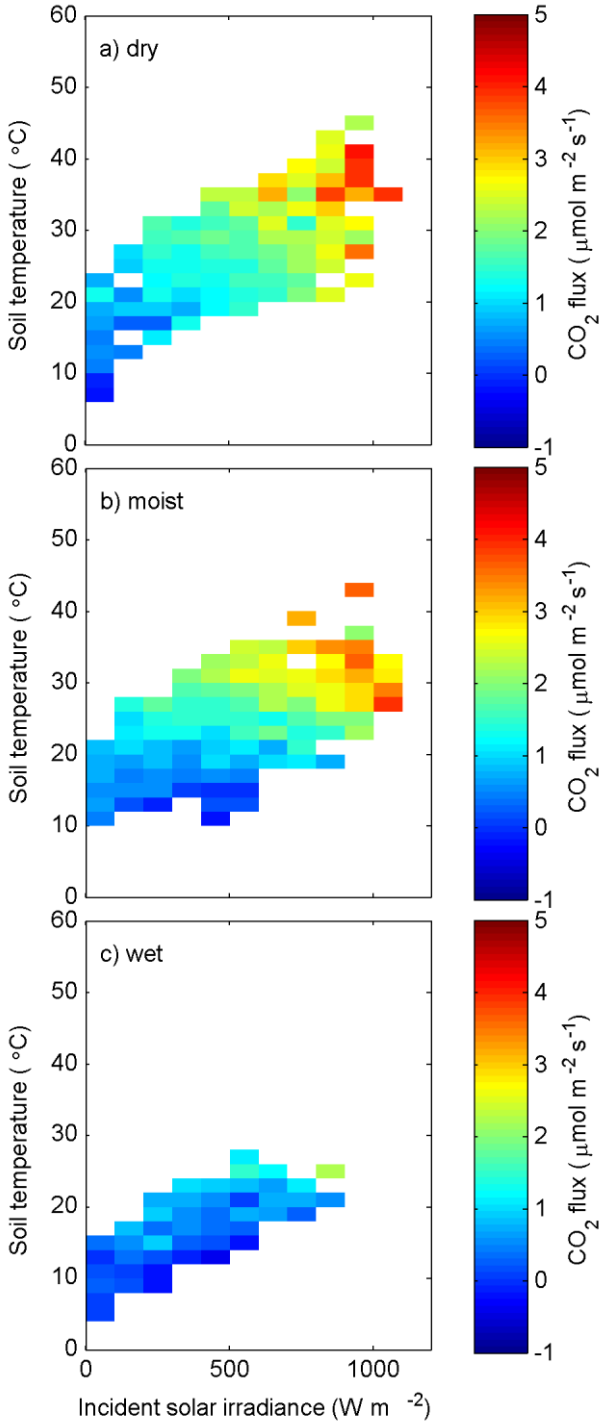

Figure 4.4 Effect of solar irradiance and soil temperature on CO_2 fluxes measured by eddy covariance at the peatland for different soil moisture contents. CO_2 fluxes were averaged by intervals defined by incident solar irradiance (bins width 100 W m^{-2}) and soil temperature at 5 mm depth (bin width 2 °C) under a) dry (volumetric moisture content of peat at 50 mm depth VMC < 0.5 m^3 m^{-3}), b) moist (0.5 m^3 m^{-3}<VMC< 0.56 m^3 m^{-3}) and c) wet (VMC > 0.56 m^3 m^{-3}) conditions. Figure was reprinted from (Rutledge et al., 2010) with permission from John Wiley and Sons.

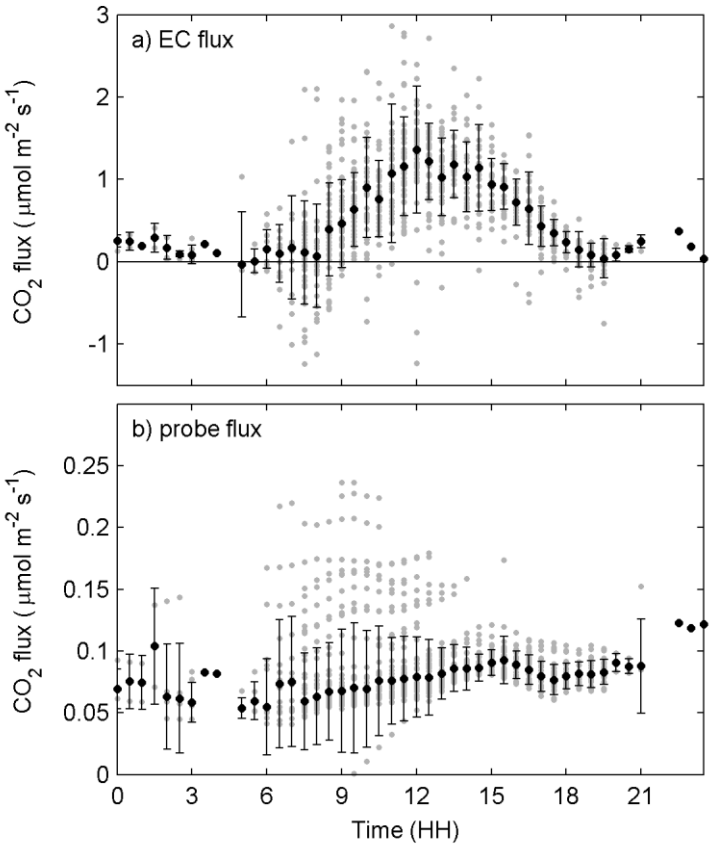

Figure 4.5 All available data (grey dots) and mean diurnal variation (black dots) for a) EC flux and b) probe flux during the dry season at the grassland. Error bars are ± 1 standard deviation. Note that the scales on the y-axes differ between the panels.

The 'typical day approach' resulted in the mean diurnal variation of EC and probe fluxes presented in Figure 4.5. Daily sums of fluxes are listed in Table 4.3. The approach using mean diurnal variation resulted in larger estimates for the irradiance-induced portion of the total CO_2 flux than the lookup table approach described above (82 % vs. 58 %, Table 4.3).

Table 4.3 Estimates of cumulative C losses (as CO_2) from the grassland for a typical day in the dry season. Fluxes are in g C m^{-2} d^{-1}. The results of the lookup table are added for comparison.

	Mean of data	Lookup table
Total flux	0.451	0.314
Biological flux	0.0830 (probe)	0.128 (median of night-time EC)
PD flux *	0.368	0.186
Ratio PD/EC	0.82	0.58

* calculated by subtracting the biological flux from the total flux

4.4 Discussion

4.4.1. Size of total and irradiance-induced flux

The estimated yearly CO_2 losses from the bare peat of 269 g C m^{-2} y^{-1} (or between 203 and 225 g C m^{-2} y^{-1} without the irradiance-induced component of the flux) fall within the wide range of CO_2 losses measured from other bare peatlands, which ranged from 62-2,628 g C m^{-2} y^{-1} (see Table 2.3), with the majority of measured respiration rates falling below 1278 g C m^{-2} y^{-1}. Many of these studies measuring CO_2 losses from bare peat only report fluxes summed over (spring and) summer, which probably results in relatively high average rates that are not representative of the whole year. The value established at the current study site is an average for two whole years, which might explain why it lies at the low end of the range in values presented in Table 2.3.

The annual carbon loss via photodegradation at the peatland (34–66 g C m^{-2} yr^{-1}) was substantial compared to net ecosystem production (NEP) for other ecosystems (e.g. average NEP across a range of ecosystems was 181 g C m^{-2} yr^{-1} (Baldocchi, 2008a)). Estimates of irradiance-induced CO_2 fluxes at the grassland varied from 16 to 32 g C m^{-2} for the 2007 dry season, depending on the method used for calculation. The irradiance-induced flux made up 58 to 82% of the total flux (Table 4.3). Of these two estimates, the one that was derived from EC data using the lookup table (58%) was likely the most reliable, because it depended on data collected using only one method (EC) at one study site. This estimate is at the upper end of the range of estimates of the contribution of photodegradation to mass loss in dry ecosystems of between 32 and 60% given by Austin & Vivanco (2006) and Gallo et al. (2009).

During midday on sunny days in summer, when incoming solar irradiance and temperature were highest, the CO_2 efflux due to photodegradation contributed as much as 62% and 92% of the total half-hourly CO_2 flux from the peatland and grassland respectively. While the absolute values of irradiance-induced fluxes were generally smaller at the grassland than at the peatland (Figures 4.1 and 4.3), the large percentage contribution of photodegradation at the grassland was mostly caused by the very low biological CO_2 fluxes during the

dry period (generally < 0.1 µmol CO_2 m^{-2} s^{-1}, see Figure 4.5). In contrast, biological fluxes at the peatland were highest during summer (see Section 6.3.1).

At the grassland, much of the standing dead grass tends to disappear during the dry season even when conditions are too dry for microbial degradation (compare photos at the beginning and end of the dry season in Figure 3.11). With a contribution of almost 60% to the total CO_2 flux, photodegradation appears to be the major pathway for degradation of the grass during these dry periods.

Even though the percentage contribution of photodegradation to the total CO_2 flux at the grassland site was high, the absolute CO_2 fluxes during dry seasons are generally much lower than during wet seasons when microbes are not limited by moisture (e.g. Xu and Baldocchi, 2004; Xu et al., 2004). For example, annual average ecosystem respiration at the grassland site from 2000 to 2006 was estimated to be > 900 g C m^{-2} y^{-1} (Ma et al., 2007). However, compared to the average NEE (38 g C m^{-2} y^{-1}; Ma et al., 2007) the dry season irradiance-induced flux of 16 g C m^{-2} y^{-1} is substantial.

The estimates of the CO_2 loss through photodegradation at both the peatland (34–66 g C m^{-2} yr^{-1}) and the grassland (16 g C m^{-2} for the dry season) are much greater than the estimate presented by Brandt et al. (2009), who extrapolated CO_2 flux measurements made from sterile litter in microcosms to field conditions. They estimated irradiance-induced CO_2 loss of 4 g C m^{-2} yr^{-1} from litter in a desert grassland in New Mexico by assuming that 100% of the surface area was covered with litter. The causes for this large difference between the measurements of this study and the estimate from Brandt et al. (2009) are as yet unclear, but are likely to be related to differences in substrate species/quality and experimental conditions (e.g., sterile conditions in the microcosms vs. non-sterile conditions in the field and partial blocking of irradiance by the sides of the microcosm). In the next chapter, the comparison between measurements made in the field and in microcosms or containers will be explored further. More attention will be paid to the potential drivers causing the difference in findings between studies.

The calculated CO_2 loss from the peatland can be converted to a depth of peat decomposed each year. Using the dry bulk density of 135 kg m^{-3} and assuming the carbon content of OM is approximately 50% (Blanco-Canqui and Lal, 2004; Joosten and Clarke, 2002) the CO_2 loss of 270 g C m^{-2} y^{-1} equates to change in peat level (subsidence) of 2.5 mm y^{-1}, of which 0.45 mm is caused by photodegradation.

4.4.2. Potential implications for other ecosystems

Results of the current study suggest that photodegradation may be an important contributor to CO_2 loss in a potentially wide range of ecosystems where soil organic matter, litter and/or standing dead material are exposed to solar irradiance (Smith et al., 2010; Throop and Archer, 2009). Ecosystems that might be affected include arid and semi-arid ecosystems, barren peat areas in tundra, bare burnt areas, ecosystems that are sparsely vegetated like shrublands, savannas and other grasslands, agricultural sites after cultivation or harvest (especially when crop residues are left on the surface), deciduous forests after leaf fall, ecosystems during prolonged drought, or ecosystems with a naturally large amount of exposed standing dead material like peat bogs (Thompson et al., 1999) and other wetlands (Kuehn et al., 2004). The magnitude of photodegradation in these other ecosystems is likely to be less than the 34–66 g C m^{-2} yr^{-1} that was found at the peatland because the conditions will be less favourable for photodegradation. Most ecosystems have a lower amount of accumulated exposed OM (especially arid and semi-arid ecosystems) or the dead OM is only exposed to solar irradiance during part of the year (e.g. harvested cropland or ecosystems during seasonal drought like the Californian grassland). In some ecosystems, OM will be exposed to levels of incoming solar irradiance that are lower than in this study, (e.g. exposed peat in tundra in boreal regions (Repo et al., 2009) and deciduous forests where litter will only be exposed in winter). In other ecosystems, for example Australian woodland savannas, the senesced understory is burned every few years (Beringer et al., 2007), in which case the cumulative impact of photodegradation on the CO_2 losses will also be small. However, breakdown of OM by photodegradation might still affect the

carbon cycling and functioning of these ecosystems as photodegradation could reduce the accumulation of dead grasses and therefore fuel load and intensity of the fires.

In many vegetated terrestrial ecosystems much of the dead organic matter (litter and SOM) is shaded from sunlight by live leaves above. Studies into the production of carbon monoxide resulting from photodegradation suggest that live leaves are 9 to 10 times less susceptible to photodegradation than senesced litter (Tarr et al., 1995; Yonemura et al., 1999). This could be explained by a variety of protection and repair mechanisms in plants that prevent or limit the damage to their tissue from harmful UV (Caldwell et al., 1999; Yonemura et al., 1999). In contrast, Anesio et al. (1999) found that the difference in CO_2 production between fresh and aged litter exposed to UV-A and UV-B irradiance could fully be explained by the difference in exposed leaf area perpendicular to the direction of the radiation source, with the emitted CO_2 per area exposed being equal between live and dead leaves. These findings would suggest even live material might be susceptible to photodegradation.

4.4.3. Implications for measurements and modelling

There are several important implications of photodegradation for the current approaches to measurement and interpretation of CO_2 fluxes.

Measurements of carbon lost from soil

Opaque chambers and soil CO_2 profiles are commonly used to measure CO_2 efflux from the soil surface and may significantly underestimate actual CO_2 fluxes because they do not measure the irradiance-induced portion of the CO_2 flux. For example, when the contribution of photodegradation to the total CO_2 flux was at its maximum, chamber and soil probe readings of CO_2 flux underestimated the total CO_2 efflux by as much as 75 and 90% for the peatland and grassland respectively. Also, for studies which aim to measure net ecosystem exchange of CO_2 of vegetated ecosystems using transparent chambers placed over plants, it is important that the chambers are transparent not only to photosynthetically active radiation, but also to radiation in the UV wavelengths.

Otherwise, the photodegradation component of the CO_2 efflux might be underestimated, leading to overestimates of the net CO_2 sequestration.

Partitioning of NEE

Ecosystem studies of carbon cycling using the EC methodology measure net CO_2 exchange and generally aim to partition the net daytime flux of CO_2 (NEE) into photosynthesis (GPP, carbon gained by the ecosystem through photosynthesis) and ecosystem respiration (ER, carbon lost from the ecosystem). Refer to Section 2.2.1 and Figure 2.3 for definitions. The most commonly used approach to partition fluxes is based on the assumption that –NEE equals NEP (e.g. Baldocchi, 2008a; Desai et al., 2008; Luyssaert et al., 2009; Ma et al., 2007; Strack et al., 2008).:

$$-\mathrm{NEE} \approx \mathrm{NEP} = \mathrm{GPP} - \mathrm{ER} \qquad \textbf{Equation 4.1}$$

ER during the day is estimated either by using a model based night-time respiration rates (Desai et al., 2008; Falge et al., 2002; Reichstein et al., 2005a), or by extrapolation of the light-response curve of NEE to zero radiation (e.g. Falge et al., 2002; Gilmanov et al., 2007; Suyker and Verma, 2001; Wohlfahrt et al., 2005; Xu and Baldocchi, 2004). Daytime photosynthesis is calculated using

$$\mathrm{GPP} = \mathrm{NEP} + \mathrm{ER} \approx -\mathrm{NEE} + \mathrm{ER} \qquad \textbf{Equation 4.2}$$

However, this approach does not take into account photodegradation (and other non-respiratory CO_2 losses) that could contribute to daytime CO_2 losses from the ecosystem (Figure 2.3). If photodegradation is contributing to CO_2 losses, –NEE cannot be assumed to equal NEP, and the correct equation is

$$-\mathrm{NEE} = \mathrm{GPP} - \mathrm{ER} - \mathrm{PD} \qquad \textbf{Equation 4.3}$$

and

$$\mathrm{GPP} = \mathrm{NEP} + \mathrm{ER} = -\mathrm{NEE} + \mathrm{ER} + \mathrm{PD} \qquad \textbf{Equation 4.4}$$

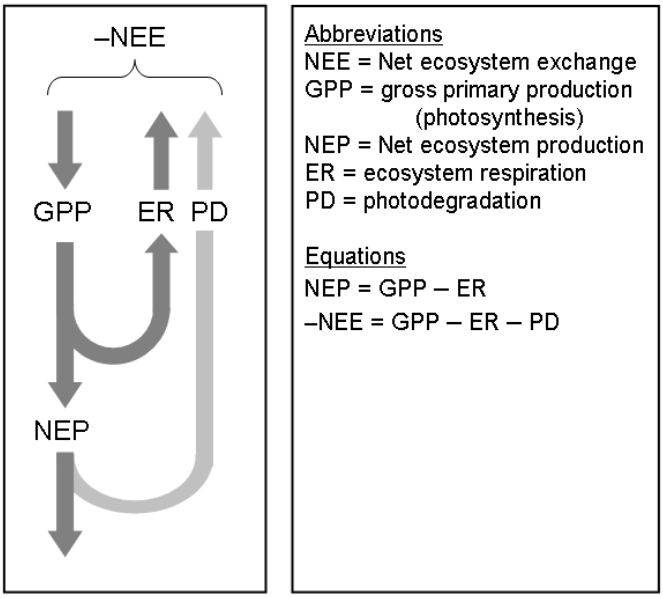

Figure 4.6 Diagram summarising the terms commonly used in describing fluxes of CO_2 in micrometeorological studies. The figure is a simplified version of Figure 2.3, was adapted from Luyssaert et al. (2007) and is based on definitions given by Chapin et al. (2006).

In an ecosystem where irradiance-induced fluxes are substantial NEE could diverge quite substantially from –NEP. Applying Equation 4.1 (thereby neglecting photodegradation) might lead to an underestimation of the total CO_2 lost during the day, consequently leading to an underestimate of daytime photosynthesis. This is illustrated in Figure 4.7.

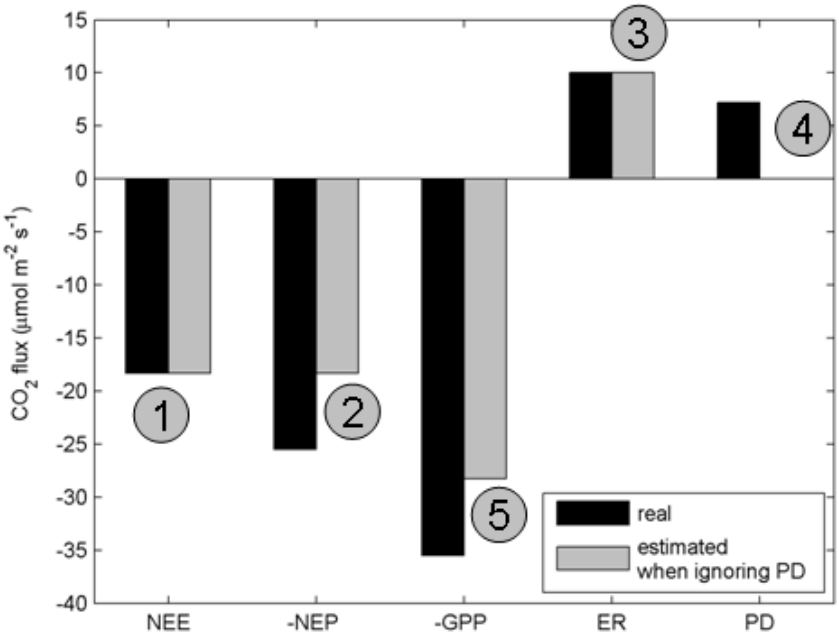

Figure 4.7 Example illustrating how the assumption that –NEE ≈ NEP (and therefore PD = 0) when partitioning NEE into its gross components can lead to an underestimation of GPP. This graph shows example actually occurring component fluxes (labelled 'real', black bars), and the component fluxes as estimated when assuming that NEE = –NEP, thereby ignoring photodegradation (grey bars). Values of fluxes serve as an example only. The steps of the flux partitioning process are indicated by the numbers in grey circles:

Step 1: NEE is measured.
Step 2: NEP is assumed the same as –NEE.
Step 3: ER is correctly estimated
Step 4: PD is (often implicitly) ignored (grey bar = 0)
Step 5: GPP is calculated using Equation 4.2 instead of Equation 4.4

The result of the incorrect assumption is that total CO_2 emissions to the atmosphere are underestimated, which leads to an underestimation of GPP by the size of PD.

Carbon cycling models

Most organic matter turnover models, like the two commonly used models CENTURY and Rothamsted (Kirschbaum, 2009), do not take into account OM decomposition through photodegradation, or only in a very simplified way (e.g. as a constant in model CenW, Kirschbaum, Oct 2009; Kirschbaum et al., 2007 and references therein). Several studies have already indicated that the traditional models that use moisture, temperature and some measure of substrate quality are unable to satisfactorily describe decomposition rates in arid regions (e.g. Meentemeyer, 1978; Montana et al., 1988; Parton and Silver, 2007; Whitford et al., 1981) where photodegradation is expected to be important. Increasing our understanding of the size and drivers of photodegradation across

a range of ecosystems is critical for continued development of carbon cycling models that properly account for irradiance-induced CO_2 losses.

4.4.4. Methodological considerations

Confidence in methodologies

The conclusions drawn in this chapter partly rely on the assumption that the three methodologies used to measure the CO_2 flux from the surface (EC, chamber and soil CO_2 probes) generally produce the same values when measuring the same CO_2 flux. In this study, good agreement was reached between night-time fluxes from EC and chamber and EC and probes (Figure 4.1 b and d), which proves the quality of the flux measurements from all three methods. At the grassland, an earlier comparison study was conducted which confirmed that values measured using the soil CO_2 probe technique were the same as those measured using a chamber (Tang et al., 2003).

Several comparison studies over bare surfaces have shown that reasonable agreement can be reached between EC and chambers (Dugas, 1993; Ham and Heilman, 2003; Kabwe et al., 2005). In some studies when night-time measurements are compared, different values are obtained from EC and chambers (e.g. Goulden et al., 1996; Lavigne et al., 1997; Ohkubo et al., 2007 and references therein). In those cases, it is usually the EC values that measure lower CO_2 efflux values than the chamber (Baldocchi, 2003; Loescher et al., 2006; Section 2.5.1). This discrepancy is often caused by the underestimation of EC fluxes resulting from the lack of turbulence at night (Drewitt et al., 2002; Goulden et al., 1996; Lavigne et al., 1997). In the current study the observed discrepancy between daytime EC and chamber/probes was reversed: EC values were larger than chamber fluxes.

Density term

Changes in temperature and water vapour concentrations cause changes in CO_2 concentrations of air close to the Earth's surface that do not reflect an exchange of CO_2 at the surface-atmosphere interface. To correct for this apparent flux caused by fluctuations in temperature and water vapour, the

density (or WPL) term needs to be added to the raw CO_2 flux data to obtain real CO_2 fluxes (Leuning, 2004; Leuning, 2007; Webb et al., 1980). The WPL term is generally largest under sunny and dry conditions (Webb et al., 1980) which were encountered both at the peatland and the grassland during summer. Under these conditions it was common for the magnitude of the density term to be larger than the raw CO_2 flux such that adding the WPL term lead to a more positive flux, which indicated larger CO_2 losses from the surface.

At the start of the study I assumed that the flux consisted exclusively of microbial respiration. However, in the peatland system, day-time EC fluxes did not agree with the chamber measurements. This observation cast doubt upon the validity of the EC fluxes and WPL term under these conditions. A review of background information on the WPL term, examples of the size of the WPL term at the study sites and an analysis of potential errors in the WPL term at the peatland and grassland can be found in Appendix D. In short, accurate determination of the density term is most challenging under hot and dry conditions because of potential error propagation (see Section D.1.2). Error propagation is the phenomenon whereby errors and uncertainties in the sensible (and the latent) heat fluxes propagate through the algorithm for the density term and therefore influence the resulting CO_2 flux and its uncertainty (Hollinger and Richardson, 2005; Liu et al., 2006; Serrano-Ortiz et al., 2008). Even though large density corrections might be undesirable, case studies of error propagation based on the peatland data with different scenarios regarding potential errors in *H*, *LE* and the raw CO_2 flux showed that it is very unlikely that the large observed differences in fluxes obtained by EC and chamber were the result of overestimation of the EC flux caused by potential error propagation through the WPL algorithm (Appendix D). These analyses corroborate the findings of several experiments designed to test the robustness of the WPL algorithm that have confirmed that even when conditions lead to large WPL terms, reliable fluxes can be obtained (Billesbach et al., 2004; Ham and Heilman, 2003; Leuning et al., 1982).

Negative NEE in winter at the peatland

At the peatland, small negative values of NEE were measured during moist and wet periods (mostly during winter and wet periods in fall and spring, see dark blue rectangles in Figure 4.4). These negative values suggest uptake of CO_2 by the peat surface. The cause of this measured uptake in not entirely clear, but two hypotheses can be posed: uptake was due to a measurement artefact caused by sensor separation or due to photosynthesis by algae. Possibly, the negative values of NEE were caused by an underestimation of the density term (see Appendix D). However, this phenomenon has only been detected in colder climates (e.g. Hirata et al. (2007) and references therein), where heating of the gas analyser caused density fluctuations that were larger than those measured using the sonic anemometer alone (Appendix D). Alternatively, the measured uptake was real. During wet periods at the peatland, puddles formed on the surface which were colonised by algae. These algae would have sequestered carbon by photosynthesis, and if CO_2 uptake was large enough it could have resulted in net negative values of NEE. The size of the total uptake of CO_2 was unknown, and was assumed negligible for the current study so that Equation 3.3 could be applied. This means that the estimate of the contribution of photodegradation to the total CO_2 flux was a conservative one. This example emphasizes the shortcomings of the current combination of techniques used to determine the size of irradiance-induced fluxes in an ecosystem where photosynthesis is taking place.

4.5 Summary

This study demonstrated that solar irradiance contributed to ecosystem CO_2 losses through the abiotic process of photodegradation of organic matter, and that these CO_2 losses were detectable at large scales under ambient conditions of soil moisture, temperature and irradiance. Irradiance-induced CO_2 fluxes were responsible for a considerable portion of the total CO_2 losses at a bare peatland in New Zealand and an annual grassland in California. Photodegradation contributed 13-25% of the annual CO_2 flux from the peatland

and 60% of the dry season CO_2 flux from the grassland and up to 62% and 90% of the summer midday CO_2 fluxes respectively.

The results show that ecosystem level studies examining CO_2 exchange cannot always neglect irradiance-induced CO_2 losses. The grassland results demonstrated that photodegradation can be responsible for a substantial portion of CO_2 losses in a natural ecosystem during the dry season, suggesting that photodegradation may be important in a wide range of ecosystems with SOM or litter exposed to solar irradiance. These ecosystems comprise very large areas on a global scale (e.g. arid and semi-arid ecosystems cover ~ 30% of the Earth's land surface (Lal, 2004)), so that even small contributions from photodegradation to CO_2 fluxes could represent large fluxes of carbon when summed globally.

Measurements of CO_2 efflux made using opaque chambers or soil CO_2 probes may seriously underestimate the real losses in ecosystems where OM is exposed to solar irradiance, because neither of these methods captures CO_2 fluxes from litter or OM exposed to solar irradiance. Photodegradation represents a daytime-specific pathway of CO_2 loss, and if photodegradation proves to contribute substantially to ecosystem-scale CO_2 loss during the day, this will invalidate the assumption made when partitioning NEE into its gross flux components, namely that daytime CO_2 losses can be modelled using night-time CO_2 losses.

Quantifying the role of photodegradation under natural field conditions is challenging. In the absence of photosynthesis, such as at the devegetated peatland or the senesced Californian grassland, photodegradation can be measured by comparing day - and night-time EC fluxes, or by comparing EC fluxes with opaque chamber fluxes. Comparison of CO_2 fluxes measured by opaque and transparent chambers should also give insight into the magnitude of CO_2 fluxes caused by photodegradation. However, in vegetated systems where water does not limit biological activity, NEE is the sum of multiple exchange processes of CO_2 (see Section 2.4.2 and Figure 2.3) which makes it very difficult to discriminate between photosynthesis, respiration and photodegradation. At

present there is no suitable technique available to disentangle the irradiance-induced flux from the biological fluxes

Despite these challenges, it is crucial that further studies are conducted in a wide variety of ecosystems to increase our understanding of the importance and drivers of photodegradation. This knowledge is needed for gaining insight into the response of carbon cycling in terrestrial ecosystems to climate change (Austin and Vivanco, 2006) and for continued development of coupled carbon-climate models. For example, the effect of changes in irradiance levels, as caused by changes in cloud cover or vegetative cover could affect decomposition rates not only indirectly (through changes in temperature), but also directly. In exposed ecosystems, these changes in irradiance levels might well be more important than changes in other climatic drivers like precipitation amount (Austin and Vivanco, 2006; Smith et al., 2010).

Chapter 5 Controls of photodegradation

5.1 Introduction

The previous chapter showed that CO_2 emitted by a bare peat surface and an annual grassland during the dry season were of both biotic and abiotic origin. In both ecosystems, photodegradation made a substantial contribution to the total CO_2 loss. Several studies have confirmed the contribution of photodegradation to OM decomposition by measuring differences in mass loss (Austin and Vivanco, 2006; Brandt et al., 2007; Day et al., 2007; Gallo et al., 2009; Henry et al., 2008) and CO_2 loss (Anesio et al., 1999; Brandt et al., 2009) from litter exposed and shaded from solar irradiance. Supplemental UV irradiance has also been found to lead to additional loss of mass (Rozema et al., 1997c; Smith et al., 2010) and CO_2 (Anesio et al., 1999; Brandt et al., 2009), although not always (Gallo et al., 2006; McLeod and Newsham, 1997; Moody et al., 2001; Newsham et al., 1997; Verhoef et al., 2000).

Solar irradiance can directly affect decomposition rates, and presumably CO_2 losses, in several ways:

- Solar irradiance can inhibit CO_2 loss from OM by *microbial inhibition*: the lowering of the abundance and activity of decomposing microbes caused by exposure of the organisms to UV irradiance (Duguay and Klironomos, 2000; Pancotto et al., 2003; Smith et al., 2010).
- Solar irradiance can increase decomposition rates by directly breaking down the compounds of OM through a process called *photodegradation*. Photodegradation in turn can lead to increased CO_2 fluxes through two mechanisms:
    - by *microbial facilitation*: the breakdown of large, often complex phenolic compounds of OM into smaller molecules can make the substrate more easily degradable by microbes, thereby indirectly enhancing microbial degradation and resulting CO_2 efflux (Day et al., 2007; Gallo et al., 2009; Gallo et al., 2006; Henry et al., 2008; Pauli, 1964) and

- by *photochemical mineralisation*: the direct breakdown of OM into inorganic carbon, i.e. dissolved inorganic carbon in water and CO_2 in air, which can take place even in the absence of active microbes (Anesio et al., 1999; Brandt et al., 2009).

Recently, studies have started to address the potential controls of irradiance-induced mass loss by photodegradation of litter and identified that the availability of OM, the exposure of litter and SOM to light, light intensity, litter species, litter density, wavelength and moisture conditions can affect this process (Brandt et al., 2007; Gallo et al., 2009; Gallo et al., 2006; Pancotto et al., 2005; Smith et al., 2010; Zepp et al., 2007). While most studies have focussed on mass loss, the studies by Anesio et al. (1999) and Brandt et al. (2009) are the only ones that have investigated the size of irradiance-induced CO_2 fluxes and its controls at small scales. None of these studies have investigated the effect of solar irradiance on soils.

Although traditionally radiation in the UV-B region of the solar spectrum was assumed to be predominantly responsible for photodegradation, radiation in wavelengths other than UV-B (i.e. UV-A and visible) have been found to contribute substantially to irradiance-induced loss of mass (Austin and Vivanco, 2006) and CO_2 (Anesio et al., 1999; Brandt et al., 2009) as well. While a linear relationship is often assumed between solar (or UV) irradiance intensity and photodegradation (Flint et al., 2003), no studies have directly investigated this assumption by measuring mass or CO_2 loss from terrestrial litter under a range of radiation intensities. Similarly, the effects of temperature and moisture on terrestrial photodegradation rates are largely unknown. Two studies comparing the effect of UV irradiance on mass loss of litter under wet and dry conditions found that UV irradiance led to an increase in mass loss under dry conditions, while UV irradiance had no (Brandt et al., 2007) or a negative (Smith et al., 2010) effect on mass loss under wet conditions. This different effect of exposure to UV between dry and wet litter was explained by the greater importance of microbial decomposition under wet conditions and the greater role of microbial inhibition by UV leading to a smaller mass loss in the litter exposed to (extra) UV compared to the wet control samples. Both Anesio et al. (1999) and Brandt et al. (2009)

examined the effect of irradiance on a variety of litter substrates, but could not detect differences when fluxes were expressed on an exposed-area basis (µmol m^{-2} s^{-1}), even though various studies suggest that litter chemistry – for example the lignin fraction – might affect rates of photodegradation (Day et al., 2007; Gehrke et al., 1995; Henry et al., 2008; Moorhead and Callaghan, 1994; Rozema et al., 1997). Since the study by Moorhead and Callaghan in 1994, little information has become available about the chemical pathways of CO_2 production by photochemical decomposition. One interesting question, namely whether CO_2 production from terrestrial litter relies on availability of atmospheric oxygen, has only been addressed by one recent study (Cory et al., 2008) which suggested that irradiance-induced CO_2 production partly relies on a direct reaction with atmospheric oxygen.

In addition to photochemical decomposition, thermal decomposition of grass litter has been found to result in production of carbon monoxide (CO) at ambient temperatures (Schade et al., 1999). Although conceivable that similar mechanisms could cause CO_2 losses as well, no literature could be found addressing CO_2 losses from OM as a result of thermal decomposition at ambient temperatures.

In this chapter, the field data from the peatland and grassland will be examined more closely to shed light on the controls of the abiotic portion of the CO_2 flux. In addition to the fully observational field measurements where no manipulation or 'treatments' were applied, measurements were made on a much smaller scale using a closed chamber system (see Section 3.4) that will be referred to as the 'container'. The instantaneous response of the CO_2 efflux from organic substrates to exposure to solar irradiance was measured using this newly developed setup which allowed manipulation of substrate, wavelengths and oxygen availability. Results showing the controls of radiation, temperature, O_2, light wavelength and different substrates will be presented in this chapter. The objectives of this chapter are:

1. Investigate the data for evidence of photochemical mineralisation, microbial facilitation or thermal decomposition as potential processes contributing to non-biological CO_2 losses.

2. Examine the sensitivity of irradiance-induced CO_2 flux to changes in radiation (i.e. determine the dose-response relationship) and look into potential interactive controls of radiation with temperature and moisture.
3. Evaluate to what extent irradiance in UV-B, UV-A and visible region of the solar spectrum cause irradiance-induced CO_2 losses.
4. Explore the response of different substrates to exposure to solar irradiance.
5. Determine whether irradiance-induced CO_2 production takes place in the absence of atmospheric oxygen.

The experimental setup measuring instantaneous CO_2 fluxes was developed during the course of this study, and after discussion of the results, the suitability of the experimental setup will be evaluated and recommendations will made on how to improve it for future experiments.

Some of the findings presented in this chapter are part of a paper that has been accepted for publication by Global Change Biology (Rutledge et al., 2010).

5.2 Methods

5.2.1. Measurements

In this chapter, the field data presented in Chapter 4 will be further examined. Refer to Sections 3.2, 3.3 and 3.5.1 for a description of the field sites and field methods.

Additionally, a small closed chamber system transparent to visible and UV light (henceforth referred to as the 'container') was designed to verify the control of irradiance on CO_2 fluxes as suggested by field measurements CO_2 fluxes. This method has been described in Section 3.4. In short, organic substrates in the container were alternately exposed to and shaded from solar irradiance at two or three minute intervals, while the CO_2 concentration, irradiance levels and temperature was continuously monitored. Substrates were

air-dried to limit microbial activity. Four experiments were conducted to study the controls of temperature, irradiance level, wavelength, different substrates and the availability of oxygen on the production of irradiance-induced CO_2 fluxes (Sections 3.4.5-3.4.8 and Table 2.1). For some analyses, data from more than one experiment were used.

Note that the peat used in Experiment A, B and D was taken from the peatland in New Zealand, and this common substrate between field and container studies allowed for comparison between results of the different studies. In contrast, the grass used for the substrate experiment (Experiment C) was not the same as the grass at the grassland study site in California, and therefore direct comparison of CO_2 fluxes measured in the field and the container is not possible.

Table 5.1 Summary of experiments with the container. See Section 3.4 for more information.

Experiment	A	B	C	D
Driver examined	Temperature and irradiance	Wavelength	Substrate	Oxygen
Method	CO_2 fluxes from peat shaded and exposed	CO_2 fluxes from peat under different filters blocking UV-B, UV-AB or all irradiance	CO_2 fluxes from peat, grass and maize leaves shaded and exposed	CO_2 fluxes from peat in air and nitrogen gas (to expel oxygen)
Dates in 2007	3,4,5 Feb	29,30 Mar, 1 Apr	2,22,23 Apr	3,6, 17 Apr

5.2.2. Data analysis

Dose-response relationship or coefficient

In this chapter, the sensitivity of the irradiance-induced CO_2 flux to changes in irradiance will be examined. In photochemistry the term “quantum yield” is commonly used as an indicator of the efficiency of a process (Anslyn and Dougherty, 2006). Quantum yield can be defined as “the amount of product (number of molecules) formed per unit time divided by the quanta of light absorbed per unit volume per unit time” (Osburn and Morris, 2003), or an equivalent equation with rates instead of amounts (Anslyn and Dougherty, 2006; Wayne, 1988). Following this definition, measurements of absorbed number of

photons are required to calculate the quantum yield. However, in the current study, only the incoming shortwave irradiance was measured (except for a 3-month period between November 2007 and January 2008 when outgoing irradiance was also measured, Section 3.3.3). No measurements were obtained about which portion of this irradiance was absorbed, which would have required continuous measurements of shortwave outgoing irradiance or albedo. Also, measurements were in energy flux density units (W m^{-2}) instead of photon flux densities (mol photons m^{-2} s^{-1}). Therefore, the sensitivity of the irradiance-induced CO_2 flux to changes in irradiance will be calculated as follows:

Sensitivity = rate of CO_2 production per unit surface divided by the irradiance the OM is exposed to per unit time per unit surface.

Units are µmol CO_2 m^{-2} s^{-1} /J s^{-1} m^{-2} = µmol CO_2 J^{-1}. This sensitivity will be referred to as the "dose-response relationship" or "dose response coefficient" after the term used in Flint and Caldwell (2003) and Flint (2003). This term is used to specify either the response to absorbed irradiance (e.g. Kieber et al., 1990) or to incoming irradiance (exposure). As explained above, in this study, the dose-response coefficient of CO_2 production will be related to incoming (but not necessarily absorbed) irradiance.

Statistics

Experiment B (wavelengths) was performed in a block design, whereby treatments were randomly applied to blocks of four measurements (full sun, block UV-B, block UV-AB and block all). Data were analysed using an analysis of variance (ANOVA) adjusted for covariates irradiance and temperature. This analysis was done using GenStat (Version 11.1.0.1535).

5.3 Results

5.3.1. Photodegradation in the field

In Chapter 4, evidence was provided of the direct effect of solar irradiance on the emitted CO_2 from the peatland and grassland. Figure 4.3 showed that increasing CO_2 flux coincided with an increase in solar irradiance, even when comparing measurements made at the same temperature. In this

section, the controls of temperature, moisture and irradiance will be explored further.

Temperature and irradiance

Figure 4.1 showed that the increase of irradiance-induced CO_2 production coincided with an increase in solar irradiance. Because temperature and solar irradiance are closely correlated (Figure 4.2), irradiance-induced CO_2 fluxes (estimated as EC flux minus chamber or probe flux) also increased with increasing temperature (Figure 5.1).

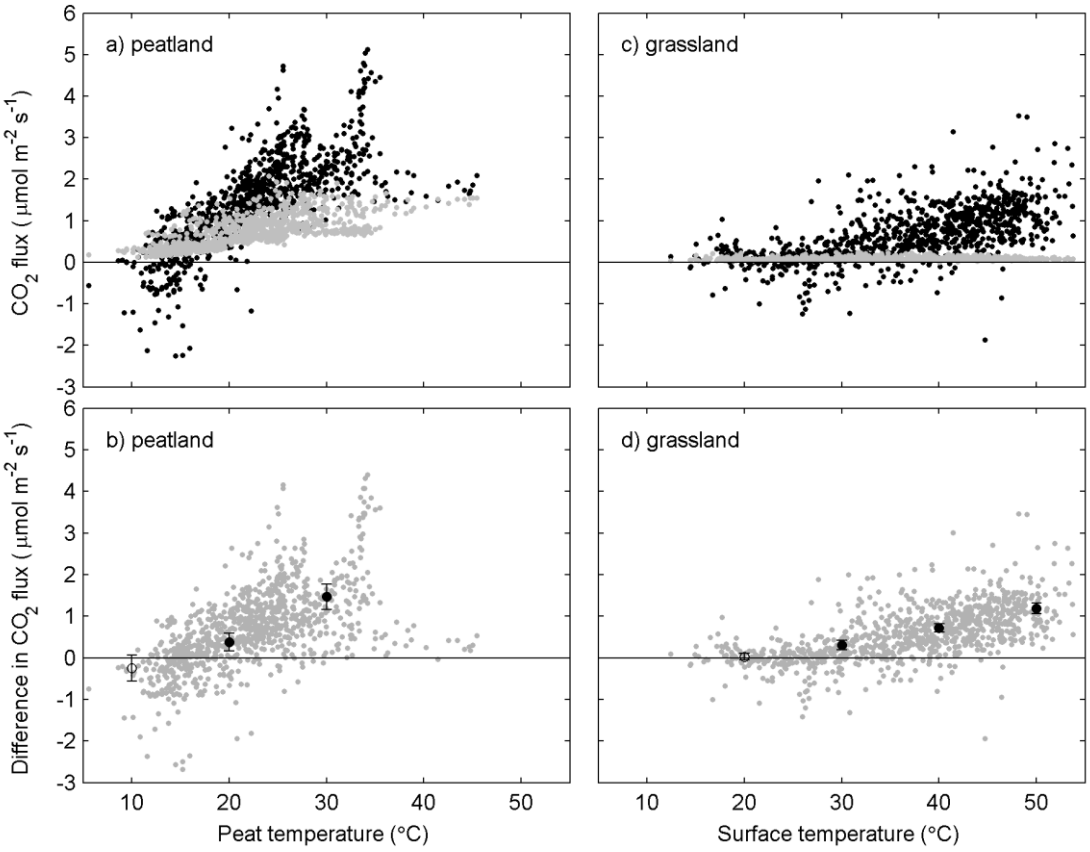

Figure 5.1 Illustration of the effect of temperature on CO_2 fluxes measured at the peatland (panels a and b) and the grassland (panels c and d). Fluxes were measured by eddy covariance (black points, panels a and c), opaque chamber (for peatland, grey points in panel a) and soil CO_2 probes (for grassland, grey points in panel c). Grey points in panels b and d are the difference in flux between total CO_2 flux (from EC) and biological CO_2 flux (from chamber or probes). Positive values depict instances where the EC system measured larger CO_2 fluxes than the chamber or probes. Black circles in panels b and d are daily averaged bin averages with error bars showing 95% confidence intervals. For the open circles, the difference between the total and biological CO_2 flux were not statistically different from zero (one sample t-test at a 95% significance level). For the filled symbols, the difference was statistically different from zero.

To investigate whether temperature affected the sensitivity of the irradiance-induced flux to changes in irradiance (i.e. the dose-response relationship, Section 5.2.2) at the grassland, regressions of irradiance-induced CO_2 flux (i.e. total flux from EC minus biological flux from probes) on solar irradiance were calculated in different bands of surface temperature. The response of CO_2 flux to an increase in irradiance seemed to be stronger at higher temperatures, as indicated by the steeper slopes at higher temperatures in Figure 5.2. This would suggest that there is an interaction between temperature and radiation. However, because half-hourly data were auto-correlated in time, regressions are displayed for illustrative purposes only and do not constitute proof for an interactive relationship between temperature and irradiance.

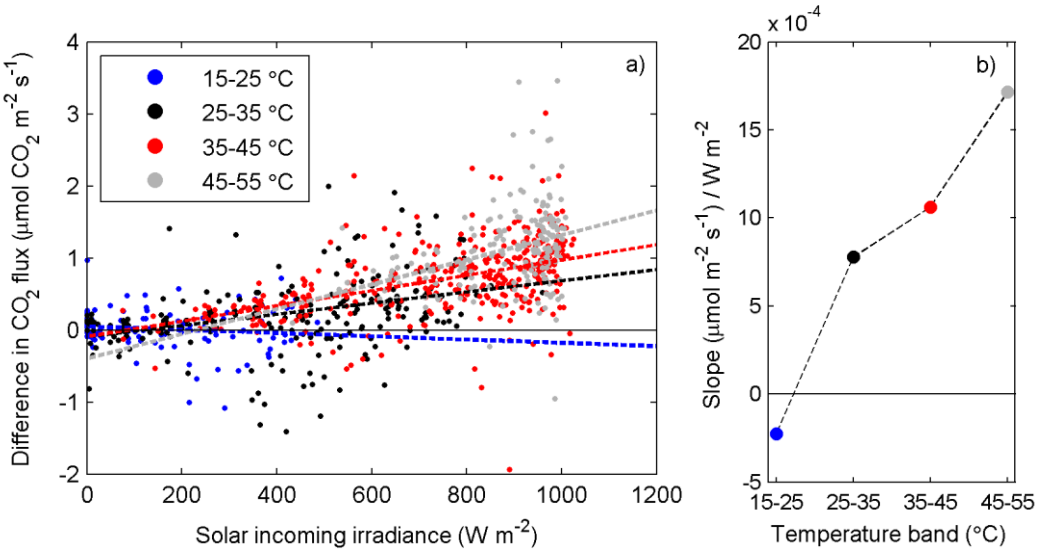

Figure 5.2 Illustration of the effect of solar irradiance on irradiance-induced CO_2 fluxes measured at the grassland. Regression of irradiance-induced flux (EC flux minus probe flux) against measured levels of solar irradiance in different surface temperature bands (panel a). Dots depict half-hourly data, and the dashed lines are corresponding linear regressions. All regressions (except the regression for 15-25 °C) were significant ($p<0.001$). Panel b shows the value of the slopes from panel a in the different temperature bands.

A similar analysis was conducted for the peatland (Figure 5.3), and the general trend of steeper slopes at greater temperatures was confirmed. In the band with lowest temperatures (5-15°C), negative fluxes measured at intermediate irradiance levels (400-500 W m^{-2}), resulted in a negative slope, which might have been the result of photosynthesis by algae under wet, cool winter conditions (see also Section 4.4.4). At the band containing greatest temperatures (35-45°C), a very high sensitivity was observed (Figure 5.3), but

because the regression was only based on a small number of data points, reliability of this regression was likely to be limited. Again, because half-hourly data were auto-correlated in time, regressions are displayed for illustrative purposes only and do not constitute proof for an interactive relationship between temperature and irradiance. Note that a direct comparison between the results from the grassland and peatland is limited because the temperature was not measured at the same depth; whereas at the grassland, measurements were made of the surface temperature (derived from measured upward longwave radiation), at the peatland temperature measurements were made at 5 mm depth.

In summary, at both the grassland and the peatland sites data suggested that the dose response coefficient increased with increasing temperature and therefore also with increasing irradiance (Figure 5.4).

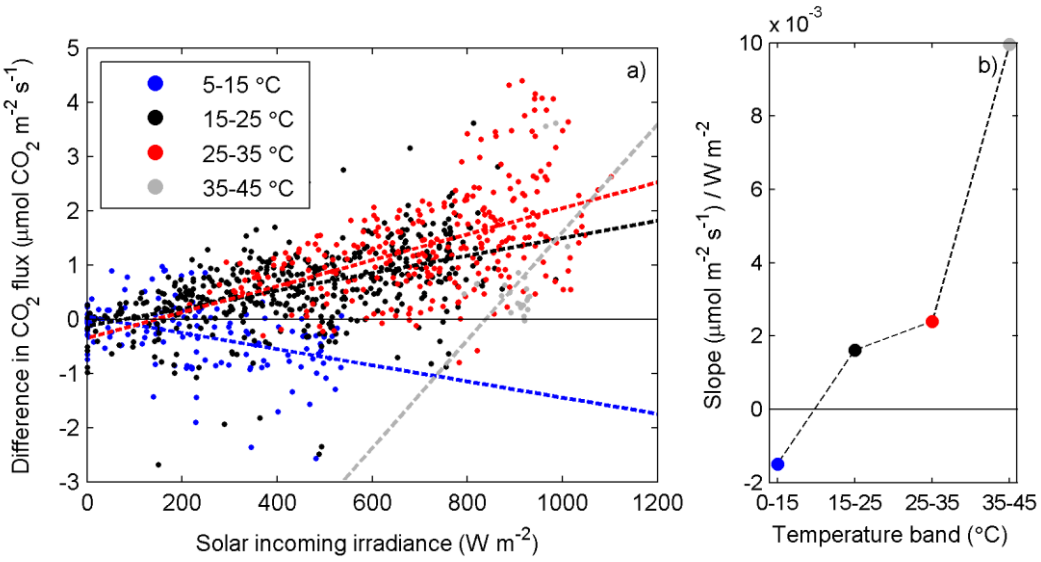

Figure 5.3 Illustration of the effect of solar irradiance on irradiance-induced CO_2 fluxes measured at the peatland. Regression of irradiance-induced flux (EC flux minus chamber flux) against measured levels of solar irradiance in different peat temperature bands (panel a). Dots depict half-hourly data, and the dashed lines are corresponding linear regressions. All regressions (except the regression for 35-45 °C) were significant ($p<0.001$). Panel b shows the value of the slopes from panel a in the different temperature bands.

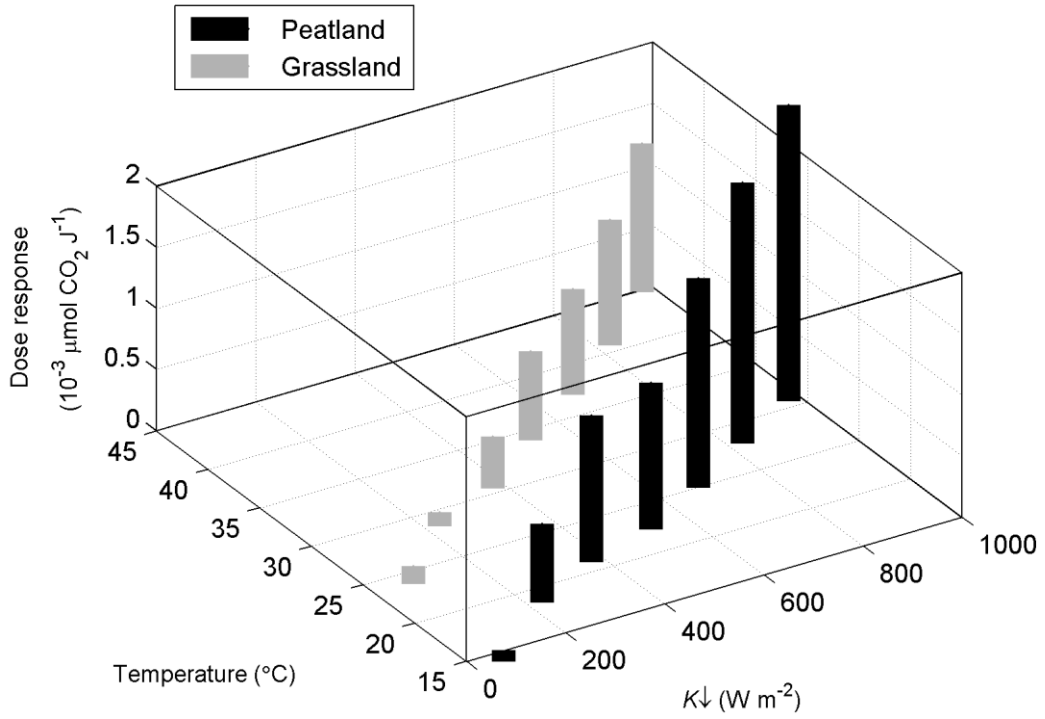

Figure 5.4 Dose-response relationship of irradiance-induced CO_2 flux at the peatland (black bars) and grassland (grey bars) as a function of incoming solar irradiance and peat temperature at 5 mm depth (at the peatland) or surface temperature (at the grassland). Irradiance-induced CO_2 flux was calculated by total flux (from EC) minus biological flux (from chamber at the peatland or probes at the grassland, see Figures 4.1 and 5.1). Values were obtained by grouping the data in bins of solar irradiance (bin width 150 Wm^{-2}). For each of these bins, the average irradiance-induced CO_2 flux, temperature and dose response (=average CO_2 flux/average solar irradiance) were calculated. The dose response was plotted against the average calculated temperature and the mid point of the solar irradiance bins.

Wavelength

Irradiance in wavelength shorter than 400 nm (UV-A and UV-B) was not measured at the field sites. However, estimates of hourly UV-B irradiance were available from National Institute of Water and Atmospheric Research (NIWA) for Paeroa, a site 19 km from the peatland (Shiona et al., 2006; Section 3.1.5 and Appendix C).

An analysis of these modelled hourly data showed that UV irradiance generally increased when levels of global radiation increased (Figure 5.5a). However, the ratio between estimated UV-B dose (280-320 nm) and measured global radiation (400 – 1100 nm) was not constant: at higher levels of solar irradiance, a larger proportion of total energy received from the sun was in the UV-B range (Figure 5.5b).

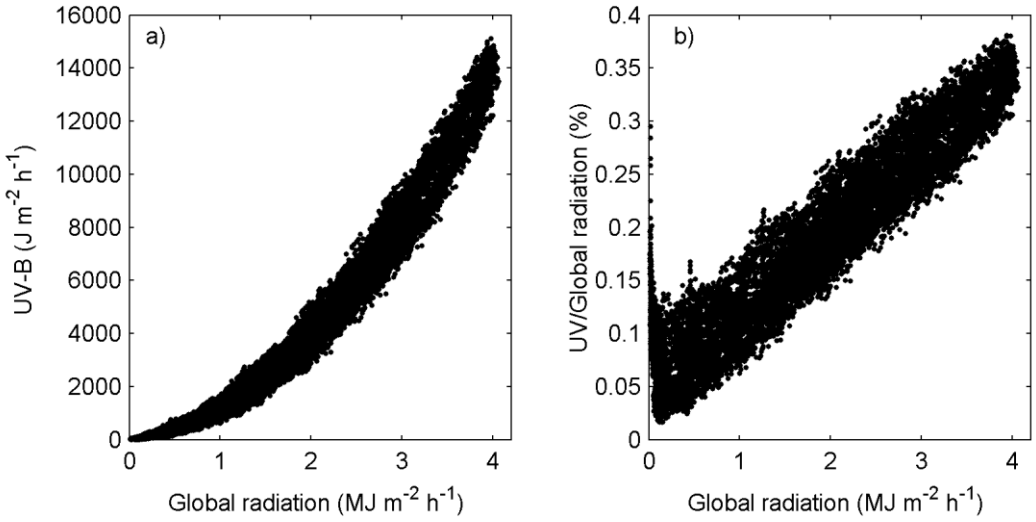

Figure 5.5 UV-B radiation (280-320nm) as a function of global radiation (300 – 1500 nm; panel a) The ratio between UV-B radiation and global radiation as a function of global radiation (panel b). Hourly data were estimates for Paeroa, 19 km from the field site and made available by NIWA. All available hourly data for 2005, 2006 and 2007 are shown.

The proportion of total energy in the UV-B wavelength band was largest when solar zenith angle (SZA) was smallest, and dropped off with increasing SZA (i.e. in the morning and afternoon, Figure 5.6).

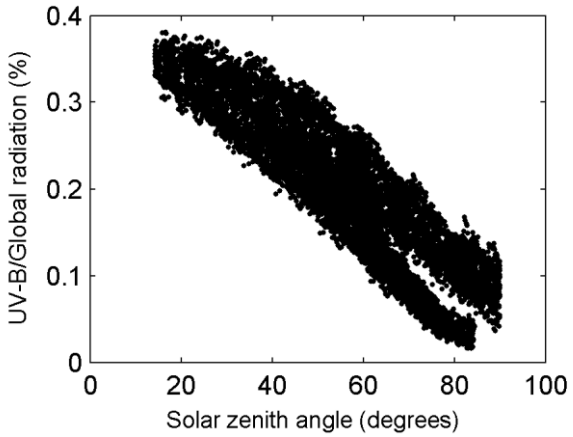

Figure 5.6 The ratio between UV-B radiation (280-320nm) and global radiation (300 – 1500 nm) as a function of solar zenith angle. Hourly data were estimates for Paeroa, 19 km from the field site and made available by NIWA. All available hourly data for 2005, 2006 and 2007 are shown.

On a diurnal scale, this disproportional effect of the SZA on irradiance in the UV wavelengths is shown by a clear diurnal variation in the UV/global irradiance ratio with the highest proportion of UV-B being received around solar noon (Figure 5.7a). Similar changes were observed throughout the year: during

December and January (summer) the proportion of UV-B irradiance was almost twice as large as the proportion during June and July (winter; Figure 5.7b).

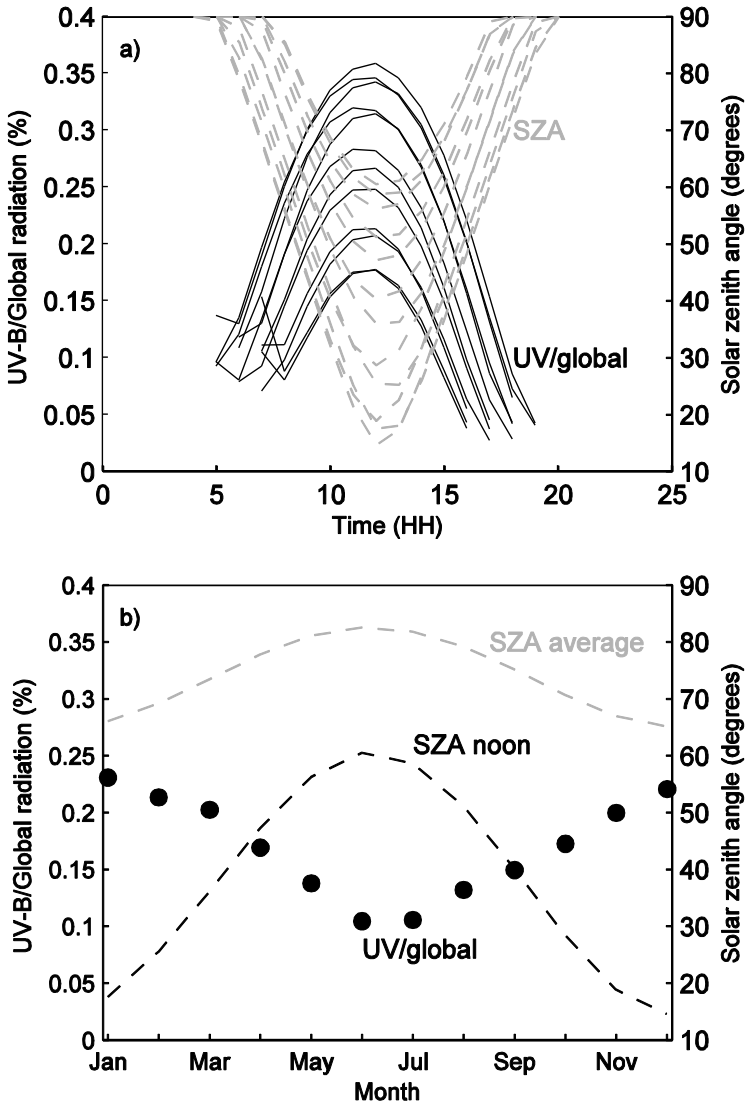

Figure 5.7 The ratio between estimated UV-B irradiance (derived from NIWA data) and global irradiance measured at the peatland as a function of a) time of day and b) month between June 2005 and July 2007. Mean diurnal variations of solar zenith angle (SZA) and UV/global irradiance ratio were calculated per month of the year (panel a). Panel b shows the mean monthly values of the UV/global irradiance ratio and solar zenith angle (grey dashed line). The black dotted line is the average of the SZA at solar noon for each month. All available hourly data for 2005, 2006 and 2007 were used to calculate the monthly averages.

For the peatland, estimates of UV-B irradiance (280-320 nm) were derived by adjusting the calculated values for clear sky UV irradiance for Paeroa (from NIWA) for clouds observed at the peatland (see Section 3.5.2 and Appendix C). The trend of difference in CO_2 flux between EC and chamber with

UV-B irradiance closely resembled the trend observed with total incoming irradiance: the difference of CO_2 flux between EC and chamber increased with increasing UV irradiance (Figure 5.8; compare Figure 4.1).

The response of the irradiance-induced CO_2 flux to increases in measured global irradiance increased with increasing UV-B irradiance (Figure 5.9).

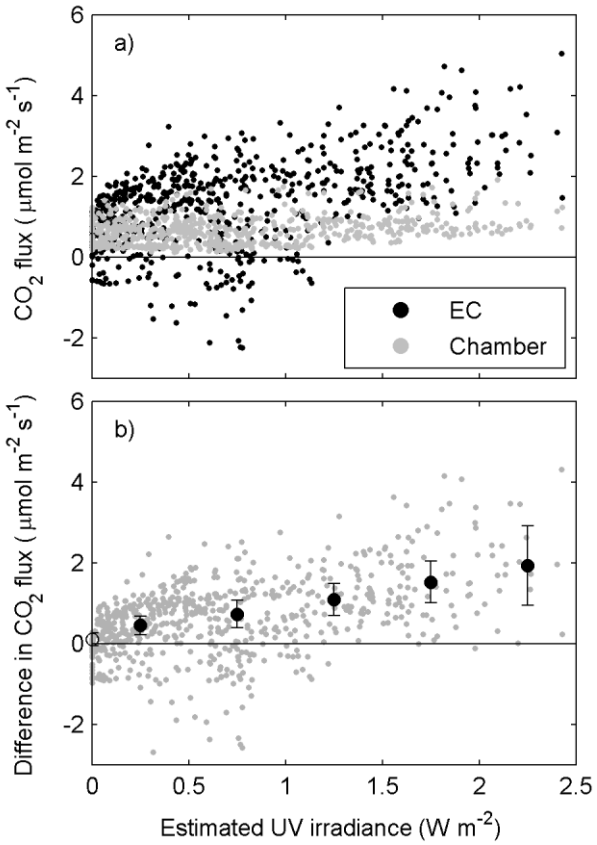

Figure 5.8 Illustration of the effect of UV irradiance on CO_2 fluxes measured at the peatland. Fluxes were measured by eddy covariance (black points, panel a) and opaque chamber (grey points in panel a). Grey points in panel b are the difference in flux between total CO_2 flux (from EC) and biological CO_2 flux (from chamber). Positive values depict instances where the EC system measured larger CO_2 fluxes than the chamber. Black circles in panel b are daily averaged bin averages with error bars showing 95% confidence intervals. For the open circles, the difference between the total and biological CO_2 flux were not statistically different from zero (one sample t-test at a 95% significance level). For the filled symbols, the difference was statistically different from zero.

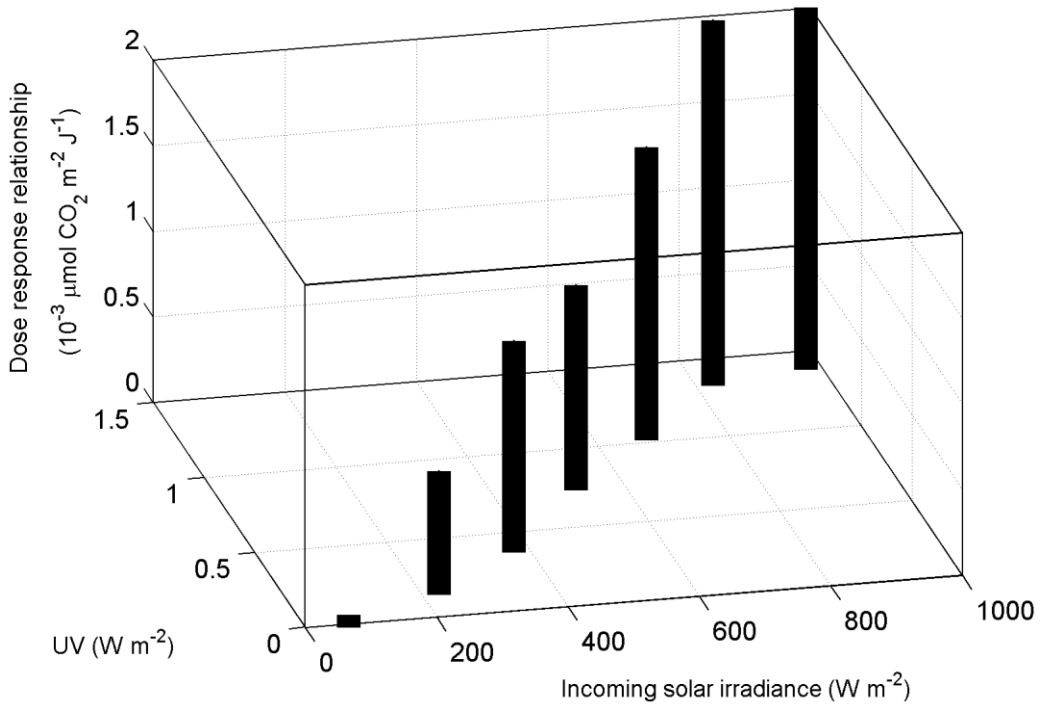

Figure 5.9 Dose-response relationship of irradiance-induced CO_2 flux at the peatland as a function of incoming solar irradiance and estimated UV-B. Irradiance-induced CO_2 flux was calculated by total flux (from EC) minus biological flux (from chamber at the peatland or probes at the grassland, see Figures 4.1 and 5.1). Values were obtained by grouping the data in bins of solar irradiance (bin width 150 Wm^{-2}). For each of these bins, the average irradiance-induced CO_2 flux, UV irradiance and dose response (=average CO_2 flux/average solar irradiance) were calculated. The dose response was plotted against the average calculated UV irradiance and the mid point of the solar irradiance bins.

Moisture content

In addition to solar irradiance and temperature, moisture content also co-correlated during the measurement period at the peatland. Regressions of irradiance-induced CO_2 flux (i.e. total flux from EC minus biological flux from chamber) on solar irradiance were calculated in different bands of volumetric moisture contents. The similar slopes between VMC bands (Figure 5.10) provided little evidence that the response of CO_2 flux to an increase in irradiance was affected by the moisture status of the peat. However, because half-hourly data were auto-correlated in time, regressions are displayed for illustrative purposes only and do not constitute proof for the lack of interactive relationship between moisture content and irradiance. Additionally, measurements of volumetric moisture content were made at 45 mm depth instead of at the surface. Moisture

conditions at that depth would have differed from those at the surface, especially during summer when the top of the peat layer dried out substantially and formed a dry crust over the surface.

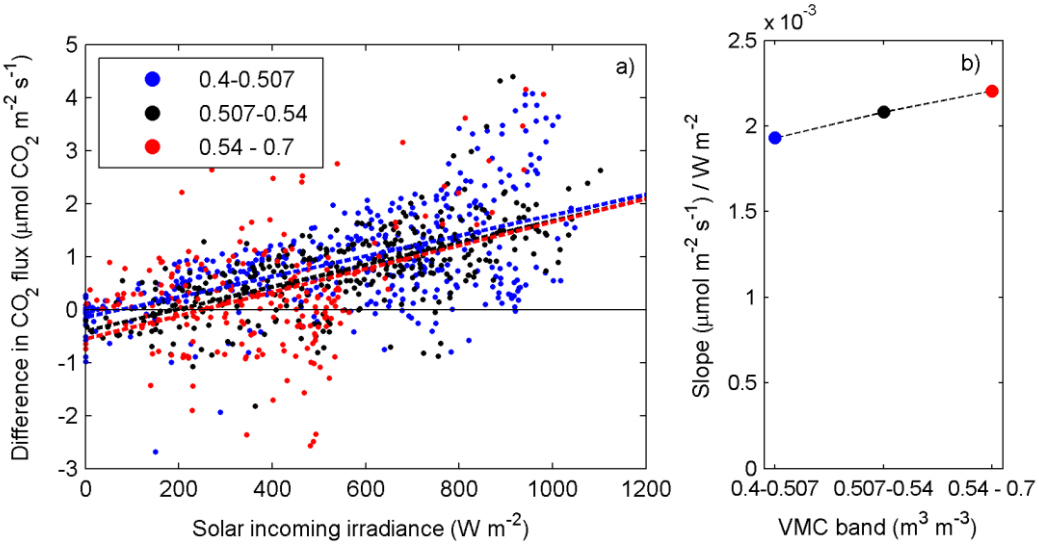

Figure 5.10 Illustration of the effect of solar irradiance on irradiance induced CO_2 fluxes measured at the peatland. Regression of irradiance-induced flux (EC flux minus chamber flux) against measured levels of solar irradiance in bands of different volumetric moisture contents of peat measured at 45 mm depth (panel a). Dots depict half-hourly data, and the dashed lines are corresponding linear regressions. Moisture groups were chosen to contain an equal number of data points. Regressions for 0.4 – 0.507 m^3 m^{-3} and 0.507-0.54 m^3 m^{-3} were significant ($p<0.001$). Panel b shows the value of the slopes from panel a in the different VMC bands.

5.3.2. Photodegradation in the container experiment

To verify the control of irradiance on CO_2 fluxes as suggested by field measurements CO_2 fluxes were measured from peat in a small container transparent to visible and UV light (see Section 3.4; Experiment A). Peat was air-dried to limit microbial activity. Peat in the container was alternately shaded and exposed to sunlight at two minute intervals while CO_2 concentration and peat temperature were monitored.

The increase in CO_2 concentration on exposure to solar irradiance was nearly instantaneous (Figure 5.11), and the immediate effect on the rate of increase in CO_2 concentration caused by passing clouds can clearly be seen (Figure 5.11 g,h).

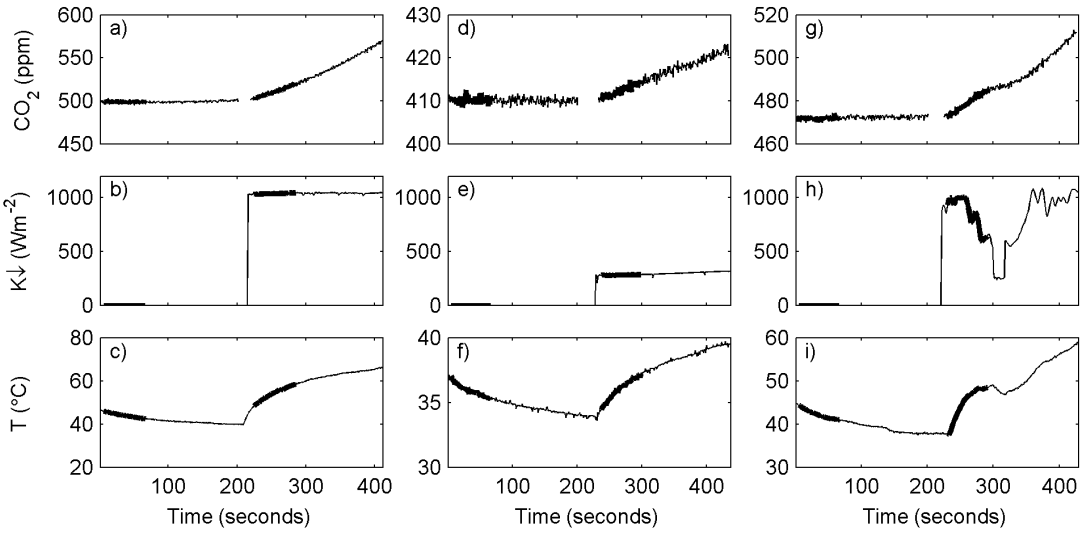

Figure 5.11 Example data of the small scale container experiment. CO_2 molar fraction (panels a, d and g), incident solar irradiance (panels b, e and h) and peat temperature (panels c, f and i) during three sets of two consecutive runs: Runs 8 and 9 (panel a, b and c), with CO_2 fluxes of –0.01 (shade) and 0.39 (sun) µmol CO_2 m^{-2} s^{-1} respectively; Runs 80 and 81 (panel d, e and f) with CO_2 fluxes of 0.01 and 0.09 µmol CO_2 m^{-2} s^{-1} respectively; Runs 86 and 87 (panels g, h and i) with CO_2 fluxes 0 and 0.29 µmol CO_2 m^{-2} s^{-1} respectively. Individual runs were 200 seconds long. Bold lines indicate the CO_2 concentration data that were used for flux calculation (60 seconds) and the matching irradiance and temperature data. The container was shaded from the sun when irradiance ($K\downarrow$) was 0 Wm^{-2}. Please note that scales on y-axes differ between graphs of CO_2 concentration (top panels) and graphs of temperature (bottom panels). Figure was reprinted from (Rutledge et al., 2010) with permission from John Wiley and Sons.

Experiment A: Temperature and irradiance

CO_2 fluxes from air-dried peat measured in the dark for Experiment A (2-4 Feb 2009) were around zero (or even slightly negative), indicating that microbial respiration was negligible (Figure 5.12). When exposed to solar irradiance, CO_2 fluxes from the peat increased considerably. Even at high temperatures (>60 °C), CO_2 fluxes in the dark remained close to zero while fluxes from peat exposed to solar irradiance were greater than 0.5 µmol CO_2 m^{-2} s^{-1} at the same temperature (Figure 5.12a). The CO_2 flux increased linearly with increasing radiation (Figure 5.12b).

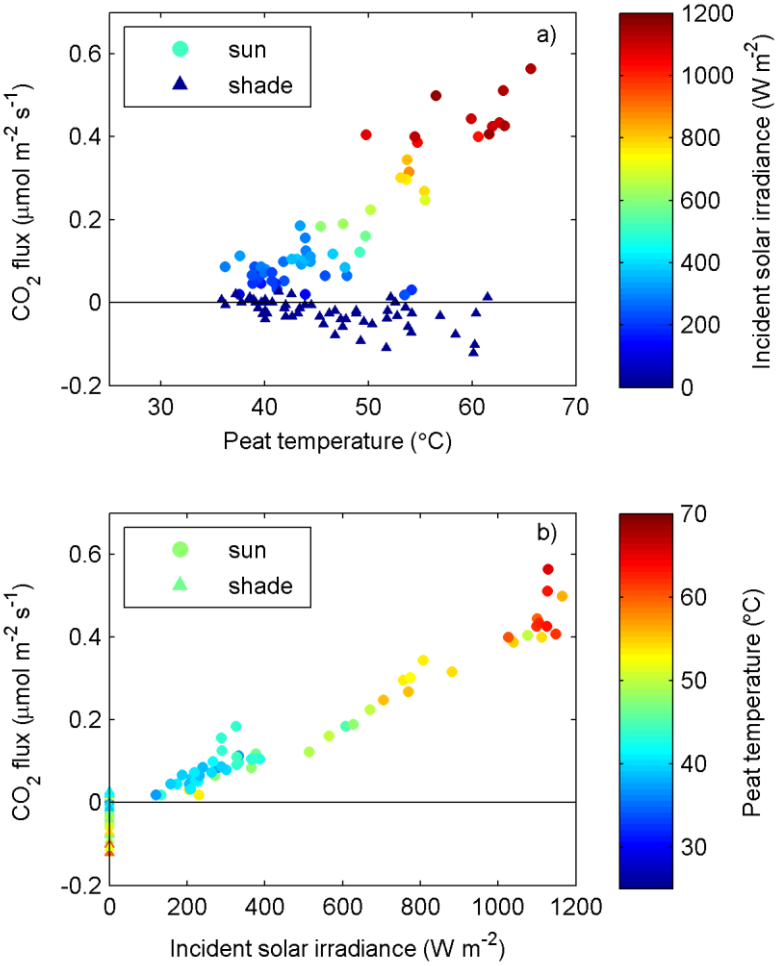

Figure 5.12 Response of CO_2 flux from peat to exposure to solar irradiance as a function of a) peat temperature and b) solar irradiance. CO_2 flux from peat in a transparent container alternately exposed to (circles) and shaded from (triangles) solar irradiance. Data presented for experiment A only. Panel a was reprinted from Rutledge et al. (2010) with permission from John Wiley and Sons.

Visual inspection of the data collected during the sun runs strongly suggested that irradiance was the main driver of the CO_2 flux, as indicated by the difference in CO_2 production between sun and shade runs, even at high temperatures (Figure 5.12). Regression analysis confirmed that irradiance intensity explained a large proportion of the variability in CO_2 flux during sun runs in addition to the variation explained by temperature and temperature squared (Table 5.2). In addition to temperature, the temperature squared term was included in the regression equation to prove that even after including two terms with temperature, solar irradiance still added explanatory power to the regression at a highly significant level. The percentage of the variance explained

by this regression was 94.9%, whereas the regression using irradiance alone explained as much as 93.7% of the variation.

Table 5.2 Estimates of coefficients of regression equation on sun run data of Experiment A (*n* = 75). Adjusted R^2 for the regression was 0.949, with F = 458.4 and p< 0.0001.

	Coefficient	Standard error	*t*-statistic	*P* value
Constant	0.55	0.17	3.3	0.0014
Temperature	-0.0252	0.0067	-3.8	0.0003
$Temperature^2$	-0.00027	0.0001	4.0	0.0001
Irradiance	0.000380	0.00002	17	<0.0001

Summed over all experiments (A-D), measurements of CO_2 production from air dried peat exposed to sunlight in the presence of atmospheric oxygen were made between February and April 2009 (see Table 3.2). The response of the CO_2 flux to irradiance varied between different months (Figure 5.13). CO_2 fluxes measured in April were approximately half as large as fluxes measured in February under similarly high irradiance conditions (Figure 5.13). Comparison of fluxes measured at irradiance of 1100 Wm^{-2} suggested that the dose-response relationship dropped from 0.40 $\cdot 10^{-3}$ µmol CO_2 J^{-1} (0.44 µmol CO_2 m^{-2} s^{-1} /1100W m^{-2}) in February to 0.24 $\cdot 10^{-3}$ µmol CO_2 J^{-1} in April (0.27 µmol CO_2 m^{-2} s^{-1} /1100W m^{-2} ; Figure 5.13)

The potential causes for this difference between months in response of the CO_2 flux to irradiance will be discussed in Section 5.4.5 . When presenting the results of experiments B, C and D, data will only be shown in the graphs if they had been collected less than approximately one month apart.

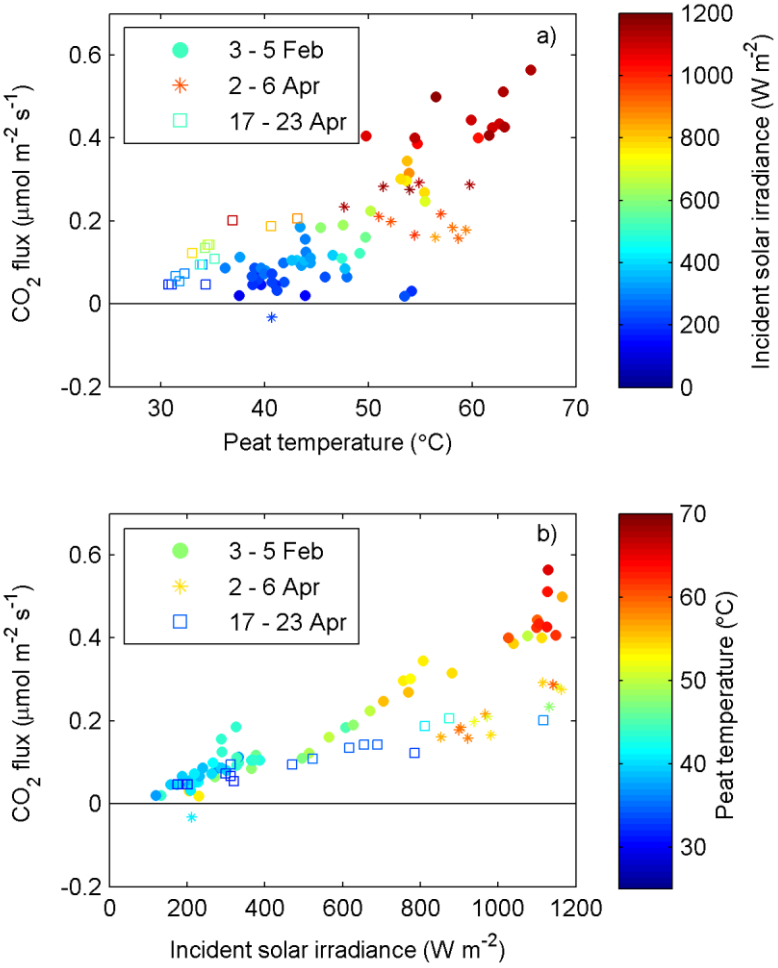

Figure 5.13 Response of CO_2 flux from peat to exposure to solar irradiance as a function of a) peat temperature and b) solar irradiance at different dates. Data are presented from the 60 seconds sun runs (without additional cover) for experiment A, C and D. Data from experiment B were excluded because an additional quartz cover was used for the sun runs in that experiment.

Experiment B: Wavelength

Before the experiment was conducted using the container with the quartz top, a pilot study was conducted using the container with its' original polystyrene top. Transmittance of the plastic was 0.88, 0.76, and 0.31 for visible (400 – 700 nm), UV-A (320 – 400 nm) and UV-B (280 – 320 nm) irradiance respectively, which meant that most of the UV-B (69%) was blocked by the plastic and did not reach the peat. Even though little UV-B reached the peat, a strong response of CO_2 production to exposure to radiation was observed (Figure 5.14)

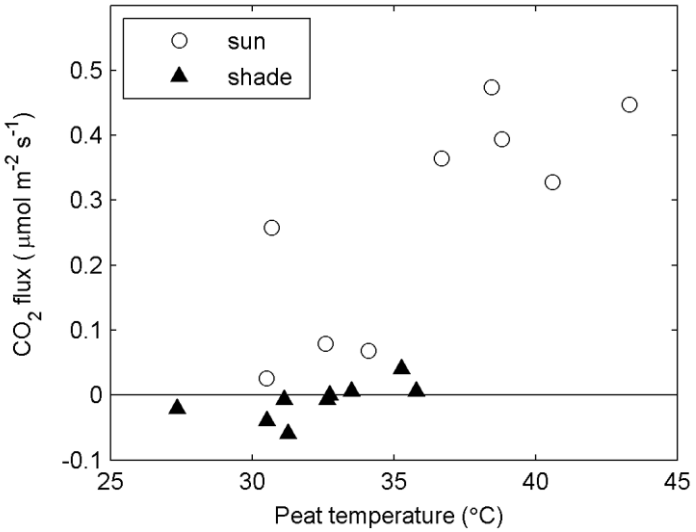

Figure 5.14 Response of CO_2 flux to exposure to solar irradiance as a function of peat temperature. CO_2 flux from peat in a partially transparent container with the polystyrene top alternatively exposed to (circles) and shaded from (triangles) solar irradiance during a pilot study. Fluxes were measured during 18 runs on 20 Nov 2008. Irradiance data were not available.

In a follow-up experiment (experiment B), a range of different filters was used to filter out radiation at different wavelengths. At high solar irradiance levels, visual inspection of the data does not show a clear difference between the CO_2 fluxes observed when filtering out different parts of the solar spectrum (Figure 5.15).

However, an analysis of variance with temperature and irradiance as covariates revealed that there was a difference in CO_2 flux between wavelength treatments ($P < 0.001$). The mean fluxes (adjusted for the covariates) were 0.3155 µmol CO_2 m^{-2} s^{-1} for the full sun treatment, 0.2769 µmol CO_2 m^{-2} s^{-1} for the –UVB treatment and 0.2662 µmol CO_2 m^{-2} s^{-1} for the – UVAB treatment. The standard error of the mean was 0.00984 µmol CO_2 m^{-2} s^{-1}, indicating that the fluxes in full sun were significantly higher than the fluxes recorded while blocking part of the solar spectrum. Although the average flux was higher for the –UVB treatment than the –UVAB treatment, this difference was not significant. Peat temperatures were not found to differ between treatments ($P < 0.001$).

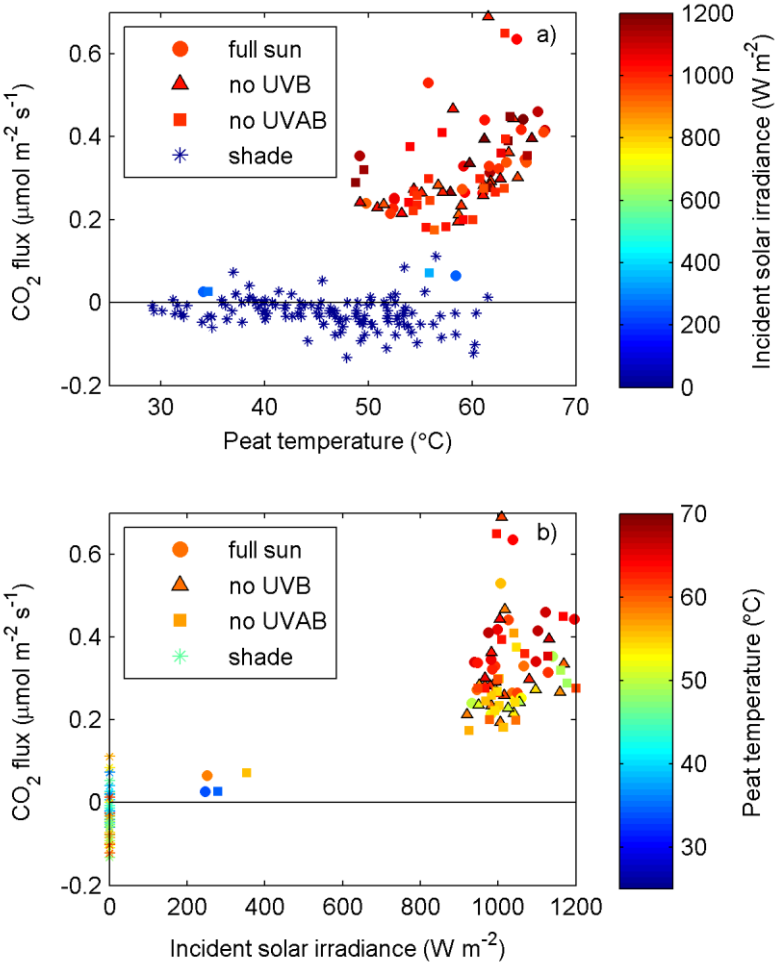

Figure 5.15 Response of CO_2 flux from peat to exposure to solar irradiance as a function of a) peat temperature and b) solar irradiance. Peat in a transparent container was exposed to four levels of solar irradiance: full solar spectrum (circles), solar irradiance with UV-B blocked (triangles), solar irradiance with UV-AB blocked (squares), and shade (asterisks). Data presented for experiment B only.

Experiment C: Substrates

CO_2 fluxes from dead, dried grass were slightly less than zero in the shade (-0.0055 ± 0.0051 µmol CO_2 m^{-2} s^{-1} (mean ± 95% confidence interval)) and larger than zero (0.0454 ± 0.0066 µmol CO_2 m^{-2} s^{-1} (mean ± 95% confidence interval)) when the container was exposed to solar irradiance (Figure 5.16). Regression analysis of sun run data using a constant, grass temperature and irradiance as predictors showed that irradiance was a significant predictor of CO_2 flux ($P < 0.001$), in contrast to grass temperature ($P = 0.141$) which did not improve the regression ($n = 42$, adjusted R^2 for total regression = 0.47).

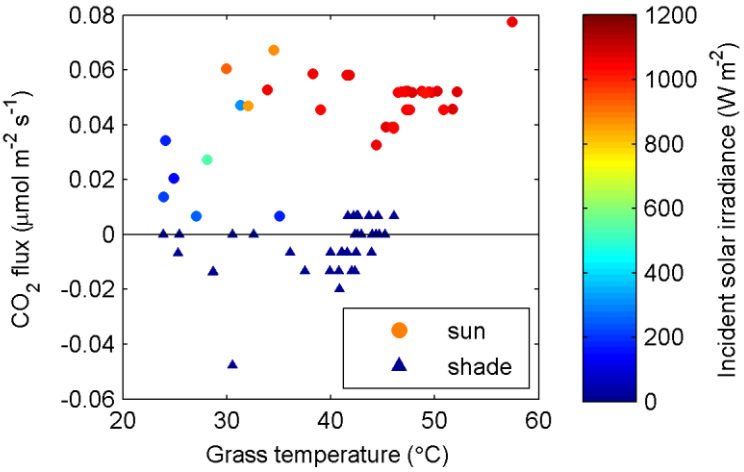

Figure 5.16 Response of CO_2 flux from dead, dried grass to exposure to solar irradiance as a function of grass temperature. CO_2 flux from grass in a transparent container alternatively exposed to (circles) and shaded from (triangles) solar irradiance. Note that the scales of x and y axes are different from Figure 5.12.

Similarly, CO_2 fluxes from dead maize leaves were zero in the shade (0.0023 ± 0.0104 µmol CO_2 m^{-2} s^{-1} (mean ± 95% confidence interval)) and greater than zero (0.0660 ± 0.0135 µmol CO_2 m^{-2} s^{-1} (mean ± 95% confidence interval)) when the container was exposed to solar irradiance (Figure 5.17). Regression analysis of sun run data using a constant, maize temperature and irradiance as predictors showed that irradiance was a significant predictor of CO_2 flux ($P < 0.001$), in contrast to maize temperature ($P = 0.87$) which did not improve the regression (n= 17, adjusted R^2 for total regression = 0.66).

The CO_2 fluxes from grass and maize leaves were much smaller than those observed from peat even when measured at the same irradiance and temperature levels and on the same days (Figure 5.18).

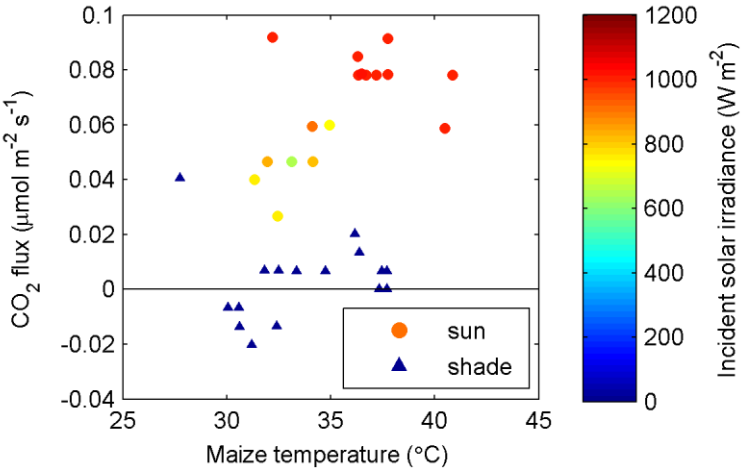

Figure 5.17 Response of CO_2 flux from dead, dried maize leaves to exposure to solar irradiance as a function of leaf temperature. CO_2 flux from maize leaves in a transparent container alternatively exposed to (circles) and shaded from (triangles) solar irradiance. Note that the scales of x and y axes are different from Figures 5.12 and 5.16.

Experiment D: Availability of oxygen

To test whether atmospheric oxygen was required for the production of CO_2 through photodegradation, the measurement setup was flushed with nitrogen gas to expel the oxygen (see Section 3.4.8). The average CO_2 flux from the peat in the presence of oxygen during experiment D was 0.1460 ± 0.037 µmol CO_2 m^{-2} s^{-1} (mean ± 95% confidence interval), and 0.1600 ± 0.049 µmol CO_2 m^{-2} s^{-1} (mean ± 95% confidence interval) when flushed with N_2. CO_2 fluxes in N_2 seemed to show a very similar relationship with temperature and irradiance to CO_2 fluxes measured in air (Figure 5.19). Regression analysis of sun run data collected when the system was flushed with nitrogen using a constant, peat temperature and irradiance as predictors showed that irradiance was a significant predictor of CO_2 flux ($P < 0.001$), in contrast to peat temperature ($P = 0.34$) which did not improve the regression ($n = 33$, adjusted $R^2 = 0.52$).

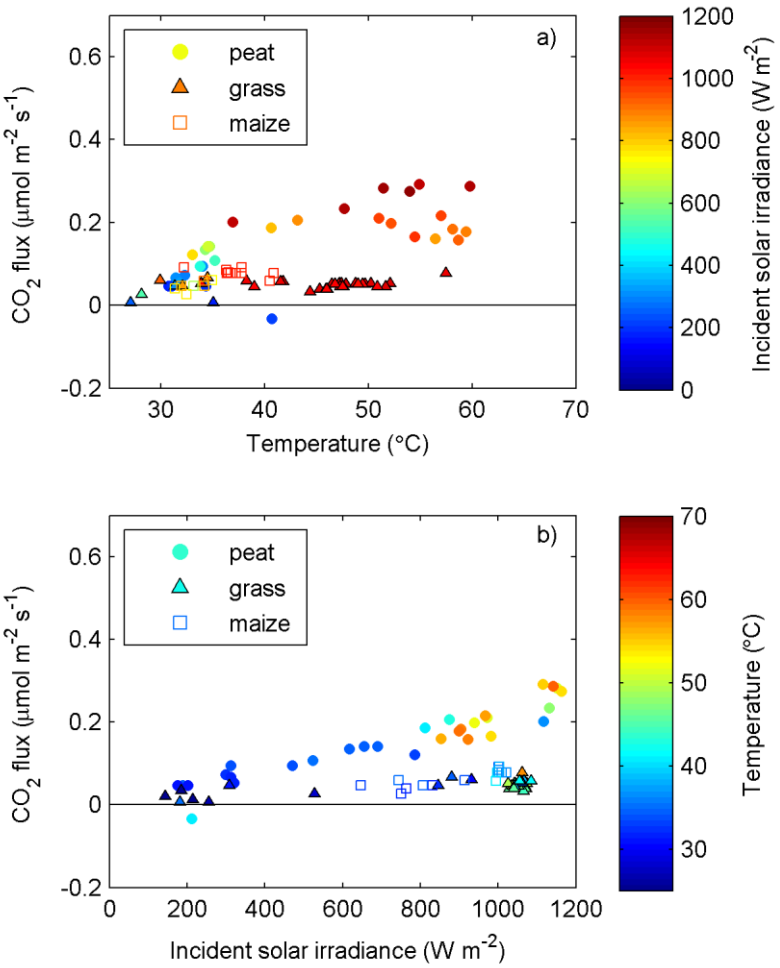

Figure 5.18 Response of CO_2 flux from peat (circles), grass (triangles) and maize leaves (squares) to exposure to solar irradiance as a function of a) substrate temperature and b) solar irradiance. Peat data are shown for experiment C and D (measurements between 2 - 23 April). Grass and maize data were from experiment C only (measurements between 2-23 April).

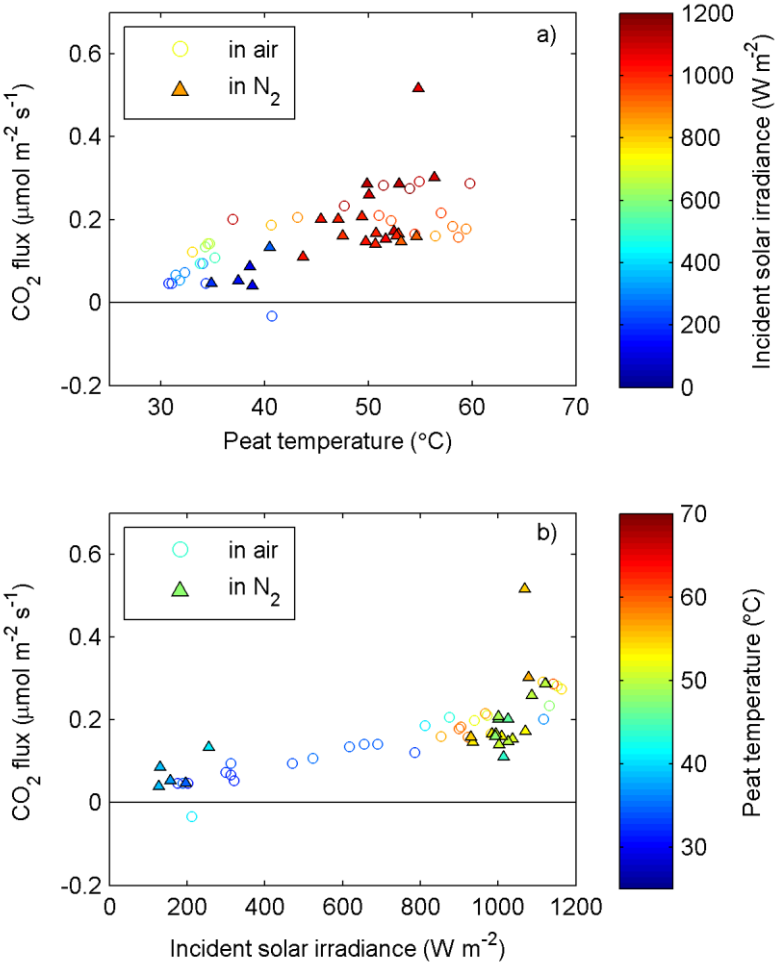

Figure 5.19 Response of CO_2 flux from peat to exposure to solar irradiance in the presence (circles) and absence (triangles) of oxygen as a function of a) peat temperature and b) solar irradiance. Data from experiment C and D are shown (measurements between 2 April and 23 April).

5.3.3. Differential scanning calorimetry to identify thermal decomposition

To investigate whether thermal decomposition of the peat might have taken place in the field, peat was analysed using differential scanning calorimetry (DSC). Results from representative runs are shown in Figure 5.20. Positive values of the heat flux in this graph show that more energy was required to heat up the peat + sample pan than just the sample pan. Because the wet peat contained much more water than the dry peat (which might have absorbed water while the sample was being prepared) larger heat fluxes were observed for the wet peat. Part of the energy might have been used for evaporation. The change in slope of both lines has been referred to as a 'glass transition' (Schaumann and

Antelmann, 2000; Schaumann and LeBoeuf, 2005), and will not be discussed here. None of the samples displayed any sign of thermal decomposition.

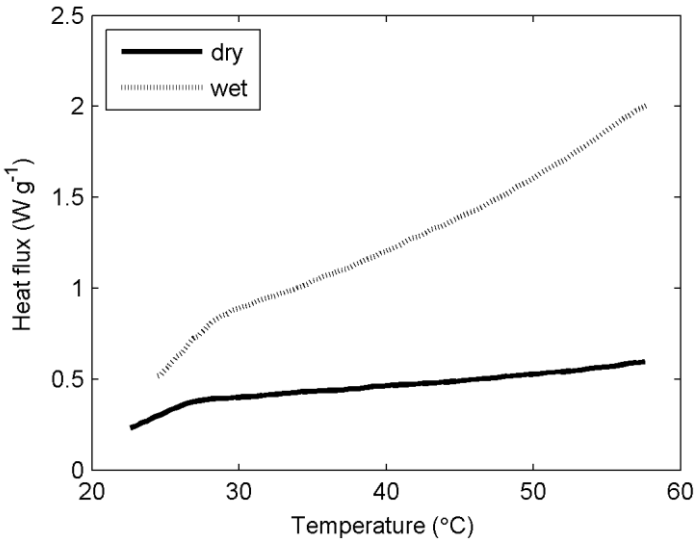

Figure 5.20. Results from differential scanning calorimetry analyses on wet and dry peat. Two representative runs out of 10 are shown. Heat flow > 0 depicts endothermic (i.e. heat-absorbing) heat flux.

5.4 Discussion

5.4.1. Pathways of abiotic CO_2 production

CO_2 production through photodegradation

There are two possible pathways for irradiance-induced CO_2 production from OM: the direct abiotic process of photochemical mineralisation and the indirect process of microbial facilitation, whereby partial breakdown of OM by irradiance enhances subsequent microbial activity (Section 2.7.2). Additionally, exposure to solar irradiance can lead to a decrease in CO_2 emissions caused by microbial inhibition (Section 2.7.2).

In the container experiment, photochemical mineralisation was the sole pathway leading to CO_2 loss because the dry peat samples did not support biological activity, as shown by the near-zero CO_2 fluxes during the shade runs. Photochemical mineralisation of OM to CO_2 has only been shown before on longer timescales (>24 hours) by exposing litter in jars to UV-B irradiance (Anesio et al., 1999) and solar irradiance (Brandt et al., 2009).

The net positive effect of solar irradiance on CO_2 fluxes observed at the field sites implied that the combined effect of photochemical mineralisation and possibly microbial facilitation was larger than the negative effect of UV on microbial activity at the surface.

At the grassland, low microbial respiration rates measured under dry conditions strongly suggested photochemical mineralisation as the main pathway for CO_2 loss. While data from wetter periods when microbial facilitation may have been important were deliberately excluded in the current analyses, there was evidence that this process may also contribute to CO_2 losses during the dry season at the grassland. Previous studies observed large pulses of CO_2 resulting from rapid microbial respiration following small, infrequent rain events (Xu and Baldocchi, 2004; Xu et al., 2004). Rates of CO_2 production in the dry season following rain can be greater than rates during the growing season when microbial mineralisation of labile root exudates and plant respiration also contribute to the total CO_2 flux (Xu and Baldocchi, 2004). Such large pulses are common during dry seasons in a wide range of semi-arid ecosystems (Fierer and Schimel, 2003; Huxman et al., 2004; Jarvis et al., 2007) but uncertainty still exists about the origin of the labile carbon that is mineralised. Hypotheses proposed to explain this phenomenon are:

1) drying and re-wetting breaks down soil aggregates, making previously physically protected SOM available for the surviving microbes (Austin et al., 2004; Jarvis et al., 2007 and references therein).
2) to avoid dehydration and death when the soil starts to dry out, microbes take up osmolytes, or solutes, to reduce their internal water potential. Then, when the soil rewets, the microbes must dispose of the accumulated intra-cellular osmolytes, in order to prevent rupture of the cell wall caused by too much uptake of water (Fierer and Schimel, 2003; Schimel et al., 2007). These organic compounds can either be respired to CO_2 by the cell, or transported out of the cell, where they are available for decomposition.
3) Drought stress can kill microbes that are not able to acclimate (Fierer and Schimel, 2003; Luo and Zhou, 2006; Schimel et al., 2007; Van Gestel et al.,

1991) and carbon and nutrients from the dead microbes becomes available for decomposition by the surviving microbes.

Results from the current study present the further hypothesis that part of the available labile substrates mineralised to CO_2 by microbes after a rain pulse are the product of partial breakdown of the OM by solar irradiance prior to rain, making substrates more available to microbes. This might explain why at the grassland, cumulative carbon losses via the pulses were larger at exposed sites than at shaded sites (Xu et al., 2004). This hypothesis for asynchronous microbial facilitation also fits well with the observation that the size of the CO_2 pulses tends to be proportional to the length of time since the last rainfall event (Jarvis et al., 2007; Sponseller, 2007).

For the peatland study site, where microbial respiration continued at the time of year when photodegradation was greatest, it was not possible to separate the contribution of photochemical mineralisation and microbial facilitation to the irradiance-induced CO_2 flux.

No evidence for CO_2 production through thermal degradation

Little information is available about the abiotic process of thermal decomposition (or thermal degradation) of organic matter to CO_2 at ambient temperatures. Whereas Schade et al. (1999) observed emissions of carbon monoxide (CO) as a result of thermal decomposition of litter, no studies could be found with similar observations of CO_2 emissions due to thermal decomposition at ambient temperatures.

Based on the field data, it was not possible to determine conclusively whether thermal decomposition was occurring. Figure 4.3 shows a small increase of total CO_2 flux with increasing temperature (when the radiation levels are kept constant), but this likely reflected the stimulation of microbial activity by increasing temperatures. The lack of CO_2 production at high temperatures (~60°C) in the dark during the container experiment suggested that thermal oxidation to CO_2 was not taking place (or were overwhelmed by the process that was causing the small negative fluxes, see Section 5.4.8 and Appendix E). Analysis

of the peat using differential scanning calorimetry (DSC) also showed no evidence for thermal decomposition of peat between 20 and 60°C, suggesting that thermal decomposition would not have taken place at the peatland and in the container at these temperatures. This agrees with other DSC studies of organic matter, which only observed breakdown at much higher temperatures (e.g. Barros et al., 2007; Pietro and Paola, 2004; Schaumann and LeBoeuf, 2005 supporting information).

5.4.2. Control by moisture

Results from the peatland site suggested that moisture content of the peat did not affect the response of CO_2 losses to absorption of solar irradiance: photodegradation was taking place under both wet and dry conditions (Figure 5.10). However, this conclusion is based on measurements of VMC at 45 mm depth because no measurements of VMC were made at the surface of the peat. Only one previous study examined the effect of moisture status on mass loss of litter caused by photodegradation. Smith et al. (2010) showed that in the samples with normal levels of microbial activity (i.e. mass loss was caused by both microbial degradation and photodegradation), the effect of UV-B irradiance on mass loss was largely determined by the moisture status of the litter. They found that exposure to extra UV-B enhanced mass loss in dry samples, whereas it inhibited mass loss in wet samples (Smith et al., 2010). This difference was explained by the inhibiting effect of UV-B irradiance on microbes in the wet samples. In the dry samples, microbial respiration was already hindered by lack of moisture and extra UV-B irradiance did not further restrict microbial activity. At the peatland, increases in irradiance continued to be associated with increases of CO_2 losses (Figure 5.10) suggesting that microbial inhibition was a process of minor importance at the peatland.

Smith et al. (2010) also examined the effect of water on photodegradation in samples with reduced microbial activity, but because of the longer duration of the experiments they were unable to fully suppress microbial activity, which complicated the interpretation of the data. To uncover the direct effect of water availability on CO_2 fluxes through photochemical mineralisation a

manipulative study which alters the moisture status of OM under sterile conditions would be most insightful.

5.4.3. Control by wavelength

From the field measurements, it was not possible to conclude which wavelengths were most important in controlling irradiance-induced CO_2 emissions. Levels of UV irradiance at any given solar zenith angle are typically strongly correlated to the levels of incoming solar irradiance (Figure 5.5) (Bodeker and McKenzie, 1996) and both measured global radiation ($K\downarrow$, 400 – 1100 nm) and estimated UV radiation (Section 3.5.2) showed a similar relationship with CO_2 flux (Figures 4.1 and 5.8).

Results obtained with the container using different filters showed that even when radiation in the UV range was (partially) blocked using Plexiglass or soda glass (which block UV-AB and UV-B, respectively), photodegradation still occurred (Figure 5.15). However, statistical analyses showed that CO_2 production rates were lower in the –UV-AB and – UV-B treatment compared to the full sun treatment (Section 5.3.2). It seemed that the majority of the CO_2 production (~86%) was caused by the exposure to visible light.

Other studies also found that radiation with wavelengths longer than those in the UV range (i.e. visible) can contribute substantially to photodegradation (Anesio et al., 1999; Austin and Vivanco, 2006; Schade et al., 1999). However, the contribution of visible light to the total irradiance flux found in the current study was considerably higher than that found in the most comparable study by Brandt et al. (2009), who found that 48% of the measured CO_2 flux was the result of exposure to visible light.

The results obtained using the container, together with findings of Brandt et al. (2009) make it very likely that UV irradiance was contributing to the measured CO_2 efflux at the study sites as well.

5.4.4. Control by temperature

Irradiance-induced CO_2 production in the field seemed to increase with increasing temperature (Figures 5.1 and 5.4). This potential interactive effect of temperature and irradiance on rates of irradiance-induced CO_2 production will be discussed as part of the next section.

5.4.5. Control by radiation and co-varying factors

Results from both the field and container studies showed that irradiance - induced CO_2 losses increased with increases in irradiance (Figures 4.1 and 5.12). The sensitivity of the irradiance-induced CO_2 flux to changes in solar irradiance seemed to vary between experiments, seasons and irradiance and temperature conditions (Table 5.3), and will be discussed in the rest of this section.

Linearity of dose-response relationship

Data from the container experiment showed a roughly linear response of CO_2 production to irradiance (Figure 5.12), whereas the field data suggested that the sensitivity of OM to exposure to solar irradiance might have increased with increasing global irradiance, UV-B irradiance and temperature (Figures 5.4 and 5.9).

As expected, solar irradiance conditions were strongly correlated with temperature and UV-B irradiance, and because the field experiment was fully observational (i.e. no manipulation of natural conditions was attempted) it was not possible to separate the potential controls that were most important in determining the variability in dose-response relationship in the field. However, several potential explanations can be put forward to explain non-linearity of the response of the irradiance-induced CO_2 flux to changes in solar irradiance.

- *Reaction pathways.* Organic matter is made up of many complex compounds which might react with photons (Moorhead and Callaghan, 1994). It is likely that a multitude of reaction pathways is responsible for the observed CO_2 losses (Moorhead and Callaghan, 1994; Wayne, 1988).

Table 5.3 Different values of dose-response relationships derived from data obtained using different methods.

	Method	Time scale	Dose–response (10^{-3} µmol CO_2 J^{-1})	Derived from	Described or displayed in
Field results					
Peatland NZ,	EC – chamber at max K↓	30 minutes	1.9	1.8 µmol CO_2 m^{-2} s^{-1} /975W m^{-2}	Figure 4.1 & Figure 5.4
Peatland NZ,	EC – chamber at intermediate K↓	30 minutes	1.2	0.6 µmol CO_2 m^{-2} s^{-1} /525W m^{-2}	Figure 4.1 & Figure 5.4
Peatland NZ,	EC – chamber at low K↓	30 minutes	0.7	0.16 µmol CO_2 m^{-2} s^{-1}/225W m^{-2}	Figure 4.1 & Figure 5.4
Peatland NZ, extrapolated for year	extrapolated using LUT* for EC flux and regression for chamber flux	year	0.80	50.2 g C m^{-2} y^{-1} / $5.2 \cdot 10^{9}$ J m^{-2} y^{-1}	Section 4.3.2
Grassland CA	EC – probes at max K↓	30 minutes	1.2	1.16 µmol CO_2 m^{-2} s^{-1}/975W m^{-2}	Figure 4.1& Figure 5.4
Grassland CA	EC – probes at intermediate K↓	30 minutes	0.7	0.37µmol CO_2 m^{-2} s^{-1}/525W m^{-2}	Figure 4.1& Figure 5.4
Grassland CA	EC – probes at low K↓	30 minutes	0.12	0.027µmol CO_2 m^{-2} s^{-1}/225W m^{-2}	Figure 4.1& Figure 5.4
Grassland CA, extrapolated for dry season	Extrapolated using LUT* for EC flux and regression for probe flux	Dry season	0.62	15.7 g C m^{-2} $85d^{-1}$ / $2.1380 \cdot 10^{9}$ J $85d^{-1}$	Section 4.3.2
Grassland CA for a "typical day"	Sum(EC flux) – sum(probe flux)/ sum(K↓)	day	1.2	$3.76 \cdot 10^{4}$ µmol CO_2 m^{-2} d^{-1} – $6.74 \cdot 10^{3}$ µmol CO_2 m^{-2} d^{-1}/ $2.53 \cdot 10^{7}$ J	Figure 4.5 & Section 4.3.2
"Incubation" results					
Peat in container	Total flux air - dried peat at max K↓	minutes	0.24 (Apr) 0.40 (Feb)	0.27 - 0.44 µmol CO_2 m^{-2} s^{-1}/1100W m^{-2}	Figure 5.13
Grass in container	Total flux air-dried grass at max K↓	minutes	0.05 (Apr)	0.05 µmol CO_2 m^{-2} s^{-1}/1000W m^{-2}	Figure 5.18
Maize leaves in container	Total flux air-dried grass at max K↓	minutes	0.08 (Apr)	0.08 µmol CO_2 m^{-2} s^{-1}/1000W m^{-2}	Figure 5.18
Grass litter in jar	Total flux sterile grass litter	3 days	0.10	0.6 mg CO_2-C MJ^{-1} **	Brandt et al. (2009)

*LUT = lookup table

** Brandt et al. (2009) report a 'dose response coefficient' of 0.6 mg C MJ^{-1} (page 8). Because they estimate that the sides of the microcosms shaded the litter by approximately 50%, this value was doubled (and converted to 10^{-3} µmol CO_2 J^{-1}).

Some of these pathways will involve products of photoreactions that could themselves react when a second photon is absorbed. A quadratic rise of CO_2 emissions in response to solar irradiance can be explained if two, instead of one, photons needed to be absorbed to produce one molecule of CO_2 (Schade et al., 1999).

- *Proportion of UV irradiance.* At small solar zenith angles (SZA) and high global irradiance the proportion of radiation in the UV-B wavelengths was larger than at lower levels of global irradiance (Figures 5.5 and 5.6) (Cui et al., 2008; Schade et al., 1999). This can be explained by the increase of optical path length with increasing SZA (Bodeker and McKenzie, 1996); because UV radiation has a higher sensitivity to changes in the optical path than total radiation (Caldwell and Flint, 1995; Cui et al., 2008), the ratio UV-B/global radiation was larger at high solar irradiance levels than at lower levels (Figure 5.5). This non-linear relationship might partly explain the increase of dose-response relationship because photons in the UV-B range contain more energy per photon (Anslyn and Dougherty, 2006; Atkins and de Paula, 2005) and are particularly effective in breaking molecular bonds of organic matter (Moorhead and Callaghan, 1994). However, this relative importance of UV irradiance was not confirmed by results from the container experiment which suggested that irradiance in the UV wavelength was only responsible for a small portion of the CO_2 losses (Section 5.4.3).
- *Interaction with temperature.* The increased sensitivity of irradiance-induced CO_2 flux to changes in solar irradiance at higher temperatures might indicate an interactive control between temperature and radiation (Figure 5.2). In general it has been found that (for non-photochemical reactions), an increase in temperature can result in a large increase in rate of reaction (Atkins and de Paula, 2005), especially for reactions with high activation energy. The rate of photochemical reactions can also be influenced by temperature. Temperature can affect the spatial arrangement of atoms in a molecule by altering the rotating angle of bonds, without changing the make-up (i.e. atoms and bonds) of the

molecules, so that the same molecule can exist in different so-called 'conformers' (Anslyn and Dougherty, 2006). If these different forms (or conformers) of the same molecules have different photo-reactivity or conformation-specific pathways of photo-dissociation exist (e.g. Choi et al., 2008; Khriachtchev et al., 2002), a change of the dose-response with changes in temperature would be expected.

Although Austin and Vivanco (2006) attributed the difference in mass loss between exposed and shaded litter samples fully to the difference in irradiation, they also found that surface soil temperatures in summer were significantly higher in the exposed plots compared to the shaded plots (Austin and Vivanco, 2006, Supplementary Information). This suggested that the extra mass loss at exposed sites might be controlled by increased temperature combined with higher irradiation, which would be in agreement with the findings of the current study.

No dose-response relationships are available in the literature for the response of irradiance-induced CO_2 fluxes to solar irradiance from terrestrial organic matter. Smith et al. (2010) found a linear response between irradiance and mass loss (Figure 2.6), but they only varied the irradiance in the UV-B wavelengths. Carbon monoxide emissions from terrestrial organic matter have been found to be both linear (Schade et al., 1999; Yonemura et al., 1999) and non-linear (Schade et al., 1999), depending on the dominating reaction pathway (Schade et al., 1999).

Although explanations can be found for both a linear and non-linear response of CO_2 flux with increasing radiation (and temperature), it is challenging to explain why a different response curve was found for the field and container experiments.

Different response to same irradiance levels between seasons

A difference in the response of the CO_2 flux to apparently similar irradiance levels was observed when comparing container measurements made during different months (Figure 5.13). The cause for this difference was not

clear, but one possible explanation might be the difference between months in the proportion of energy in the UV range of the solar spectrum compared to the total energy received from the sun. Whereas averaged for February, 0.21 % of the energy was in the UV-B range, this percentage dropped to 0.17% for April (Figure 5.7b). This difference was caused by the difference in solar zenith angle between the months (see above). Consequently, while measured shortwave solar irradiance in the current study might have been the same between months, UV levels would have been lower in April compared to February, which could have caused a lower CO_2 flux. However, the small (but statistically significant) increase in flux that UV irradiance was responsible for in Experiment B (Section 5.4.3), would seem to suggest it was unlikely that this small difference in UV radiation would have been solely responsible for the observed difference between CO_2 fluxes in February and April.

Another potential contributor to the difference between CO_2 fluxes in the container from peat during different months might have been the difference in temperature. In April, the temperature of the peat was generally lower than in February, even at high radiation levels (e.g. at high radiation levels, average temperature of the peat was approximately 63°C and 55°C in February and in April, respectively; Figure 5.13). If temperature interacts with radiation in controlling the CO_2 efflux, these lower temperatures in April might be responsible for part of the difference in dose-response relationship between February and April.

Dose response relationship field vs. container

The values for the dose-response coefficient found in the present study for the container experiment were in the same order of magnitude as the values found by Brandt et al. (2009) for incubations in a jar (Table 5.3). In contrast, the dose-response coefficients found in the field were generally much higher than those observed in the container: at the peatland the dose-response coefficient was $1.9 \cdot 10^{-3}$ µmol CO_2 J^{-1} at its maximum, whereas the average value found in February for the container study was only $0.40 \cdot 10^{-3}$ µmol CO_2 J^{-1} (Table 5.3). Similarly, the grassland study showed maximum dose-response coefficient of

$1.2 \cdot 10^{-3}$ µmol CO_2 J^{-1}, whereas in the container, this was only 0.05 µmol CO_2 J^{-1} for grass (in April; Table 5.3; however, bear in mind that the grass substrates were not the same between field and container study). The causes for this large difference between container and field experiments were not clear. Possible explanations could include that solar irradiance was measured next to the container. Even with the quartz top some absorption of solar irradiance would have occurred (~8%; Table 3.3), leading to lower irradiance levels reaching the peat than the measurements would have suggested. Possibly the sides of the container were partly blocking the radiation as well during measurements made when SZA were relatively large.

However, this explanation seems to insufficiently explain why the dose-responses obtained from container and field experiments would be so different from each other. Until a suitable explanation can be found, this finding emphasises the importance of field measurements in addition to lab experiments.

Brandt et al. (2009) extrapolated results from a jar-experiment to estimate irradiance-induced losses from a desert in New Mexico using a dose-response coefficient obtained from the incubations (Table 5.3). Results from the current study suggest that the dose response coefficient obtained using incubations might substantially underestimate the "real dose-response coefficient" observed in the field. If a similar underestimation occurred during the study of Brandt et al. (2009), their estimate for irradiance-induced CO_2 losses in the desert is likely to be an underestimate.

5.4.6. Influence of substrate

Comparing the size of the irradiance-induced CO_2 flux between field sites is challenging, because several factors differed between sites. However, it is noteworthy that the dose – response relationship observed at the peatland was generally higher than that observed at the grassland (e.g. at high irradiance levels of ~ 1000 Wm^{-2}, $1.9 \cdot 10^{-3}$ µmol CO_2 J^{-1} vs. $1.2 \cdot 10^{-3}$ µmol CO_2 J^{-1}, see Table 5.3). For the container experiments, an even larger difference was observed in CO_2 production between peat (0.24 µmol CO_2 J^{-1}) on the one hand and grass

(0.05 µmol CO_2 J^{-1}) and maize leaves (0.08 µmol CO_2 J^{-1}) on the other (Table 5.3). It was not possible to conclusively state what caused these differences at this stage of the research. However, several potential causes might be responsible:

- *Surface coverage in the field.* Coverage of dead organic matter was higher at the peatland than at the grassland site. At the peatland, 100% of the surface area was covered with dead OM, whereas coverage at the grassland was likely somewhat lower. For the container experiments, difference in coverage could not have caused the difference in fluxes, because for both peat and grass coverage was 100%.
- *Albedo*. In this study, the controls of irradiance-induced CO_2 fluxes were studied using solar incoming irradiance (or "incoming shortwave radiation") as one of the main drivers. However, part of this shortwave radiation was reflected at the surface and could therefore not contribute to the photodegradation process. Possibly, the use of net shortwave radiation (= incoming radiation – reflected outgoing radiation) might have been more appropriate, however, net shortwave radiation data were not available for most of the study period at the peatland.

  The albedo of a surface (outgoing shortwave radiation / incoming shortwave radiation) changes with time of day and time of year. It generally increases with decreasing moisture content and increasing solar zenith angle (Grant et al., 2000; Iqbal, 1983; Mayor et al., 1988), which causes the fraction of reflected shortwave radiation to be smaller around solar noon compared to the morning and afternoon. Values of albedo for different surfaces can vary greatly (Iqbal, 1983).

  The average daytime albedo was 0.07 at the peatland (Dec 2006 – Jan 2007), and 0.17 at the grassland (averaged over the dry period of 2007 - values around noon were 0.15). This difference in albedo would have lead to more available energy at the peatland, because a smaller portion of incoming solar irradiance was reflected. For example, at shortwave incoming radiation levels of 1000 Wm^{-2}, the net shortwave radiation would have been 80 Wm^{-2} higher at the peatland compared to the grassland (=1000 Wm^{-2} * (0.15 –0.07)). This might be a partial

explanation why CO_2 fluxes from the dark peat were larger than from the lighter coloured grass. In contrast to the albedo in the shortwave region (wavelengths > 400 nm), the albedo for UV wavelengths has been found to be larger for bare soil compared to grass (Blumthaler and Webb, 2003; Feister and Grewe, 1995; Madronich, 1993). However, the relevance of this difference is hard to estimate because no UV irradiance data were available for the grassland.

- *Temperature*. In the container, the temperature of peat was higher than that of grass or maize leaves (Figure 5.18), which might have contributed to the lower fluxes from the latter. For the field studies (where differences between CO_2 fluxes from peat and grass were much smaller) this direct comparison of temperatures was not possible because surface temperatures were not available for the peatland during most of the study period.
- *OM chemistry.* The different chemistry of peat and dead grass was likely the main cause of the difference in irradiance-induced CO_2 flux. Although no consensus has been reached about which compounds of OM are most susceptible to photodegradation (Brandt et al., 2007; Gehrke et al., 1995; Moorhead and Callaghan, 1994; Schade et al., 1999; Section 2.7.4), it is likely that the different chemical make-up of grass and peat was responsible for at least some of the difference observed between dose-response relationships between sites.

5.4.7. Control by oxygen availability

Production of CO_2 did not seem hindered by flushing the container with nitrogen gas (Figure 5.19). This was contrary to expectations: previous work had suggested that the oxygen atoms in the emitted CO_2 originated from the surrounding air (Cory et al., 2008). In contrast, Schade (1997) confirmed that CO emission continued, albeit at a lower rate, when irradiating dead plant material in a nitrogen atmosphere.

Because no means of measuring the remaining O_2 concentration was available during the nitrogen runs in the current study, it is conceivable that

enough oxygen still remained in the system to enable photodegradation, even if atmospheric oxygen was required for the formation of CO_2. This left the results of the oxygen-experiment somewhat inconclusive.

5.4.8. Methodological considerations

Previous studies have suggested that measurements of irradiance-induced CO_2 fluxes are a more sensitive method for determining rates of photodegradation than measurements of mass loss (Brandt et al., 2009; Duguay and Klironomos, 2000). Measurements of irradiance-induced CO_2 fluxes allow researchers to measure the effects of photodegradation over short time periods (in the order of weeks). For instance, during a 10-week study, Brandt et al. (2009) measured a great increase of CO_2 concentration on exposure to irradiance, whereas they were unable to detect any loss of litter mass over the same time period. Previous incubation studies monitored irradiance-induced CO_2 production with measurements of (increase in) CO_2 concentration made at least 24 hours apart (Anesio et al., 1999; Brandt et al., 2009; Duguay and Klironomos, 2000; Gehrke et al., 1995).

The current study is the first to measure the instantaneous evolution of CO_2 in response of OM being exposed to irradiance. The closed flow-through chamber system (the "container") developed in this study, with its fast response of CO_2 flux to changing conditions, presented opportunities for studying the controls of photodegradation and the susceptibility of different substrates to photodegradation.

However, several methodological challenges presented themselves during the experiments which will need to be resolved in the future. These will be discussed below.

Condensation

At times, condensation occurred in the container and tubing, even when using air-dried peat. This water would have partly blocked the solar irradiance, and might have inadvertently trapped CO_2. Using a desiccant to scrub the air from all water vapour was found to present challenges as well, as the trapped

water vapour might serve as a trap for CO_2 and interfere with the measurements. In future experiments, especially those trying to elucidate the effect of moisture content on photochemical mineralisation rates, this issue would need to be resolved.

Negative fluxes in the dark

The small negative fluxes that were observed during the dark runs and their potential causes are discussed in Appendix E. In summary, for the dark runs, the size of the negative CO_2 seemed inversely correlated with temperature, and correlated to changes in temperature during the run, i.e. fluxes were most negative at high temperatures and at times that temperature was dropping most rapidly (Figure E.3). The cause of the small negative fluxes is as yet unclear, but could be a result of (temperature-mediated) adhesion of CO_2 to peat particles or tubing and the container, evaporation and condensation of water, changes in solubility of CO_2 in water caused the temperature changes, or possible measurements artefacts caused by non-stationary temperature and moisture conditions in the container-analyser setup. In contrast, no trends in CO_2 efflux with changing temperatures were observed during the sun runs (Figure E.3).

Correlation between irradiance and temperature

Peat temperatures measured during the container experiment were high (Figure 5.12), but still representative of surface temperatures occurring in the field: surface temperatures of up to 60 °C were observed during summer at the bare peat mine (data not shown). It would be desirable to have greater overlap in temperatures between sun and shade runs; this requires an approach which allows for manipulation of temperature (i.e. a way to heat up or cool down the substrate) independent of irradiance levels.

Recommendations for future container experiments

Although the container setup was very useful for measuring irradiance-induced CO_2 losses from OM, several recommendations can be made when using a similar setup in the future:

- Replace the plastic tubing with metal or glass tubing to rule out potential degradation of the plastic under high temperatures or irradiance levels.
- Construction of an even shallower container would reduce shading of the substrates by the sides of the container. Alternatively, the whole container could be constructed from a transparent material like quartz. An additional benefit of a very shallow container would be that the area/volume ratio would be larger; thereby making the setup more suitable for measuring smaller fluxes.
- Add a way to control temperature separately from radiation.
- In addition to measuring shortwave incoming radiation, shortwave outgoing radiation should be measured as well. Measurements of radiation in the UV-A and UV-B wavelengths would provide valuable information also.

5.5 Summary

Irradiance-induced CO_2 fluxes measured at the peatland and grassland increased with increasing global irradiance, UV irradiance and temperature. Because these quantities are strongly correlated with one another, it was not possible to fully determine which factor(s) were most responsible for the variability in the observed CO_2 fluxes. The response of CO_2 flux to irradiance increased with increasing radiation and temperature, indicating potential interaction between temperature and radiation. Changes in moisture content of the peat did not seem to affect the control of irradiance on CO_2 fluxes measured in the field.

The closed flow-through chamber setup (“container”) was very suitable for measuring irradiance-induced CO_2 losses from organic matter at very high time resolution. Measurements of CO_2 flux from air-dried peat, grass and maize leaves using the container setup confirmed the production of CO_2 by photochemical mineralisation.

Container measurements showed that UV irradiance was responsible for approximately 14% of the irradiance-induced CO_2 losses. The remaining 86% was caused by visible light. In the container, CO_2 production from both grass and

maize leaves was much less than the CO_2 produced by peat: fluxes at high solar irradiance from grass and maize leaves were only 21-33% of that from peat. This difference was probably caused by a combination of difference in albedo, temperature and organic matter chemistry.

One of the main challenges that presented themselves when using the new container setup was the presence of small negative fluxes observed in the shade runs. The cause of these negative fluxes was unclear, but might have been the adsorption of CO_2 to the tubing and/or OM particles (but see Appendix E).

Approximately 5 times as much CO_2 was produced in the field compared to in the container, even when radiation levels were similar. The cause for this difference was unclear, and until this difference is resolved, extreme caution has to be taken when extrapolating the results from small-scale experiments to the field scale.

Chapter 6 Controls of microbial respiration of peat

6.1 Introduction

Globally, soils store more carbon than the atmosphere and terrestrial biosphere combined (Janzen, 2004). The main pathway for carbon transfer from soil to the atmosphere is organic matter (OM) decomposition, primarily due to microbial activity resulting in CO_2 production (Davidson et al., 2006a; Grace and Rayment, 2000; Janzen, 2004; Luo and Zhou, 2006). CO_2 efflux measured at the soil surface is the result of both production of CO_2 in the soil profile and subsequent transport of the produced CO_2 to the soil surface (Fang and Moncrieff, 1999).

Between 16-33 % of global soil carbon is stored in peatlands (Gorham, 1991; Lappalainen, 1996; Maltby and Immirzi, 1993) and about 10 % of these peatlands have been drained for use in agriculture, forestry or for peat mining (Table 2.1; Joosten and Clarke, 2002). Peat mining involves drainage of the peatland, removal of the vegetation and extraction of the peat, after which the sites are either abandoned or attempts are made to restore the ecosystem. Whereas natural peatlands are an important sink for atmospheric CO_2 (Gorham, 1991), peatlands that are drained, mined and subsequently abandoned are often found to be persistent sources of CO_2 (Nykänen et al., 1995; Silvola et al., 1996; Sundh et al., 2000; Waddington and McNeil, 2002; Waddington and Price, 2000; Waddington and Warner, 2001). This switch from sink to source of CO_2 is caused by the destruction of the carbon fixing vegetation, while microbial respiration continues (Sundh et al., 2000; Waddington et al., 2002).

Organic matter in mineral and peat soils (of which approximately 50% is carbon; Blanco-Canqui and Lal, 2004; Luo and Zhou, 2006) improves soil structure, enhances water holding capacity and supplies nutrients for plant growth (Luo and Zhou, 2006; McLaren and Cameron, 1996). These benefits emphasize the need to conserve OM in soils and to minimise losses of carbon from soils, which requires a thorough understanding of the drivers of soil

respiration. Of additional importance is the role that soil respiration plays in the global carbon cycle and its potential effect on the global climate. Because soils constitute a large pool of carbon, even small changes in rates of soil respiration could affect atmospheric CO_2 concentration which in turn could influence global climate (Kirschbaum, 2000; Raich and Schlesinger, 1992; Rustad et al., 2000). This feedback between the terrestrial carbon cycle and climate is one of the largest uncertainties in projections of future climate (Friedlingstein et al., 2006; Jones et al., 2003; Schimel et al., 2001). Because of the important 'services' of SOM for soil quality and carbon storage, it is critical to increase our understanding of the controls and drivers of the rates of soil respiration (Rustad et al., 2000). This research involves measurements of respiration and its drivers at various time and spatial scales, and translation of these measurements into models that can accurately describe temporal and spatial patterns of carbon release from soils, thereby allowing prediction of soil respiration under changing climate conditions (Baveye, 2007), land use and management practices (Paustian et al., 2000).

In addition to substrate quality, soil temperature and moisture content are the most important controlling factors of soil respiration (Davidson et al., 2006b). Microbial activity and thus respiration rates tend to increase with increasing soil temperature over the range of temperatures commonly observed in the temperate climate zone (Davidson and Janssens, 2006; Kirschbaum, 2006; Luo and Zhou, 2006). Incubations of peat confirm the common conceptual model of the relationship between soil moisture and soil respiration which states that microbial activity is highest at intermediate soil moisture levels (e.g. Glatzel et al., 2006; Linn and Doran, 1984; Waddington et al., 2001) that are not limiting the diffusion of oxygen or substrates (Section 2.6.2; Davidson et al., 2000; Janzen, 2004; Luo and Zhou, 2006; Skopp et al., 1990). At either end of the moisture scale, soil respiration rates are expected to be lower, because of stress caused by a decrease in substrate availability and microbial physiological changes (Schimel et al., 2007) at the dry end of the spectrum (Davidson and Janssens, 2006; Luo and Zhou, 2006), or low oxygen availability limiting aerobic respiration at the wet end of the spectrum (Figure 6.1; Davidson and Janssens, 2006; Gaumont-Guay et al., 2006; Glatzel et al., 2004; Moore and Dalva, 1997;

Waddington et al., 2001 and references therein). At optimal moisture conditions, a strong relationship is generally observed between temperature and soil respiration (e.g. Fang and Moncrieff, 2001). In contrast, the control by temperature might not easily be observed if moisture levels are outside an optimal range and respiration might be inhibited by low oxygen, water or substrate levels (Kirschbaum, 2000). Several studies have concluded that when moisture conditions are either below or above optimum levels, temperature is not an important driver (e.g. Almagro et al., 2009; Jassal et al., 2008; Reichstein et al., 2002; Sowerby et al., 2008).

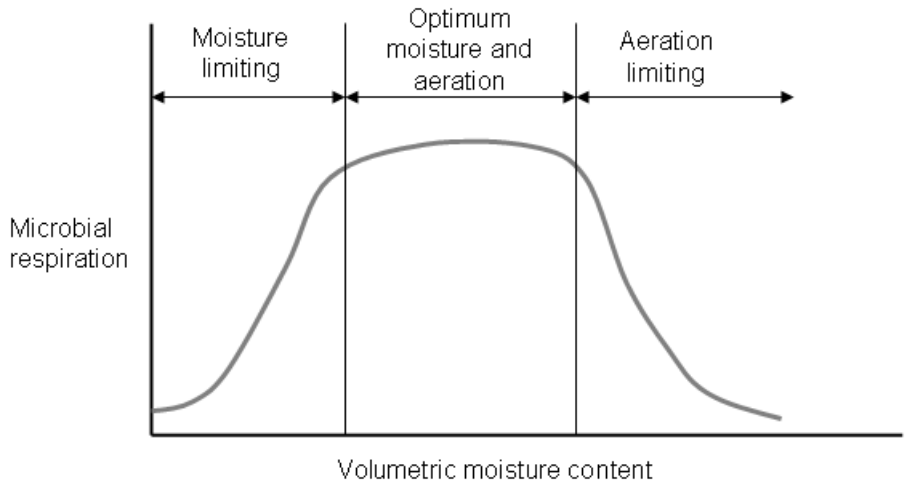

Figure 6.1 Conceptual model of the control of volumetric moisture content on microbial respiration (at a constant temperature; redrawn after Luo and Zhou, 2006).

Often, soil respiration is modelled by relatively simple linear or exponential equations based on soil temperature (Section 2.6.3; Davidson et al., 2000; Rustad et al., 2000). One of the challenges arising from this approach is the decision at which depth to measure the temperature that is used for the model (Graf et al., 2008; Richardson et al., 2006a). Different criteria have been used to determine which depth is most suitable. In many studies, the temperature is used from the depth which yields the highest R^2 of the relationship between temperature and the CO_2 flux at the surface (e.g. Carbone et al., 2008; Pavelka et al., 2007; Shi et al., 2006). Sometimes, researchers use the depth which gives the smallest hysteresis in the temperature-flux relationship (e.g. Gaumont-Guay et

al., 2006). Both methods aim to estimate which layer in the soil profile is responsible for the majority of the CO_2 production. However, especially when a thick layer of the soil is contributing to the total respiration, determining the 'best' measurement depth is challenging (Graf et al., 2008).

Factors controlling the variability of soil respiration may vary depending on the time scale one is working on (Carbone et al., 2008; J. Curiel et al., 2007). For example, Ouyang and Zheng (2000) found that daily variation of soil respiration was mostly controlled by solar radiation (and thus temperature), whereas on a monthly time scale, rainfall (and thus moisture status of the soil) was the most important factor controlling variation. Similarly, short-term (within-day) temperature sensitivity of soil respiration can be quite different than the temperature sensitivity obtained using long-term (seasonal) trends in respiration and temperature (Reichstein et al., 2005b). Modelling of soil respiration can also take place at a variety of time scales: for climate projections modelling annual or seasonal time steps might be appropriate (Kirschbaum, 2009). In contrast, when aiming to increase mechanistic understanding of the soil respiration process, within-day variation is often examined (Carbone et al., 2008; Tang et al., 2005). However, predicting soil respiration rates at this time scale can be very challenging. For example, the response of the CO_2 efflux to change in temperatures might be lagged, leading to hysteresis in the relationship between temperature and surface CO_2 flux (Bahn et al., 2008; Graf et al., 2008). Another process which makes prediction of CO_2 fluxes at high temporal resolution difficult are short-time pulses of CO_2, for example in response to rainfall (Jarvis et al., 2007).

In vegetated ecosystems, the response of microbial respiration to changing environmental conditions is often confounded by responses of plants to these changing conditions, which in turn can affect microbial respiration (e.g. Bahn et al., 2008; Tang et al., 2005). Field studies examining respiration from bare soil offer the opportunity to examine the controls on the CO_2 efflux resulting from microbial respiration alone at large scales and in the absence of plants.

The current study focuses on the controls of heterotrophic respiration (HR) by microbes at a bare peatland in New Zealand. The main objectives were to describe how temperature, moisture and depth to water table at the peatland affect the CO_2 flux at monthly, daily and within-day timescales. These findings will be compared to the conceptual model depicted in Figure 6.1. The extent to which relatively simple regression models can explain the variability in measured HR is explored and compared to results found in other peatland studies.

6.2 Methods

6.2.1. Study site and conditions

Measurements of CO_2 efflux were made at a mined peatland. The site was devoid of plants, and drained to allow mining of the peat. Depth to water table (DWT) ranged from 0.05 m in winter to 0.45 m in summer (Figure 3.2). Volumetric moisture content (VMC) was measured at two depths (45 and 105 mm). Although VMC at 45 mm stayed relatively high during summer (minimum was 0.44 $m^3\ m^{-3}$), the surface peat above the sensor dried out considerably more.

6.2.2. Measurements

To determine the rates of microbial respiration, CO_2 efflux was measured using a LI-8100 automated soil CO_2 flux system attached to a large opaque chamber (200 mm diameter – also referred to as the 'long term chamber'). Measurements were made at 15-minute intervals. Additional measurements were made using a smaller survey chamber to sample the spatial variability. Refer to Appendix F for an analysis of spatial variability of the chamber flux at the peatland. Because the long-term chamber measurements of CO_2 flux were similar in size to fluxes obtained during spatial sampling, and fluxes obtained with the long-term and survey chambers revealed comparable patterns with changes in temperature and moisture, the long-term chamber measurements were found to be appropriate for gaining a mechanistic understanding of the controls of the CO_2 efflux. The long-term chamber measurements will not be used to establish a yearly carbon budget of CO_2 at the peatland and,

consequently, possible differences in absolute size of the CO_2 fluxes were not of concern.

Photodegradation does not occur when solar radiation is absent and night-time eddy covariance (EC) measurements could potentially be used as a direct measure of microbial respiration as well. However, strict filtering necessitated by narrow lanes of bare peat in the footprint and low windspeed conditions at night leading to stable atmospheric conditions led to poor data availability with less than 3 % of the data remaining after filtering. As a result of this low data availability, chamber data were considered a more reliable data source for examination of the CO_2 flux of biological origin.

Because the peatland was not vegetated, root respiration was not contributing to the total CO_2 efflux.

Peat temperature at 30 mm depth was measured next to the chamber. Approximately 7 m away, as part of the EC setup, temperatures at more depths were also measured (5, 50, 100 mm). For much of the measuring period, an additional array of temperature probes provided information on peat temperatures at depths 20, 40, 80, 160, 240, 320, 400 and 500 mm. The volumetric moisture contents at 45 and 105 mm depth, and the depth to water table were measured as part of the EC setup also.

6.2.3. Data analysis

Monthly and daily averaged CO_2 flux

In this chapter, the controls of CO_2 flux were examined at different time scales. Both monthly and daily averages were used for the CO_2 flux, as well as 15-minute data. For the daily averages, a minimum of 50 observations (i.e. measurements of at least half a day) was required to calculate a daily average. Measurements were usually available for the total 24 hours (i.e. 96 data points per day). In contrast, for the monthly averages, the number of data points varied greatly between months. For all months when chamber data were collected, the mean diurnal variation was calculated from the average value for each hour of the day. These 24 hourly values were then averaged to obtain the mean value for

that month. The number of days making up a monthly average varied between 4 and 31.

Empirical models

In this study, several forms of regression models for the temperature control on the CO_2 flux were compared. The first was a linear relationship (Rochette et al., 1991; Wofsy et al., 1993):

$$HR = a + bT \qquad \textbf{Equation 6.1}$$

where HR is the CO_2 efflux (µmol CO_2 m^{-2} s^{-1}) of microbial origin (heterotrophic respiration), T the peat temperature (°C) and a and b are fitted parameters. Similar equations with volumetric moisture content VMC or depth to water table DWT instead of temperature will also be presented.

Two forms of exponential regression models for the temperature control on the CO_2 flux were compared. A simple exponential equation (first proposed by Van 't Hoff (1884)) was fitted in the form:

$$HR = \alpha e^{\beta T} \qquad \textbf{Equation 6.2}$$

where α is the soil respiration rate at 0°C and β is the temperature sensitivity parameter ($°C^{-1}$). Similar equations with VMC or DWT instead of T will also be presented. Using the exponential equation with temperature as the predictor, the Q_{10}, a parameter used to describe the temperature sensitivity, was calculated using $Q_{10} = e^{10 \cdot \beta}$.

An alternative exponential regression model using peat temperature is the commonly applied Lloyd and Taylor (LT) function, which was fitted in the form (Luo and Zhou, 2006):

$$HR = R_{ref} e^{E_0 \left(\frac{1}{T_{ref} - T_0} - \frac{1}{T - T_0} \right)} \qquad \textbf{Equation 6.3}$$

where the fitted parameter R_{ref} represents the respiration rate at a reference temperature, E_0 is a parameter related to the activation-energy and T_0 is the

temperature at which respiration rates are assumed to approach zero (Kirschbaum, 2000; Reichstein et al., 2003) . However, the LT function in the form presented above (with three fitted parameters R_{ref}, E_0 and T_0) has been found to be over-parameterised because the parameters are strongly correlated (Richardson and Hollinger, 2005) and different combinations of the parameters can yield equally acceptable versions of the model. For this reasons, T_0 was fixed at 227.1K, as used in the original analyses by Lloyd and Taylor (1994), and only R_{ref} and E_0 were fitted in the current study. The equivalent of the Q_{10} for the LT equation (Q_{10_LT}) does not depend on $R_{ref,}$ but does vary depending on the temperature range it is determined over, as was confirmed in experimental data (Kirschbaum, 2000 and referenced therein).

Many empirical models exist describing the simultaneous effect of soil temperature and moisture on soil respiration (e.g. Richardson et al., 2006a). In this thesis, two equations are compared that have been used in peatlands before. The first has been applied to mined peatlands in Canada by Waddington and Warner (2001)

$$\mathrm{HR} = a + b \cdot T + c \cdot DWT \qquad \textbf{Equation 6.4}$$

where T is the peat temperature (°C), DWT is the depth to water table (mm), and a, b and c are fitted constants. Often, DWT is used instead of the moisture content because it is more easily measured. The second equation was applied to various peatland study sites in Finland by Silvola (1996)

$$\ln(\mathrm{HR}) = a + b \cdot T + c \cdot DWT \qquad \textbf{Equation 6.5}$$

where a, b and c are fitted constants.

Determination of delays

For examining the controls of temperature on the within-day variation of the CO_2 flux, the monthly mean diurnal variation (MDV) was calculated for the CO_2 efflux and temperatures (T) at all depths. The delay between T at a certain depth and the CO_2 efflux measured at the surface was estimated by determining

the delay which resulted in the maximum correlation between the two signals (CO_2 flux and *T* at depth, see also Parkin and Kaspar (2003)). The same method was used to determine delay times between temperature at depth and the temperature measured close to the surface (5 mm depth).

6.3 Results

Results will be shown using data at increasingly higher time resolutions. First, monthly averaged data will be examined, after which daily averages are discussed. Within-day variations are studied using mean diurnal variation calculated monthly and a few case studies using 15-minute data.

6.3.1. Temperature, rainfall, moisture and soil respiration throughout the measurement period

Figure 6.2 shows the variation in peat temperature, rainfall, depth to water table, volumetric moisture content and chamber CO_2 flux from June 2005 – June 2008.

Typically, peat temperature peaked in January and February, which coincided with the time of lowest water table and lowest volumetric moisture contents (Figure 6.2a, b, c, see also Figure 6.3). Seasonal changes in temperature propagated from the surface downward, causing temperatures measured deeper down the peat profile to lag behind the surface temperature. Temperatures deeper in the peat displayed a smaller yearly variation than the surface temperature (Figure 6.2b).

The peat experienced larger variation in VMC at 45 mm than at 105 mm depth (Figure 6.2c). At all times, VMC measured at 105 mm was greater than 45 mm (Figure 6.2c). Around mid-November of 2007, the measured volumetric moisture content at both depths dropped to values lower than the values measured the previous two summers (dashed lines in Figure 6.2d). Even though the region experienced severe drought conditions between December 2007 and February 2008 (Mudge, 2009), it is unlikely that these measured moisture contents reflect real values, especially because VMC values failed to rise in response to rainfall and a rising water table in March and April of 2008.

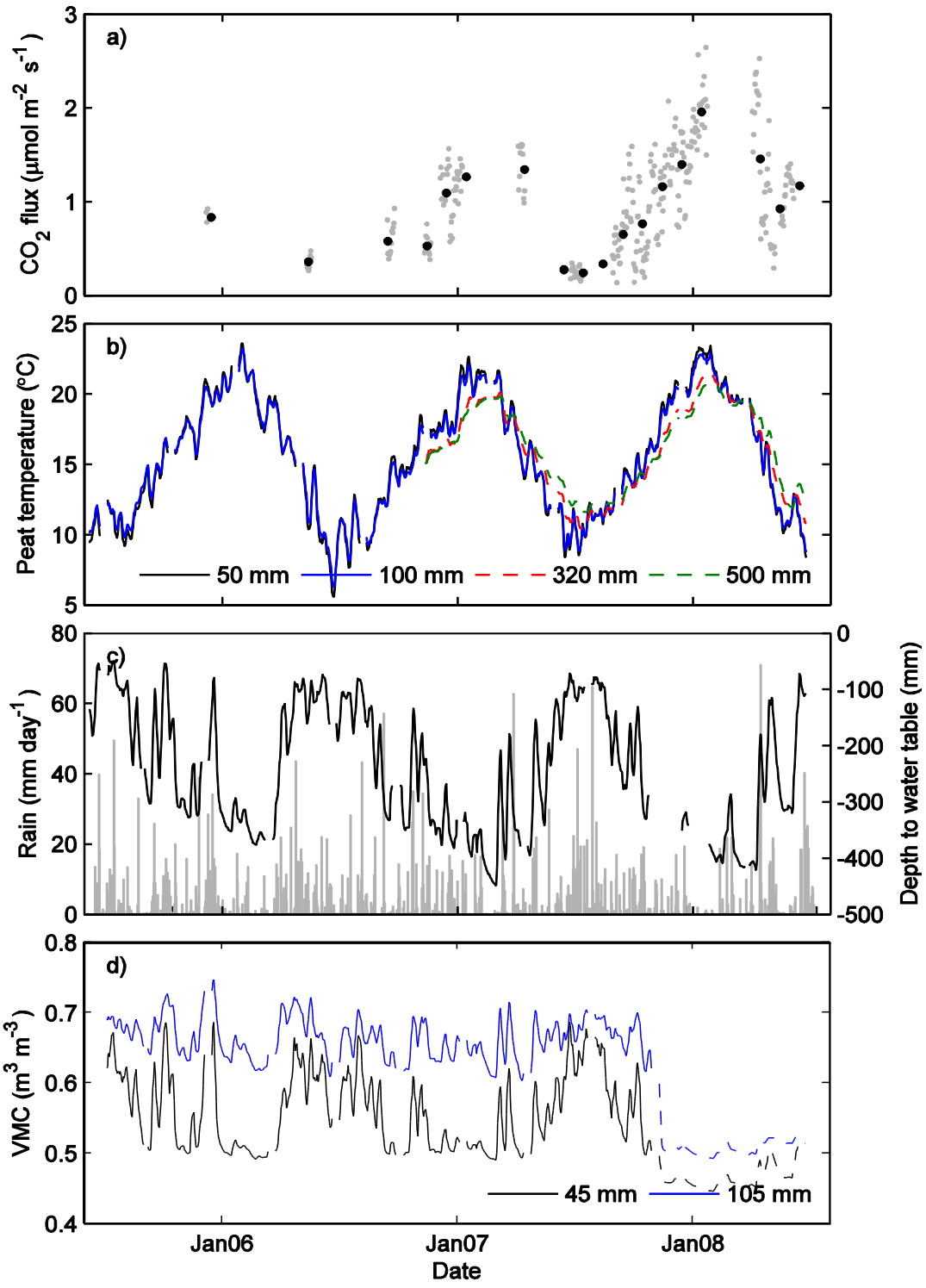

Figure 6.2 Temporal variation across three years of (a) daily (grey dots) and monthly averaged (black dots) CO_2 effluxes measured using the long-term chamber, (b) peat temperature at 50, 100, 320 and 500 mm depth, (c) rainfall (bars) and depth to water table, and (d) volumetric moisture content at 45 and 105 mm depth. VMC data not used for analysis are shown as dashed lines. All displayed values (except the CO_2 fluxes and the half-hourly rainfall) are running means calculated using a moving window of 7 days.

The most likely cause of the anomalous VMC measurements was that the dry conditions caused the peat to shrink away from the sensors, thereby limiting the contact between the sensors and the peat. The data suggest that this contact was not re-established even under wetter conditions in March/April. For this reason, VMC data obtained from November 2007 onwards were considered unreliable and were not used for further analyses in the rest of this chapter.

Monthly averaged CO_2 fluxes ranged from 0.24 µmol CO_2 m^{-2} s^{-1} during winter to 1.97 µmol CO_2 m^{-2} s^{-1} during summer Figure 6.2a).

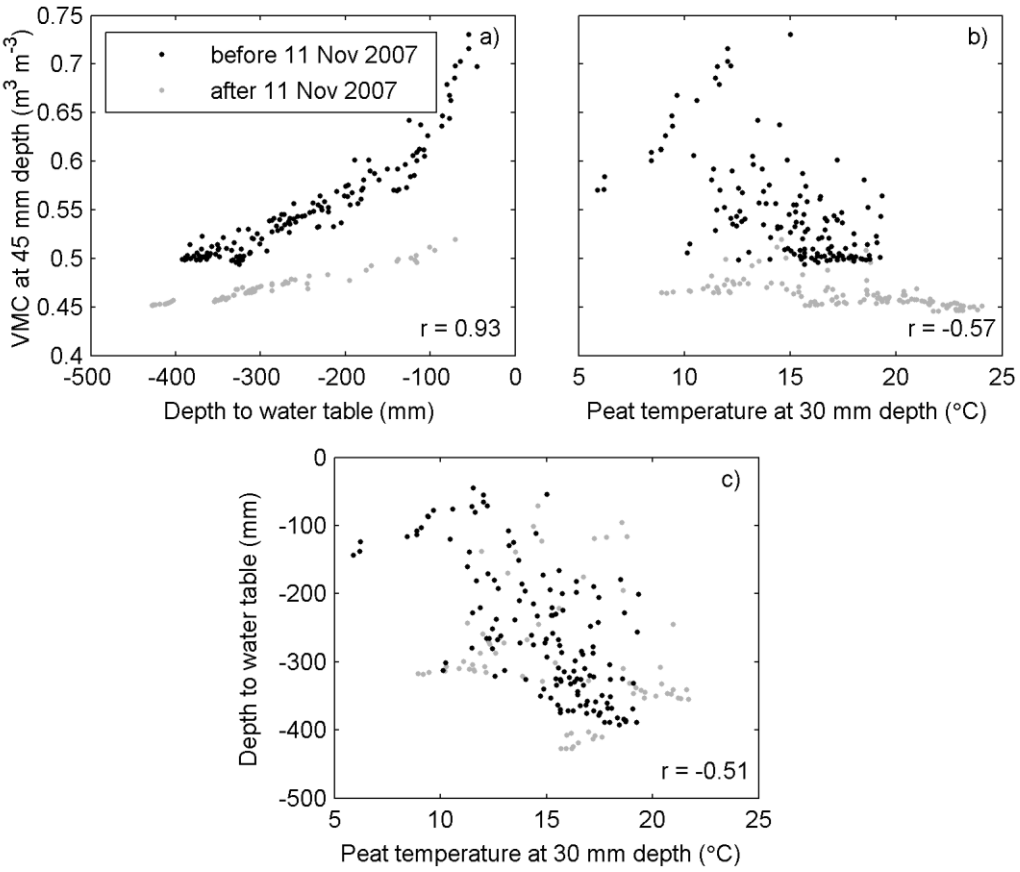

Figure 6.3 Correlation between daily averaged volumetric moisture content at 45 mm, depth to water table and peat temperature. Values of the VMC collected after 11 November 2007 (grey points) were considered unreliable (see also Figure 6.2). r denotes the correlation coefficient based on data before 11 Nov 2007.

As mentioned above, temperature, water table and moisture content were correlated in time: VMC increased with rising water tables (Figure 6.3a), and high temperatures typically occurred when the peat was relatively dry (Figure 6.3b) and the water table was deep (Figure 6.3c). Figure 6.3 also shows

that the data collected after 11 November 2007 displayed a different relationship between VMC and DWT, which was the reason not to include them in further analysis.

6.3.2. Controls of temperature, DWT and VMC – monthly averages

Figure 6.4 shows how monthly mean CO_2 fluxes responded to mean peat temperature (*T*), depth to water table (DWT) and volumetric moisture content (VMC). In general, greater CO_2 fluxes were measured with increasing peat temperature, increasing depth to water table and decreasing moisture content.

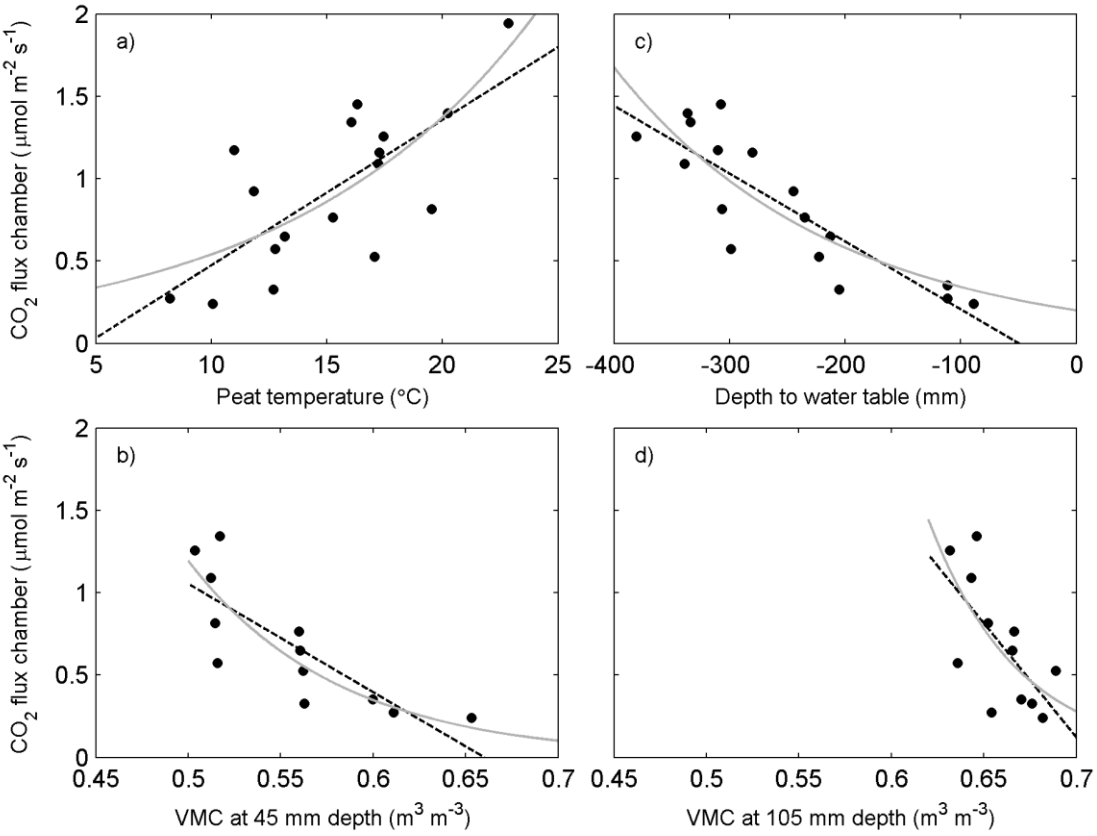

Figure 6.4 Monthly averaged CO_2 flux measured by the long-term chamber as a function of the means of a) peat temperature at 30 mm depth, b) volumetric moisture content at 45 mm depth c) depth to water table and d) volumetric moisture content at 105 mm depth. Linear and exponential fits are shown as dashed black lines and grey line, respectively. VMC data collected after November 2007 onwards were not included (see Section 6.3.1), hence the smaller number of points in panels b and d. Coefficients of the regression equations are shown in Table 6.1.

Comparison of the regression equations of HR vs. *T*, DWT and VMC revealed that the regression of the flux vs. VMC at 45 mm depth and DWT explain most of the variation (Table 6.1). The lowest R^2 was found when regressing against VMC at 105 mm depth (Table 6.1). Differences in explained portion of the variance between the linear and exponential regressions were small. For DWT, the linear regression explained slightly more of the variance compared to the exponential regression, whereas for *T* and VMC it was the other way around.

Table 6.1 Coefficients of regression equations displayed in Figure 6.4. y = CO_2 flux measured by the chamber. Peat temperature was measured at 30 mm depth next to the chamber. R^2 is the proportion of the variance explained by the regression.

	Linear $y = a + bx$			Exponential $y = ae^{bx}$		
x	*a*	*b*	R^2	*a*	*b*	R^2
Temperature	-0.410	0.088	0.49	0.212	0.093	0.51
DWT	-0.206	-0.004	0.72	0.202	-0.005	0.71
VMC 45 mm	4.34	-6.58	0.62	566	-12.3	0.68
VMC 105 mm	9.82	-13.9	0.39	$5.02 \cdot 10^5$	-20.6	0.40

6.3.3. Controls of temperature, DWT and VMC – daily averages

Similar to the trends revealed when examining monthly averaged data, daily averaged CO_2 flux increased with increasing peat temperature, dropping water table and decreasing volumetric moisture content (Figure 6.5).

The regression equations of HR vs. DWT explained more of the variation (71%) than regressions against peat temperature or VMC (indicated by the highest R^2, Table 6.2). In general, the exponential regressions were slightly better than the linear regressions (i.e. resulted in higher R^2, Table 6.2). The lowest R^2 was found for regressions against peat temperature at 30 mm depth and VMC at 105 mm ($R^2 < 0.46$, Table 6.2). For *T*, DWT and VMC at -45 mm, the exponential regression explained more of the variance compared to the linear regression, whereas for VMC at -105 mm slightly more of the variance was explained by the linear regression.

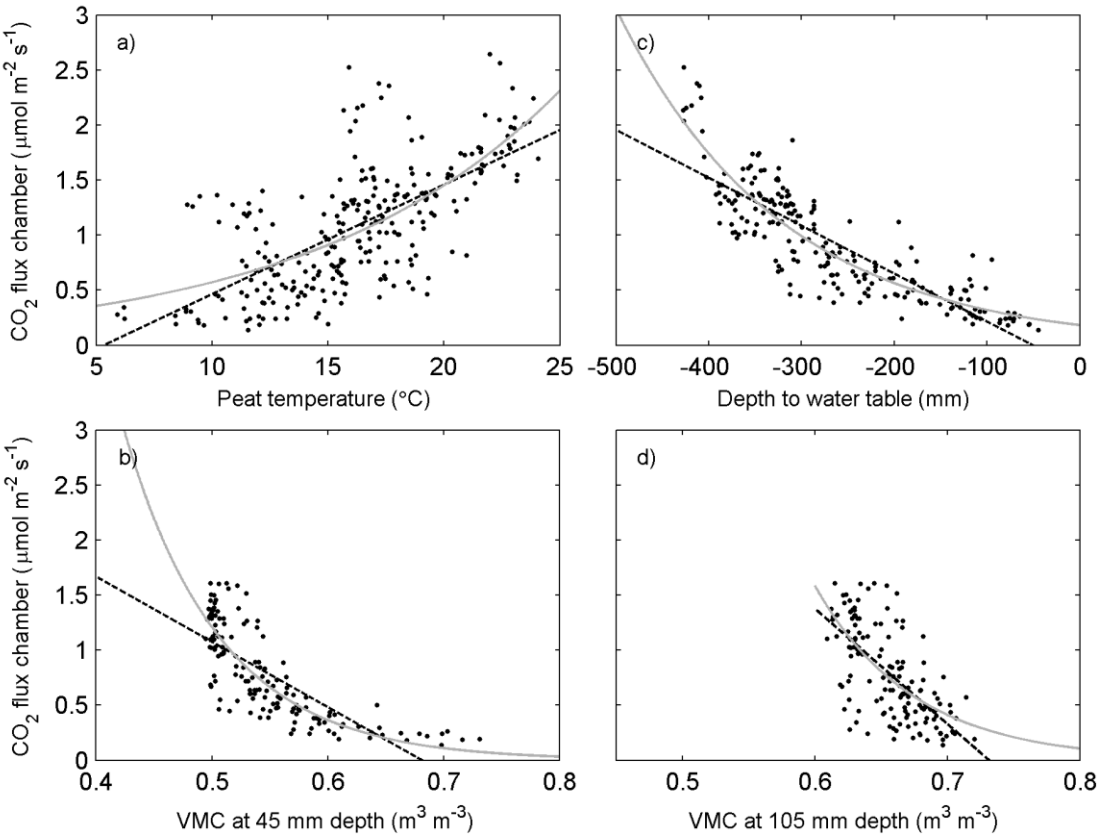

Figure 6.5 Daily averaged CO_2 flux measured by the long-term chamber as a function of a) peat temperature at 30 mm depth, b) volumetric moisture content at 45 mm depth c) depth to water table and d) volumetric moisture content at 105 mm depth. Linear and exponential fits are shown as dashed black lines and grey line, respectively. VMC data collected after 11 November 2007 onwards were not included (see Section 6.3.1), hence the smaller number of points in panels b and d. Coefficients of the regression equations are shown in Table 6.2.

Table 6.2 Coefficients of regression equations displayed in Figure 6.5 that were based on daily averaged data. y = CO_2 flux measured by the chamber. Peat temperature was measured at 30 mm depth directly adjacent to the chamber. R^2 is the proportion of the variance explained by the regression adjusted for the degrees of freedom.

	Linear $y = a + bx$			Exponential $y = ae^{bx}$		
x	*A*	*b*	R^2	*a*	*b*	R^2
Temperature	-0.529	0.099	0.45	0.225	0.093	0.47
DWT	-0.221	-0.004	0.71	0.182	-0.006	0.77
VMC -45 mm	4.04	-5.93	0.58	482	-12.0	0.68
VMC -105 mm	7.69	-10.5	0.45	5059	-13.4	0.44

Model HR with temperature

Fitting the Lloyd and Taylor (LT) equation (Eq. 6.3) using the peat temperature measured directly next to the chamber at 30 mm depth resulted in a R_{10} of 0.53 ± 0.068 µmol CO_2 m^{-2} s^{-1} and an Eo of 379.4 ± 52 (mean ± 95% confidence interval, n = 266, R^2 = 0.47, Figure 6.6). The equivalent of the Q_{10} for the Lloyd and Taylor equation (Q_{10_LT}) between 10 and 20 °C was 2.79. For the exponential equation, the calculated Q_{10} was 2.53. The respiration rate at 10 °C (R_{10}) determined by the exponential regression was 0.57 µmol CO_2 m^{-2} s^{-1}.

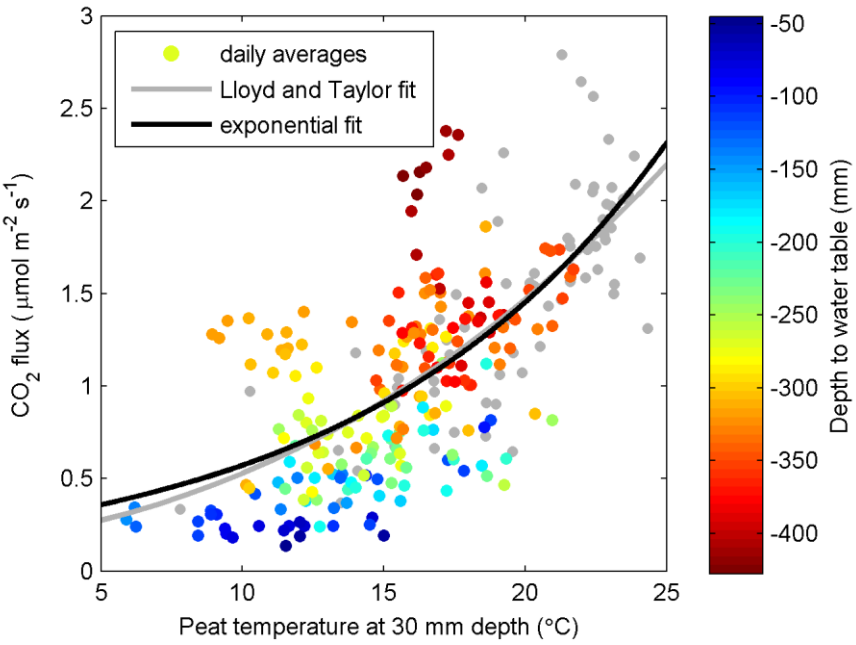

Figure 6.6 Relationship between daily averaged peat temperature at 30 mm depth and CO_2 flux. Colours depict the depth to water table. For the grey points, no information on the water table was available.

Partway into the experiment, an array of temperature sensors was installed between 20 and 500 mm depth 7 m from the chamber setup (Section 3.3.3). Fitting an exponential equation to the daily averaged flux data as a function of peat temperature obtained with the temperature sensors at deeper depths resulted in increasing values for the Q_{10} with increasing depths (Figure 6.7a). Calculated Q_{10} values ranged from 2.31 using the temperature at 20 mm depth to 4.66 using the temperature at 400 mm. The portion of the variation explained by the regressions showed a general increase with depth and varied between 0.41 and 0.52 (Figure 6.7b).

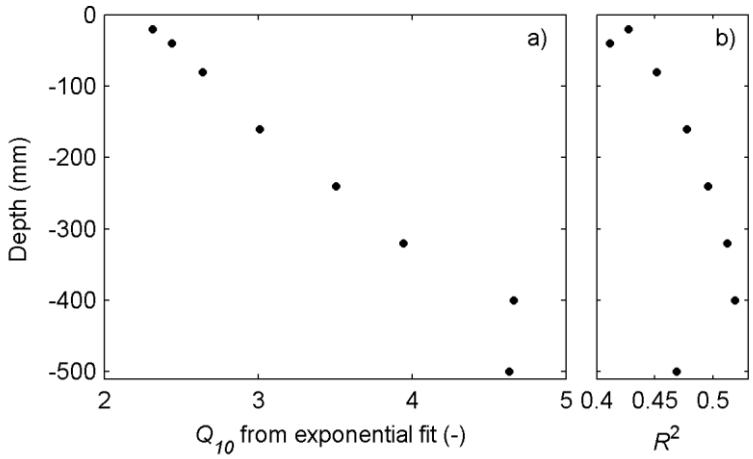

Figure 6.7 Change in apparent Q_{10} and R^2 (calculated from an exponential fit) with changing depth of temperature measurement.

To check whether an average temperature of the CO_2-producing layer above the water table might be a better predictor of the CO_2 efflux, CO_2 flux was regressed against the mean temperature of the peat layer above the water table instead of the 30 mm-temperature. The equation $\mathrm{HR} = 0.19 \cdot e^{0.11 \cdot T}$ was found, with an adjusted R^2 of 0.31 (Q_{10} = 2.87). This was a poorer fit (lower R^2) than the fit that was found for the regressions with the 30 mm temperature measured next to the chamber, or the fits using any of the individual temperatures along the temperature profile (Figure 6.7).

Interactive control of moisture and temperature on HR

To examine the interactive control of water table and temperature, regressions between temperature and respiration were made separated in groups of DWT (3 groups, -450 mm < DWT < 300 mm, -300 mm < DWT < -150 mm and -150 mm < DWT < 0 mm). However, due to large scatter and reduced number of measurements per group, regressions were not significant and comparison of the response of flux to changes in temperature was not possible (data not shown).

To model the interactive control of moisture status and temperature on the CO_2 flux, two regression equations using DWT and the 30 mm peat temperature were fitted (Equations 6.4 and 6.5). The 30 mm temperature was included for this model because it was the only temperature measured directly

next to the chamber and therefore assumed to be most representative. As a measure of moisture status of the peat, DWT was chosen over VMC, because the regressions presented above (Figure 6.5 and Table 6.2) showed that DWT was likely a more important driver as suggested by the higher R^2. Coefficients of the two empirical models for the CO_2 flux are shown in Table 6.3. Both regressions explained a large portion of the variation in the data, with R^2 of 0.76 for the model predicting HR (Eq. 6.4), and a R^2 of 0.86 for the model predicting ln(HR) (Eq. 6.5).

Table 6.3 Coefficients of multiple regression equations of daily averaged CO_2 flux on peat temperature at 30 mm and depth to water table. R^2 is the proportion of the variance explained by the regression adjusted for the degrees of freedom

	Source	*a*	*b*	*c*	*P*	R^2
$HR = a + b \cdot T + c \cdot DWT$	Waddington and Warner (2001)	-0.358	0.0208	-0.0038	<0.001	0.76
$\ln(HR) = a + b \cdot T + c \cdot DWT$	Silvola (1996)	-1.98	0.0182	-0.0056	<0.001	0.86

The data and the model predicting ln(HR) are shown in Figure 6.8. The model clearly showed that water table position was the dominant driver of the CO_2 efflux. The response of the CO_2 flux to changes in temperature seemed slightly greater at deeper DWT.

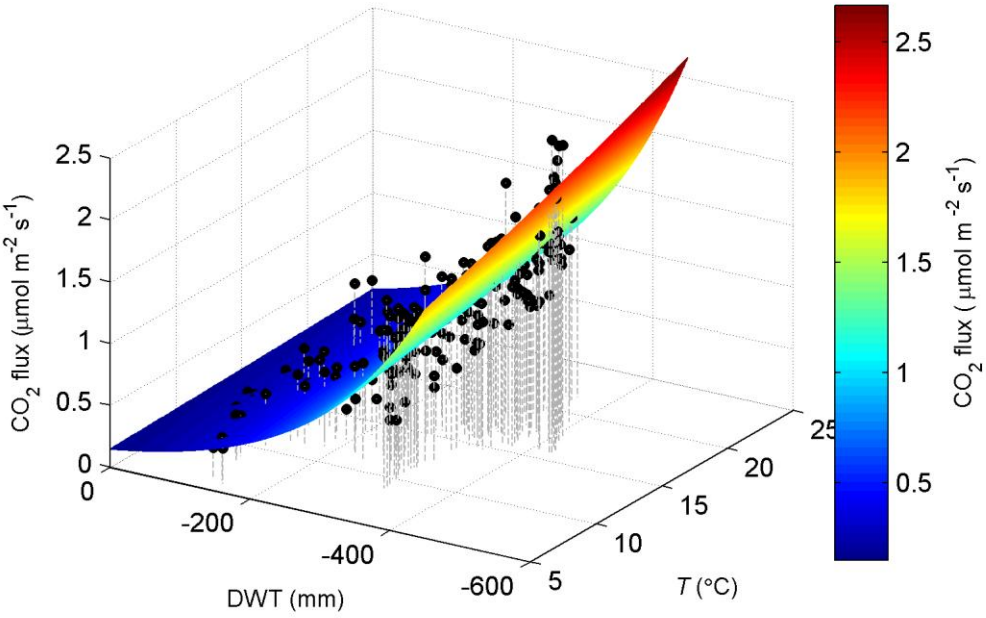

Figure 6.8 Daily averaged flux data (black dots) as a function of depth to water table and peat temperature at 30 mm depth. Coloured plane is the fitted non-linear model used before by Silvola (1996) (ln(HR) = a + b·*T* + c·*DWT*). Regression results are summarised in Table 6.3.

Comparison of measured and predicted values for the two models revealed that residuals were generally smaller than 0.5 µmol CO_2 m^{-2} s^{-1} (Figure 6.9). Larger residuals were found when large values of HR were observed and both models underestimated HR. The ln(HR) model used by Silvola (1996) performed slightly better in these instances (Figure 6.9).

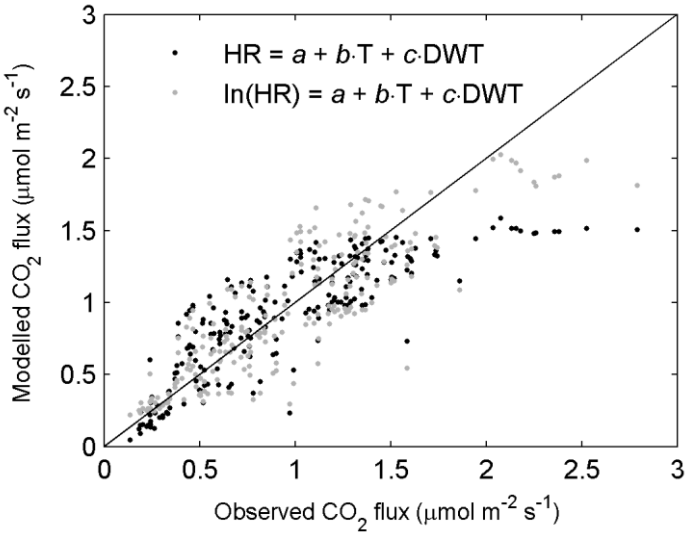

Figure 6.9 Comparison of modelled and observed daily averaged CO_2 fluxes using the models described in Section 6.2.3. The coefficients of the regression equations are shown in Table 6.3.

6.3.4. Controls of temperature – within-day timescale

In this section, the control of temperature on microbial respiration within the diurnal cycle will be examined using graphs of mean diurnal variation of flux and peat temperature calculated for each month.

Diurnal variation of peat temperature and HR

Temperature at 30 mm depth typically showed a clear diurnal pattern and peaked around 1600 NZST, regardless of the time of year (Figure 6.10a). In contrast, the mean diurnal variation of the CO_2 flux did not always display a clear diurnal trend (Figure 1.5b). In some summer months (December, January and February), the flux changed significantly during the course of the day, for example in Dec 2006, Jan 2007 and Jan 2008 (Figure 1.5b). Fluxes in the late afternoon were lower than those during the night in those instances. Other months, for example September 2007 and May 2008, displayed hardly any diurnal variation (Figure 1.5b). This difference between the diurnal courses of surface temperature and CO_2 efflux for different times of year is examined below.

Relationship between HR and peat temperature

Figure 6.11 shows an example of the mean diurnal variation of the CO_2 flux and the peat temperature at 30 mm depth for July 2007. During winter (June-July-August) the water table was typically shallowest (Figure 6.2) and temperature peaked in the late afternoon. The CO_2 flux did not change much over the course of the day, but a very small increase in flux could be observed mid-afternoon (Figure 6.11a). The observed relationship between CO_2 efflux and surface temperature was therefore positive (Figure 6.11b).

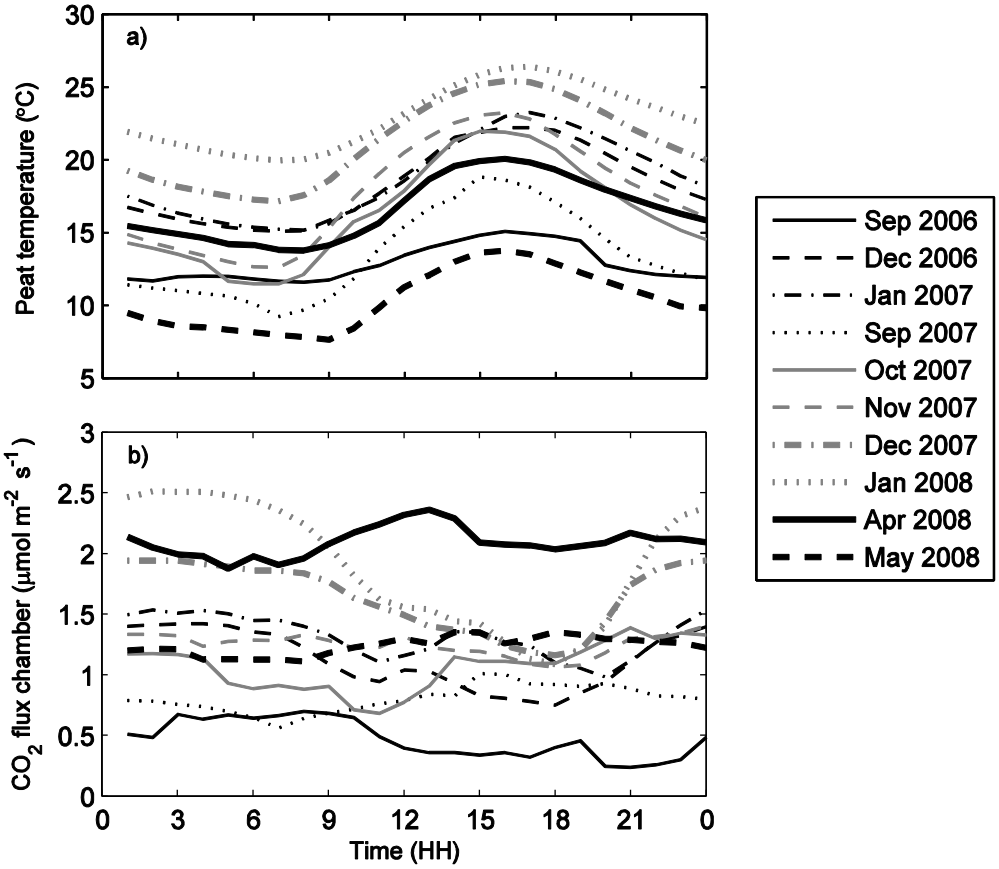

Figure 6.10 Mean diurnal variation of a) peat temperature (measured at 30 mm depth) and b) CO_2 flux measured by the chamber for 10 different months between September 2006 and May 2008. Time 0 is midnight, 12 is noon.

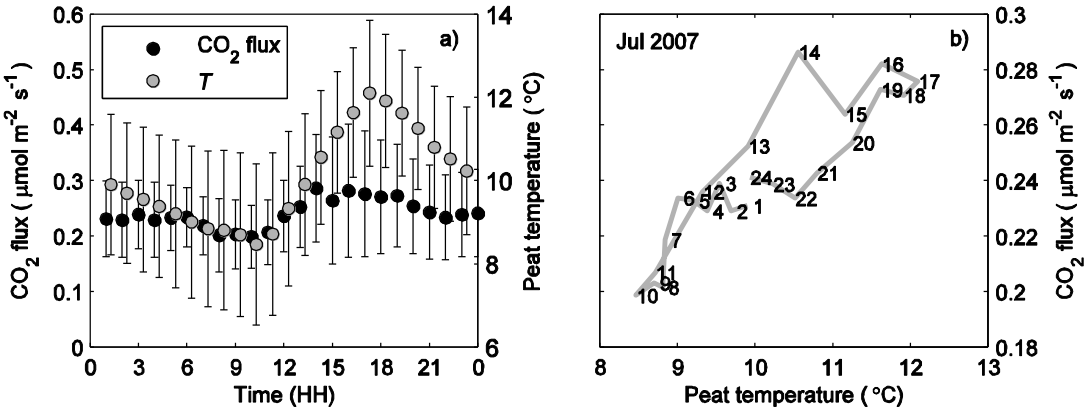

Figure 6.11 a) Mean diurnal variation of CO_2 flux and peat temperature measured at 30 mm depth for July 2007 when water table was relatively shallow (-89 mm). Error bars are standard deviations. *T* data points were slightly offset to avoid overlap of the error bars. b) Relationship between peat temperature at 30 mm depth and CO_2 flux for July 2007. The numbers in panel a) refer to the hours of the day.

During summer (December-January-February), the water table depth was typically below -350 mm (Figure 6.2) and a different daily pattern was observed in the CO_2 flux. As an example, the mean diurnal variation of temperature and CO_2 efflux are shown for December 2006 (Figure 6.12). Similar to wet conditions, the peat temperature close to the surface peaked in the late afternoon (Figure 6.12a). In contrast, the CO_2 flux was at its lowest value at that time of the day with highest rates of CO_2 efflux occurring at night. This pattern resulted in a negative relationship between near-surface peat temperature and the CO_2 efflux (Figure 6.12b).

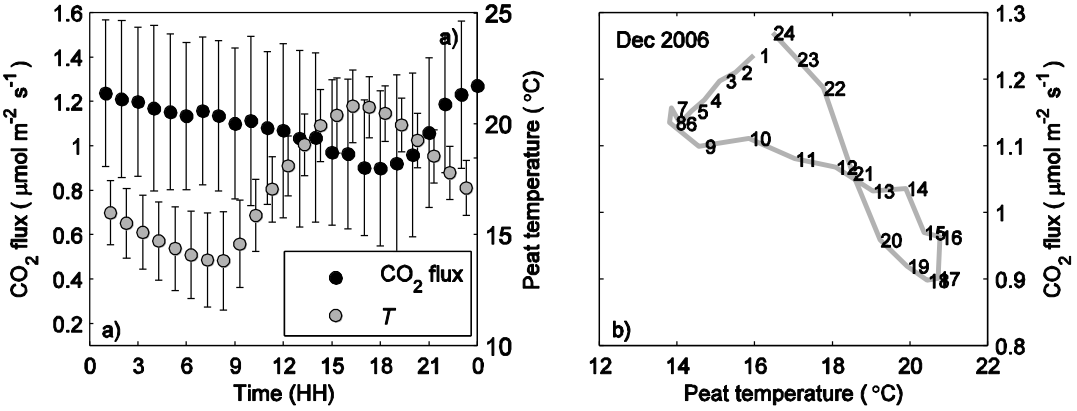

Figure 6.12 a) Mean diurnal variation of CO_2 flux and peat temperature measured at -30 mm depth for December 2006 when water table was relatively deep (-339 mm). Error bars are standard deviations. *T* data was slightly offset to avoid overlap of the error bars. b) Relationship between peat temperature at 30 mm depth and CO_2 flux for December 2006. The numbers in panel a) refer to the hours of the day.

Change in relationship between HR and temperature with depth

Examination of changes in temperature with depth show that temperatures measured further down the peat profile typically lagged behind the peak in surface temperature (see Figure 6.13 for an example). Also, the amplitude of the daily temperature range decreased with depth (Figure 6.13). The change in phase and amplitude with measurement depth implied that different relationships would be found between peat temperature at different depths and the CO_2 efflux measured at the surface.

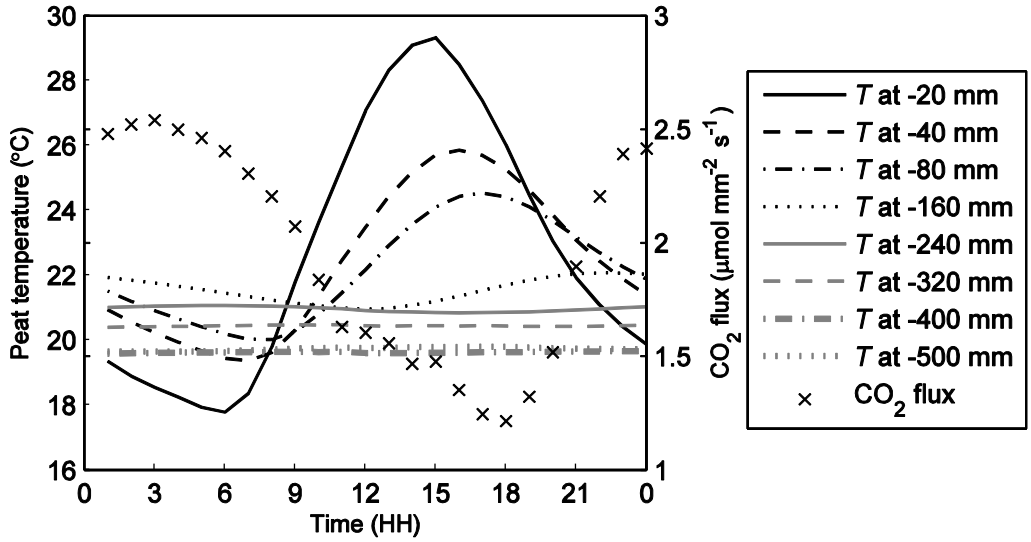

Figure 6.13 Mean diurnal variation of surface CO_2 flux and peat temperature at various depths down the peat profile calculated for all available data in January 2008 when water table was deep.

As an example of the relationship between CO_2 efflux at the surface and peat temperature measured at different depths during summer, the left-most panels of Figure 6.14 show the relationship between peat temperature at different depths and the measured CO_2 efflux for December 2006. A negative relationship between temperature and CO_2 flux was found for *T* at -5, -20, -40 and -80 mm (Figure 6.14 a, b, c and d). When regressing the CO_2 flux against the temperature at -160 mm, a weak positive relationship was found (Figure 6.14 e and f). At -240 and -400 mm, hardly any change in temperature was detected on a diurnal time scale (Figure 6.14g).

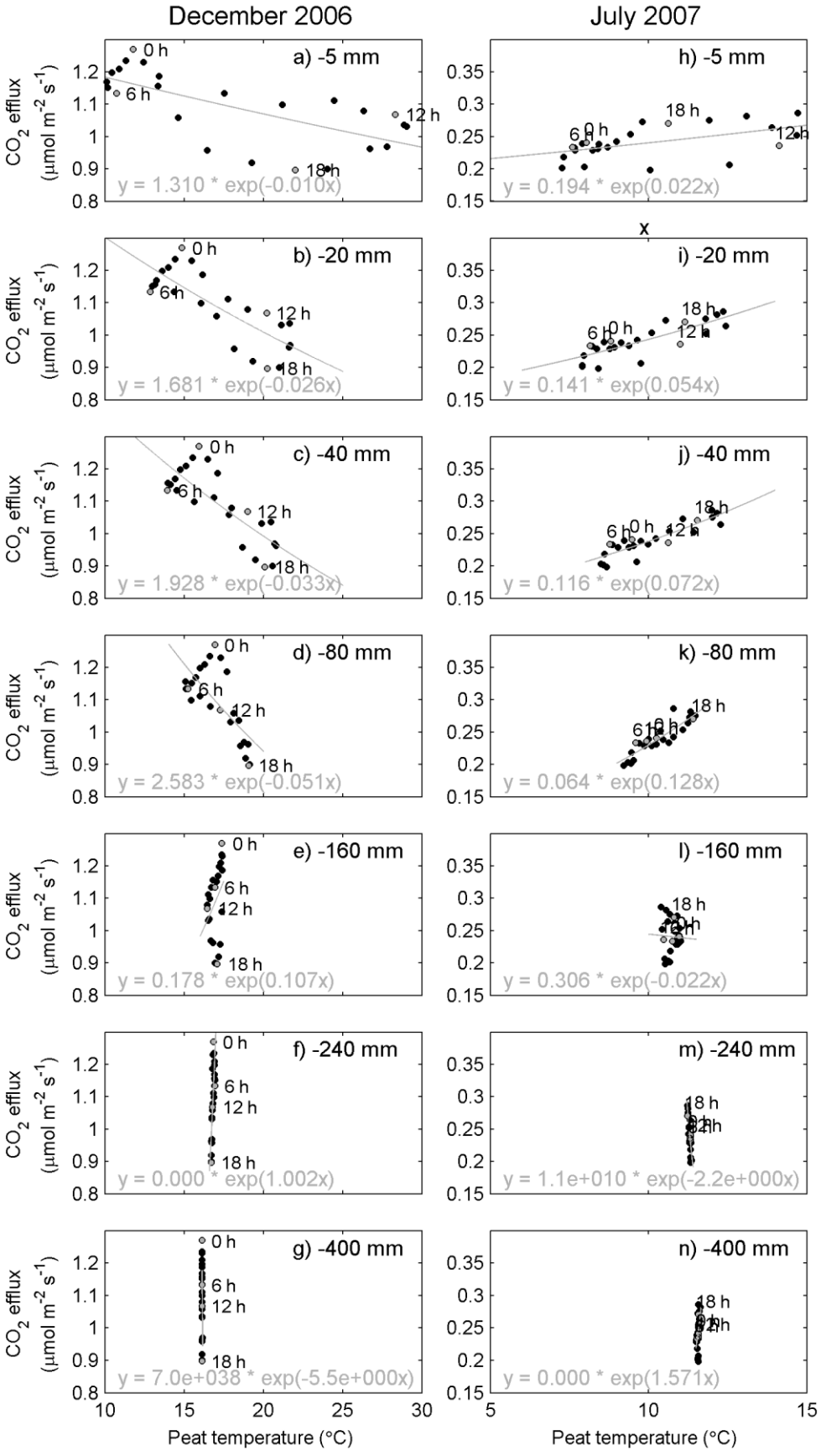

Figure 6.14 Exponential regressions of CO_2 efflux against peat temperature measured at different depths for December 2006 when the water table was -339 mm (a-g) and July 2007 when water table was -89 mm (h-n).

Data collected in July 2007 served as an example for temperature and flux values in winter under wet conditions (Figure 6.14h-n). This time, the positive relationship between temperature and flux observed at the shallow depth persisted until 80 mm depth (Figure 6.14 h, I, j and k). At the deeper depths (-160 mm), the relationship reversed with CO_2 flux values decreasing as temperatures increased (Figure 6.14 l). As in summer, no temporal variation was observed in the temperature signal at the daily time scale at 240 and 400 mm depth (Figure 6.14 n).

The Q_{10} value was calculated for each depth and both example months of Figure 6.14 (Table 6.4). Values of Q_{10} varied between 0.6 and 3.6, excluding the regression using temperatures at the deepest depths (-240 and -400 mm), which resulted in non-realistically small or large Q_{10}'s caused by the lack of temperature change during the day.

Table 6.4 Temperature sensitivity of the CO_2 flux at the surface to changes of temperature at various depths for two contrasting months. Modelled values were calculated using the exponential regression equations shown in Figure 6.14 that were based on the mean diurnal variation in temperature at depth and CO_2 flux at the surface.

T measurement depth	Temperature sensitivity	
	December 2006	July 2007
-5 mm	0.90	1.2
-20 mm	0.78	1.7
-40 mm	0.72	2.1
-80 mm	0.60	3.6
-160 mm	2.9	0.80
-240 mm	$2.3 \cdot 10^4$	0
-400 mm	0	$6.6 \cdot 10^6$

Delays between temperature measured near the surface and temperature further down the peat profile were determined by shifting the temperature-at-depth signal in time until a maximum positive correlation was found between the two temperatures. Also, the delay between the temperature signals at depth and the surface CO_2 flux were determined. Again, the lag in temperature signal with depth was clearly observed both in summer (Figure 6.15a) and winter (Figure 6.15b; compare Figure 6.13). In December 2006, when the water table was relatively deep, the delay between the CO_2 flux signal and the surface temperature signal was approximately -12 hours, i.e. the CO_2 flux

signal peaked 12 hours before the temperature signal (Figure 6.15). Because a 24 hours cycle was used to determine the delays, this is the same as a delay of +12 (= -12 + 24) hours, i.e. the temperature peaked 12 hours before the CO_2 flux. This delay between peat temperature and CO_2 efflux decreased for temperature at deeper peat layers (Figure 6.15), as suggested by the pattern of heat wave propagation in Figure 6.13. Just above -240 mm, the delay between temperature and CO_2 efflux was approximately 0 (or 24) hours. Below -240 mm, the delay increased again with depth.

In July 2007, when the water table was close to the surface, peaks in near-surface temperature and CO_2 flux occurred almost at the same time. Surface temperature lagged approximately 1 hour behind the CO_2 flux. The change in delay between temperature and surface CO_2 flux with depth followed the increase of delay between surface temperature and temperature at depth closely (i.e. the two lines in Figure 6.15 run nearly parallel).

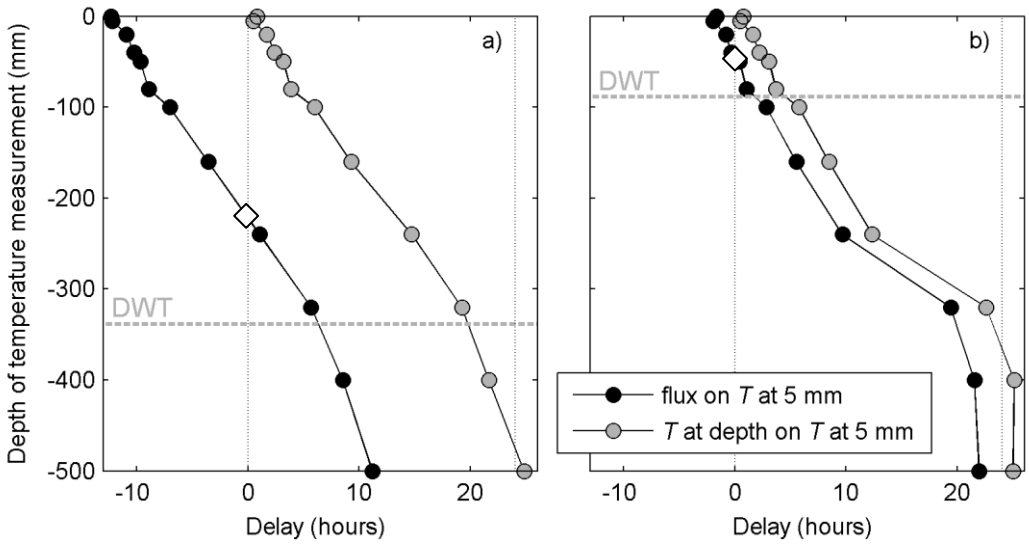

Figure 6.15 Lag of peat temperature measured at depth compared to the shallow peat temperature (grey dots) and of the CO_2 efflux (measured at the surface) compared to the temperature at depth for a) December 2006 and b) July 2007. Delays were determined from monthly mean diurnal variations of flux and peat temperature. Values for depth to water table (grey dotted line) were averaged monthly. The depth at which the delay between peat temperature and the surface CO_2 flux is zero hours is indicated by a white diamond.

The depth at which signals of *T* at depth were in phase with the surface CO_2 flux signal (i.e. the depth of the white diamonds in Figure 6.15, which is the depth of zero delay) correlated reasonably well with the depth to water table

(Figure 6.16). Regression of the depth of zero delay between peat temperature and surface CO_2 flux against DWT explained 74 % of the variation (Figure 6.16).

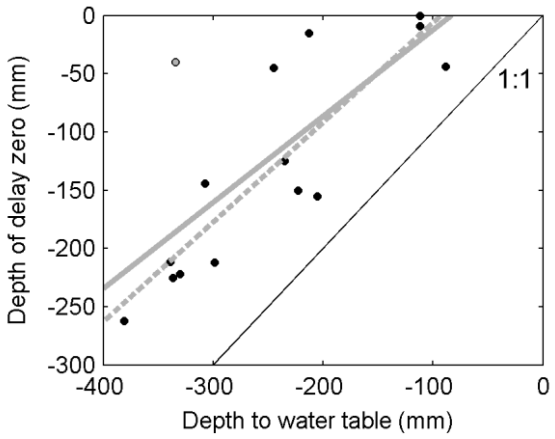

Figure 6.16 Relationship between the depth to water table and the depth at which the delay between peat temperature and the surface CO_2 flux is zero hours. Values for depth to water table were averaged monthly, and delays were determined from monthly mean diurnal variations of flux and peat temperature. Each dot represents the depth at which the delay between peat temperature and surface CO_2 flux was approximately zero. As an example, this depth is indicated by white diamonds in Figure 6.15 for December 2006 and July 2007. The solid grey line is the linear regression y = a +b·x with a = 61.5 and b = 0.740 (p = 0.0012, adj. R^2= 0.57), and the dotted grey line is the linear regression with one outlier (grey point) removed (a = 79.4, b = 0.856, P < 0.001, adj. R^2 = 0.74). The black line is the 1:1 line.

Hysteresis of the CO_2 flux-temperature relationship on a within-day scale

As illustrated in Figure 6.14, regression of hourly-averaged CO_2 flux on surface temperature leads to both positive and negative relationships between flux and temperature depending on the time of year and moisture conditions of the peat. Additionally, during many months, hysteresis was observed (i.e. at the same peat temperature the CO_2 flux was different during the cooling and the heating phase). For example, in December 2006, CO_2 fluxes were greater in the morning than in afternoon, even though the temperature at the surface was the same (Figure 6.14a). In general, this hysteresis was more pronounced during months with low water tables than during months with high water tables (data not shown).

In an attempt to find a more suitable temperature for developing an empirical temperature model based on hourly data, fluxes were also regressed against the mean temperature of the peat above the DWT. However, these regressions resembled the regression against surface temperature closely (data

not shown) and for several months, the negative relationships remained and/or hysteresis was still observed.

In summary, the relationship between temperature and CO_2 efflux at the diurnal time scale was somewhat ambiguous. Whereas under wet conditions, diurnal variation of temperature and CO_2 efflux were 'in phase', during dry conditions maxima in CO_2 flux occurred at the time of minimum surface temperature. Because the heat wave propagated down the peat profile causing a lag in the temperature signal with depth, a depth could be identified where the temperature signal (at depth) and the CO_2 flux measured at the surface were in phase. This 'depth of apparent zero delay' was related to the water table depth. In addition to the change in temperature vs. CO_2 flux relationship with change in depth of temperature measurement, the relationship between temperature and CO_2 flux displayed hysteretic behaviour that was more pronounced during months with deep water tables.

6.3.5. Short-term effects of rainfall and moisture on CO_2 efflux – within-day time scale

Rainfall events suppressed the CO_2 flux

To illustrate how rainfall and volumetric moisture content affected the temporal variation of the CO_2 flux at short time-scales (i.e. hours to days), example time series of 15-minute data of rainfall, DWT, VMC, peat temperature and CO_2 flux are presented below.

Figure 6.17 shows an example of the immediate suppression of the CO_2 flux when the peat column in wetted up after a rainfall event totalling 6.2 mm on 7 November 2006. The water table rose from –290 mm to –90 mm, leading to an increase in VMC at both 105 and 45 mm (Figure 6.17b). CO_2 efflux at the start of the rainfall event was around 0.77 µmol CO_2 m^{-2} s^{-1}, and went down to 0.45 µmol CO_2 m^{-2} s^{-1} after rainfall.

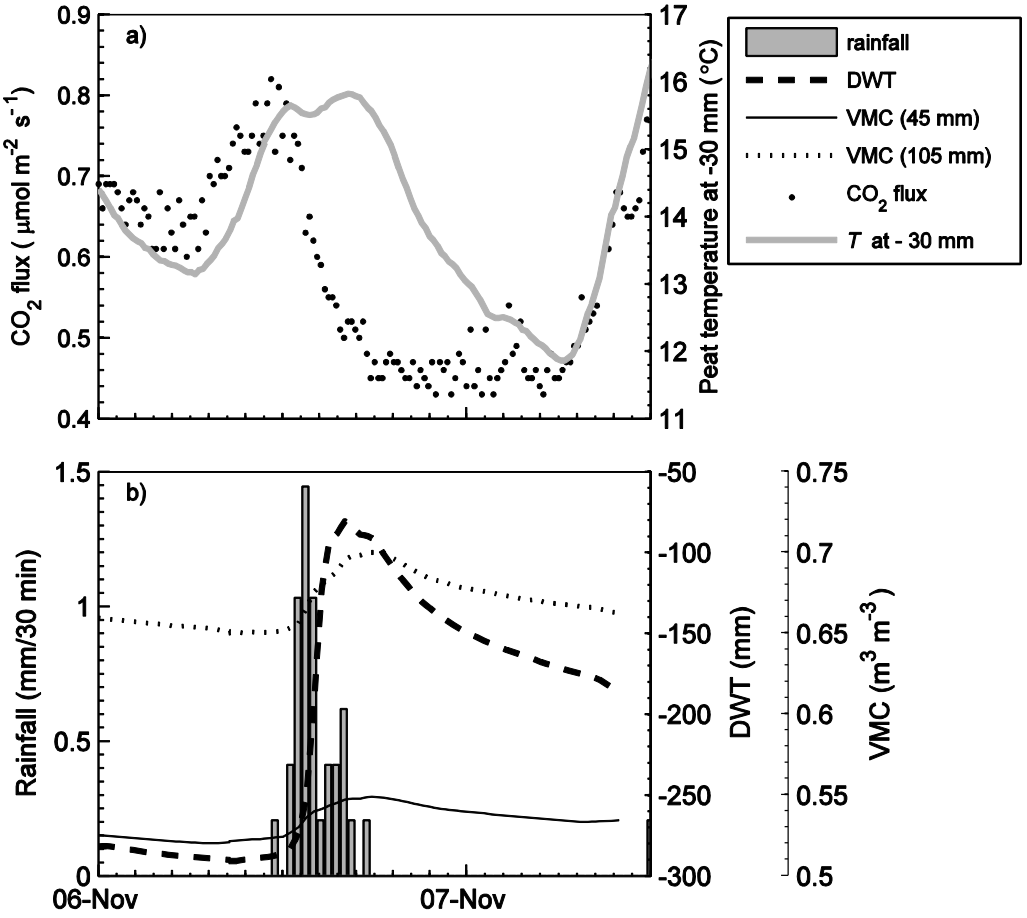

Figure 6.17 Example of the suppression of soil respiration caused by saturation of the peat column on 6 November 2007. Date labels on the x-axes indicate the start of the day (at midnight).

Figure 6.18 shows an example of the effect of rainfall on the CO_2 flux during winter when the water table generally was much closer to the peat surface than during the November 2007 example. In response to the first 15.3 mm rainfall episode between the afternoon of 29 June and 2 am the following morning, DWT rose from -149 mm before the rain to -38 mm after the rain. During this time, the CO_2 flux decreased from 0.41 µmol CO_2 m^{-2} s^{-1} before the rain to 0.10 µmol CO_2 m^{-2} s^{-1} after the rain. As soon as the rainfall stopped, the water table started dropping and CO_2 flux recovered slightly until the next large rainfall event (19.8 mm total) which started at 500 NZST on 30 June. Again, DWT rose and CO_2 fluxes dropped. This pattern of decreasing fluxes during rainfall and recovery as soon as rainfall stopped repeated itself several times after this (Figure 6.18).

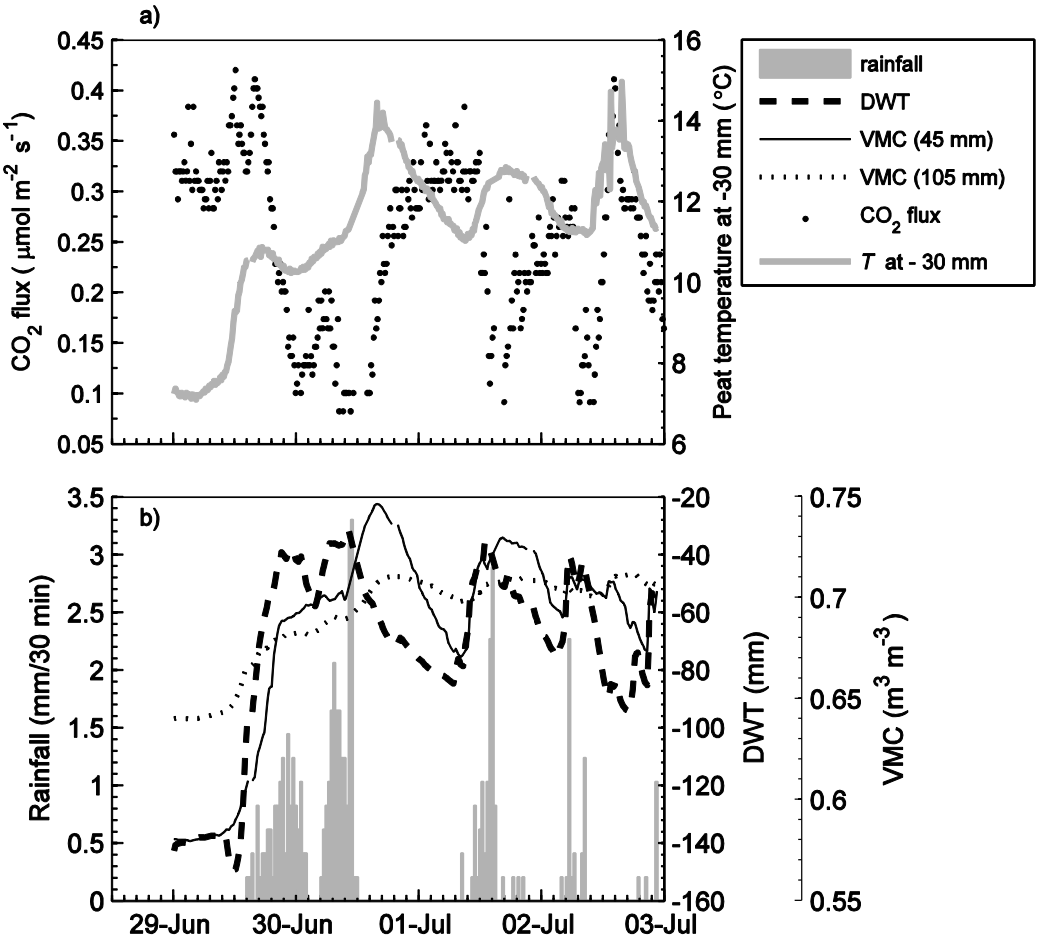

Figure 6.18 Example of the suppression of soil respiration caused by saturation of the peat column between 29 Jun and 3 Jul 2007. Date labels on the x-axes indicate the start of the day (at midnight).

Rainfall events enhanced the CO_2 flux

In addition to events where rainfall caused significant decreases in CO_2 efflux, a few instances were observed where rainfall caused a short-term increase in CO_2 flux. Figure 6.19 shows an example from 17 December 2006, when the water table level was relatively deep (< -380 mm, Figure 6.19b). Precipitation falling in one rainfall event (6.0 mm) did not affect the VMC at 45 mm or the water table depth (Figure 6.19b), but lead to a marked increase in CO_2 efflux. CO_2 flux was 0.6 µmol CO_2 m^{-2} s^{-1} during the rain and increased to 2.35 µmol CO_2 m^{-2} s^{-1} directly after the rain, which was markedly higher than the rates at the same time of day during previous days that did not experience rainfall (Figure 6.19).

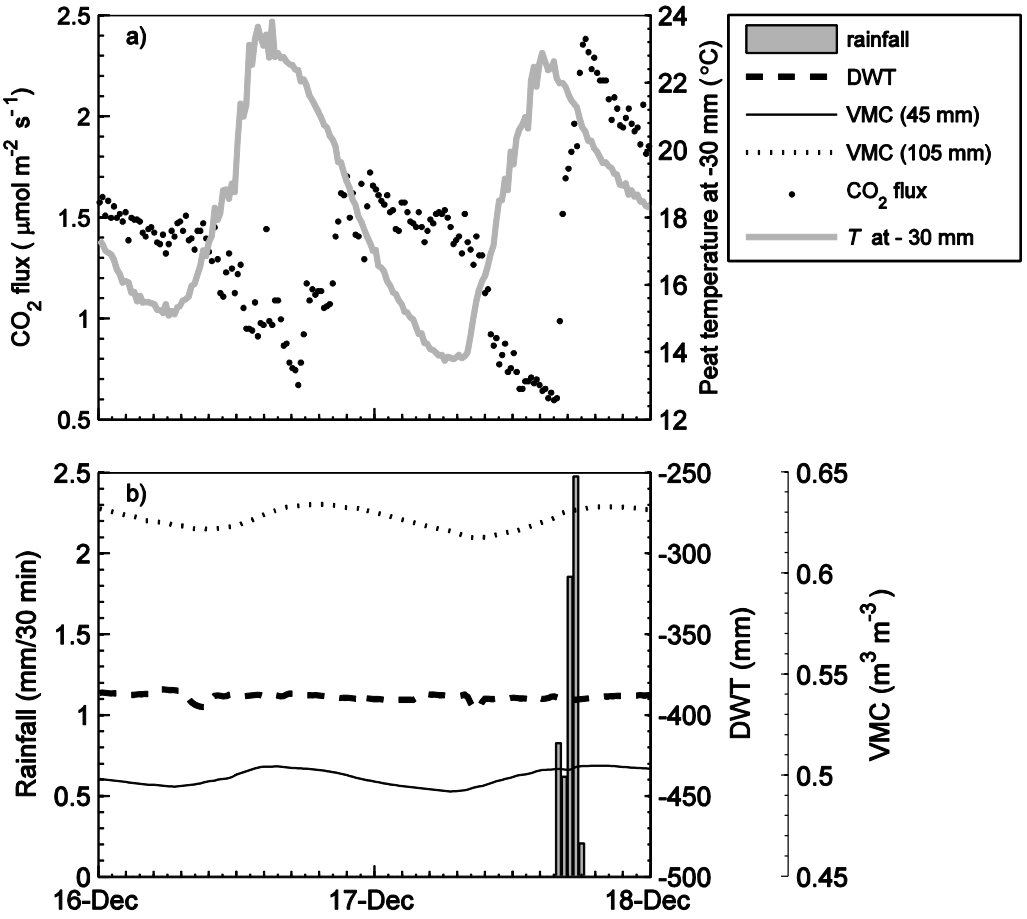

Figure 6.19 Example of the stimulation of soil respiration caused by wetting up of the peat surface on 17 December 2006. Date labels on the x-axes indicate the start of the day (at midnight).

Possible enhancement of the CO_2 flux by dewfall at night in summer

Under summer conditions when CO_2 flux was inversely correlated to surface temperature peak fluxes were observed at night. The example time series of two days in December 2006 show that these 'plateaus' of maximum fluxes coincided well with 'plateaus' of high relative humidity (RH) as measured in the chamber (Figure 6.20 a and c). Therefore, a positive relationship between RH and flux was observed (Figure 6.20d). During the night, the difference between the near-surface temperature of the peat and the dew point temperature of the air was minimal, and sometimes less than 0°C (Figure 6.20b), indicating that condensation (dewfall) might have occurred at the peat surface during these summer nights.

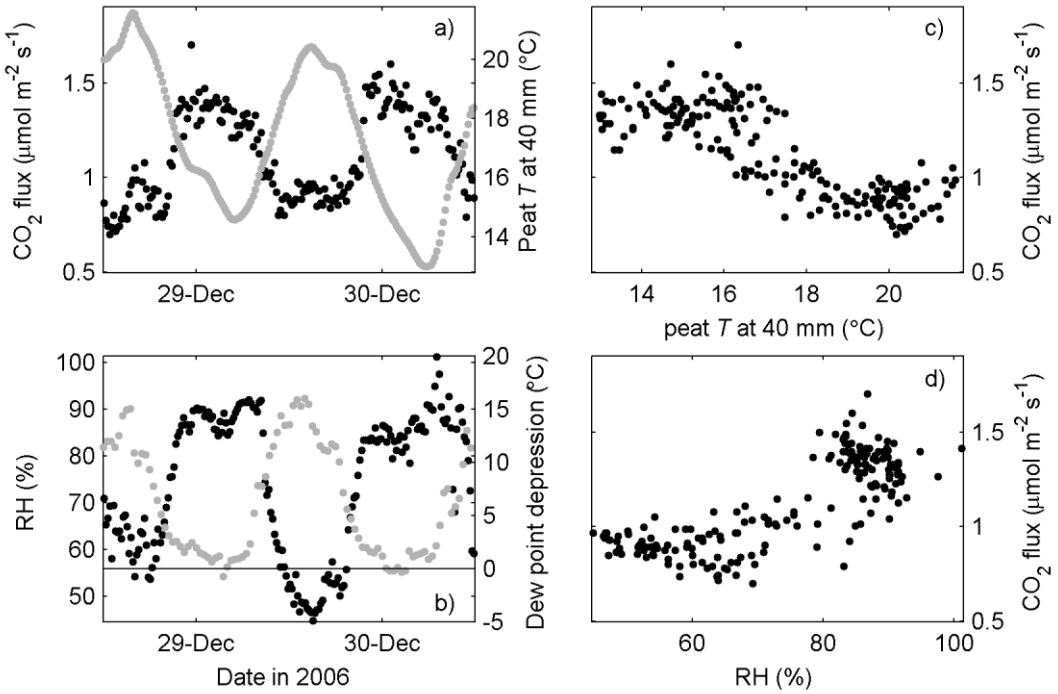

Figure 6.20 Diurnal variation of a) CO_2 flux (black points) and peat temperature at -40 mm depth (grey points), b) relative humidity (black points) and dew point depression (grey points) for two days when water table was low (-358mm) in December 2006. The dew point depression was calculated as the difference between surface peat temperature (at 5 mm depth) and dew point temperature of the air. Date labels on the x-axes of panels a and b indicate the start of the day (at midnight). Relationship of peat temperature (c) and relative humidity (d) to surface CO_2 flux during the same two days.

6.3.6. Modelling CO_2 flux at the within-day time scale

Figure 6.21 shows how measured respiration rates changed with changes in near-surface temperature, water table and volumetric moisture content at 45 and 105 mm depth. On average, the same general trends could be observed as with the daily averaged values (Section 6.3.3): increasing CO_2 fluxes were accompanied by increasing near-surface temperatures, deeper water table and lower volumetric moisture values.

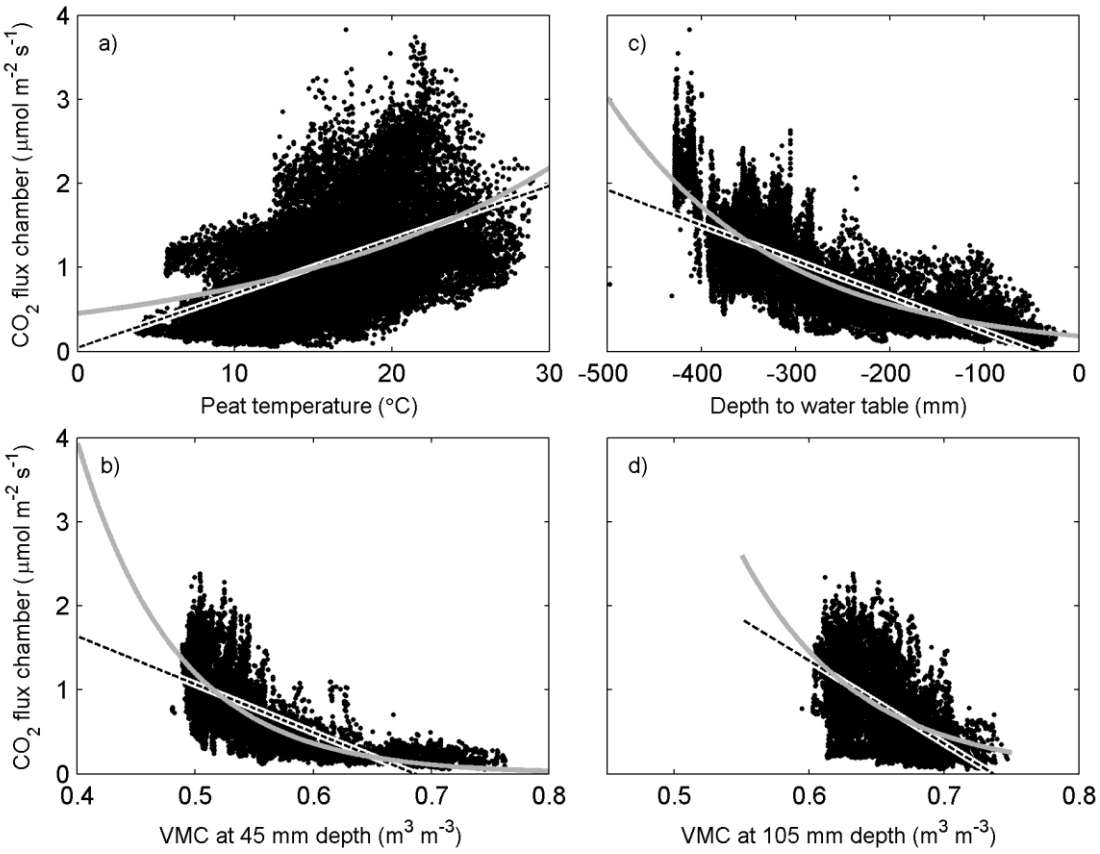

Figure 6.21 All 15-minute CO_2 flux measurements by the long-term chamber as a function of a) peat temperature at 30 mm depth, b) volumetric moisture content at 45 mm depth c) depth to water table and d) volumetric moisture content at 105 mm depth. Linear and exponential fits are shown as dashed black lines and grey line, respectively. VMC data collected after 11 November 2007 onwards were not included, hence the smaller number of points in panels c and d. Coefficients of the regression equations are shown in Table 6.5.

Overall, regression equations applied to data at this high temporal resolution explained less of the variation compared to the regression applied to daily averaged data, as revealed by the lower R^2 values (compare Tables 6.2 and 6.5) and larger scatter in the graphs (compare Figures 6.5 and 6.21). Especially the regression against temperature (Figure 6.21a) showed much scatter. Similar to the regressions on daily averaged data, DWT was the most powerful predictor of CO_2 fluxes at the 15 minute time scale (as indicated by the highest R^2 in Table 6.5).

Table 6.5 Coefficients of regression equations displayed in Figure 6.21 that were based on 15-minute data. y = CO_2 flux measured by the chamber. Peat temperature was measured at 30 mm depth directly adjacent to the chamber. R^2 is the proportion of the variance explained by the regression adjusted for the degrees of freedom.

	Linear $y = a + bx$			Exponential $y = ae^{bx}$		
x	*a*	*b*	R^2	*a*	*b*	R^2
Temperature	0.043	0.064	0.218	0.450	0.053	0.200
DWT	-0.185	-0.004	0.609	0.182	-0.006	0.67
VMC 45 mm	3.93	-5.72	0.474	463	-11.9	0.57
VMC 105 mm	7.26	-9.85	0.361	1543	-11.6	0.34

As with the daily averaged data (Section 6.3.3), the interactive models that combine the effect of temperature and DWT (Equations 6.4 and 6.5) were fitted to the 15-minute data. Coefficients of the two models are shown in Table 6.6. Both regressions explained a reasonable portion of the variation in the data, with R^2 of 0.67 for the model predicting HR (Eq. 6.4), and an R^2 of 0.79 for the model predicting ln(HR) (Eq. 6.5).

Table 6.6 Coefficients of multiple regression equations of 15-minute CO_2 flux on peat temperature at 30 mm and depth to water table. R^2 is the proportion of the variance explained by the regression adjusted for the degrees of freedom.

	Source	*a*	*b*	*c*	*P*	R^2
$\mathrm{HR} = a + b \cdot T + c \cdot DWT$	Waddington and Warner (2001)	-0.267	0.0106	-0.0039	< 0.001	0.67
$\ln(\mathrm{HR}) = a + b \cdot T + c \cdot DWT$	Silvola (1996)	-1.97	0.0117	-0.0058	< 0.001	0.79

Comparison of measured and modelled values for the two models revealed that residuals were generally smaller than 1 µmol CO_2 m^{-2} s^{-1} (Figure 6.22). The model by Waddington and Warner (2001) (Figure 6.22a) appeared to overestimate small to intermediate fluxes (between around 0 and 1 µmol CO_2 m^{-2} s^{-1}), but underestimated fluxes larger than 1.5 µmol CO_2 m^{-2} s^{-1}. The ln(HR) model used by Silvola (1996) performed better when higher respiration rates were observed.

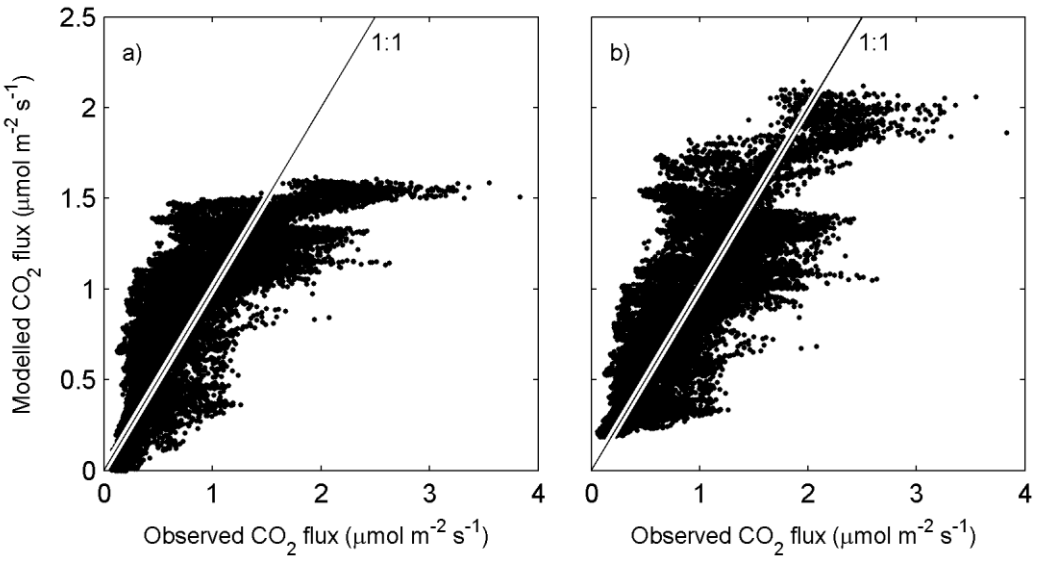

Figure 6.22 Comparison of modelled and observed CO_2 fluxes using the models described in Section 6.2.3 applied to 15-minute chamber data. a) performance of the model proposed by Waddington and Warner (2001), b) performance of the model proposed by Silvola et al. (1996), see Section 6.2.3. The coefficients of the regression equations are shown in Table 6.6.

6.4 Discussion

The main objective of this study was to describe how temperature, moisture and depth to water table affect respiration rates at the monthly, daily and within-day timescales. One of the aims was to examine whether the pattern that is often observed in lab and field studies – with lowered respiration rates at both the dry and the wet end of the moisture spectrum – could be observed at the peatland. Also, the performance of two relatively simple regression models was examined.

The discussion of the results will start by comparing the monthly averaged rates of soil respiration measured at the peatland to rates found in the literature for comparable ecosystems (Section 6.4.1). Monthly averaged respiration rates are also used to identify the dominant seasonal controls on respiration rates. This is followed by a discussion of the control by water table depth, moisture content and rain (Section 6.4.2). This section is split into two subsections addressing different mechanisms: the first section addresses how DWT controlled the oxygen conditions in the peat layer (thereby affecting respiration rates), and the second describing how moisture conditions might have affected respiration rates. Within these two subsections, data on the daily

and the within-day timescales will be discussed separately. The control of CO_2 efflux by temperature is examined after this (Section 6.4.3). Temperature sensitivity and the effect of depth of the temperature measurement will be considered separately for daily averaged data, and within-day data. The fourth section deliberates on the interactive control on respiration rates by DWT and temperature and describes to what extent the hypothesised behaviour illustrated by the conceptual model described in Section 6.1 could be observed at the peatland (Section 6.4.4). The last section describes the results of the two interactive models used in this study (Section 6.4.5).

6.4.1. Monthly respiration rates

At the peatland, monthly mean soil respiration rates varied between 0.25 g C m^{-2} d^{-1} in winter and 2.03 g C m^{-2} d^{-1} in summer (Figure 6.2). These CO_2 fluxes fall well within the range of peat respiration values found in other studies over bare peatlands in the northern hemisphere (Table 2.3). In contrast, the values found at the study site were relatively low compared to average value of 7.2 g C m^{-2} d^{-1} reported for temperate vegetated peatland ecosystems by Roehm (2005). Likely causes of the larger CO_2 losses from the vegetated peatlands are the input of young and labile organic matter by the vegetation and the contribution of root-associated respiration to the total CO_2 efflux. The decrease in peat respiration after draining and mining has been found by other studies also. Glatzel et al. (2004) and Waddington et al. (2001) found lower aerobic CO_2 production rates at recently harvested peat sites in Canada compared to pristine peatlands using laboratory incubations. Glatzel et al. (2004) suggested that harvesting may have reduced C substrate and nutrient availability which might in turn have led to decreased microbial biomass (Croft et al., 2001; Glatzel et al., 2004). Similarly, Waddington et al. (2001) reasoned that the removal of the surface layer with its fresh OM readily available to microbes at the harvested sites led to more recalcitrant material at the surface and lowered the potential for CO_2 emissions. This hypothesis was supported by incubations of peat from different depths that showed a decrease of CO_2 production potential with depth (Glatzel et al., 2006; Hogg et al., 1992; Waddington et al., 2001), suggesting a

decrease of substrate quality with depth (Glatzel et al., 2006; Waddington et al., 2001).

Similarly, Nieveen et al. (2005) measured average (night-time) losses of 3.3 g C m^{-2} d^{-1} from a drained peatland under pasture 62 km from the study site between May 2002 and May 2003. The causes for the higher CO_2 losses found at the pasture site were likely the lower water table depth (especially in winter) increasing the aerobic peat layer, inputs of young and easily degradable organic matter from the pasture, the contribution of autotrophic respiration to the total CO_2 efflux and possibly, stimulated microbial respiration caused by the higher nutrient status resulting from fertilisation (e.g. Kechavarzi et al., 2010)

The monthly averaged chamber fluxes at the mined peatland were largest when peat temperature was greatest, DWT deepest and VMC lowest (Figure 6.4). Although fluxes generally increased with increasing peat temperature (Figure 6.4), the regressions of CO_2 flux vs. DWT or VMC explained more variance than the regression vs. peat temperature (Table 6.1), suggesting that moisture status or the thickness of the unsaturated zone were more important controls on soil respiration than temperature.

6.4.2. Control of the CO_2 efflux by DWT, moisture content and rain

Control of thickness of the aerobic layer by DWT

Daily averaged data

The CO_2 efflux at the study site measured at the surface increased exponentially as the depth to water table increased (Figure 6.5). Because oxygen diffusion is greatly reduced under water-logged conditions (Luo and Zhou, 2006), microbial respiration and thus CO_2 production in the aerobic layer above the water table generally takes place at a much higher rate than CO_2 production below the water table (Glatzel et al., 2006; McNeil and Waddington, 2003; Waddington et al., 2002). As a result, changes in DWT and therefore the thickness of the layer of aerobic peat producing CO_2 explained much of the variation observed in the daily averaged CO_2 effluxes (Figure 6.5). This control of DWT on the aerobic layer is potentially larger in peat soils than mineral soils.

Whereas mineral soils contain most organic matter in the top of the profile (Jobbagy and Jackson, 2000), peat soils have high OM availability throughout the profile (Graf et al., 2008). This means that microbial activity is not limited to a thin, easily identifiable layer, but instead the CO_2 efflux measured at the surface is the sum of all respired CO_2 produced along the peat profile (Graf et al., 2008; Pavelka et al., 2007). Several peatland studies have examined the effect of water table drawdown on respiration rates and observed a positive response of respiration as the water table dropped (Freeman et al., 1993; Jauhiainen et al., 2005; Laiho, 2006; Moore and Dalva, 1993; Silvola et al., 1996). This response of increased carbon losses to drying of peatlands has also been found in modelling studies (Schimel et al., 1994).

The lowering of the water table caused by draining peatlands used for agriculture or forestry is considered the main cause of the high peat respiration rates in drained (but not necessarily mined) systems compared to pristine wetlands (Laiho, 2006; Waddington et al., 2002). Even a small change in DWT can have large implications for CO_2 losses, as shown by Waddington et al. (2002). In comparing two contrasting years, they found that respiration rates were more than 70% lower during the wetter summer, even though the difference in mean water table between the two summer was only 60 mm (Waddington et al., 2002).

Increased methane oxidation might also have contributed to the relatively high values of the CO_2 flux when the water table was deep. Wetlands soils are stratified vertically into an anaerobic submerged zone of CH_4 production and an overlying aerobic zone of CH_4 oxidation (Le Mer and Roger, 2001; Whalen, 2005). This means that only part of the produced methane is emitted to the atmosphere. Between 60 to 90% of the produced CH_4 diffusing upwards from the layer below the water table is intercepted and oxidised in the aerobic layer above (Le Mer and Roger, 2001). The ratio of production to oxidation typically decreases with increasing thickness of the aerobic layer (i.e. lowering of the water table; Rodhe and Svensson, 1995; Sundh et al., 1995; Waddington and Price, 2000) because of decreased production and increased oxidation of methane (Bridgham et al., 2006; Lai, 2009; Nykänen et al., 1995; Rodhe and

Svensson, 1995). However, because carbon losses as methane are generally relatively small (< 10 g C m^{-2} y^{-1} was estimated as the global median emissions for wetlands (Aselmann and Crutzen, 1990; Le Mer and Roger, 2001)) the contribution of this oxidised methane to the carbon losses at peatland in the current study were likely small compared to losses as CO_2 resulting from microbial respiration.

Within-day variation

The controls exerted by rainfall and DWT on the CO_2 flux at the study site could also be observed at the within-day time scale. Several instances were identified whereby rainfall events caused a rapid rise in water table, leading to an instant decrease in CO_2 flux (Figures 6.17 and 6.18). This decrease in emitted CO_2 in response to the rising water table could be the result of anaerobic conditions limiting both CO_2 production along the peat profile (Glatzel et al., 2006; McNeil and Waddington, 2003; Waddington et al., 2002) and the transport of the produced CO_2 to the peat surface (by limiting the CO_2 diffusion; Jassal et al. 2005).

Typically, the water table dropped rapidly as soon as rainfall stopped. In some instances, a rapid increase in CO_2 flux was observed (e.g. Figure 6.18). This response to the lowering of the water table suggested that oxygen limitation was alleviated and diffusion of CO_2 enabled by the lowering of the water table. This stimulating effect of drying after rainfall had been shown in a wetting-and-drying experiment in a mined peatland in Canada (Waddington et al., 2002), where respiration rates were found to drop in response to a 24 mm rainfall event, but recovered within 2.5 hours after simulated rainfall stopped. Comparison of different simulated rainfall intensities showed that larger rainfall events caused longer recovery times (Waddington et al., 2002). This stimulating response to lowering of the water table after rainfall was not easily recognisable in many instances during the current, purely observational study, possibly because other potential drivers (i.e. water table, VMC and temperatures along the profile) co-varied at the same time and confounded the response.

Control of VMC by DWT

Daily averaged data

In addition to determining the depth of the aerobic layer of peat, DWT also affected moisture levels of the peat above it (Figure 6.3). At the field site, VMC close to the surface was always less than the moisture content deeper down the peat profile (Figure 6.2). DWT never dropped below 450 mm and the lowest moisture content recorded at 45 mm depth was 0.44 m^3 m^{-3} (Figure 6.2). CO_2 fluxes measured at the surface did not decrease when moisture conditions at 45 mm were low (Figures 6.4 and 6.5), suggesting that moisture never limited CO_2 production. However, incubation studies using peat have shown that respiration rates decline at low moisture contents (e.g. Glatzel et al., 2006; Waddington et al., 2001). At the peatland, low moisture availability might have limited microbial activity at the very surface; however, because no data were collected on the vertical partitioning of the CO_2 production a decrease in daily-averaged respiration rates from the surface layer could not be detected by measuring the total CO_2 flux at the surface. Possibly, CO_2 production in the surface layer was limited under dry conditions, but was more than compensated for by the increase in CO_2 production caused by the increase in the thickness of the aerated layer as a result of a deep water table.

Within-day variation

The controls exerted by rainfall and VMC on the CO_2 flux at the study site could also be observed at the much shorter, within-day time scale.

Under dry and hot conditions in summer, a dry crust formed over the surface and the surface peat was observed to be much drier than the recorded values of VMC at 45 mm suggested. During the study period, there were few occasions in summer when the CO_2 flux increased rapidly in response to (small amounts of) rainfall. In some instances (e.g. Figure 6.19), the infiltrating water reached neither the water table, nor the moisture sensor at -45 mm. This suggested that all precipitation was absorbed by the peat above 45 mm depth. The large response of the CO_2 flux to rainfall suggested that microbial activity in the dry surface layer of peat might have been limited by lack of moisture in

summer which was temporarily alleviated by the rainfall. In addition to microbes at the very surface being affected by drought stress, it was very likely that the diffusion of soluble substrates to the microbes was limited by lack of water before the rainfall, thereby causing low respiration rates (Davidson et al., 2006a).

Another indication that microbes at the surface might have been stressed by lack of moisture or substrate was that the diurnal variation of the CO_2 flux during dry months displayed a maximum at night (Figures 6.12 and 6.20), which was also the time when relative humidity was highest (Figure 6.20). At times, the surface temperature of the peat was lower than the dew point temperature of the air (see e.g. Figure 6.20) indicating that condensation onto the surface could have taken place during these nights (Agam and Berliner, 2006; Oke, 1990). This could have enabled microbial activity and respiration at the peat surface by temporarily relieving water stress (Agam and Berliner, 2006; Dirks et al., 2010). Microbial activity might even have been enhanced by absorption of water vapour from the atmosphere when relative humidity was high, without dew formation taking place (Agam and Berliner, 2006; Dirks et al., 2010; Kuehn et al., 2004; Nagy and Macauley, 1982).

6.4.3. Control of the CO_2 efflux by temperature

Daily and monthly averaged data

Temperature sensitivity

At the daily and monthly time scales, CO_2 production generally increased with increasing peat temperature (Figures 6.4 and 6.5). Using daily averaged fluxes and the temperature at 30 mm depth measured next to the chamber, a (equivalent) Q_{10} of 2.79 or 2.53 was calculated using the Lloyd and Taylor and exponential equations, respectively. Both (equivalent) Q_{10} values were slightly higher than the theoretical value of 2 that is expected for biological processes (Davidson and Janssens, 2006) and fell well within the range of Q_{10} values found for peat in other studies (commonly found to vary between 2 and 3; Blodau, 2002 and references therein; Moore and Dalva, 1993; Xiang and Freeman, 2009).

The effect of temperature measurement depth

At the seasonal time scale, temperature at depth lagged behind the surface temperature and displayed a decrease in amplitude with increasing depth (Figure 6.2b). This presents a challenge when deciding which depth to choose for the temperature measurements (Graf et al., 2008; Richardson et al., 2006a) when aiming to determine the sensitivity of the CO_2 efflux to changes in soil temperature or when deciding which temperature to use for modelling. Temperature sensitivity derived from regressions of daily averaged CO_2 efflux against temperature varied depending on the depth at which the temperature was measured (Figure 6.7). Using daily averaged values, apparent temperature sensitivity (expressed as Q_{10}) when calculated with the temperature at -400 mm was more than twice as large as the temperature sensitivity calculated using the shallow -20 mm temperature (Figure 6.7a). There was a small increase in R^2 when using temperatures deeper down, until 400 mm depth (Figure 6.7b).

This increase of apparent temperature sensitivity when using temperatures from increasingly deeper depths (Figure 6.7) is commonly observed (Gaumont-Guay et al., 2006; Graf et al., 2008; Khomik et al., 2006; Pavelka et al., 2007). Because the temperate signal is 'muted' with depth, the same fluctuations in respiration are related to smaller fluctuations in temperature, leading to larger *apparent* temperature sensitivity (Davidson et al., 1998; Janssens and Pilegaard, 2003; Pavelka et al., 2007). However, this dependence of the observed Q_{10} on measurement depth should not be confused with the hypothesized increased temperature sensitivity of stable, recalcitrant organic compounds found in deeper soil layers compared to labile organic matter which is frequently found closer to the surface (Graf et al., 2008; Section 2.6.2 and references therein).

Using the mean temperature of the aerated layer above the water table to obtain a value for the temperature sensitivity resulted in a Q_{10} of 2.87 (Section 6.3.3), which sits within the range of Q_{10}'s obtained using temperatures at individual depths (Figure 6.7a). Although the fit was relatively poor (R^2 = 0.31), the obtained Q_{10} might be closer to the "real" Q_{10} of the peat than the Q_{10} obtained using the relatively shallow 30-mm temperature, because a modelling

study by Graf et al. (2008) suggested that using the temperature in the middle of the respiring soil layer (comparable to the mean temperature of the peat layer used here) yielded apparent Q_{10} closest to the 'real' Q_{10}.

Within-day variation

Hysteresis

During most months, hysteresis was observed when examining how hourly averaged temperature related to CO_2 efflux (e.g. Figure 6.14). In this situation, the flux observed at a certain temperature depended on the time of day, or whether the temperature was rising or falling. Hysteretic behaviour can be caused by several factors. Bahn et al. (2008) list the most important contributing processes as:

- the difference in time of day at which optimum temperatures occurs at different depths down the soil profile, as caused by the heat wave propagating down (Reichstein et al., 2005b)
- additional lags introduced by time it takes the produced CO_2 to diffuse to the soil's surface (Luo and Zhou, 2006)
- confounding co-varying controls that display a different diurnal variation than temperature. The most commonly identified factor in vegetated ecosystems is the diurnal variation of photosynthesis regulating substrate supply to microbes in the rhizosphere (Carbone et al., 2008; Gaumont-Guay et al., 2006; Riveros-Iregui et al., 2007; Tang et al., 2005). Another potential co-varying control causing hysteresis with temperature could be if soil moisture varies close to a threshold value (Carbone et al., 2008).

At the peatland, it was likely that hysteresis in the temperature – CO_2 efflux relationship was caused by a combination of some of the factors listed above. However, the lack of plants at the peatland ruled out the possibility of the diurnal variation in photosynthesis causing this hysteresis.

Similar to the pattern observed at the seasonal time scale, the within-day pattern of changes in temperature at depth displayed a smaller diurnal variation and a phase shift compared to the temperature near the surface (see e.g. Figure 6.13; van Wijk and de Vries (1963). This meant that peat layers at different

depths were subject to different temperatures at any one time during the day. Especially in summer, temperature maxima at the bottom of the aerated (=CO_2 producing) peat occurred up to 20 hours after the maximum at the surface (e.g. Figure 6.15) which would have lead to an asynchronous occurrence of maximum CO_2 production with depth. In the current study, no estimates were made of the time it takes for CO_2 to diffuse from deeper depth to the peat surface, which would add to the lag time. Because the peatland was not vegetated, it did not have a varying supply of fresh substrate that could have caused hysteresis. However, the increase in moisture availability at the peat surface at night – caused by dew or absorption of water vapour from the atmosphere – might have temporarily increased substrate diffusion to the microbial microsites at that time of day. This possible diurnal pattern in moisture availability might have been an important driver of the diurnal variation observed in summer, which displayed maximum values at night, when surface temperatures were lowest (Figure 6.20).

For the discussion of the temperature sensitivity at the within-day timescale, the hysteretic behaviour of CO_2 flux and temperature will be ignored, and the results of simple regressions (which average out the effect of hysteresis) will be used.

Temperature sensitivity and the effect of temperature measurement depth

Within-day temperature sensitivities derived using temperatures at different depths varied greatly (Figure 6.14). Because of the dampening and the phase shift of the temperature signal with depth, both positive and negative relationships were found between temperature at depth and CO_2 flux (Figure 6.14), resulting in values of Q_{10} between 0.6 and 3.6. Whereas under wet conditions respiration rates increased with increasing near-surface temperature (Figure 6.14h), the opposite was true under dry conditions when CO_2 flux was inversely related to near-surface temperatures (Figure 6.14a). Under these dry conditions, none of the temperatures measured at any of the depths appeared to explain the diurnal pattern in HR (Figures 6.13 and 6.14). Similar to the results based on daily averaged values, regressions using mean temperature above the water table (which was assumed to represent the mean temperature of the CO_2

producing peat layer) instead of the temperature close to the surface did not provide a better prediction than shallow temperatures.

It was obvious that none of the regressions using within-day variation of *T* and respiration rates were very useful for determining temperature sensitivities. Pavelka et al. (2007) and Gaumont-Guay et al. (2006) concluded the same, when they calculated Q_{10} values between 150 and 800 respectively based on diurnal variation of fluxes and temperatures deeper down the soil profile. In a modelling study by Graf et al. (2008), it was also concluded that when relatively short time series are used for determination of temperature sensitivity (i.e. shorter than 6 months), highly irregular apparent Q_{10} can be obtained because the time series do not cover at least one annual cycle.

Using monthly averaged within-day variations of flux and peat temperature with depth, the average depth was calculated at which the delay between peat temperature and surface CO_2 flux was minimal (Figure 6.16). This analysis indicated that the depth at which the temperature signal was in phase with the surface CO_2 flux was related to the depth of the water table (Figure 6.16). The depth-of-zero-delay was located just above the water table, at approximately 74-86% of the DWT. It is tempting to conclude that this depth indicated the layer most actively contributing to the total CO_2 flux. Others have suggested that in the peat layer just above the water table moisture and oxygen conditions might be optimal, enabling optimum diffusion of both oxygen and substrates (Glatzel et al., 2006). However, the data presented here do not directly provide evidence that the depth of minimum delay between temperature and surface CO_2 flux can be interpreted as the depth of "optimum CO_2 production" or "depth representative of the CO_2 production layer", because diffusion time was not taken into account in this analysis. It is very unlikely that this transport between depth of production and the peat surface was instantaneous. Also, because the depth of zero delay was calculated using the 24 hours cycle of the mean diurnal variation, an apparent 0 hour delay might actually indicate a 24-hour delay. Thirdly, during several months with deep water table, the depth-of-zero-apparent-delay was below -200 mm. As shown in Figure 6.13, the amplitude of the diurnal temperature variation at this depth was very

small (< 1°C), which makes it unlikely that that temperature changes at these depths were mainly responsible for the daily variation in surface CO_2 efflux, which were more than 1 µmol CO_2 m^{-2} s^{-1} during most summer months (see e.g. Figure 6.13).

Summarising the results concerning temperature sensitivity of the CO_2 flux obtained at both daily and within-day time scale, the accurate determination of the temperature sensitivity of peat respiration at the study site proved to be challenging and highly dependent on the depth chosen for the temperature measurement. It was clear that determination of the temperature sensitivity using the diurnal patterns of *T* and HR lead to very unrealistic values for Q_{10}. However, even after values were averaged by day, as recommended by Graf et al. (2008), it was still unclear which value for Q_{10} represented the best estimate for the 'real' Q_{10}. Several studies have suggested that field studies might not be the most appropriate method for determining temperature sensitivity of soil respiration (Graf et al., 2008; Kirschbaum, 2000). Especially because the layer of peat contributing to the total CO_2 losses was relatively thick and varied seasonally, the total CO_2 efflux measured at the surface was made up of CO_2 produced in many layers subject to different temperatures at any one time, which makes finding the 'best depth' for determination of the temperature sensitivity prone to errors (Graf et al., 2008). As Davidson et al. (1998) point out it would be preferable to determine the temperature sensitivity of CO_2 production for each soil layer separately, instead of trying to relate the sum of all CO_2 produced to the temperature measured at one subjectively chosen depth.

6.4.4. Interactive control of peat respiration by temperature and DWT

Because the current study was a field study, controlling factors of the CO_2 efflux (like temperature, moisture content, water table depth and the relative contribution of the peat layers to the total CO_2 production) co-varied in time (Figure 6.3; Reichstein et al., 2005b). Often, summers are dry and warm and winters are cool and wet, making it hard to separate the effect of *T* and moisture

on HR. Also, VMC (or DWT) and temperature are not completely independent in the field: apart from temperature increasing in summer because of larger energy inputs from the sun, the moisture content partly controls the temperature regime of the surface layer of peat. The magnitude of temperature fluctuations tends to increase with decreasing moisture content because the loss of water in the top layers leads to a decrease in specific heat and thermal conductivity (Waddington et al., 2002).

Changes in moisture and aeration conditions might have had a confounding effect on the temperature response of the measured respiration rates in the field as determined in Section 6.4.3 (Davidson et al., 1998; Kirschbaum, 2000). For this reason, incubations under controlled conditions in a laboratory are sometimes suggested to be a more appropriate means of obtaining estimates for the temperature sensitivity (Graf et al., 2008; Kirschbaum, 2000). However, these laboratory incubations are conducted under highly artificial conditions and have their own drawbacks (Luo and Zhou, 2006), such as physical disturbance of the soil (Bradford et al., 2009) and depletion of available organic matter (Kirschbaum, 2000).

In studies examining soil respiration in the field, it is commonly observed that the response of HR to changes in a controlling factor might be confounded if one of the other factors is limiting. For example, Waddington et al. (2001) found that addition of oxygen to deeper peat layers did not increase CO_2 production much, probably because substrate quality was constraining HR. Or, as mentioned in Section 6.1, in several non-peatland ecosystems no (or only a small) response to temperature changes could be detected when moisture conditions were limiting microbial activity (e.g. Mudge, 2009; Reichstein et al., 2002; Sowerby et al., 2008). At the peatland, daily averaged temperature continued to have a positive effect on HR regardless of DWT, although the response of HR to temperature did seem smaller under the wet conditions compared to dry conditions (Figure 6.8). This pattern corresponded with the conceptual model depicted in Figure 6.1, which implies that under wet conditions, oxygen might be limiting HR, and moisture conditions might confound the temperature response. The conceptual model described in the introduction also suggested that dry

conditions might confound the response of respiration to changes in temperature, but these conditions were never encountered at the peatland throughout the whole peat profile as discussed in Section 6.4.2.

6.4.5. Modelling respiration from peat

Models of soil respiration are needed to help increase understanding about soil respiration and to predict the likely response of the CO_2 efflux from soils to the atmosphere (and therefore the global soil carbon pool) to changing climatic conditions and/or management practises. For predicting the effect of climate changes, modelling at seasonal time steps is appropriate. However, when the aim is to increase understanding of the underlying mechanisms of soil respiration, much smaller time steps are often required.

Inspection of the 15-minute data showed that respiration rates did not show a clear relationship with peat temperature at any one depth or with the mean temperature of the aerobic layer (Section 6.3.4). Hysteresis was observed in the relationship between *T* and HR, and especially under dry conditions an apparent inverse relationship between near-surface temperature and CO_2 flux was common. On top of this, rainfall events were observed to cause pulses of CO_2 emission or complete suppression of the CO_2 flux. This set of complex interacting effects, together with processes that might not have been identified, posed a great challenge when trying to understand what controlled CO_2 effluxes at this time scale. At the within-day time scale, near-surface peat temperature was shown to be a very poor predictor of the CO_2 flux (Figure 6.21 and Table 6.5) and CO_2 flux seemed mostly driven by DWT. Even though the two models predicting the CO_2 flux based on *T* at 30 mm and DWT (Equations 6.4 and 6.5) were able to explain between 67% and 79% of the variation in the data, the large residuals of both models indicate that the regression models are a poor tool for predicting CO_2 fluxes at this within-day time scale (Figure 6.22). However, for the purpose of predicting future CO_2 losses and understanding the impacts of management practices on CO_2 losses modelling CO_2 effluxes at the fine within-day time scale is probably not necessary.

Using daily averaged DWT and temperature at 30 mm improved the performance of both models. The linear and non-linear model explained 76 and 86% of the variation, respectively (Figure 6.8 and Table 6.3). For such relatively simple regression models, this was regarded as adequate, and at the high end of the range of R^2 values found in other peatland studies (e.g. Silvola et al., 1996; Waddington et al., 2002).

Even though the simple regression models applied to daily averaged data explained much of the observed variation in soil respiration, and were able to identify DWT as the most important driver of CO_2 fluxes, they are of limited value when trying to increase detailed understanding about the underlying processes (Luo and Zhou, 2006). Even in a relatively simple ecosystem like the bare peatland, several processes interact to determine the measured rate of CO_2 efflux as a result of heterotrophic respiration. Rate of CO_2 production, change in storage of CO_2 in the soil (or peat) and transport of CO_2 to the surface together determine the efflux of CO_2 at any one time. The change in the thickness of the CO_2-producing layer depending on the position of the water table added complexity at the peatland. Moisture content and temperature affect CO_2 production, storage and transport both directly and indirectly (Davidson and Janssens, 2006). Whereas regression models like the ones tested in this study shed little light on how these processes interact to result in the final measured CO_2 flux (especially at the within-day timescale), mechanistic or 'process-based' models can be used to study the combined effect of the processes that make up soil respiration (Luo and Zhou, 2006). These models describe either CO_2 production (e.g. RothC (Coleman and Jenkinson, 2008) or CENTURY (Parton et al., 2001)), or CO_2 production and diffusion (e.g. Fang and Moncrieff, 1999; Jassal et al., 2004), and can be used to gain more detailed insight into the various mechanisms underlying soil respiration. These process based models are more suited, for example, to examine the vertical partitioning of the CO_2 production, changes of temperature sensitivity with depth (e.g. Davidson et al., 2006b), and short-term dynamics of soil CO_2 efflux. However, mechanistic models can be complex, have greater requirements with regards to site-specific input variables

(Khomik et al., 2009), are difficult to validate (Reichstein et al., 2003) and consequently fell outside the scope of the current study.

6.5 Summary

Measurements made using an automatic chamber were used to investigate the control of depth to water table (DWT), volumetric moisture content (VMC) and peat temperature (*T*) on the CO_2 efflux resulting from heterotrophic respiration (HR) at a bare peatland.

The highest daily averaged values for HR were measured in summer and were associated with high temperatures, deep water tables and low values for surface VMC. Using simple regression equations, DWT appeared the most important driver of the daily averaged CO_2 flux (highest R^2). The most important effect of DWT was probably its control of the depth of the aerated layer of peat, which varied between 50 mm in winter and 440 mm in summer. Because diffusion of oxygen is 10,000 times faster in air than in water, this increase of the aerated peat layer would have greatly increased the contribution of microbes in deeper peat layer to the total CO_2 flux.

There was evidence that microbial activity in the very top layer of the peat might have been moisture limited in summer: highest HR were measured at night when dew formation and absorption of water vapour might have served as a source of water and small rainfall events occasionally caused large increases in CO_2 efflux.

However, because the total CO_2 flux at the surface was the result of microbial activity within a thick layer of peat, this potential decrease of microbial activity at the very surface, caused by low moisture conditions, did not cause a decrease in total daily averaged CO_2 flux, as drying of the surface was accompanied by an increase in the aerated layer. This means that, for the bare peatland, the conceptual model with decreased microbial activity at both ends of the moisture scale (i.e. either too dry or too wet, Figure 6.1), was not fully observed. However, under wet conditions, low fluxes were observed, accompanied by a weak response of HR to temperature, most likely because

much of the peat profile was saturated and lack of oxygen limited the rate of respiration.

Temperature sensitivity could not be determined with certainty using daily averaged values for the temperature and CO_2 flux, because the obtained Q_{10} values varied depending on the depth chosen for the temperature measurements. Also, moisture conditions were likely to have confounded the temperature response. The observed Q_{10} based on the average temperature of the peat layer above the water table was 2.87, which sat within the range of Q_{10}'s obtained using temperatures at individual depths and was comparable to Q_{10}'s found in other peatland ecosystems. Data collected at a higher time resolution (i.e. 15 minute data) proved very unsuitable for determination of the temperature sensitivity.

Simple regression models using DWT and *T*, applied previously at other peatlands (Silvola et al., 1996; Waddington and Warner, 2001), were able to explain 76–86 % of the variation in daily averaged HR. Using the mean temperature of the peat layer above the water table did not improve the proportion of explained variation. Possibly inclusion of more variables (e.g. temperature at a second depth (Reichstein et al., 2005b)) might improve the quality of the model. Alternatively, a mechanistic model which explicitly models the processes of CO_2 production at different depths and CO_2 transport though the peat might lead to a higher proportion of explained variance, and increase understanding of the underlying processes of soil respiration.

Because peatlands generally contain a deep layer of partly decomposed organic matter, they are a large store of carbon at a global scale. This study indicated that the position of the water table depth was the main driver of CO_2 effluxes from the bare peatland. This suggests that changes in hydrological conditions (for example those due to global change or change of management) might be more important than changes in temperature for determining CO_2 losses from bare peatlands.

Chapter 7 Summary and conclusions

7.1 Introduction and review of thesis objectives

Soil carbon is important because it increases soil quality and productivity through increasing water holding capacity, nutrient retention and improving soil structure (Luo and Zhou, 2006; McLaren and Cameron, 1996). Soil carbon also forms a large store of terrestrial carbon, which, if (partly) lost to the atmosphere as CO_2, would have major implications for the global climate (Davidson and Janssens, 2006; Friedlingstein et al., 2006; Jones et al., 2003; Kirschbaum, 2004).

Because of the important functions of soil carbon for soil quality and the global carbon cycle, it is of utmost importance to improve our understanding of the drivers and magnitude of CO_2 losses from soils. Uncertainty still exists about what controls losses of CO_2 through heterotrophic respiration by microbes (Jones et al., 2003; Trumbore, 2006). The abiotic process of photodegradation has only recently been identified as a contributor to CO_2 losses from litter at small scales (Anesio et al., 1999; Brandt et al., 2009), and no studies have estimated the contribution of photodegradation to CO_2 losses from SOM and litter at larger scales.

The aim of this thesis was to increase understanding about the controls of CO_2 losses from terrestrial organic matter. This overall aim was divided into three objectives (See also Section 1.2):

1. Determine the contribution of photodegradation to total CO_2 losses
2. Investigate the controls of irradiance-induced CO_2 production
3. Examine the controls of microbial respiration rates at a bare peatland.

CO_2 fluxes were measured at a bare peatland using eddy covariance and chambers. Differences between the CO_2 fluxes measured by these two methods indicated that photodegradation contributed to CO_2 losses, in addition to microbial respiration. Observations of CO_2 fluxes from a grassland in California collected during the dry summer period when plants had died were also

examined for evidence of photodegradation. Furthermore, short incubations in a small closed chamber setup (referred to as the 'container') were used to study irradiance-induced CO_2 losses and its controls.

The following five sections will summarise the results and conclusions related to the objectives listed above. The final section will describe recommendations for further research.

7.2 Magnitude of CO_2 efflux resulting from microbial decomposition and photodegradation

At both the bare peatland in New Zealand and the summer-dead grassland in California, incoming solar radiation exerted direct control over the CO_2 efflux at ecosystem scales through the process of photodegradation of organic matter (OM) under ambient conditions of soil moisture, temperature and radiation. The contribution of irradiance-induced CO_2 fluxes was quantified by comparing eddy covariance (EC) measurements (which determined the total CO_2 efflux) with the CO_2 flux measured using either an opaque chamber (at the peatland) or the CO_2 gradient technique (at the grassland). In addition, comparisons were made between EC fluxes obtained at night and during the day under similar temperature and moisture conditions. At the peatland, total annual CO_2 losses were estimated to be 269 g C m^{-2} y^{-1} of which between 13% and 25% was the result of photodegradation. For the grassland, the irradiance-induced portion of the CO_2 flux could only be estimated when photosynthesis was not taking place, i.e. during the summer period when the grass had senesced. Excluding periods during and immediately after rain, total CO_2 losses during the dry summer period (~3 months) were estimated to be 27 g C m^{-2} (or 0.31 g C m^{-2} d^{-1}), of which approximately 60% was irradiance-induced.

The detection of substantial production of irradiance-induced CO_2 from two very different ecosystems suggested that photodegradation might also occur in other ecosystems with exposed OM, such as sparsely vegetated arid and semi-arid ecosystems, savannas, croplands after harvest or ecosystems during drought. This contribution is currently not recognised in conceptual and numerical models of ecosystem carbon cycling.

Another implication of these results is that the method of flux partitioning commonly applied in ecosystem CO_2 exchange research using EC, whereby daytime CO_2 losses are modelled based on measured night-time CO_2 losses, might be invalid if photodegradation contributed substantially to ecosystem-scale CO_2 losses during the day. Consequently, especially in ecosystems where much of the dead organic matter is exposed to solar radiation, it is advisable to carefully test whether light intensity affects the CO_2 losses from litter and soil, for example by using transparent chambers and comparing measurements made during the night and day.

7.3 Mechanisms of irradiance-induced CO_2 production

There are several ways by which solar irradiance can affect CO_2 losses from terrestrial organic matter. Solar irradiance can directly break down bonds in OM, either into smaller organic molecules that can be further decomposed by microbes (microbial facilitation), or completely to CO_2 (photochemical mineralisation). In contrast, exposure of OM to UV irradiance can also have a negative effect on surface-dwelling microbes (microbial inhibition), thereby potentially lowering CO_2 losses by microbial respiration.

At both the peatland and the grassland, CO_2 fluxes measured in the presence of solar radiation were greater than those in the dark under that same moisture and temperature conditions, suggesting that the mechanisms that enhanced CO_2 losses (i.e. microbial facilitation and photochemical mineralisation) overshadowed any possible negative effect of radiation on microbes.

The CO_2 fluxes measured during the container study were the result of photochemical mineralisation alone, because the organic matter in the container was too dry to support microbial activity and CO_2 fluxes in the dark were zero. It is likely that, in the field, photochemical mineralisation also was the main CO_2 producing mechanism, although data obtained during previous studies do suggest that asynchronous microbial facilitation might have occurred at the grassland. Solar irradiance might partly break down OM during the dry season, thereby making substrates available for microbial decomposition as soon as

moisture limitations for microbes are alleviated by rainfall. Consequently, microbial decomposition facilitated by photodegradation may be a mechanism contributing to the 'Birch effect'.

7.4 Controls of irradiance-induced CO_2 production

Both field and container measurements indicated that the intensity of solar irradiance was the most important factor controlling rates of CO_2 losses through photodegradation. In the field, the sensitivity of CO_2 production to incoming solar irradiance (or dose-response coefficient, here defined as moles of CO_2 produced per unit of energy of incoming solar irradiance) seemed to increase with increasing solar irradiance, temperature and UV irradiance. Moisture status of the peat did not seem to affect irradiance-induced CO_2 losses.

Container incubations performed while blocking part of the solar spectrum indicated that irradiance in the UV region of the solar spectrum was responsible for approximately 14% of the total CO_2 losses by photodegradation. This estimate for the contribution of UV irradiance was lower than the contribution found by Brandt et al. (2009), who found a contribution of 48% to the CO_2 flux caused by UV. Incubations also showed that senesced grass and maize leaves produced less CO_2 when exposed to solar irradiance than peat (0.05 and 0.08 µmol CO_2 m^{-2} s^{-1} for grass and maize respectively compared to 0.24 µmol CO_2 m^{-2} s^{-1} for peat at high irradiance levels). Evidently, different substrates responded differently to irradiance, but the causes of these different responses were not clear. Most likely, the irradiance-induced CO_2 production is associated with albedo of the substrate and the organic matter chemistry.

In the field, irradiance-induced CO_2 fluxes observed at high irradiance intensities were almost 5 times larger than those observed in the container when expressed on an area basis. The cause for this difference is not known, and until an explanation can be found, this finding stresses the importance of conducting field experiments in addition to small scale (lab) experiments.

7.5 Controls of microbial respiration at the peatland

The position of the water table was the main driver of the CO_2 flux resulting from microbial respiration at the peatland. The water table depth determined thickness of the aerated peat layer in which aerobic respiration could take place. At the average daily time scale, temperature positively affected respiration rates. The observed Q_{10} increased from 2.3 when using the peat temperature at 20 mm depth for the Q_{10} calculation, to 4.7 when using the peat temperature at 400 mm depth. Because of this dependence of Q_{10} on the measurement depth of the temperature, and likely confounding effects of changing moisture conditions throughout the year on the observed temperature sensitivity, it was not possible to determine the 'true temperature sensitivity'. Possibly, the Q_{10} of 2.8 calculated using the mean temperature of the peat layer above the water table (which varied throughout the year) was the best estimate of the temperature sensitivity.

Two simple regression models previously used in northern hemisphere peatlands could be fitted to predict 76-86% of the observed variation in the daily averaged CO_2 flux based on water table depth and peat temperature.

Within-day variation of CO_2 flux could not easily be explained using peat temperature. In winter, when the water table was shallow, a weak peak in CO_2 efflux was observed during the warmest part of the day, but in summer, when the water table was deep, the CO_2 efflux peaked during the night when surface temperatures were lowest. This pattern was probably caused by the complex interplay of the greater thickness of the CO_2 producing layer in summer compared to winter, the propagation of the diurnal heat wave down the soil profile (causing a phase shift and decrease in amplitude with depth) and a range of diffusion times depending on which depth the CO_2 was produced at. Consequently, without more detailed mechanistic modelling, accurate prediction of the within-day variation of the CO_2 efflux was not possible. However, for the purpose of predicting future CO_2 losses and increasing understanding of the effects of management practices, modelling at the daily averaged timescale, or seasonal timescale, is probably sufficient.

7.6 A new conceptual model

Presented below is a new conceptual model of CO_2 losses from terrestrial organic matter based on the findings of the current study at a bare peatland and an annual grassland (Figure 7.1).

The process of microbial respiration (blue solid line in Figure 7.1) has traditionally been assumed to be solely responsible for the decomposition of organic matter and therefore production of CO_2 from soil and litter. Although some uncertainties remain (Jones et al., 2003; Trumbore, 2006), the effects of temperature and moisture on microbial respiration and CO_2 losses are reasonably well understood in many ecosystems (blue dashed lines in Figure 7.1).

The abiotic process of photodegradation has been ignored in most ecosystem carbon cycling studies and, in contrast to microbial respiration, there is only very limited understanding of mechanisms of photodegradation, the abiotic drivers and its importance for ecosystems worldwide.

Results of the current study suggest that photodegradation should be included to the conceptual model (red lines in Figure 7.1) as a mechanism contributing to decomposition and CO_2 production.

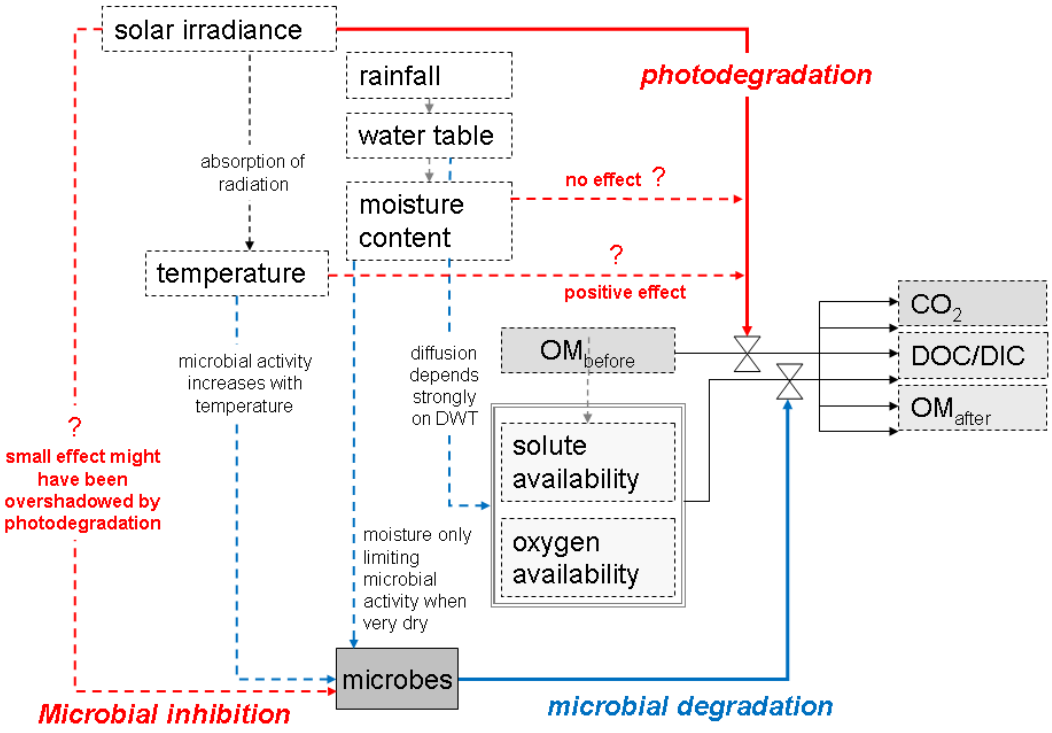

Figure 7.1 In addition to microbial decomposition and its controls (in blue), photodegradation and its controls (in red) need to be added to the conceptual model of CO_2 losses from terrestrial organic matter (based on the current study at the peatland and the grassland).

7.7 Recommendations for further research

The conceptual model presented above (Section 7.6, Figure 7.1) needs to be tested in a range of other ecosystems and greater understanding needs to be developed of the environmental controls. Controlled manipulative laboratory studies are most suited to help us gain knowledge about the mechanisms of photodegradation and to help disentangle the different abiotic controls such as temperature, moisture, substrate species and quality, wavelength distribution and irradiance intensity. The container setup developed in this research allows rapid testing of the influence of these parameters on irradiance-induced CO_2 losses. However, to gain insight into the importance of photodegradation to total CO_2 fluxes under more realistic conditions, field studies with measurements made under natural field conditions and at appropriate scales are crucial (Smith et al., 2010; Yue et al., 1998). Therefore, future research into photodegradation of terrestrial organic matter should combine small scale controlled experiments

and large scale field experiments. Recommendations for both small scale studies and field studies will be made in Sections 7.7.1 and 7.7.2, respectively.

After testing the conceptual model in a wide range of ecosystem and increasing understanding about the mechanisms and controls of photodegradation, numerical models need to be developed that describe the magnitude of photodegradation and irradiance-induced CO_2 losses under different environmental conditions. Section 7.7.3 will present some considerations for future modelling work.

7.7.1. Small scale studies

Small scale studies like the real-time incubations presented in Chapter 5 could be used to disentangle the controls of photodegradation. Of special interest are:

- Separating the effect of temperature and solar irradiance on photodegradation and the examination of interactive effects of temperature and radiation.
- Determining the effect of moisture on photodegradation (both in the presence and absence of microbial activity).
- Examining the potential contribution of photodegradation to the Birch effect (the often-observed pulse of CO_2 emission in response to rainfall after periods of prolonged drought) by measuring biological respiration from incubated litter that has been re-wetted after different durations of exposure to solar irradiance.
- Studying the susceptibility of different substrates (dead litter and soil, but also live and partly senesced leaves) to photodegradation. When combined with determination of the substrate chemistry before and after exposure this might shed light on which compounds are most responsible for the irradiance-induced CO_2 fluxes.

7.7.2. Field studies

At the larger scale, field studies should be focused on measuring irradiance-induced CO_2 fluxes from different ecosystems with exposed dead organic matter, for example, sparsely vegetated shrublands, savannas, seasonal grasslands, agricultural fields after ploughing and other ecosystems during seasonal droughts. This will require a combination of methods. In addition to the eddy covariance systems, opaque chambers and soil CO_2 profiles that were used in this study, transparent chambers could be used to measure the total (= CO_2 from biological + abiotic processes) CO_2 production.

In addition to new field studies, data from previous studies can be used to gain insight into the importance of photodegradation for the total CO_2 flux in other ecosystems. The FLUXNET database (http://www.fluxnet.ornl.gov/) is a large repository for CO_2 flux and supporting data collected across the globe, and these data could be subjected to similar analyses to those presented in Chapter 4 to estimate the contribution of photodegradation to CO_2 losses.

Currently, no technique is available for partitioning the total CO_2 flux measured in vegetated ecosystem into photosynthesis, biological respiration and photodegradation. If a method were developed that facilitated this partitioning, this would greatly enhance the research into irradiance-induced CO_2 losses.

The current study has only examined the extent to which photodegradation affects the carbon cycling in ecosystems. However, in addition to affecting decomposition rates (determined as mass loss) and CO_2 losses, photodegradation also might affect ecosystem functioning via the release of nutrients from OM. Photodegradation, in contrast to microbial decomposition, does not require nutrients, because “physical processes have no metabolic nutrient requirements” (Brandt, 2009). For example, a few studies have already identified that decomposition by photodegradation was not accompanied by nitrogen immobilisation (Brandt et al., 2007; Parton and Silver, 2007), as is often observed in microbial decomposition (Swift et al., 1979). It has been hypothesised that where photodegradation is the dominant decomposing process, carbon and nutrient cycling may be decoupled (Brandt, 2009).

Therefore, a key question to be addressed in future research is to determine the role of photodegradation in nutrient cycling.

7.7.3. Modelling

Previous studies have identified that models of carbon cycling which predict organic matter decomposition as a function of temperature and moisture perform poorly in dry ecosystems where photodegradation is likely to contribute considerably to the total mass loss (Parton and Silver, 2007). The current study highlights the need for photodegradation to be separately accounted for in carbon cycling models and coupled carbon-climate models.

Although much is still unknown about the drivers of photodegradation, it seems apparent that decomposition and CO_2 production resulting from photodegradation differ from decomposition and CO_2 production as a result of microbial activity in several aspects:

- Solar irradiance is the most important direct driver of decomposition by photodegradation, rather than moisture, temperature and nutrient status of OM which are important drivers of microbial degradation
- In carbon models, decomposition rates of OM often depend on the remaining mass of OM. However, for photodegradation, the remaining mass of the OM is not relevant, because photodegradation rates are controlled by exposed area instead of remaining mass. Only OM exposed to solar irradiance can photodegrade, and therefore, the ratio of exposed to shaded litter will be more important than absolute amounts of litter.
- Although consensus has not been reached, several studies report that lignin, a compound of OM that is typically slowest to be decomposed by microbes and therefore regarded as ‘stable’, might be most susceptible to photodegradation.

Consequently, carbon cycling models aimed at predicting decomposition in ecosystems where photodegradation is important would need to address these differences between the environmental controls of biological decomposition and photodegradation.

Photodegradation is an underexplored and potentially important component of ecosystem-scale CO_2 emissions which is likely to be a fruitful area of research in the future.

References

Aciego Pietri, J.C. and Brookes, P.C., 2008. Relationships between soil pH and microbial properties in a UK arable soil. Soil Biology and Biochemistry, 40(7): 1856-1861.

Adair, E.C. et al., 2008. Simple three-pool model accurately describes patterns of long-term litter decomposition in diverse climates. Global Change Biology, 14(11): 2636-2660.

Agam, N. and Berliner, P.R., 2006. Dew formation and water vapor adsorption in semi-arid environments -A review. Journal of Arid Environments, 65(4): 572-590.

Almagro, M., López, J., Querejeta, J.I. and Martínez-Mena, M., 2009. Temperature dependence of soil CO_2 efflux is strongly modulated by seasonal patterns of moisture availability in a Mediterranean ecosystem. Soil Biology and Biochemistry, 41(3): 594-605.

Amundson, R., 2001. The carbon budget in soils. Annual Review of Earth and Planetary Sciences, 29: 535-562.

Andrady, A.L., Hamid, H.S. and Torikai, A., 2007. Effects of stratospheric ozone depletion and climate change on materials damage. Photochemical and Photobiological Sciences, 6: 311-318.

Andriesse, J.P., 1988. Nature and management of tropical peat soil, FAO Soil Bulletin 59. FAO - Food and agricultural organization of the United Nations, Rome, http://www.fao.org/docrep/x5872e/x5872e00.htm#Contents.

Anesio, A.M., Tranvik, L.J. and Graneli, W., 1999. Production of inorganic carbon from aquatic macrophytes by solar radiation. Ecology, 80(6): 1852-1859.

Anslyn, E.V. and Dougherty, D.A., 2006. Modern physical organic chemistry. University Science Books, Sausalito, 1095 pp.

Armentano, T.V. and Menges, E.S., 1986. Patterns of change in the carbon balance of organic soil-wetlands of the temperate zone. Journal of Ecology, 74: 755-774.

Armentano, T.V. and Verhoeven, J.T.A., 1988. The contribution of freshwater wetlands to the global biogeochemical cycles of carbon, nitrogen and sulphur. Wetlands and Shallow Water Bodies 1 SPB. Academic Publishing, The Hague.

Arrhenius, S., 1889. Über die Reaktionsgeschwindigkeit bei der Inversion von Rohrzucker durch Säuren. Z.Phys.Chem., 4: 226-248.

Aselmann, I. and Crutzen, P.J., 1990. A global inventory of wetland distribution and seasonality, net primary productivity and estimated methane emissions. In: A.F. Bouwman (Editor), Soils and the greenhouse effect. John Wiley & Sons Ltd., Chichester, pp. 441-449.

Atkins, P. and de Paula, J., 2005. Elements of physical chemistry. Oxford University Press, New York, 627 pp.

Aubinet, M. et al., 2005. Comparing CO_2 storage and advection conditions at night at different CarboEuroflux sites. Boundary-Layer Meteorology, 116(1): 63-93.

Aubinet, M. et al., 2000. Estimates of the annual net carbon and water exchanges of forests: the Euroflux methodology. Advances in Ecological Research, 30: 113-175.

Austin, A.T. and Ballaré, C.L., 2010. Dual role of lignin in plant litter decomposition in terrestrial ecosystems. Proceedings of the National Academy of Sciences, 107(10): 4618-4622.

Austin, A.T. and Vivanco, L., 2006. Plant litter decomposition in a semi-arid ecosystem controlled by photodegradation. Nature, 442(7102): 555-558.

Austin, A.T. et al., 2004. Water pulses and biogeochemical cycles in arid and semiarid ecosystems. Oecologia, 141(2): 221-235.

Bahn, M. et al., 2008. Soil respiration in European grasslands in relation to climate and assimilate supply. Ecosystems, 11: 1352-1367.

Bain, W.G. et al., 2005. Wind-induced error in the measurement of soil respiration using closed dynamic chambers. Agricultural and Forest Meteorology, 131(3-4): 225.

Baker, J.M. and Griffis, T.J., 2005. Examining strategies to improve the carbon balance of corn/soybean agriculture using eddy covariance and mass balance techniques. Agricultural and Forest Meteorology, 128(3-4): 163-177.

Baldocchi, D., 2008a. Breathing of the terrestrial biosphere: lessons learned from a global network of carbon dioxide flux measurement systems. Australian Journal of Botany, 56(1): 1-26.

Baldocchi, D., 2008b. Editorial: FLUXNET, Quo vadis. In: D. Baldocchi and R. Vargas (Editors), FluxLetter - The Newsletter of FLUXNET. FLUXNET Office, Berkely, pp. 17, http://www.fluxnet.ornl.gov/fluxnet/FluxLetter_Vol1_No2.pdf.

Baldocchi, D. et al., 2001. FLUXNET: A new tool to study the temporal and spatial variability of ecosystem-scale carbon dioxide and energy flux densities. Bulletin of the American Meteorological Society, 82(11): 2415-2434.

Baldocchi, D., Tang, J.W. and Xu, L.K., 2006. How switches and lags in biophysical regulators affect spatial-temporal variation of soil respiration in an oak-grass savanna. Journal of Geophysical Research-Biogeosciences, 111(G02008): doi:10.1029/2005JG000063.

Baldocchi, D.D., 2003. Assessing the eddy covariance technique for evaluating carbon dioxide exchange rates of ecosystems: past, present and future. Global Change Biology, 9(4): 479-492.

Baldocchi, D.D., Hicks, B.B. and Meyers, T.P., 1988. Measuring biosphere-atmosphere exchanges of biologically related gases with micrometeorological methods. Ecology, 69(5): 1331-1340.

Baldocchi, D.D., Xu, L. and Kiang, N., 2004. How plant functional-type, weather, seasonal drought, and soil physical properties alter water and energy fluxes of an oak-grass savanna and an annual grassland. Agricultural and Forest Meteorology, 123(1-2): 13-39.

Balser, T.C. and Wixon, D.L., 2009. Investigating biological control over soil carbon temperature sensitivity. Global Change Biology, 15(12): 2935-3949.

Barros, N., Salgado, J. and Feijóo, S., 2007. Calorimetry and soil. Thermochimica Acta, 458(1-2): 11-17.

Baveye, P.C., 2007. Soils and runaway global warming: terra incognita. Journal of Soil and Water Conservation, 62(6): 139A-143A.

Berg, B., 2000. Litter decomposition and organic matter turnover in northern forest soils. Forest Ecology and Management, 133(1-2): 13-22.

Berg, B. and McClaugherty, C., 2008. Plant litter - Decomposition, humus formation, carbon sequestration. Springer, Berlin-Heidelberg, 338 pp.

Berg, B., Wessen, B. and Ekbohm, G., 1982. Nitrogen level and decomposition in Scots pine needle litter. Oikos, 38: 291-296.

Beringer, J., Hutley, L.B., Tapper, N.J. and Cernusak, L.A., 2007. Savanna fires and their impact on net ecosystem productivity in North Australia. Global Change Biology, 13(5): 990-1004.

Bertilsson, S. and Tranvik, L.J., 2000. Photochemical transformation of dissolved organic matter in lakes. Limnology and Oceanography, 45(4): 753-762.

Billesbach, D.P., Fischer, M.L., Torn, M.S. and Berry, J.A., 2004. A portable eddy covariance system for the measurement of ecosystem–atmosphere exchange of CO_2, water vapor, and energy. Journal of Atmospheric and Oceanic Technology, 21: 639-650.

Blakemore, L.C., Searle, P.L. and Daly, B.K., 1987. Methods for chemical analysis of soils. N.Z. Soil Bureau Scientific Report 80.

Blanco-Canqui, H. and Lal, R., 2004. Mechanisms of carbon sequestration in soil aggregates. Critical Reviews in Plant Sciences, 23(6): 481-504.

Blodau, C., 2002. Carbon cycling in peatlands - A review of processes and controls. Environmental Reviews, 10(2): 111-134.

Blodau, C. et al., 2007. Belowground carbon turnover in a temperate ombrotrophic bog. Global Biogeochemical Cycles, 21(1): B1021-B1021.

Blumthaler, M. and Webb, A.R., 2003. UVR climatology. In: E.W. Helbling and H. Zagarese (Editors), UV effects in aquatic organisms and ecosystems. Royal Society of Chemistry, Cambridge UK pp. 21-58.

Bodeker, G.E. and McKenzie, R.L., 1996. An algorithm for inferring surface UV irradiance including cloud effects. Journal of Applied Meteorology, 35: 1860-1877.

Bolstad, P.V., Davis, K.J., Martin, J., Cook, B.D. and Wang, W., 2004. Component and whole-system respiration fluxes in northern deciduous forests. Tree Physiology, 24: 493-504.

Bond-Lamberty, B., Wang, C. and Gower, S.T., 2004. A global relationship between the heterotrophic and autotrophic components of soil respiration? Global Change Biology, 10(10): 1756.

Boone, R.D., Nadelhoffer, K.J., Canary, J.D. and Kaye, J.P., 1998. Roots exert a strong influence on the temperature sensitivity of soil respiration. Nature, 396: 570-572.

Bornman, J.F. and Teramura, A.H., 1993. Effects of ultraviolet-B radiation on terrestrial plants. In: A.R. Young, L.O. Björn, J. Moan and W. Nultsch (Editors), Environmental UV Photobiology. Plenum Press, New York, pp. 427-471.

Bosatta, E. and Ågren, G.I., 1999. Soil organic matter quality interpreted thermodynamically. Soil Biology and Biochemistry, 31(13): 1889-1891.

Bradford, M.A., Watts, B.W. and Davies, C.A., 2009. Thermal adaptation of heterotrophic soil respiration in laboratory microcosms. Global Change Biology: "Accepted Article"; doi: 10.1111/j.1365-2486.2009.02040.x.

Brandt, L.A., 2009. The role of photodegradation in plant litter decomposition in grassland ecosystems, University of Minnesota, St Paul, 154 pp.

Brandt, L.A., Bohnet, C. and King, J.Y., 2009. Photochemically induced carbon dioxide production as a mechanism for carbon loss from plant litter in arid ecosystems. Journal of Geophysical Research, 114(G02004): doi:10.1029/2008JG000772.

Brandt, L.A., King, J.Y. and Milchunas, D.G., 2007. Effects of ultraviolet radiation on litter decomposition depend on precipitation and litter chemistry in a shortgrass steppe ecosystem. Global Change Biology, 13: 2193-2205.

Bridgham, S.D., Megonigal, J.P., Keller, J.K., Bliss, N.B. and Trettin, C., 2007. Chapter 13, Wetlands. In: A.W. King et al. (Editors), The first state of the carbon cycle report (SOCCR). The North American carbon budget and implications for the global carbon cycle. US Climate Change Science Program, Synthesis and Assessment Product 2.2. National Oceanic and Atmospheric Administration, National Climatic Data Centre, Asheville, NC, pp. 242.

Bridgham, S.D. and Richardson, C.J., 1992. Mechanisms controlling soil respiration (CO_2 and CH_4) in southern peatlands. Soil Biology & Biochemistry, 34(11): 1089-1099.

Bridgham, S.D. and Richardson, C.J., 2003. Endogenous versus exogenous nutrient control over decomposition and mineralization in North Carolina peatlands. Biogeochemistry, 65: 151-178.

Buchmann, N., Guehl, J.M., Barigah, T.S. and Ehleringer, J.R., 1997. Interseasonal comparison of CO_2 concentrations, isotopic composition, and carbon dynamics in an Amazonian rainforest (French Guiana). Oecologia, 110(1): 120-131.

Burba, G., Anderson, D., Xu, L. and McDermitt, D., 2005a. Solving the off-season uptake problem: correcting fluxes measured with the LI-7500 for the effects of instrument surface heating. Progress report of the ongoing study. Part I: Theory, AmeriFlux 2005 Annual Meeting, Boulder, CO.

Burba, G., Anderson, D., Xu, L. and McDermitt, D., 2005b. Solving the off-season uptake problem: correcting fluxes measured with the LI-7500 for the effects of instrument surface heating. Progress report of the ongoing study. Part II: Results, AmeriFlux 2005 Annual Meeting, Boulder, CO.

Burba, G., Anderson, D., Xu, L. and McDermitt, D., 2006. Correcting apparent off-season CO_2 uptake due to surface heating of an openpath gas analyzer: progress report of an ongoing experiment, Proceedings of the 27th Annual Conference of Agricultural and Forest Meteorology, San Diego, CA.

Burba, G.G., McDermitt, D.K., Grelle, A., Anderson, D.J. and Xu, L.K., 2008. Addressing the influence of instrument surface heat exchange on the measurements of CO_2 flux from open-path gas analyzers. Global Change Biology, 14(8): 1854-1876.

Caldwell, M., Searles, P.S., Flint, S.D. and Barnes, P.W., 1999. Terrestrial ecosystem responses to solar UV-B radiation mediated by vegetation,

microbes and abiotic photochemistry. In: M.C. Press, J.D. Scholes and M.G. Barker (Editors), Physiological Plant Ecology. Blackwell, Oxford, pp. 241-262.

Caldwell, M.M. and Flint, S.D., 1995. Lighting considerations in controlled environments for nonphotosynthetic plant responses to blue and ultraviolet radiation. In: T.W. Tibbitts (Editor), Proceedings international lighting in controlled environments workshop. National Aeronautics and Space Administration, , Ames Research Station, Moffett Field, CA., pp. 113-124.

Caldwell, M.M. and Flint, S.D., 1997. Uses of biological spectral weighting functions and the need of scaling for the ozone reduction problem. Plant Ecology, 128(1/2): 66-76.

Carbone, M.S., Winston, G.C. and Trumbore, S.E., 2008. Soil respiration in perennial grass and shrub ecosystems: Linking environmental controls with plant and microbial sources on seasonal and diel timescales. Journal of Geophysical Research-Biogeosciences, 113(G02022, doi:10.1029/2007JG000611).

Chapin, F. et al., 2006. Reconciling carbon-cycle concepts, terminology, and methods. Ecosystems, 9(7): 1041-1050.

Charman, D., 2002. Peatlands and environmental change. Wiley.

Chen, S., Lin, G., Huang, J. and He, M., 2008. Responses of soil respiration to simulated precipitation pulses in semiarid steppe under different grazing regimes. Journal of Plant Ecology, 1(4): 237-246.

Choi, S. et al., 2008. Ionization spectroscopy of conformational isomers of propanal: the origin of the conformational preference. The Journal of Physical Chemistry A, 112(23): 5060-5063.

Christen, A., 2005. Impact for the LICOR 7500 lag correction on field data sampled 2000-2003 at the University of Basel. Institute of Meteorology, Climatology and Remote Sensing. University of Basel, pp. 4, http://pages.unibas.ch/geo/mcr/Projects/BUBBLE/docs/7500note.pdf.

Christensen, P.A., Dilks, A., Egerton, T.A. and Temperley, J., 1999. Infrared spectroscopic evaluation of the photodegradation of paint. Part I: The UV degradation of acrylic films pigmented with titanium dioxide. Journal of Materials Science, 34(23): 5689-5700.

Clarkson, B. and Fergie, S., 2002. The challenge of restoring a Waikato peat bog, Wet & Wild, Newsletter of the National Wetland Trust. National Wetland Trust of New Zealand, pp. 3.

Clymo, R.S., 1984. The limits to peat bog growth. Philosophical Transactions of the Royal Society of London.Series B, Biological Sciences, 303(1117): 605-654.

Coleman, K. and Jenkinson, D.S., 2008. ROTHC - 26.3: A model for the turnover of carbon in soil. Model description and windows user guide. ISBN 0 951 4456 8 5, Rothamsted Research, Harpenden, Herts.

Conant, R.T. et al., 2008. Sensitivity of organic matter decomposition to warming varies with its quality. Global Change Biology, 14(4): 868-877.

Convey, P. et al., 2002. Response of Antarctic terrestrial microarthropods to long-term climate manipulations. Ecology, 83(11): 3130-3140.

Cory, R.M., Powers, H., McDowell, N. and Rahn, T., 2008. Photodegradation of leaf litter in water-limited ecosystems, Fall Meeting AGU, Abstract B21E-04.

Cotrufo, M.F., Piermatteo, D., Marzaioli, F. and Ngao, J., 2008. Leaf litter decomposition process in forest ecosystem: A comparison of methods, 93rd ESA Annual Meeting, Milwaukee.

Cui, X. et al., 2008. Diurnal and seasonal variations of UV radiation on the northern edge of the Qinghai-Tibetan Plateau. Agricultural and Forest Meteorology, 148(1): 144-151.

Culf, A.D., Foken, T. and Gash, J.H.C., 2004. The energy balance closure problem. In: P. Kabat, M. Claussen and P.A. Dirmeyer (Editors), Vegetation, water, humans and the climate. A new perspective on an interactive system. Springer, Berlin, Heidelberg, pp. 159-166.

Dalias, P., Anderson, J.M., Bottner, P. and Coûteaux, M.-M., 2001. Temperature responses of carbon mineralization in conifer forest soils from different regional climates incubated under standard laboratory conditions. Global Change Biology, 7(2): 181-192.

Davidson, E.A., Belk, E. and Boone, R.D., 1998. Soil water content and temperature as independent or confounded factors controlling soil respiration in a temperate mixed hardwood forest. Global Change Biology, 4(2): 217-227.

Davidson, E.A. and Janssens, I.A., 2006. Temperature sensitivity of soil carbon decomposition and feedbacks to climate change. Nature, 440(7081): 165-173.

Davidson, E.A., Janssens, I.A. and Luo, Y., 2006a. On the variability of respiration in terrestrial ecosystems: moving beyond Q_{10}. Global Change Biology, 12(2): 154-164.

Davidson, E.A., Savage, K.E., Trumbore, S.E. and Borken, W., 2006b. Vertical partitioning of CO_2 production within a temperate forest soil. Global Change Biology, 12(6): 944-956.

Davidson, E.A., Savage.K, Verchot, L.V. and Navarro, R., 2002. Minimizing artifacts and biases in chamber-based measurements of soil respiration. Agricultural and Forest Meteorology, 113: 21-37.

Davidson, E.A., Verchot, L.V., Cattânio, J.H., Ackerman, I.L. and Carvalho, J.E.M., 2000. Effects of soil water content on soil respiration in forests and cattle pastures of eastern Amazonia. Biogeochemistry, 48(1): 53-69.

Day, T.A., Vogelmann, T.C. and DeLucia, E.H., 1992. Are Some Plant Life Forms More Effective than Others in Screening out Ultraviolet-B Radiation? Oecologia, 92(4): 513-519.

Day, T.A., Zhang, E.T. and Ruhland, C.T., 2007. Exposure to solar UV-B radiation accelerates mass and lignin loss of *Larrea tridentata* litter in the Sonoran Desert. Plant Ecology, 193(2): 185-194.

DeLucia, E.H., Day, T.A. and Vogelman, T.C., 1992. Ultraviolet-B and visible light penetration into needles of two species of subalpine conifers during foliar development. Plant, Cell and Environment, 15(8): 921-929.

Denmead, O.T., 1983. Micrometeorological methods for measuring gaseous losses of nitrogen in the field. In: J.R. Freney and J.R. Simpson (Editors),

Gaseous Loss of Nitrogen from Plant-Soil Systems. Martinus Nijhoff The Hague, pp. 133-157.

Denmead, O.T. and Raupach, M.R., 1993. Methods for measuring atmospheric gas transport in agricultural and forest systems. In: J.M. Duxbury, L.A. Harper, A.R. Mosier and D.E. Rolston (Editors), Agricultural ecosystem effects on trace gases and global climate change. American Society of Agronomy, Madison, pp. 19-43.

Denward, C.M.T. and Tranvik, L.J., 1998. Effects of solar radiation on aquatic macrophyte litter decomposition. Oikos, 82(1): 51-58.

Derbyshire, H., Miller, E. and Turkulin, H., 1997. Investigations into the photodegradation of wood using microtensile testing. European Journal of Wood and Wood Products, 55(5): 287-291.

Desai, A.R. et al., 2008. Cross-site evaluation of eddy covariance GPP and RE decomposition techniques. Agricultural and Forest Meteorology, 148(6-7): 821-838.

Dirks, I., Navon, Y., Kanas, D., Dumbur, R. and Grünzweig, J.M., 2010. Atmospheric water vapor as driver of litter decomposition in Mediterranean shrubland and grassland during rainless seasons. Global Change Biology: Accepted Article. doi: 10.1111/j.1365-2486.2010.02172.x.

Dorrepaal, E. et al., 2009. Carbon respiration from subsurface peat accelerated by climate warming in the subarctic. Nature, 460(7255): 616-619.

Drewitt, G.B. et al., 2002. Measuring forest floor CO_2 fluxes in a Douglas-fir forest. Agricultural and Forest Meteorology, 110(4): 299-317.

Duan, Z. and Sun, R., 2003. An improved model calculating CO_2 solubility in pure water and aqueous NaCl solutions from 273 to 533 K and from 0 to 2000 bar. Chemical Geology, 193(3-4): 257-271.

Dugas, W.A., 1993. Micrometeorological and chamber measurements of CO_2 flux from bare soil. Agricultural and Forest Meteorology, 67: 115-128.

Duguay, K.J. and Klironomos, J.N., 2000. Direct and indirect effects of enhanced UV-B radiation on the decomposing and competitive abilities of saprobic fungi. Applied Soil Ecology, 14(2): 157-164.

Emmerich, W.E., 2003. Carbon dioxide fluxes in a semiarid environment with high carbonate soils. Agricultural and Forest Meteorology, 116(1-2): 91-102.

Eriksen, J. and Jensen, L.S., 2001. Soil respiration, nitrogen mineralization and uptake in barley following cultivation of grazed grasslands. Biology and Fertility of Soils, 33(2): 139-145.

Falge, E. et al., 2001a. Gap filling strategies for defensible annual sums of net ecosystem exchange. Agricultural and Forest Meteorology, 107: 43-69.

Falge, E. et al., 2001b. Gap filling strategies for long term energy flux data sets. Agricultural and Forest Meteorology, 107: 71-77.

Falge, E. et al., 2002. Seasonality of ecosystem respiration and gross primary production as derived from FLUXNET measurements. Agricultural and Forest Meteorology, 113(1-4): 53-74.

Fang, C. and Moncrieff, J.B., 1996. Simple and fast technique to measure CO_2 profiles in soil. Soil Biology & Biochemistry, 30(14): 2107-2112.

Fang, C. and Moncrieff, J.B., 1999. A model for soil CO_2 production and transport 1: Model development. Agricultural and Forest Meteorology, 95(4): 225-236.

Fang, C. and Moncrieff, J.B., 2001. The dependence of soil CO_2 efflux on temperature. Soil Biology and Biochemistry, 33(2): 155-165.

Fang, C., Smith, P., Moncrieff, J.B. and Smith, J.U., 2005. Similar response of labile and resistant soil organic matter pools to changes in temperature. Nature, 433(7021): 57-59.

Feigenwinter, C., Bernhofer, C. and Vogt, R., 2004. The influence of advection on the short term CO_2-budget in and above a forest canopy. Boundary-Layer Meteorology, 113(2): 201-224.

Feister, U. and Grewe, R., 1995. Spectral albedo measurements in the UV and visible region over different types of surfaces. Photochemistry and Photobiology, 62: 736-744.

Fernando, S.S., Christensen, P.A., Egerton, T.A. and White, J.R., 2009. Humidity dependence of carbon dioxide generation during photodegradation of biaxially oriented polypropylene in oxygen. Polymer Degradation and Stability, 94(1): 83-89.

Fierer, N., Allen, A.S., Schimel, J.P. and Holden, P.A., 2003. Controls on microbial CO_2 production: a comparison of surface and subsurface soil horizons. Global Change Biology, 9(9): 1322-1332.

Fierer, N., Chadwick, O.A. and Trumbore, S.E., 2005a. Production of CO_2 in soil profiles of a California annual grassland. Ecosystems, 8(4): 412-429.

Fierer, N., Craine, J.M., McLauchlan, K. and Schimel, J.P., 2005b. Litter quality and the temperature sensitivity of decomposition. Ecology, 86(2): 320-326.

Fierer, N. and Schimel, J.P., 2003. A proposed mechanism for the pulse in carbon dioxide production commonly observed following the rapid rewetting of a dry soil. Soil Science Society of America Journal, 67(3): 798-805.

Finnigan, J.J., Clement, R., Malhi, Y., Leuning, R. and Cleugh, A.H., 2003. A re-evaluation of long-term flux measurement techniques part I: averaging and coordinate rotation. Boundary Layer Meteorology, 107(1): 1-48.

Flint, S.D. and Caldwell, M.M., 2003. Field testing of UV biological spectral weighting functions for higher plants. Physiologia Plantarum, 117(1): 145-153.

Flint, S.D., Ryel, R.J. and Caldwell, M.M., 2003. Ecosystem UV-B experiments in terrestrial communities: a review of recent findings and methodologies. Agricultural and Forest Meteorology, 120(1-4): 177-189.

Foken, T. et al., 2004. Post-field data quality control. In: X. Lee, W. Massman and B. Law (Editors), Handbook of micrometeorology; A guide for surface flux measurement and analysis. Atmospheric and oceanographic sciences library. Kluwer Academic Publisher, Dordrecht, The Netherlands, pp. 181-208.

Fontaine, S. et al., 2007. Stability of organic carbon in deep soil layers controlled by fresh carbon supply. Nature, 450(7167): 277-280.

Fontaine, S., Mariotti, A. and Abbadie, L., 2003. The priming effect of organic matter: a question of microbial competition? Soil Biology and Biochemistry, 35(6): 837-843.

Freeman, C., Lock, M.A. and Reynolds, B., 1993. Fluxes of CO_2 , CH_4 and N_2O from a Welsh peatland following simulation of water table draw-down: Potential feedback of climatic change. Biochemistry, 19: 51-60.

Friedlingstein, P. et al., 2006. Climate-carbon cycle feedback analysis: results from the C_4MIP model intercomparison. Journal of Climate, 19(14): 3337-3353.

Gallo, M.E., Porras-Alfaro, A., Odenbach, K.J. and Sinsabaugh, R.L., 2009. Photoacceleration of plant litter decomposition in an arid environment. Soil Biology and Biochemistry, 41(7): 1433-1441.

Gallo, M.E., Sinsabaugh, R.L. and Cabaniss, S.E., 2006. The role of ultraviolet radiation in litter decomposition in arid ecosystems. Applied Soil Ecology, 34(1): 82-91.

Gaumont-Guay, D. et al., 2006. Interpreting the dependence of soil respiration on soil temperature and water content in a boreal aspen stand. Agricultural and Forest Meteorology, 140(1-4): 220-235.

Gehrke, C., Johanson, U., Callaghan, T.V., Chadwick, D. and Robinson, C.H., 1995. The impact of enhanced ultraviolet-B radiation on litter quality and decomposition processes in *Vaccinium* leaves from the subarctic. Oikos, 72(2): 213-222.

Geissbühler, P., Siegwolf, R. and Eugster, W., 2000. Eddy covariance measurements on mountain slopes: the advantage of surface-normal sensor orientation over a vertical set-up. Boundary-Layer Meteorology, 96(3): 371-392.

George, B., Suttie, E., Merlin, A. and Deglise, X., 2005. Photodegradation and photostabilisation of wood - the state of the art. Polymer Degradation and Stability, 88(2): 268-274.

Giardina, C.P. and Ryan, M.G., 2000. Evidence that decomposition rates of organic carbon in mineral soil do not vary with temperature. Nature, 404(6780): 858-861.

Gilmanov, T.G. et al., 2007. Partitioning European grassland net ecosystem CO_2 exchange into gross primary productivity and ecosystem respiration using light response function analysis. Agriculture, Ecosystems & Environment, 121(1-2): 93-120.

Glatzel, S., Basiliko, N. and Moore, T., 2004. Carbon dioxide and methane production potentials of peats from natural, harvested, and restored sites, eastern Quebec, Canada. Wetlands, 24(2): 261-267.

Glatzel, S., Lemke, S. and Gerold, G., 2006. Short-term effects of an exceptionally hot and dry summer on decomposition of surface peat in a restored temperate bog. European Journal of Soil Biology, 42(4): 219-229.

Gorham, E., 1991. Northern peatlands: Role in the global carbon cycle and probable responses to global warming. Ecological Applications, 1(2): 182-195.

Goulden, M.L., Munger, J.W., Fan, S.M., Daube, B.C. and Wofsy, S.C., 1996. Measurements of carbon sequestration by long-term eddy covariance: methods and a critical evaluation of accuracy. Global Change Biology, 2: 169-182.

Graf, A. et al., 2008. Measurement depth effects on the apparent temperature sensitivity of soil respiration in field studies. Biogeosciences, 5(4): 1175-1188.

Grant, I.F., Prata, A.J. and Cechet, R.P., 2000. The impact of the diurnal variation of albedo on the remote sensing of the daily mean albedo of grassland. Journal of Applied Meteorology, 39(2): 234-244.

Grelle, A. and Burba, G., 2007. Fine-wire thermometer to correct CO_2 fluxes by open-path analyzers for artificial density fluctuations. Agricultural and Forest Meteorology, 147(1-2): 48-57.

Gu, L. et al., 2005. Objective threshold determination for nighttime eddy flux filtering. Agricultural and Forest Meteorology, 128(3-4): 179-197.

Gu, L., Post, W.M. and King, A.W., 2004. Fast labile carbon turnover obscures sensitivity of heterotrophic respiration from soil to temperature: A model analysis. Global Biogeochemical Cycles, 18, GB1022, doi:10.1029/2003GB002119.

Ham, J.M. and Heilman, J.L., 2003. Experimental test of density and energy-balance corrections on carbon dioxide flux as measured using open-path eddy covariance. Agronomy Journal, 95(6): 1393-1403.

Hamada, Y. and Tanaka, T., 2001. Dynamics of carbon dioxide in soil profiles based on long-term field observation. Hydrological Processes, 15(10): 1829-1845.

Hanson, P.J., Edwards, N.T., Garten, C.T. and Andrews, J.A., 2000. Separating root and soil microbial contributions to soil respiration: A review of methods and observations. Biogeochemistry, 48(1): 115-146.

Harden, J.W. et al., 2000. The role of fire in the boreal carbon budget. Global Change Biology, 6(S1): 174-184.

Hartley, I.P. and Ineson, P., 2008. Substrate quality and the temperature sensitivity of soil organic matter decomposition. Soil Biology and Biochemistry, 40(7): 1567-1574.

Haslwanter, A., Hammerle, A. and Wohlfahrt, G., 2008. Open-path vs. closed-path eddy covariance measurements of the net ecosystem carbon dioxide and water vapour exchange: A long-term perspective. Agricultural and Forest Meteorology, 149(2): 291-302.

Henry, H.A.L., Brizgys, K. and Field, C.B., 2008. Litter decomposition in a California annual grassland: Interactions between photodegradation and litter layer thickness. Ecosystems, 11(4): 545-554.

Heusinkveld, B.G., Jacobs, A.F.G. and Holtslag, A.A.M., 2008. Effect of open-path gas analyzer wetness on eddy covariance flux measurements: A proposed solution. Agricultural and Forest Meteorology, 148(10): 1563-1573.

Hibbard, K.A., Law, B.E., Reichstein, M. and Sulzman, J., 2005. An analysis of soil respiration across northern hemisphere temperate ecosystems. Biogeochemistry, 73(1): 29-70.

Hirano, T., Kim, H. and Tanaka, Y., 2003. Long-term half-hourly measurement of soil CO_2 concentration and soil respiration in a temperate deciduous forest. Journal of Geophysical Research, 108(D20): 4631, doi:10.1029/2003JD003766.

Hirata, R. et al., 2007. Seasonal and interannual variations in carbon dioxide exchange of a temperate larch forest. Agricultural and Forest Meteorology, 147(3-4): 110-124.

Hogg, E.H., Lieffers, V.J. and Wein, R.W., 1992. Potential carbon losses from peat profiles: effects of temperature, drought cycles and fire. Ecological Applications, 2(3): 298-306.

Hollinger, D.Y. and Richardson, A.D., 2005. Uncertainty in eddy covariance measurements and its application to physiological models. Tree Physiology, 25: 873-885.

Horst, T.W. and Weil, J.C., 1992. Footprint estimation for scalar flux measurements in the atmospheric surface layer. Boundary - Layer Meteorology, 59: 279-296.

Hutyra, L.R. et al., 2008. Resolving systematic errors in estimates of net ecosystem exchange of CO_2 and ecosystem respiration in a tropical forest biome. Agricultural and Forest Meteorology, 148(8-9): 1266-1279.

Huxman, T.E. et al., 2004. Precipitation pulses and carbon fluxes in semiarid and arid ecosystems. Oecologia, 141(2): 254-268.

Immirzi, C.P., Maltby, E. and Clymo, R.S., 1992. The global status of peatlands and their role in carbon cycling. A report for Friends of the Earth by the Wetland Ecosystem Research Group, Dept Geography, University of Exeter. Friends of the Earth, London.

IPCC, 2007. Summary for Policymakers. In: S. Solomon et al. (Editors), Climate Change 2007: The physical science basis. Contribution of Working Group I to the Fourth Assessment Report of the Intergovernmental Panel on Climate Change. Cambridge University Press, Cambridge, United Kingdom and New York, NY, USA, pp. 18.

Iqbal, M., 1983. An introduction to solar radiation Academic Press, Ontario, 390 pp.

J. Curiel, Y. et al., 2007. Microbial soil respiration and its dependency on carbon inputs, soil temperature and moisture. Global Change Biology, 13(9): 2018-2035.

Janssens, I.A. et al., 2001. Productivity overshadows temperature in determining soil and ecosystem respiration across European forests. Global Change Biology, 7: 269-278.

Janssens, I.A. and Pilegaard, K., 2003. Large seasonal changes in Q_{10} of soil respiration in a beech forest. Global Change Biology, 9(6): 911-918.

Janzen, H.H., 2004. Carbon cycling in earth systems - a soil science perspective. Agriculture, Ecosystems & Environment, 104: 399-417.

Jarvis, P. et al., 2007. Drying and wetting of Mediterranean soils stimulates decomposition and carbon dioxide emission: the "Birch effect". Tree Physiology, 27: 929-940.

Jassal, R. et al., 2005. Relationship between soil CO_2 concentrations and forest-floor CO_2 effluxes. Agricultural and Forest Meteorology, 130(3-4): 176-192.

Jassal, R.S. et al., 2004. A model of the production and transport of CO_2 in soil: predicting soil CO_2 concentrations and CO_2 efflux from a forest floor. Agricultural and Forest Meteorology, 124(3-4): 219-236.

Jassal, R.S., Black, T.A., Novak, M.D., Gaumont-Guay, D. and Nesic, Z., 2008. Effect of soil water stress on soil respiration and its temperature sensitivity in an 18-year-old temperate Douglas-fir stand. Global Change Biology, 14(6): 1305-1318.

Jauhiainen, J., Takahashi, H., Heikkinen, J.E.P., Martikainen, P.J. and Vasander, H., 2005. Carbon fluxes from a tropical peat swamp forest floor. Global Change Biology, 11(10): 1788-1797.

Jenkinson, D.S., Andrew, S.P.S., Lynch, J.M., Goss, M.J. and Tinker, P.B., 1990. The turnover of organic carbon and nitrogen in soil. Philosophical Transactions: Biological Sciences, 329(1255): 361-368.

Jin, X., Wang, S. and Zhou, Y., 2008. Microbial CO_2 production from surface and subsurface soil as affected by temperature, moisture, and nitrogen fertilisation. Australian Journal of Soil Research, 46(3): 273-280.

Jobbagy, E.G. and Jackson, R.B., 2000. The vertical distribution of soil organic carbon and its relation to climate and vegetation. Ecological Applications, 10(2): 423-436.

Jones, C.D., Cox, P. and Huntingford, C., 2003. Uncertainty in climate-carbon-cycle projections associated with the sensitivity of soil respiration to temperature. Tellus, 55B(2): 642-648.

Joosten, H. and Clarke, D., 2002. Wise use of mires and peatlands - background and principles including a framework for decision-making. International Mire Conservation Group and International Peat Society, Saarijärvi, Finland, 302 pp.

Kabwe, L.K., Farrell, R.E., Carey, S.K., Hendry, M.J. and Wilson, G.W., 2005. Characterizing spatial and temporal variations in CO_2 fluxes from ground surface using three complimentary measurement techniques. Journal of Hydrology, 311(1-4): 80-90.

Kakani, V.G., Reddy, K.R., Zhao, D. and Sailaja, K., 2003. Field crop responses to ultraviolet-B radiation: a review. Agricultural and Forest Meteorology, 120(1-4): 191-218.

Karberg, N.J., Scott, N.A. and Giardina, C.P., 2008. Methods for estimating litter decomposition. In: C.M. Hoover (Editor), Field measurements for forest carbon monitoring. Springer Netherlands, pp. 103-111.

Katagi, T., 2004. Photodegradation of pesticides on plant and soil surfaces. Reviews of Environmental Contamination and Toxicology, 182: 1-189.

Kechavarzi, C., Dawson, Q., Bartlett, M. and Leeds-Harrison, P.B., 2010. The role of soil moisture, temperature and nutrient amendment on CO_2 efflux from agricultural peat soil microcosms. Geoderma, 154(3-4): 203-210.

Kelly, G.B. and Williams, J.C., 1981. Inhibition of light sensitivity of papers treated with diethyl zinc, Preservation of Paper and Textiles of Historic and Artistic Value II. Advances in Chemistry. American Chemical Society, Washington, D. C., pp. 109-117.

Khomik, M., Arain, M.A., Liaw, K.-L. and McCaughey, J.H., 2009. Debut of a flexible model for simulating soil respiration-soil temperature relationship: Gamma model. Journal of Geophysical Research, 114(G03004): doi:10.1029/2008JG000851.

Khomik, M., Arain, M.A. and McCaughey, H., 2006. Temporal and spatial variability of soil respiration in a boreal mixedwood forest. Agricultural and Forest Meteorology, 140(1-4): 244-256.

Khriachtchev, L., Maçôas, E., Pettersson, M. and Räsänen, M., 2002. Conformational memory in photodissociation of formic acid. Journal of the American Chemical Society, 124(37): 10994-10995.

Kieber, R.J., Zhou, X. and Mopper, K., 1990. Formation of carbonyl compounds from UV-induced photodegradation of humic substances in natural waters: Fate of riverine carbon in the sea. Limnology and Oceanography, 35(7): 1503-1515.

Kirschbaum, M.U.F., 1995. The temperature dependence of soil organic matter decomposition, and the effect of global warming on soil organic C storage. Soil Biology and Biochemistry, 27(6): 753-960.

Kirschbaum, M.U.F., 2000. Will changes in soil organic carbon act as a positive or negative feedback on global warming? Biogeochemistry, 48(1): 21-51.

Kirschbaum, M.U.F., 2004. Soil respiration under prolonged soil warming: are rate reductions caused by acclimation or substrate loss? Global Change Biology, 10(11): 1870-1877.

Kirschbaum, M.U.F., 2006. The temperature dependence of organic-matter decomposition -still a topic of debate. Soil Biology and Biochemistry, 38(9): 2510-1518.

Kirschbaum, M.U.F., 2009. The temperature dependence of organic matter decomposition: seasonal temperature variations turn a sharp short-term temperature response into a more moderate annually-averaged response. Global Change Biology, "Accepted Article"; doi: 10.1111/j.1365-2486.2009.02093.x.

Kirschbaum, M.U.F., Oct 2009. Detailed description of CenW 3.1, pp. 30, http://www.kirschbaum.id.au/CenW_equations.pdf, accessed Feb 2009.

Kirschbaum, M.U.F. et al., 2007. Modelling net ecosystem carbon and water exchange of a temperate Eucalyptus *delegatensis* forest using multiple constraints. Agricultural and Forest Meteorology, 145(1-2): 48-68.

Kisselle, K.W. et al., 2002. Seasonal soil fluxes of carbon monoxide in burned and unburned Brazilian savannas. Journal of Geophysical Research - Atmospheres, 107(8051): doi:10.1029/2001JD000638

Klán, P. and Wirz, J., 2009. Photochemistry of organic compounds: from concepts to practice. John Wiley & Sons Ltd., West Sussex, 563 pp.

Klavins, M., Sire, J., Purmalis, O. and Melecis, V., 2008. Approaches to estimating humification indicators for peat, Mires and peat, Volume 3, http://www.mires-and-peat.net/. International Mire Conservation Group and International Peat Society.

Knorr, W., Prentice, I.C., House, J.I. and Holland, E.A., 2005. Long-term sensitivity of soil carbon turnover to warming. Nature, 433(7023): 298-301.

Kominami, Y., Miyama, T., Tamai, K., Nobuhiro, T. and Goto, Y., 2003. Characteristics of CO_2 flux over a forest on complex topography. Tellus B, 55: 313-321.

Kondo, F. and Tsukamoto, O., 2008. Evaluation of Webb correction on CO_2 flux by eddy covariance technique using open-path gas analyzer over asphalt surface. Journal of Agricultural Meteorology, 64: 1-8.

Kowalski, A.S., 2006. Further comment on "Reply to the comment by Kowalski on 'An alternative approach for CO_2 flux correction caused by heat and water vapour transfer' by Liu". Boundary-Layer Meteorology, 120(2): 365-366.

Kowalski, A.S. and Serrano-Ortiz, P., 2007. On the relationship between the eddy covariance, the turbulent flux, and surface exchange for a trace gas such as CO_2. Boundary-Layer Meteorology, 124(2): 129-141.

Kowalski, A.S. et al., 2008. Can flux tower research neglect geochemical CO_2 exchange? Agricultural and Forest Meteorology, 148(6-7): 1045-1054.

Kroon, P., Hensen, A., van den Bulk, W., Jongejan, P. and Vermeulen, A., 2008. The importance of reducing the systematic error due to non-linearity in N_2O flux measurements by static chambers. Nutrient Cycling in Agroecosystems, 82(2): 175-186.

Kuehn, K.A., Steiner, D. and Gessner, M.O., 2004. Diel mineralization patterns of standing-dead plant litter: implications for CO_2 flux from wetlands. Ecology, 85(9): 2504-2518.

Kurz-Besson, C., Coûteaux, M.-M., Thiéry, J.M., Berg, B. and Remacle, J., 2005. A comparison of litterbag and direct observation methods of Scots pine needle decomposition measurement. Soil Biology and Biochemistry, 37(12): 2315-2318.

Kuske, T.J., 2009. Fluxes of energy and water vapour from grazed pasture on an mineral soil in the Waikato, University of Waikato, Hamilton, 152 pp.

Kuzyakov, Y., 2006. Sources of CO_2 efflux from soil and review of partitioning methods. Soil Biology and Biochemistry, 38(3): 425-448.

Laiho, R., 2006. Decomposition in peatlands: Reconciling seemingly contrasting results on the impacts of lowered water levels. Soil Biology & Biochemistry, 38(8): 2011-2024.

Laine, A. et al., 2006. Estimating net ecosystem exchange in a patterned ecosystem: Example from blanket bog. Agricultural and Forest Meteorology, 138(1-4): 231-243.

Lal, R., 2004. Carbon sequestration in dryland ecosystems Environmental Management, 33: 528-544.

Lappalainen, E., 1996. General review on world peatland and peat resources. In: E. Lappalainen (Editor), Global Peat Resources. International Peat Society, Saarijärven, pp. 53.

Lasslop, G. et al., 2009. Separation of net ecosystem exchange into assimilation and respiration using a light response curve approach: critical issues and global evaluation. Global Change Biology, 16(1): 187-208.

Laubach, J. and Teichmann, U., 1999. Surface energy budget variability: a case study over grass with special regard to minor inhomogeneities in the source area. Theoretical and Applied Climatology, 62(1-2): 9-24.

Lavelle, P. and Martin, A., 1992. Small-scale and large-scale effects of endogeic earthworms on soil organic matter dynamics in soils of the humid tropics. Soil Biology and Biochemistry, 24(12): 1491-1498.

Lavigne, M.B. et al., 1997. Comparing nocturnal eddy covariance measurements to estimates of ecosystem respiration made by scaling chamber measurements at six coniferous boreal sites. Journal of Geophysical Research, 102(D24): 28977-28985.

Law, B.E. et al., 2001. Spatial and temporal variation in respiration in a young ponderosa pine forest during a summer drought. Agricultural and Forest Meteorology, 110(1): 27-43.

Law, B.E., Ryan, M.G. and Anthoni, P.M., 1999. Seasonal and annual respiration of a ponderosa pine ecosystem. Global Change Biology, 5(2): 169-182.

Le Mer, J. and Roger, P., 2001. Production, oxidation, emission and consumption of methane by soils: A review. European Journal of Soil Biology, 37(1): 25-50.

Lee, X., Finnigan, J. and Paw U, K.T., 2004. Coordinate systems and flux bias error. In: X. Lee, W. Massman and B. Law (Editors), Handbook of Micrometeorology - A guide for surface flux measurement and analysis. Atmospheric and oceanographic sciences library. Kluwer Academic Publishers, Dordrecht, pp. 250.

Leinweber, P., Jandl, G., Baum, C., Eckhardt, K.U. and Kandeler, E., 2008. Stability and composition of soil organic matter control respiration and soil enzyme activities. Soil Biology & Biochemistry, 40(6): 1496-1505.

Leuning, R., 2004. Measurements of trace gas fluxes in the atmosphere using eddy covariance: WPL corrections revisited. In: X. Lee, W. Massman and B. Law (Editors), Handbook of micrometeorology; A guide for surface flux measurement and analysis. Atmospheric and oceanographic sciences library. Kluwer Academic Publisher, Dordrecht, The Netherlands, pp. 119-132.

Leuning, R., 2007. The correct form of the Webb, Pearman and Leuning equation for eddy fluxes of trace gases in steady and non-steady state, horizontally homogeneous flows. Boundary-Layer Meteorology, 123(2): 263-267.

Leuning, R., Denmead, O.T., Lang, A.R.G. and Ohtaki, E., 1982. Effects of heat and water vapor transport on eddy covariance measurement of CO_2 fluxes. Boundary - Layer Meteorology, 23: 209-222.

Leuning, R. and Judd, M.J., 1996. The relative merits of open- and closed-path analysers for measurement of eddy fluxes. Global Change Biology, 2: 241-253.

Leuning, R. and King, K.M., 1992. Comparison of eddy-covariance measurements of CO_2 fluxes by open-and closed-path CO_2 analysers. Boundary-Layer Meteorology, 59: 297-311.

Liski, J., Ilvesniemi, H., Mäkelä, A. and Westman, C.J., 1999. CO_2 emissions from soil in response to climatic warming are overestimated: the decomposition of old soil organic matter is tolerant of temperature. Ambio, 28(2): 171-174.

Liu, H., 2006. Reply to the comment by Kowalski on "An alternative approach for CO_2 flux correction caused by heat and water vapour transfer". Boundary-Layer Meteorology, 120(2): 357-363.

Liu, H.P., 2005. An alternative approach for CO_2 flux correction caused by heat and water vapour transfer. Boundary-Layer Meteorology, 115(1): 151-168.

Liu, H.P., Randerson, J.T., Lindfors, J., Massman, W.J. and Foken, T., 2006. Consequences of incomplete surface energy balance closure for CO_2 fluxes from open-path CO_2/H_2O infrared gas analysers. Boundary-Layer Meteorology, 120(1): 65-85.

Liu, Q., Callaghan, T. and Zuo, Y., 2004. Effects of elevated solar UV-B radiation from ozone depletion on terrestrial ecosystems. Journal of Mountain Science, 1(3): 276-288.

Liu, X., Wan, S., Su, B., Hui, D. and Luo, Y., 2002. Response of soil CO_2 efflux to water manipulation in a tallgrass prairie ecosystem. Plant And Soil, 240(2): 213-223.

Livingston, G.P. and Hutchinson, G.L., 1995. Enclosure-based measurement of trace gas exchange: applications and sources of error. In: P.A. Matson and R.C. Harriss (Editors), Biogenic trace gases: measuring emissions from soil and water. Blackwell Science, Cambridge, pp. 14-51.

Lloyd, J. and Taylor, J.A., 1994. On the temperature dependence of soil respiration. Functional Ecology, 8: 315-323.

Loescher, H.W. et al., 2006. Uncertainties in, and interpretation of, carbon flux estimates using the eddy covariance technique. Journal of Geophysical Research-Atmospheres, 111(D21): S2190-S2190.

Luo, Y. and Zhou, X., 2006. Soil respiration and the environment. Academic Press/Elsevier, San Diego, CA, 316 pp.

Luyssaert, S. et al., 2007. CO_2 balance of boreal, temperate, and tropical forests derived from a global database. Global Change Biology, 13(12): 2509-2537.

Luyssaert, S. et al., 2009. Toward a consistency cross-check of eddy covariance flux-based and biometric estimates of ecosystem carbon balance. Global Biogeochemical Cycles, 23(GB3009): doi:10.1029/2008GB003377.

Ma, S., Baldocchi, D.D., Xu, L. and Hehn, T., 2007. Inter-annual variability in carbon dioxide exchange of an oak/grass savanna and open grassland in California. Agricultural and Forest Meteorology, 147(3-4): 157-171.

Mackay, W.P., Silva, S., Lightfoot, D.C., Pagani, M.I. and Whitford, W.G., 1986. Effect of increased soil moisture and reduced soil temperature on a desert soil arthropod community. American Midland Naturalist, 116(1): 45-56.

Madronich, S., 1993. The atmosphere and UV-B radiation at ground level. In: A.R. Young, L.O. Björn, J. Moan and W. Nultsch (Editors), Environmental UV Photobiology. Plenum Press, New York, pp. 1-39.

Madronich, S., McKenzie, R.L., Björn, L.O. and Caldwell, M.M., 1998. Changes in biologically active ultraviolet radiation reaching the Earth's surface. Journal of Photochemistry and Photobiology B: Biology, B46(1-3): 5-19.

Maljanen, M., Martikainen, P.J., Aaltonen, H. and Silvola, J., 2002. Short-term variation in fluxes of carbon dioxide, nitrous oxide and methane in cultivated and forested organic boreal soils. Soil Biology & Biochemistry, 34(5): 577-584.

Maltby, E. and Immirzi, P., 1993. Carbon dynamics in peatlands and other wetland soils regional and global perspectives. Chemosphere, 27(6): 999-1023.

Maltby, E. and Proctor, M.C.F., 1996. Peatlands: their nature and role in the biosphere. In: E. Lappalainen (Editor), Global Peat Resources. International Peat Society, Saarijärven, pp. 11.

Manning, P. et al., 2008. Direct and indirect effects of nitrogen deposition on litter decomposition. Soil Biology and Biochemistry, 40(3): 688-698.

Martikainen, P.J. and Lappalainen, E., 1996. The fluxes of greenhouse gases CO_2, CH_4 and N_2O in northern peatlands, Global Peat Resources. International Peat Society, Saarijärven, pp. 29-36.

Massman, W., 2004a. Concerning the measurement of atmospheric trace gas fluxes with open -and closed-path eddy covariance systems: the WPL terms and spectral attenuation. In: X. Lee, W. Massman and B. Law (Editors), Handbook of micrometeorology; A guide for surface flux measurement and analysis. Atmospheric and oceanographic sciences library. Kluwer Academic Publisher, Dordrecht, The Netherlands, pp. 133-160.

Massman, W., 2004b. Uncertainty in eddy covariance flux estimates resulting from spectral attenuation. In: X. Lee, W. Massman and B. Law (Editors), Handbook of micrometeorology; A guide for surface flux measurement and analysis. Atmospheric and oceanographic sciences library. Kluwer Academic Publisher, Dordrecht, The Netherlands, pp. 67-99.

Massman, W. and Tuovinen, J., 2006. An analysis and implications of alternative methods of deriving the density (WPL) terms for eddy covariance flux measurements. Boundary-Layer Meteorology, 121(2): 221-227.

Massman, W.J., 2000. A simple method for estimating frequency response corrections for eddy covariance systems. Agricultural and Forest Meteorology, 104(3): 185-198.

Massman, W.J. and Lee, X., 2002. Eddy covariance flux corrections and uncertainties in long-term studies of carbon and energy exchanges. Agricultural And Forest Meteorology, 113(1-4): 121-144.

Mauder, M., 2004. Recent problems of turbulence sensors, 2nd QA/QC Workshop for Eddy Covariance Measurements, 18-19 Jan 2004, Spoleto, Italy, http://www.geo.uni-bayreuth.de/mikrometeorologie/QC_Workshop/2ndCARBOEUROPE_QAQC_Mauder.pdf, accesses March 2008.

Mayor, S. et al., 1988. Asymmetry in the diurnal variation of surface albedo. IEEE Transactions on Geoscience and Remote Sensing 35: 879-891.

McDermitt, D., 2003. Application note for LI-7500 customers about the timing error and power cable. LI-COR, Inc., pp. 5, http://www.geo.uni-bayreuth.de/mikrometeorologie/QAQC/ExplainationoftimingproblemLI-7500.pdf, accessed Feb 2008.

McKenzie, R., Connor, B. and Bodeker, G., 1999. Increased summertime UV radiation in New Zealand in response to ozone loss. Science, 285(5434): 1709-1711.

McLaren, R.G. and Cameron, K.C., 1996. Soil science - sustainable production and environmental protection. Oxford University Press, Auckland.

McLeod, A.R. and Newsham, K.K., 1997. Impacts of elevated UV-B on forest ecosystems. In: P.J. Lumsden (Editor), Plants and UV-B: Responses to environmental change. Society for Experimental Biology seminar series. Press Syndicate of the University of Cambridge, Cambridge, pp. 355.

McMillen, R.T., 1986. A BASIC Program for EC in non-simple terrain. NOAA Tech Memo ERL ARL-147.

McMillen, R.T., 1988. An eddy correlation technique with extended applicability to non-simple terrain. Boundary-Layer Meteorology, 43: 231-245.

McNeil, P. and Waddington, J.M., 2003. Moisture control on Sphagnum growth and CO_2 exchange on a cutover bog. Journal of Applied Ecology, 40: 354-367.

Meentemeyer, V., 1978. Macroclimate the lignin control of litter decomposition rates. Ecology, 59(3): 465-472.

Melillo, J.M. and Aber, J.D., 1982. Nitrogen and lignin control of hardwood leaf litter decomposition dynamics. Ecology, 63(3): 621-626.

Mielnick, P., Dugas, W.A., Mitchell, K. and Havstad, K., 2005. Long-term measurements of CO_2 flux and evapotranspiration in a Chihuahuan desert grassland. Journal of Arid Environments, 60(3): 423-436.

Moffat, A.M. et al., 2007. Comprehensive comparison of gap-filling techniques for eddy covariance net carbon fluxes. Agricultural and Forest Meteorology, 147(3-4): 209.

Moncrieff, J. et al., 2004. Averaging, detrending, and filtering of eddy covariance time series. In: X. Lee, W. Massman and B. Law (Editors), Handbook of micrometeorology; A guide for surface flux measurement and analysis. Atmospheric and oceanographic sciences library. Kluwer Academic Publisher, Dordrecht, The Netherlands, pp. 7-32.

Moncrieff, J.B., Malhi, Y. and Leuning, R., 1996. The propagation of errors in long-term measurements of land-atmosphere fluxes of carbon and water. Global Change Biology, 2: 231-240.

Montana, C., Ezcurra, B., Carillo, A. and Delhoume, J.P., 1988. The decomposition of litter in grasslands of northern Mexico: a comparison between arid and non-arid environments. Journal of Arid Environments, 14: 55-60.

Moody, S.A. et al., 2001. The direct effects of UV-B radiation on *Betula pubescens* litter decomposing at four European field sites. Plant Ecology, 154(1-2): 27-36.

Moore, C.J., 1986. Frequency response corrections for eddy correlation systems. Boundary Layer Meteorology, 37: 17-35.

Moore, T.R. and Dalva, M., 1993. The influence of temperature and water table position on carbon dioxide and methane emissions from laboratory columns of peatland soils. Journal of Soil Science, 44: 651-664.

Moore, T.R. and Dalva, M., 1997. Methane and carbon dioxide exchange potentials of peat soils in aerobic and anaerobic laboratory incubations. Soil Biology and Biochemistry, 29(8): 1157-1164.

Moore, T.R. and Knowles, R., 1989. The influence of water table levels on methane and carbon dioxide emissions from peatland soils. Canadian Journal of Soil Science, 69: 33-38.

Moore, T.R., Roulet, N.T. and Waddington, J.M., 1998. Uncertainty in predicting the effect of climatic change on the carbon cycling of Canadian peatlands. Climatic Change, 40(2): 229-245.

Moorhead, D.L. and Callaghan, T., 1994. Effects of increasing ultraviolet-B radiation on decomposition and soil organic-matter dynamics - a synthesis and modelling study. Biology and Fertility of Soils, 18(1): 19-26.

Moorhead, D.L. and Reynolds, J.F., 1989. The contribution of abiotic processes to buried litter decomposition in the northern Chihuahuan Desert. Oecologia, 79(1): 133-135.

Moorhead, D.L. and Sinsabaugh, R.L., 2006. A theoretical model of litter decay and microbial interaction. Ecological Monographs, 76(2): 151-174.

Moran, M.A. and Zepp, R.G., 1997. Role of photoreactions in the formation of biologically labile compounds from dissolved organic matter. Limnology and Oceanography, 42(6): 1307-1316.

Moyano, F.E., Kutsch, W.L. and Schulze, E.D., 2007. Response of mycorrhizal, rhizosphere and soil basal respiration to temperature and photosynthesis in a barley field. Soil Biology & Biochemistry, 39(4): 843-853.

Mudge, P., 2009. Annual carbon balance of an intensively grazed pasture: magnitude and controls, University of Waikato, Hamilton, 147 pp.

Nagy, L.A. and Macauley, B.J., 1982. Eucalyptus leaf-litter decomposition: Effects of relative humidity and substrate moisture content. Soil Biology and Biochemistry, 14(3): 233-236.

Newsham, K.K., Greenslade, P.D., Kennedy, V.H. and McLeod, A.R., 1999. Elevated UV-B radiation incident on *Quercus robur* leaf canopies enhances decomposition of resulting leaf litter in soil. Global Change Biology, 5(4): 403-409.

Newsham, K.K., McLeod, A.R., Roberts, J.D., Greemslade, P.D. and Emmett, B.A., 1997. Direct effects of elevated UV-B radiation on the decomposition of *Quercus robur* leaf litter. Oikos, 79: 592-602.

Nieveen, J.P., Campbell, D.I., Schipper, L.A. and Blair, I.J., 2005. Carbon exchange of grazed pasture on a drained peat soil. Global Change Biology, 11: 607-618.

NIWA, 2007. National Climate Database. National Institute of Water and Atmospheric Research, http://cliflo.niwa.co.nz/.

Norman, J.M., Garcia, R. and Verma, S.B., 1992. Soil surface CO_2 fluxes and the carbon budget of a grassland. Journal of Geophysical Research, 97(D17): 18,845-18,853.

Nykänen, H., Alm, J., Lang, K., Silvola, J. and Martikainen, P., 1995. Emissions of CH_4 , N_2O and CO_2 from a virgin fen and a fen drained for grassland in Finland. Journal of Biogeography, 22(2-3): 351-357.

Ohkubo, S., Kosugi, Y., Takanashi, S., Mitani, T. and Tani, M., 2007. Comparison of the eddy covariance and automated closed chamber methods for evaluating nocturnal CO_2 exchange in a Japanese cypress forest. Agricultural and Forest Meteorology, 142(1): 50.

Oke, T.R., 1990. Boundary Layer Climates. Routledge, London and New York, 435 pp.

Ono, K., Miyata, A. and Yamada, T., 2007. Apparent downward CO_2 flux observed with open-path eddy covariance over a non-vegetated surface. Theoretical and Applied Climatology: 195-208.

Orchard, V.A. and Cook, F.J., 1983. Relationship between soil respiration and soil moisture. Soil Biology and Biochemistry, 15(4): 447-453.

Osburn, C.L. and Morris, D.P., 2003. Photochemistry of chromophoric dissolved organic matter in natural waters. In: E.W. Helbling and H. Zagarese (Editors), UV effects in aquatic organisms and ecosystems. Royal Society of Chemistry, Cambridge UK pp. 187-217.

Ouyang, Y. and Zheng, C., 2000. Surficial processes and CO_2 flux in soil ecosystem. Journal of Hydrology, 234(1-2): 54-70.

Pancotto, V.A. et al., 2003. Solar UV-B decreases decomposition in herbaceous plant litter in Tierra del Fuego, Argentina: potential role of an altered decomposer community. Global Change Biology, 9(10): 1465-1474.

Pancotto, V.A., Sala, O.E., Robson, T.M., Caldwell, M.M. and Scopel, A.L., 2005. Direct and indirect effects of solar ultraviolet-B radiation on long-term decomposition. Global Change Biology, 11(11): 1982-1989.

Parkin, T.B. and Kaspar, T.C., 2003. Temperature controls on diurnal carbon dioxide flux: implications for estimating soil carbon loss. Soil Science Society of America Journal, 67(6): 1763-1772.

Parshotam, A., 1996. The Rothamsted soil-carbon turnover model -- discrete to continuous form. Ecological Modelling, 86(2-3): 283-289.

Parsons, A.N., Barrett, J.E., Wall, D.H. and Virginia, R.A., 2004. Soil carbon dioxide flux in Antarctic dry valley ecosystems. Ecosystems, 7(3): 286-295.

Parton, B., Ojima, D., Del Grosso, S. and Keough, C., 2001. CENTURY tutorial; Supplement to CENTURY user's manual, pp. 140, http://www.nrel.colostate.edu/projects/century/century_tutorial.pdf, accessed Feb 2009.

Parton, W. and Silver, W.L., 2007. Global-scale similarities in nitrogen release patterns during long-term decomposition. Science, 315(5814): 361-364.

Parton, W.J., Schimel, D.S., Cole, C.V. and Ojima, D.S., 1987. Analysis of factors controlling soil organic matter levels in Great Plains Grasslands. Soil Science Society of America Journal, 51(5): 1173-1179.

Pauli, F., 1964. Soil fertility problem in arid and semi-arid lands. Nature, 204: 1286-1288.

Paustian, K., Six, J., Elliott, E.T. and Hunt, H.W., 2000. Management options for reducing CO_2 emissions from agricultural soils. Biogeochemistry, 48(1): 147-163.

Pavelka, M., Acosta, M., Marek, M.V., Kutsch, W. and Janous, D., 2007. Dependence of the Q_{10} values on the depth of the soil temperature measuring point. Plant and Soil, 292(1-2): 171-179.

Paw, K.T., Baldocchi, D.D., Meyers, T.P. and Wilson, K.B., 2000. Correction of eddy-covariance measurements incorporating both advective effects and density fluxes. Boundary-Layer Meteorology, 97(3): 487-511.

Pendall, E. et al., 2004. Below-ground process responses to elevated CO_2 and temperature: a discussion of observations, measurement methods, and models. New Phytologist, 162(2): 311-322.

Petrone, R.M., Waddington, J.M. and Price, J.S., 2003. Ecosystem-scale flux of CO_2 from a restored vacuum harvested peatland. Wetlands Ecology and Management, 11(6): 419-432.

Pietro, M. and Paola, C., 2004. Thermal analysis for the evaluation of the organic matter evolution during municipal solid waste aerobic composting process. Thermochimica Acta, 413(1-2): 209-214.

Pirisi, F.M., Cabras, P., Garau, V.L., Melis, M. and Secchi, E., 1996. Photodegradation of pesticides. Photolysis rates and half-life of pirimicarb and its metabolites in reactions in water and in solid phase. Journal of Agricultural and Food Chemistry, 44(8): 2417-2422.

Raich, J.W. and Potter, C., 1995. Global patterns of carbon dioxide emissions from soils. Global Biogeochemical Cycles, 9(1): 23-36.

Raich, J.W. and Schlesinger, W.H., 1992. The global carbon dioxide flux in soil respiration and its relationship to vegetation and climate. Tellus, 44B: 81-99.

Raich, J.W. and Tufekciogul, A., 2000. Vegetation and soil respiration: Correlations and controls. Biogeochemistry, 48(1): 71-90.

Randerson, J.T., Chapin III, F.S., Harden, J.W., Neff, J.C. and Harmon, M.E., 2002. Net ecosystem production: A comprehensive measure of net carbon accumulation by ecosystems. Ecological Applications, 12(4): 937-947.

Rayment, M.B. and Jarvis, P.G., 2000. Temporal and spatial variation of soil CO_2 efflux in a Canadian boreal forest. Soil Biology and Biochemistry, 32(1): 35-45.

Reda, I. and Andreas, A., 2003. Solar position algorithm for solar radiation application. Technical report NREL/TP-560-34302, National Renewable Energy Laboratory (NREL), Colorado.

Reichstein, M., Bednorz, F., Broll, G. and Kätterer, T., 2000. Temperature dependence of carbon mineralisation: conclusions from a long-term incubation of subalpine soil samples. Soil Biology and Biochemistry, 32(7): 947-958.

Reichstein, M. et al., 2005a. On the separation of net ecosystem exchange into assimilation and ecosystem respiration: review and improved algorithm. Global Change Biology, 11(9): 1424-1439.

Reichstein, M., Jens-Arne, S., Angeli, A.C. and Tenhunen, J.D., 2005b. Does the temperature sensitivity of decomposition of soil organic matter depend upon water content, soil horizon, or incubation time? Global Change Biology, 11(10): 1754-1767.

Reichstein, M. et al., 2005c. Temperature sensitivity of decomposition in relation to soil organic matter pools: critique and outlook. Biogeosciences, 2(4): 317-321.

Reichstein, M. et al., 2003. Modeling temporal and large-scale spatial variability of soil respiration from soil water availability, temperature and vegetation productivity indices. Global Biochemical Cycles, 17(4): 15.1-15.15.

Reichstein, M. et al., 2002. Ecosystem respiration in two Mediterranean evergreen holm oak forests: drought effects and decomposition dynamics. Functional Ecology, 16(1): 27-39.

Reicosky, D.C. et al., 1999. Effects of residue management and controlled traffic on carbon dioxide and water loss. Soil and Tillage Research, 52(3-4): 153-165.

Repo, M.E. et al., 2009. Large N_2O emissions from cryoturbated peat soil in tundra Nature Geoscience, 3: 189-192.

Rey, A. and Jarvis, P., 2006. Modelling the effect of temperature on carbon mineralization rates across a network of European forest sites (FORCAST). Global Change Biology, 12(10): 1894-1908.

Richardson, A.D. et al., 2006a. Comparing simple respiration models for eddy flux and dynamic chamber data. Agricultural and Forest Meteorology, 141(2-4): 219-234.

Richardson, A.D. and Hollinger, D.Y., 2005. Statistical modeling of ecosystem respiration using eddy covariance data: Maximum likelihood parameter

estimation, and Monte Carlo simulation of model and parameter uncertainty, applied to three simple models. Agricultural and Forest Meteorology, 131(3-4): 191-208.

Richardson, A.D. et al., 2006b. A multi-site analysis of random error in tower-based measurements of carbon and energy fluxes. Agricultural and Forest Meteorology, 136(1-2): 1-18.

Riveros-Iregui, D.A. et al., 2007. Diurnal hysteresis between soil CO_2 and soil temperature is controlled by soil water content. Geophysical Research Letters, 34(L17404): doi: 10.1029/2007GL030938.

Rochette, P., Desjardins, R. and Pattey, E., 1991. Spatial and temporal variability of soil respiration in agricultural fields. Canadian Journal Of Soil Science, 71: 189-196.

Roehm, C.L., 2005. Respiration in wetland ecosystems. In: P.A. Giorgio and P.J.I.B. Williams (Editors), Respiration in aquatic ecosystems. Oxford University Press, New York, pp. 83-103.

Roy, V., 2004. Matlab script sun_position.m. In: Matlab Central (Editor), File Exchange. The Mathworks, Natick, pp. http://www.mathworks.com/matlabcentral/fileexchange/4605.

Rozema, J. et al., 1997a. Effects of UV-B radiation on terrestrial plants and ecosystems: interaction with CO_2 enrichment. Plant Ecology, 128(1): 183-191.

Rozema, J. et al., 1997b. Stratospheric ozone reduction and ecosystem processes: enhanced UV-B radiation affects chemical quality and decomposition of leaves of the dune grassland species *Calamagrostis epigeios*. Plant Ecology, 128(1): 285-294.

Rozema, J. et al., 1997c. Stratospheric ozone reduction and ecosystem processes: Enhanced UV-B radiation affects chemical quality and decomposition of leaves of the dune grassland species Calamagrostis epigeios. Plant Ecology, 128(1-2): 284-294.

Rozema, J., van de Staaij, J., Björn, L.O. and Caldwell, M., 1997d. UV-B as an environmental factor in plant life: stress and regulation. Trends in Ecology & Evolution, 12(1): 22-28.

Rustad, L.E. et al., 2001. A meta-analysis of the response of soil respiration, net nitrogen mineralization, and aboveground plant growth to experimental ecosystem warming. Oecologia, 126: 543.

Rustad, L.E., Huntington, T.G. and Boone, R.D., 2000. Controls on soil respiration: Implications for climate change. Biogeochemistry, 48(1): 1-6.

Rutledge, S., Campbell, D.I., Baldocchi, D. and Schipper, L.A., 2010. Photodegradation leads to increased CO_2 losses from terrestrial organic matter. Global Change Biology: "Accepted Article"; doi: 10.1111/j.1365-2486.2009.02149.x

Ryan, M.G. and Law, B.E., 2005. Interpreting, measuring, and modeling soil respiration. Biogeochemistry, 73(1): 3-27.

Salomé, C., Nunan, N., Pouteau, V., Lerch, T.Z. and Chenu, C., 2010. Carbon dynamics in topsoil and in subsoil may be controlled by different regulatory mechanisms. Global Change Biology, 16(1): 416-426.

Savage, K.E. and Davidson, E.A., 2003. A comparison of manual and automated systems for soil CO_2 flux measurements: trade-offs between spatial and temporal resolution. Journal of Experimental Botany, 54(384): 891.

Schade, G.W., 1997. CO-Emissionen aus abgestorbener, pflanzlicher Biomasse, Johannes Gutenberg Universität, Mainz, Germany.

Schade, G.W., Hofmann, R.-M. and Crutzen, P.J., 1999. CO emissions from degrading plant matter (I). Measurements Tellus B, 51(5): 889-908.

Schaefer, D., Steinberger, Y. and Whitford, W.G., 1985. The failure of nitrogen and lignin control of decomposition in a north American desert. Oecologia, 65(3): 382-386.

Schaumann, G.E. and Antelmann, O., 2000. Thermal characteristics of soil organic matter measured by DSC: A hint on a glass transition. Journal of Plant Nutrition and Soil Science, 163(2): 179-181.

Schaumann, G.E. and LeBoeuf, E.J., 2005. Glass transitions in peat: their relevance and the impact of water. Environmental Science & Technology, 39: 800-806.

Schimel, D.S. et al., 1994. Climatic, edaphic, and biotic controls over storage and turnover of carbon in soils. Global Biogeochem. Cycles, 8(3): 279-293.

Schimel, D.S. et al., 2001. Recent patterns and mechanisms of carbon exchange by terrestrial ecosystems. Nature, 414: 169-172.

Schimel, J., Balser, T.C. and Wallenstein, M., 2007. Microbial stress-response physiology and its implications for ecosystem function. Ecology, 88(6): 1386-1394.

Schindlbacher, A., Zechmeister-Boltenstern, S. and Jandl, R., 2008. Carbon losses due to soil warming: Do autotrophic and heterotrophic soil respiration respond equally? Global Change Biology, 15(4): 901-913.

Schipper, L.A., Clarkson, B.R., Vojvodic-Vukovic, M. and Webster, R., 2002. Restoring cut-over restiad peat bogs: A factorial experiment of nutrients, seed and cultivation. Ecological Engineering, 19: 29-40.

Schmid, H.P., 2002. Footprint modeling for vegetation atmosphere exchange studies: a review and perspective. Agricultural and Forest Meteorology, 113: 159.

Schotanus, P., Nieuwstadt, F.T.M. and de Bruin, H.A.R., 1983. Temperature measurement with a sonic anemometer and its application to heat and moisture fluxes. Boundary Layer Meteorology, 26: 81-90.

Schuepp, P.H., Leclerc, M.Y., Macpherson, J.I. and Desjardins, R.L., 1990. Footprint prediction of scalar fluxes from analytical solutions of the diffusion equation. Boundary Layer Meteorology, 50: 355-373.

Searles, P.S., Kropp, B.R., Flint, S.D. and Caldwell, M.M., 2001. Influence of solar UV-B radiation on peatland microbial communities of southern Argentinia. New Phytologist, 152(2): 213.

Serrano-Ortiz, P., Kowalski, A., Domingo, F., Ruiz, B. and Alados-Arboledas, L., 2008. Consequences of uncertainties in CO_2 density for estimating net ecosystem CO_2 exchange by open-path eddy covariance. Boundary-Layer Meteorology, 126(2): 209-218.

Serrano-Ortiz, P. et al., 2010. Hidden, abiotic CO_2 flows and gaseous reservoirs in the terrestrial carbon cycle: Review and perspectives. Agricultural and Forest Meteorology, 150(3): 321-329.

Shi, P.-L., Zhang, X.-Z., Zhong, Z.-M. and Ouyang, H., 2006. Diurnal and seasonal variability of soil CO_2 efflux in a cropland ecosystem on the Tibetan Plateau. Agricultural and Forest Meteorology, 137(3-4): 220-233.

Shibu, M.E., Leffelaar, P.A., Van Keulen, H. and Aggarwal, P.K., 2006. Quantitative description of soil organic matter dynamics - A review of approaches with reference to rice-based cropping systems. Geoderma, 137(1-2): 1-18.

Shiona, H. et al., 2006. UV Atlas 2.1.5 Build number 0. National Institute of Water and Atmospheric Research (NIWA), http://www.niwa.co.nz/our-services/online-services/uv-and-ozone/uv-atlas.

Shurpali, N.J., Verma, S.B. and Kim, J., 1995. Carbon dioxide exchange in a peatland ecosystem. Journal of Geophysical Research, 100(D7): 14319.

Silvola, J., Alm, J., Ahlholm, U., Nykänen, H. and Martikainen, P.J., 1996. CO_2 fluxes from peat in boreal mire under varying temperature and moisture conditions. Journal of Ecology, 84: 219-228.

Sjörs, H., 1981. The zonation of northern peatlands and their importance for the carbon balance of the atmosphere. International Journal of Ecology & Environmental Sciences, 7: 11-14.

Smith, C.A., Gerlock, J.L. and Carter, R.O., 2001. Determination of ultraviolet light absorber longevity and distribution in automotive paint systems using ultraviolet micro-spectroscopy. Polymer Degradation and Stability, 72(1): 89-97.

Smith, W., Gao, W. and Steltzer, H., 2009. Current and future impacts of ultraviolet radiation on the terrestrial carbon balance. Frontiers of Earth Science in China, 3(1): 34-41.

Smith, W.K., Gao, W., Steltzer, H., Wallenstein, M.D. and Tree, R., 2010. Moisture availability influences the effect of ultraviolet-B radiation on leaf litter decomposition. Global Change Biology, 16: 484-495.

Sorrell, B. et al., 2004. Wetland management and restoration. In: P. Mosley and J. Harding (Editors), New Zealand Limnological Society and New Zealand Hydrological Society, Caxton Press. The Caxton Press, Christchurch, pp. 40.1-40.2.

Sottocornola, M. and Kiely, G., 2010. Hydro-meteorological controls on the CO_2 exchange variation in an Irish blanket bog. Agricultural and Forest Meteorology, 150(2): 287-297.

Sowerby, A., Emmett, B.A., Tietema, A. and Beier, C., 2008. Contrasting effects of repeated summer drought on soil carbon efflux in hydric and mesic heathland soils. Global Change Biology, 14(10): 2388-2404.

Sponseller, R.A., 2007. Precipitation pulses and soil CO_2 flux in a Sonoran Desert ecosystem. Global Change Biology, 13(2): 426-436.

Steinweg, J.M., Plante, A.F., Conant, R.T., Paul, E.A. and Tanaka, D.L., 2008. Patterns of substrate utilization during long-term incubations at different temperatures. Soil Biology and Biochemistry, 40(11): 2722-2728.

Stewart, J.M. and Wheatly, R.E., 1990. Estimates of CO_2 production from eroding peat surfaces. Soil Biology and Biochemistry, 22(1): 65-68.

Strack, M., 2008. Executive summary for policymakers "Peatland in global change". In: M. Strack (Editor), Peatlands and climate change. International Peat Society, Saarijärvi, pp. 9-12.

Strack, M., Waddington, J.M., Turetsky, M., Roulet, N.T. and Byrne, K.A., 2008. Northern peatlands, greenhouse gas exchange and climate change. In: M. Strack (Editor), Peatlands and climate change. International Peat Society, Saarijärvi, pp. 44-69.

Subke, J.-A., Inglima, I. and Francesca Cotrufo, M., 2006. Trends and methodological impacts in soil CO_2 efflux partitioning: A metaanalytical review. Global Change Biology, 12(6): 921-943.

Subke, J.A. and Tenhunen, J.D., 2004. Direct measurements of CO_2 flux below a spruce forest canopy. Agricultural and Forest Meteorology, 126(1-2): 157-168.

Suyker, A.E. and Verma, S.B., 2001. Year-round observations of the net ecosystem exchange of carbon dioxide in a native tallgrass prairie. Global Change Biology, 7(3): 279-289.

Swift, M.J., Heal, O.W. and Anderson, J.M., 1979. Decomposition in terrestrial ecosystems. Blackwell Scientific Publication, Oxford London Edinburgh Melbourne, 372 pp.

Tang, J. and Baldocchi, D.D., 2005. Spatial and temporal variation in soil respiration in an oak-grass savanna ecosystem in California and its partitioning into autotrophic and heterotrophic components. Biogeochemistry, 73(1): 183-207.

Tang, J., Baldocchi, D.D., Qi, Y. and Xu, L., 2003. Assessing soil CO_2 efflux using continuous measurements of CO_2 profiles in soils with small solid-state sensors. Agricultural and Forest Meteorology, 118: 207-220.

Tang, J., Baldocchi, D.D. and Xu, L., 2005. Tree photosynthesis modulates soil respiration on a diurnal time scale. Global Change Biology, 11(8): 1298-1304.

Tang, J.W. et al., 2008. Ecosystem respiration and its components in an old-growth forest in the Great Lakes region of the United States. Agricultural and Forest Meteorology, 148(2): 171-185.

Tarr, M.A., Miller, W.L. and Zepp , R.G., 1995. Direct carbon monoxide photoproduction from plant matter. Journal of Geophysical Research, 100(D6): 11,403-11,413.

Taylor, B.R., Parkinson, D. and Parsons, W.F.J., 1989. Nitrogen and lignin content as predictors of litter decay rates: a microcosm test. Ecology, 70(1): 97-104.

The Ameriflux Workshop Team, 2003. Summary and synthesis of recommendations of the AmeriFlux workshop on standardization of flux analysis and diagnostics, Corvallis, Oregon, August 2002, Corvallis, http://public.ornl.gov/ameriflux/workshops/workshop-20020827-CorvallisOR-summary.doc.

Thompson, M.A., Campbell, D.I. and Spronken-Smith, R.A., 1999. Evaporation from natural and modified raised peat bogs in New Zealand. Agricultural and Forest Meteorology, 95(2): 85-98.

Throop, H.L. and Archer, S.R., 2009. Resolving the dryland decomposition conundrum: some new perspectives on potential drivers. In: U. Lüttge, W. Beyshchlag, B. Büdel and D. Francis (Editors), Progress in Botany. Springer-Verlag Berlin Heidelberg, pp. 171-194.

Tjoelker, M.G., Oleksyn, J. and Reich, P.B., 2001. Modelling respiration of vegetation: evidence for a general temperature-dependent Q_{10}. Global Change Biology, 7(2): 223-230.

Torikai, A. and Hasegawa, H., 1999. Accelerated photodegradation of poly(vinyl chloride). Polymer Degradation and Stability, 63(3): 441-445.

Trumbore, S., 2000. Age of soil organic matter and soil respiration: radiocarbon constraints on belowground C dynamics. Ecological Applications, 10(2): 399-411.

Trumbore, S., 2006. Carbon respired by terrestrial ecosystems - recent progress and challenges. Global Change Biology, 12(2): 141-153.

Tuomi, M., Vanhala, P., Karhu, K., Fritze, H. and Liski, J., 2008. Heterotrophic soil respiration - Comparison of different models describing its temperature dependence. Ecological Modelling, 211: 182-190.

Turunen, J., Tomppo, E., Tolonen, K. and Reinikainen, A., 2002. Estimating carbon accumulation rates of undrained mires in Finland - application to boreal and subarctic regions. Holocene, 12(1): 69-80.

Twine, T.E. et al., 2000. Correcting eddy-covariance flux underestimates over a grassland. Agricultural and Forest Meteorology, 103: 279-300.

Updegraff, K., Bridgham, S.D., Pastor, J., Weishampel, P. and Harth, C., 2004. Response of CO_2 and CH_4 emissions from peatlands to warming and water table manipulation. Ecological Applications, 11(2): 311-326.

Vähätalo, A., Søndergaard, M., Schlüter, L. and Markager, S., 1998. Impact of solar radiation on the decomposition on detrital leaves of eelgrass *Zostera marina*. Marine Ecology Progress Series, 197: 107-117.

van der Wal, A., van Veen, J.A., Pijl, A.S., Summerbell, R.C. and de Boer, W., 2006. Constraints on development of fungal biomass and decomposition processes during restoration of arable sandy soils. Soil Biology and Biochemistry, 38(9): 2890-2902.

Van Gestel, M., Ladd, J.N. and Amato, M., 1991. Carbon and nitrogen mineralization from two soils of contrasting texture and microaggregate stability: Influence of sequential fumigation, drying and storage. Soil Biology and Biochemistry, 23(4): 313-322.

van Gorsel, E. et al., 2009. Estimating nocturnal ecosystem respiration from the vertical turbulent flux and change in storage of CO_2. Agricultural and Forest Meteorology, 149(11): 1919-1930.

van Gorsel, E. et al., 2008. Application of an alternative method to derive reliable estimates of nighttime respiration from eddy covariance measurements in moderately complex topography. Agricultural and Forest Meteorology, 148(6-7): 1174-1180.

Van Gorsel, E., Leuning, R., Cleugh, H.A., Keith, H. and Suni, T., 2007. Nocturnal carbon efflux: reconciliation of eddy covariance and chamber measurements using an alternative to the u_*-threshold filtering technique. Tellus B, 59(3): 397-403.

van Wijk, W.R. and de Vries, D.A., 1963. Periodic temperature variations in a homogeneous soil. In: W.R. Van Wijk (Editor), Physics of plant environment. John Wiley & Sons, New York, pp. 102-140.

van't Hoff, J.H., 1884. Études de dynamique chemique. Frederik Muller and Co., Amsterdam, The Netherlands.

Vanderbilt, K.L., White, C.S., Hopkins, O. and Craig, J.A., 2008. Aboveground decomposition in arid environments: Results of a long-term study in central New Mexico. Journal of Arid Environments, 72(5): 696-709.

Verhoef, H.A., Verspagen, J.M.H. and Zoomer, H.R., 2000. Direct and indirect effects of ultraviolet-B radiation on soil biota, decomposition and nutrient fluxes in dune grassland soil systems. Biology and Fertility of Soils, 31(5): 366-371.

Vigano, I. et al., 2008. Effect of UV radiation and temperature on the emission of methane from plant biomass and structural components. Biogeosciences, 5(3): 937-947.

Vossbrinck, C.R., Coleman, D.C. and Woolley, T.A., 1979. Abiotic and biotic factors in litter decomposition in a semiarid grassland. Ecology, 60(2): 265-271.

Waddington, J.M., Rotenberg, P.A. and Warren, F.J., 2001. Peat CO_2 production in a natural and cutover peatland: Implications for restoration. Biogeochemistry, 54(2): 115-130.

Waddington, J.M. and Warner, K.D., 2001. Atmospheric CO_2 sequestration in restored mined peatlands. Ecoscience, 8(3): 359-368.

Waddington, J.M., Warner, K.D. and Kennedy, G.W., 2002. Cutover peatlands: A persistent source of atmospheric CO_2. Global Biogeochemical Cycles, 16(1): 1002, doi:10.1029/2001GB001398.

Wayne, C.E. and Wayne, R.P., 1996. Photochemistry. Oxford chemistry primers 39. Oxford University Press, New York, 92 pp.

Wayne, R.P., 1988. Principles and applications of photochemistry. Oxford University Press,, New York.

Webb, E.K., Pearman, G.J. and Leuning, R., 1980. Correction of flux measurements for density effects due to heat and water vapour transfer. Quarterly Journal of the Royal Meteorological Society, 106: 85-100.

Webster, K.L., Creed, I.F., Skowronski, M.D. and Kaheil, Y.H., 2009. Comparison of the performance of statistical models that predict soil respiration from forests. Soil Science Society Of America Journal, 73(4): 1157-1167.

Weiss, N.S., 1993. Complex mixtures and indoor air pollution: overview of epidemiologic methods Environmental Health Perspectives Supplements 101 (S4): 179-181.

Wetterstedt, J.Å.M., Persson, T. and Ågren, G.I., 2009. Temperature sensitivity and substrate quality in soil organic matter decomposition; results of an incubation study with three substrates. Global Change Biology, "Accepted Article"; doi: 10.1111/j.1365-2486.2009.02112.x.

Wetzel, R.G., 2003. Solar radiation as an ecosystem modulator. In: E.W. Helbling and H. Zagarese (Editors), UV effects in aquatic organisms and ecosystems. Royal Society of Chemistry, Cambridge UK pp. 3-18.

Whalen, S.C., 2005. Biogeochemistry of methane exchange between natural wetlands and the atmosphere. Environmental Engineering Science, 22(1): 73-94.

Whitford, W.G. et al., 1981. Exceptions to the AET model: deserts and clear-cut forest. Ecology, 62(1): 275-277.

Wiebe, R. and Gaddy, V.L., 1940. The solubility of carbon dioxide in water at various temperatures from 12 to 40°C and at pressures to 500 atmospheres. Journal of the American Chemical Society, 62(4): 815-817.

Wilczak, J.M., Oncley, S.P. and Stage, S.A., 2001. Sonic anemometer tilt correction algorithms. Boundary Layer Meteorology, 99: 127-150.

Williams, R.S., 2005. Weathering of wood. In: R.M. Rowell (Editor), Handbook of wood chemistry and wood composites. CRC Press, Florida, pp. 139-185.

Wilson, K. et al., 2002. Energy balance closure at FLUXNET sites. Agricultural and Forest Meteorology, 113: 223-243.

Wofsy, S.C. et al., 1993. Net exchange of CO_2 in a mid-latitude forest. Science, 260: 1314-1317.

Wohlfahrt, G. et al., 2005. Quantifying nighttime ecosystem respiration of a meadow using eddy covariance, chambers and modelling. Agricultural and Forest Meteorology, 128(3-4): 141-162.

Wohlfahrt, G., Fenstermaker, L.F. and Arnone, J.A., 2008. Large annual net ecosystem CO_2 uptake of a Mojave Desert ecosystem. Global Change Biology, 14(7): 1475-1487.

Wolf, A., Saliendra, N., Akshalov, K., Johnson, D.A. and Laca, E., 2008. Effects of different eddy covariance correction schemes on energy balance closure and comparisons with the modified Bowen ratio system. Agricultural and Forest Meteorology, 148(6-7): 942-952.

Wolters, V., 2000. Invertebrate control of soil organic matter stability. Biology and Fertility of Soils, 31(1): 1-19.

Wyngaard, J.C., 1990. Scalar fluxes in the planetary boundary layer - theory, modeling, and measurement. Boundary Layer Meteorology, 50: 49-75.

Xiang, W. and Freeman, C., 2009. Annual variation of temperature sensitivity of soil organic carbon decomposition in North peatlands: implications for thermal responses of carbon cycling to global warming. Environmental Geology, 58(3): 499-508.

Xu, L. and Baldocchi, D.D., 2004. Seasonal variation in carbon dioxide exchange over a Mediterranean annual grassland in California. Agricultural and Forest Meteorology, 123(1-2): 79-96.

Xu, L., Baldocchi, D.D. and Tang, J., 2004. How soil moisture, rain pulses, and growth alter the response of ecosystem respiration to temperature. Global Biogeochemical Cycles, 18(GB4002): doi:10.1029/2004GB002281.

Yonemura, S., Morokuma, M., Kawashima, S. and Tsuruta, H., 1999. Carbon monoxide photoproduction from rice and maize leaves. Atmospheric Environment, 33(18): 2915-2920.

Yue, M., Li, Y. and Wang, X., 1998. Effects of enhanced ultraviolet-B radiation on plant nutrients and decomposition of spring wheat under field conditions. Environmental and Experimental Botany, 40(3): 187-196.

Zeller, C. et al., 2001. Analysis of inadvertent microprocessor lag time on eddy covariance results. Journal of Applied Meteorology, 40(9): 1640-1646.

Zepp, R.G., 2003. Solar ultraviolet radiation and aquatic carbon, nitrogen, sulfur and metals cycles. In: E.W. Helbling and H. Zagarese (Editors), UV effects in aquatic organisms and ecosystems. Royal Society of Chemistry, Cambridge UK pp. 137-183.

Zepp, R.G., Erickson, D.J., Paul, N.D. and Sulzberger, B., 2007. Interactive effects of solar UV radiation and climate change on biogeochemical cycling. Photochemical & Photobiological Sciences, 6(3): 286-300.

Appendix A Global Change Biology paper

Global Change Biology

Global Change Biology (2010), doi: 10.1111/j.1365-2486.2009.02149.x

Photodegradation leads to increased carbon dioxide losses from terrestrial organic matter

SUSANNA RUTLEDGE*, DAVID I. CAMPBELL*, DENNIS BALDOCCHI† and LOUIS A. SCHIPPER*

*Department of Earth and Ocean Sciences, University of Waikato, Private Bag 3105, Hamilton, New Zealand, †Department of Environmental Science, Policy and Management, Ecosystems Science Division, University of California, Berkeley, CA, USA

Abstract

CO_2 production in terrestrial ecosystems is generally assumed to be solely biologically driven while the role of abiotic processes has been largely overlooked. In addition to microbial decomposition, photodegradation – the direct breakdown of organic matter (OM) by solar irradiance – has been found to contribute to litter mass loss in dry ecosystems. Previous small-scale studies have shown that litter degradation by irradiance is accompanied by emissions of CO_2. However, the contribution of photodegradation to total CO_2 losses at ecosystems scales is unknown. This study determined the proportion of the total CO_2 losses caused by photodegradation in two ecosystems: a bare peatland in New Zealand and a seasonally dry grassland in California. The direct effect of solar irradiance on CO_2 production was examined by comparing daytime CO_2 fluxes measured using eddy covariance (EC) systems with simultaneous measurements made using an opaque chamber and the soil CO_2 gradient technique, and with nighttime EC measurements under the same soil temperature and moisture conditions. In addition, a transparent chamber was used to directly measure CO_2 fluxes from OM caused by solar irradiance. Photodegradation contributed 19% of the annual CO_2 flux from the peatland and almost 60% of the dry season CO_2 flux from the grassland, and up to 62% and 92% of the summer mid-day CO_2 fluxes, respectively. Our results suggest that photodegradation may be important in a wide range of ecosystems with exposed OM. Furthermore, the practice of partitioning daytime ecosystem CO_2 exchange into its gross components by assuming that total daytime CO_2 losses can be approximated using estimates of biological respiration alone may be in error. To obtain robust estimates of global ecosystem–atmosphere carbon transfers, the contribution of photodegradation to OM decomposition must be quantified for other ecosystems and the results incorporated into coupled carbon–climate models.

Keywords: abiotic decomposition, carbon cycle, carbon dioxide (CO_2) emission, eddy correlation, grassland, photodegradation, peatland, rain pulse, respiration, solar radiation

Received 5 October 2009; revised version received 16 November 2009 and accepted 19 November 2009

Introduction

Microbial decomposition of organic matter (OM) is regarded as one of the dominant processes resulting in CO_2 production in terrestrial ecosystems (Grace & Rayment, 2000; Janzen, 2004). Temperature, moisture and substrate quality are generally considered the main factors controlling decomposition because of their strong influence on decomposer activity (Luo & Zhou, 2006). However, abiotic processes like physical fragmentation by wind and water, leaching, and photodegradation (Vanderbilt *et al.*, 2008) can also contribute to decomposition of litter and soil organic matter (SOM). Of these, photodegradation is well known to be important in cycling of aquatic OM (Zepp, 2003), but the relevance of photodegradation in OM cycling in terrestrial ecosystems is poorly understood (Brandt *et al.*, 2009; Smith *et al.*, 2010; Throop & Archer, 2009).

Photodegradation is the process by which solar irradiance directly breaks down the compounds of OM, increasing CO_2 fluxes through either photochemical mineralization or microbial facilitation. Photochemical mineralization is the direct breakdown of OM to CO_2 and has been demonstrated in the absence of microbial activity (Anesio *et al.*, 1999; Brandt *et al.*, 2009). Microbial facilitation is the breakdown by solar irradiance of large organic compounds into smaller molecules that can subsequently be degraded by microbes (Gallo *et al.*, 2006, 2009; Day *et al.*, 2007; Henry *et al.*, 2008).

Photodegradation can contribute to mass loss of litter in sparsely vegetated arid and semi-arid environments (see review Throop & Archer, 2009). Litter mass loss has been found to be greater under ambient solar irradiance than reduced irradiance using a range of filters blocking different wavelength bands (Austin & Vivanco, 2006;

Correspondence: Susanna Rutledge, tel. + 64 7 838 4466, extn. 6229, fax + 64 7 856 0115, e-mail: sj52@students.waikato.ac.nz

Brandt *et al.*, 2007; Day *et al.*, 2007; Gallo *et al.*, 2009). Supplemental UV-B irradiance may also increase mass loss (Rozema *et al.*, 1997; Smith *et al.*, 2010), although not always (Gehrke *et al.*, 1995; Newsham *et al.*, 1997; Verhoef *et al.*, 2000; Moody *et al.*, 2001).

Photodegradation is likely most important in arid and semi-arid regions with open canopies, large amounts of standing dead material, and high radiative loads (Austin & Vivanco, 2006; Throop & Archer, 2009) and where microbial activity is inhibited by water limitation and possibly by exposure to high UV irradiance (Gehrke *et al.*, 1995; Pancotto *et al.*, 2003; Austin & Vivanco, 2006; Brandt *et al.*, 2009; Smith *et al.*, 2010). Although previously UV-B irradiance was considered to be responsible for the vast majority of photodegradation, irradiance in other parts of the solar spectrum (i.e. UV-A and visible) can also contribute to OM decomposition and gaseous carbon losses (Anesio *et al.*, 1999; Austin & Vivanco, 2006; Brandt *et al.*, 2009).

Field studies of photodegradation have focussed on mass loss of litter (Austin & Vivanco, 2006; Brandt *et al.*, 2007; Day *et al.*, 2007; Henry *et al.*, 2008) but have not determined the contribution of photodegradation to ecosystem scale CO_2 losses. Our objective was to determine the extent to which photodegradation contributed to CO_2 losses from two contrasting ecosystems: an exposed de-vegetated peatland in New Zealand and an annual (seasonally dry) grassland in California. These ecosystems were selected because they had significant surface OM exposed to high ambient levels of solar irradiance when microbial activity was low due to water limitation. CO_2 fluxes were measured using a combination of eddy covariance (EC), chamber and soil CO_2 gradient measurements that allowed us to determine the potential influence of solar irradiance on the CO_2 flux. These field studies were complemented with a controlled experiment where instantaneous CO_2 fluxes were measured from peat that was alternately exposed to and shaded from natural solar irradiance in a small transparent container.

Site descriptions and methods

Peatland study site

The peatland study site was an exposed, de-vegetated peat bog at Torehape, in the Hauraki Plains of the North Island of New Zealand (37°19′S, 175°27′E, 3 m elevation). The vegetation and the top 1 m of peat had been removed as part of a peat mining operation. Measurements started directly after mining had finished. A further 8 m of peat remained and the site remained un-vegetated throughout the study. The site was drained to make mining activities possible with drains approximately 40 m apart. Lanes of bare peat between drains were 900 m long. Dominant vegetation before mining at Torehape was *Sporadanthus ferrugineus* over a lower storey of *Empodisma minus* and *Sphagnum cristatum* (Schipper *et al.*, 2002). Dry bulk density of the peat (depth 0–150 mm) was 0.135 g cm^{-3}, and OM content was 92%, measured by loss on ignition. Mean annual air temperature at a nearby climate station was 15.2 °C and average rainfall 1150 mm yr^{-1} (1970–2000). During the experiment water table depth varied from 0.45 m during summer to 0.05 m during winter. Volumetric moisture content (VMC) measured at 50 mm depth varied from 0.49 $m^3 m^{-3}$ during summer to 0.68 $m^3 m^{-3}$ during winter. In summer, the surface peat got very dry and formed a dry crust over the surface, leading to much drier surface conditions than the VMC at 50 mm implied.

Grassland study site

EC measurements of CO_2 flux were made at an annual grassland site (Vaira Ranch, part of the AmeriFlux network) located in the lower foothills of the Sierra Nevada, near Ione, CA (38.4133°N; 120.9508°W, 129 m elevation). The soil is an Exchequer very rocky silt loam (Lithic xerorthents). Soil bulk density at the surface (0–300 mm) was 1.43 ± 0.10 g cm^{-3}. The site was relatively flat and upwind fetch exceeded 200 m. Species composition included *Brachypodium distachyon, Hypochaeris glabra, Trifolium dubium, Trifolium hirtum, Dichelostemma volubile* and *Erodium botrys* (Xu & Baldocchi, 2004). The measurements of soil CO_2 flux using a belowground CO_2 flux gradient system were collected at a companion site (Tonzi Ranch) located 2 km from the grassland site (38.4311°N, 120.966°W, 177 m elevation). This site is composed of oak/grass savanna. The soil is an Auburn very rocky silt loam (Lithic haploxerepts) with a soil bulk density at the surface (0–30 cm) of 1.64 ± 0.11 g cm^{-3} (Baldocchi *et al.*, 2004). Species of annual herbs and exotic grasses in the understory included *Brachypodium distachyon, Hypochaeris glabra, Bromus madritensis* and *Cynosurus echinatus* (Baldocchi *et al.*, 2006). The climate of the region can be described as Mediterranean, with hot and dry summers and cool and wet winters. Mean annual air temperature at a nearby climate station was 16.3 °C and average rainfall 559 mm yr^{-1} (1959–1977) (Baldocchi *et al.*, 2004). The general absence of precipitation during summer (May–November) causes the grass to die (Xu *et al.*, 2004) and limits soil respiration (Tang & Baldocchi, 2005).

Instrumentation EC and flux processing

CO_2 fluxes were measured using the EC technique (Baldocchi, 2003). At the peatland, EC measurements were made over a period of 2 years (Jun 2005–May 2007). Instruments were mounted at 1.5 m above the peat surface until March 2007 and thereafter at 2.5 m. The system consisted of a sonic anemometer (CSAT-3, Campbell Scientific Inc. (CSI), Logan, UT, USA) and an open-path infrared H_2O/CO_2 gas analyser (LI-7500, LI-COR Inc., Lincoln, NE, USA). A CR23x datalogger (CSI) sampled signals of the CSAT-3 and the LI-7500 and calculated raw fluxes. At the grassland the EC system was mounted at 2.0 m above the ground. It consisted of a sonic

anemometer (Model 1352, Gill Instruments Ltd, Lymington, UK) and a LI-7500 gas analyser. Raw data were recorded on a laptop computer. At both sites the sampling rate was 10 Hz. To compute half-hourly CO_2 fluxes from the raw data at the peatland we applied coordinate rotation (McMillen, 1986), corrected for sonic temperature (Schotanus *et al.*, 1983) and high-frequency loss (Moore, 1986) and added the density correction term (Webb *et al.*, 1980). We refer to Xu & Baldocchi (2004) and Baldocchi *et al.* (2004) for detailed information on computational procedures applied to the grassland data.

EC data filtering

For the peatland, EC data were only used when footprint analyses (Schuepp *et al.*, 1990) showed that 80% or more of the flux originated from the bare peat. Further data were discarded when wind direction was from behind the tower to avoid possible flow distortion. Data were discarded also when rainfall or dew caused unreliable readings from the LI-7500 or when friction velocity was $<0.2\,m\,s^{-1}$. The friction velocity threshold was chosen conservatively to ensure only the very best data were used for analysis. Because of these strict criteria we discarded 89% of the data points, leaving ~4000 half-hourly averages of CO_2 flux for analysis.

For the grassland, data were only used for the period in 2007 when vegetation had senesced. Data were selected for periods when the soil VMC at 50 mm was $<0.038\,m^3\,m^{-3}$ to ensure that photosynthesis was zero. Data were discarded when collected during rainfall, and 7 days thereafter. No gap-filling of missing data was applied for either site.

Additional field measurements

At the peatland, repeated chamber measurements were made using a LI-8100 automated soil CO_2 flux system (LI-COR Inc.). We used a long-term chamber (LI-8100-101, soil collar 200 mm in diameter) to measure the temporal variation of the CO_2 fluxes from one collar installed 10 m from the EC system. Measurements were made every 15 min. A SP Lite pyranometer (Kipp & Zonen, Delft, the Netherlands) mounted at 2.4 m was used to measure incident solar irradiance ($K\downarrow$, wavelengths between 400 and 1100 nm). Soil temperature at 5 mm was measured using an averaging thermocouple (four prongs) buried close to the EC tower and long-term chamber. VMC was measured at 50 mm depth using a CS615 water content reflectometer (CSI) calibrated in the lab for peat.

At the grassland, measurements of soil respiration were collected using a belowground CO_2 flux gradient system (Tang *et al.*, 2003). Soil CO_2 concentrations were measured using probes at depths of 0.02, 0.08, 0.16 and 0.24 m. The profile was measured approximately 20 m away from trees, and tree roots had negligible influence on the measurements, based on transect measurements of soil respiration using a manual chamber system (Tang & Baldocchi, 2005). CO_2 concentrations in the soil air were measured by solid-state infrared gas analyzer probes (GMT 222 and GMT 221, Vaisala, Helsinki, Finland). Soil CO_2 efflux rates were computed using flux–gradient theory. Refer to Tang *et al.* (2003) and Baldocchi *et al.* (2006) for detailed descriptions of the measurements and flux calculations. We used a four-component net radiometer (CNR1, Kipp & Zonen) mounted at 2.5 m to measure incident solar irradiance ($K\downarrow$, wavelengths between 310 and 2800 nm) and upward longwave radiation. The latter was used to calculate the surface temperature. Soil VMC was measured with frequency-domain reflectometer probes (ML2x, Delta-T Devices, Burwell, Cambridge, UK) at a depth of 50 mm.

Container experiment

To confirm the direct control of solar irradiance on CO_2 effluxes an additional small-scale chamber experiment was conducted, whereby CO_2 fluxes from air-dried peat were measured in a small closed chamber (volume 270 mL). To make the distinction between the chamber used in the field (see previous section) and this small home-made closed chamber, we will refer to the latter as the 'container.' We replaced the top of the polystyrene container with a quartz plate 3.175 mm thick (GM Associates Inc., Oakland, CA, USA) to increase transmittance to 0.91, 0.93 and 0.93 for visible (400–700 nm), UV-A (320–400 nm) and UV-B (280–320 nm) irradiance, respectively, as measured by a Cary 100 UV-Vis spectrophotometer (Varian Inc., Palo Alto, CA, USA). A thin layer of peat in the container (approximately 4 g, just sufficient to cover the bottom of the container) was alternately shaded from and exposed to sunlight. CO_2 concentration was measured every second using a LI-8100 infrared gas analyser (LI-COR Inc.) in runs of 140 or 200 s. The container was flushed with ambient air after every 10 runs. Because of the fast response of the CO_2 flux to changes in temperature and irradiance conditions, fluxes were calculated from the change in CO_2 concentration over 1 min, beginning 6 s after the run started (i.e. 7–66 s). The first 6 s of each run were discarded to allow for travel time of air from the container to the infra-red gas analyser. The shorter run length ensured temperatures between sun and shade runs overlapped, thus allowing direct comparison between sun and shade runs of equal mean temperature. Test runs ($n = 14$), where the empty container was exposed to sunlight, confirmed that uptake or release of CO_2 by the container materials in response to exposure to irradiance was negligible (0.0159 and $0.0055\,\mu mol\,CO_2\,m^{-2}\,s^{-1}$ for sun and shade runs, respectively) and not significantly different from zero.

Peat temperature was measured with four thermocouples of which the average was used. Average peat temperatures ranged from 35 to 65 °C and were representative of surface temperatures occurring in the field: surface temperatures of up to 60 °C were observed during summer at the peatland. The experiment ran over 3 days (February 3–5, 2009) during 5 h centered on midday. On each day, a new peat sample was used. The total number of runs used in the analyses was 114 (57 with the container shaded, 57 with the container exposed).

Estimation of cumulative CO_2 losses

To calculate yearly CO_2 losses from the peatland, a model was constructed using lookup tables of EC fluxes defined by bins of VMC at 50 mm depth (three bins with equal number of data

points: VMC $< 0.50\,m^3\,m^{-3}$, $0.50\,m^3\,m^{-3} <$ VMC $< 0.56\,m^3\,m^{-3}$ and VMC $> 0.56\,m^3\,m^{-3}$), incident solar irradiance (bins of $100\,W\,m^{-2}$) and soil temperature at 5 mm depth (bins of 2 °C). Each bin required a minimum of five data points to make an average. To estimate the irradiance-induced part of the flux for each time step, we took the difference between the CO_2 flux from the lookup table, and the estimated dark (night-time) CO_2 flux at the same temperature and in the same moisture bin. Night-time CO_2 fluxes were estimated using two different regression equations of CO_2 flux as a function of soil temperature for each soil moisture class. As a conservative estimate of the night-time flux, we used a linear regression between soil temperature and measured flux ($R^2 = 0.64$, 0.45, 0.24 for dry, medium and wet soil moisture classes, respectively). As a second estimate of night-time flux, we fitted the Lloyd and Taylor equation (Lloyd & Taylor, 1994; $R^2 = 0.76$, 0.71, 0.02 for dry, medium and wet soil moisture classes, respectively). By combining the daytime value for the CO_2 flux from the lookup table with the two estimates for night-time flux and summing the values over the year, two estimates were calculated for annual contribution of photodegradation to the total CO_2 flux.

For the grassland site, a very similar but slightly simpler method was used to estimate the cumulative contribution of irradiance-induced CO_2 flux to the total CO_2 flux during the dry season. A lookup table of EC fluxes, defined by bins of incident solar irradiance (bins of $100\,W\,m^{-2}$) and surface temperature (bins of 2 °C), was made using the data from the dry season. Soil moisture was not used for the lookup table because the values of soil VMC were very low with a very narrow range during the senescent period ($0.03\,m^3\,m^{-3} <$ VMC $< 0.038\,m^3\,m^{-3}$); therefore no effect of moisture was expected. Night-time CO_2 fluxes were estimated using the median value of all night-time EC measurements during the dry period, because night-time EC flux showed no clear trend with surface temperature (data not shown). An estimate for the cumulative contribution of photodegradation to the total CO_2 flux during the dry season was calculated by subtracting the estimated night-time flux from the daytime value for the CO_2 flux from the lookup table and summing all half-hourly values for the dry season.

Statistics

We tested whether solar irradiance explained a statistically significant proportion of variation in abiotic flux (here defined as 'the CO_2 flux measured using EC minus CO_2 flux measured using chamber or soil probes') in addition to the variation explained by temperature and soil moisture. The multiple regression analysis was carried out using the RAR1 procedure in GENSTAT (Version 11.1.0.1535). Fitted terms were: a constant, temperature, soil moisture content and solar irradiance. The analysis used residual maximum likelihood to model correlated regression errors for contiguous blocks of observations (i.e. within observation days).

To test whether the differences between CO_2 fluxes measured by EC and those measured by chamber or soil probes were significantly different from zero at different levels of solar irradiance a one-sample *t*-test was used (95% significance level, MATLAB, Version 7.3.0.267, R2006b). Before testing, flux differences were binned by incoming solar irradiance (bin width $150\,W\,m^{-2}$) and averaged daily by bin to avoid issues with correlated data within observation days.

Results

Effect of solar irradiance on CO_2 fluxes – field experiments

To examine the effect of incident solar irradiance ($K\downarrow$) on the CO_2 fluxes measured by EC fluxes, we first compared them with fluxes measured by chamber (chamber fluxes) and soil probes (probe fluxes) for different levels of solar irradiance. At night ($K\downarrow = 0\,W\,m^{-2}$), EC fluxes agreed well with chamber and probe fluxes (Fig. 1).

However, during the day ($K\downarrow > 0\,W\,m^{-2}$) there was a large discrepancy between EC fluxes and fluxes measured by chamber and soil probes. This discrepancy increased with increasing incident solar irradiance (Fig. 1b and d). At the peatland, the average difference between EC and chamber fluxes at high irradiances ($K\downarrow$ around $1000\,W\,m^{-2}$) was almost $2\,\mu mol\,m^{-2}\,s^{-1}$ (Fig. 1b). The EC flux was approximately 2.5 times larger than the chamber flux in those instances. At the grassland, the average difference between EC and probe fluxes at high irradiances was $1.1\,\mu mol\,m^{-2}\,s^{-1}$ (Fig. 1d). The EC flux was 12 times larger than the probe flux in those instances.

Multiple regression analyses confirmed that for both sites the effect of solar irradiance explained a significant proportion of variation in the discrepancy between the EC CO_2 fluxes and chamber or soil CO_2 fluxes in addition to the variation explained by soil temperature and soil moisture ($P < 0.001$, Table 1).

To visually separate the controls of temperature and solar irradiance on CO_2 fluxes, we compared day- and night-time measurements made using EC in the same temperature ranges (Fig. 2). This comparison showed that solar irradiance had a direct effect on CO_2 fluxes measured by EC. At both sites, CO_2 fluxes were much greater during the day than at night when comparing fluxes measured at equal temperatures (Fig. 2), further suggesting that photodegradation was an important process explaining the difference between day- and night-time EC fluxes. At the peatland, the effect of irradiance on the CO_2 flux was most pronounced when the surface peat was dry, but could also be observed when the peat was moist (Fig. 3).

Effect of solar irradiance on CO_2 fluxes – container experiment

Exposing peat to sunlight in the transparent container markedly increased CO_2 flux (Fig. 4). CO_2 fluxes in the

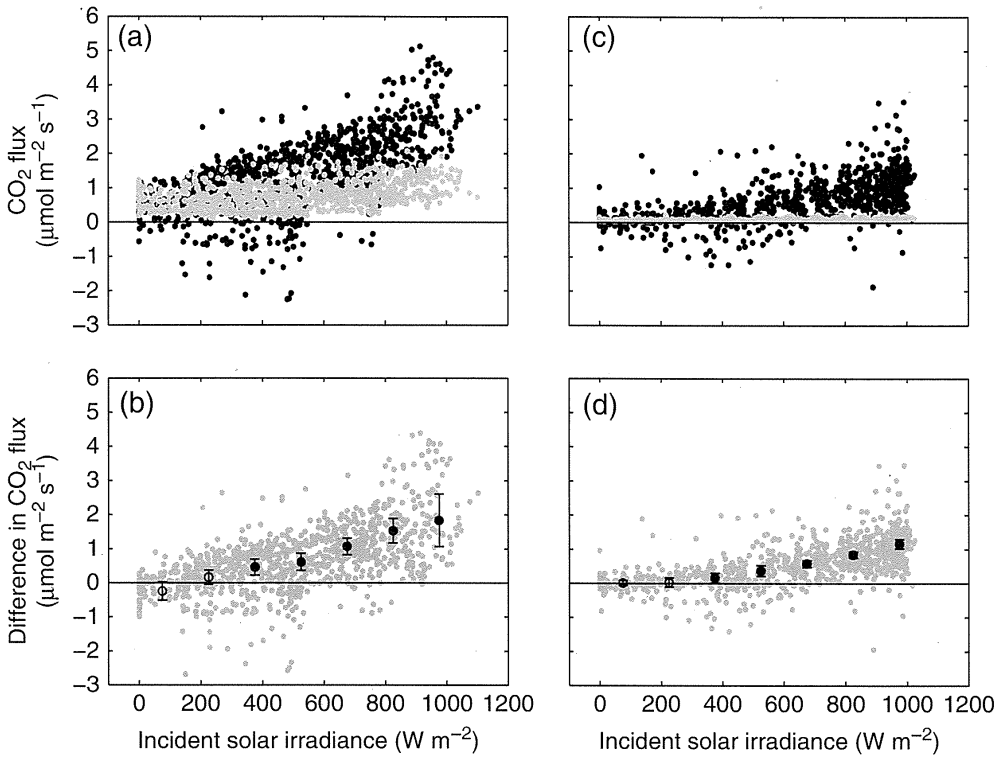

Fig. 1 Illustration of the effect of irradiance on CO_2 fluxes measured at the peatland (a and b) and the grassland (c and d). Fluxes were measured by eddy covariance (black points, a and c), opaque chamber (for peatland, gray points in a) and soil CO_2 probes (for grassland, gray points in c). Gray points in (b and d) are the difference in flux between total CO_2 flux (from EC) and biological CO_2 flux (from chamber or probes). Positive values depict instances where the EC system measured larger CO_2 fluxes than the chamber or probes. Black circles in (b and d) are daily averaged bin averages with error bars showing 95% confidence intervals. For the open circles, the difference between the total and biological CO_2 flux were not statistically different from zero (one sample *t*-test at a 95% significance level). For the filled symbols, the difference was statistically different from zero.

Table 1 Estimates of parameters of multiple regression analyses on peatland and grassland data

Parameter	Estimate coefficient	Standard error	*t*-statistic	*P* value
Peatland (n = 908)				
Constant	−1.2	1.43	−0.82	0.415
Soil temperature	0.042	0.013	3.3	0.001
Soil moisture content	−0.20	2.5	−0.08	0.937
Solar irradiance	0.0019	0.00020	9.2	<0.001
Grassland (n = 885)				
Constant	−0.48	0.64	−0.76	0.448
Surface temperature	0.025	0.00603	4.2	<0.001
Soil moisture content	−7.1	20	−0.35	0.728
Solar irradiance	0.00065	0.00015	4.3	<0.001

Multiple regression equation with abiotic flux (here defined as 'the CO_2 flux measured using eddy covariance minus the CO_2 flux measured using chamber or soil probes') as dependent variable and temperature, soil moisture content and solar irradiance as independent variables. The percentage of the variance that was explained by the total regression was 27.0% and 24.7% for the peatland and grassland regressions, respectively. The number of observations is represented by *n*.

 Global Change Biology, doi: 10.1111/j.1365-2486.2009.02149.x

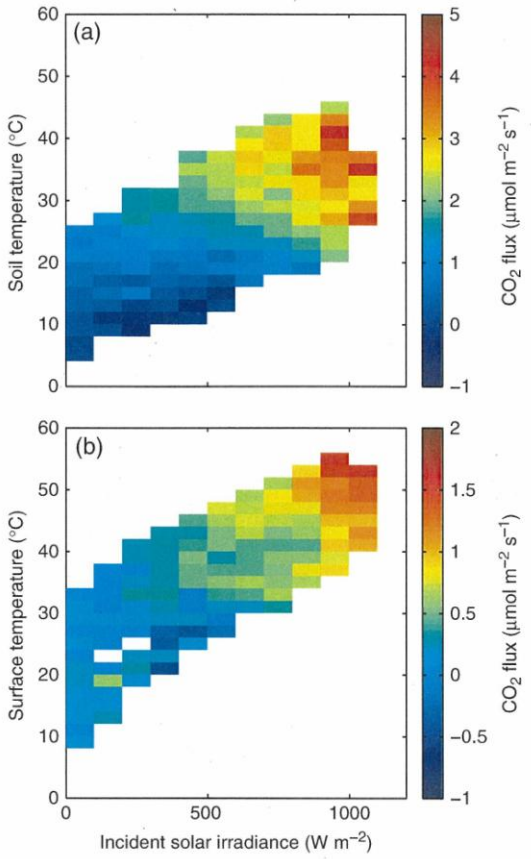

Fig. 2 Effect of solar irradiance and temperature on CO_2 fluxes measured by eddy covariance above (a) the bare peatland and (b) the annual grassland. CO_2 fluxes were averaged across intervals defined by incident solar irradiance (bin width 100 W m^{-2}) and temperature (bin width 2 °C). Note that the scales on the color axes are different between panels. For the peatland, similar graphs with data split into three groups based on volumetric moisture content of the peat are shown in Fig. 3.

dark (irradiance = 0 W m^{-2}) were around zero because low moisture availability constrained microbial decomposition. Even at high temperatures (>60 °C) CO_2 fluxes in the dark remained around zero while fluxes from peat exposed to sunlight were over 0.5 μmol m^{-2} s^{-1} at the same temperature (Fig. 4). The increase in CO_2 concentration on exposure to solar irradiance was nearly instantaneous (Fig. 5), and the immediate effect on the rate of increase in CO_2 concentration caused by passing clouds can clearly be seen (Fig. 5g and h). We observed small negative fluxes in the dark (Fig. 4) that were likely due to adsorption of CO_2 to the plastic or desiccant in the tubing at higher temperatures, even though we confirmed that the container materials did not emit or take up CO_2 by exposing the empty container to solar irradiance. However, the temperature in the container was generally higher when peat was present compared with the empty container because the peat was still warm after absorbing solar irradiance in the sun run preceding the shade run. We suspect that this absorption is affected by temperature only (Fig. 4) which means that shaded and exposed measurements made at the same temperature are still comparable.

Estimates of the contribution of irradiation-induced CO_2 fluxes

For the peatland, the total CO_2 losses for June 2005–May 2007 averaged 269 g C m^{-2} yr^{-1}. The estimate of the annual contribution of photodegradation to the total flux depended on the equation used to model the biological fluxes in the dark and ranged from 34 (using the Lloyd and Taylor equation) to 66 g C m^{-2} yr^{-1} (using a linear equation), representing 13% and 25% of total CO_2 flux, respectively.

For the grassland, the contribution of photodegradation could only be estimated for the dry season when no uptake of CO_2 by photosynthesis was taking place. During the entire 2007 dry season, the CO_2 loss from the grassland was estimated to be 27 g C m^{-2} (or 0.314 g C m^{-2} day^{-1}), of which approximately 16 g C m^{-2} (or 0.186 g C m^{-2} day^{-1}) was irradiation induced, equalling almost 60% of the total dry season CO_2 flux.

Discussion

Size of the irradiance-induced flux

During midday on sunny days in summer, when incoming solar irradiance and temperature were highest, the CO_2 efflux due to photodegradation contributed as much as 62% and 92% of the total half-hourly CO_2 flux from the peatland and grassland, respectively. The magnitude of the annual carbon loss via photodegradation at the peatland (34–66 g C m^{-2} yr^{-1}) was substantial compared with net ecosystem production (NEP) documented for other ecosystems [e.g. average NEP across a range of ecosystems was 181 g C m^{-2} yr^{-1} (Baldocchi, 2008)].

Our estimates of photodegradation at the peatland (34–66 g C m^{-2} yr^{-1}) and the grassland (16 g C m^{-2} for the dry season) were much greater than the estimate made by Brandt *et al.* (2009), who extrapolated measurements made from sterile litter in microcosms to field conditions. They estimated irradiance-induced CO_2 loss of 4 g C m^{-2} yr^{-1} from litter in a desert grassland in New Mexico assuming that 100% of the surface area

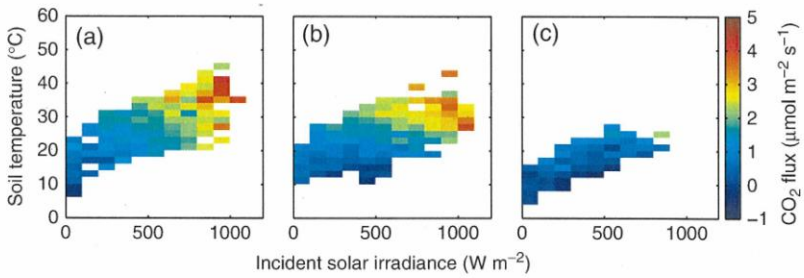

Fig. 3 Effect of solar irradiance and soil temperature on CO_2 fluxes measured by eddy covariance at the peatland for different soil moisture contents. CO_2 fluxes were averaged by intervals defined by incident solar irradiance (bins width 100 W m^{-2}) and soil temperature at 5 mm depth (bin width 2 °C) under (a) dry (volumetric moisture content of peat at 50 mm depth VMC <0.5 m^3 m^{-3}, (b) moist (0.5 m^3 m^{-3} < VMC < 0.56m^3 m^{-3}) and (c) wet (VMC > 0.56m^3 m^{-3}) conditions.

was covered with litter. The causes of the difference between our measurements and their estimate are likely due to differences in substrate species/quality and experimental conditions (e.g. sterile conditions in the microcosms vs. nonsterile conditions in the field and partial blocking of irradiance by the sides of the microcosm).

For the grassland, the irradiance-induced CO_2 losses formed almost 60% of the total CO_2 flux during the dry season. This is at the upper end of the range of estimates (32–60%) of the contribution of photodegradation to mass loss in dry ecosystems given by Austin & Vivanco (2006) and Gallo *et al.* (2009). Even though the percentage contribution of photodegradation to the total CO_2 flux at the grassland site was high, the absolute CO_2 fluxes during dry seasons are generally much lower than during wet seasons when microbes are not limited by moisture (e.g. Xu & Baldocchi, 2004; Xu *et al.*, 2004). For example, annual average ecosystem respiration at the grassland site from 2000 to 2006 was estimated to be >900 g C m^{-2} yr^{-1} (Ma *et al.*, 2007). However, compared with the average net ecosystem exchange (NEE) for the same years (38 g C m^{-2} yr^{-1}; Ma *et al.*, 2007) the dry season irradiance-induced flux of 16 g C m^{-2} yr^{-1} was substantial.

Potential pathways of irradiance-induced CO_2 production

There are two possible pathways for irradiance-induced CO_2 production from OM: the direct abiotic process of photochemical mineralization and the indirect process of microbial facilitation, whereby partial breakdown of OM by irradiance enhances subsequent microbial activity. In the container experiment, photochemical mineralization was the sole pathway leading to CO_2 loss because the dry peat samples did not support biological activity. At the grassland, low microbial respiration rates measured under dry conditions also strongly suggested photochemical mineralization as the main pathway for CO_2 loss. While we deliberately excluded data from wetter periods when microbial facilitation may have been important, there is evidence that this process may also contribute to CO_2 losses during the dry season. Previous studies observed large pulses of CO_2 resulting from rapid microbial respiration following small, infrequent rain events (Xu & Baldocchi, 2004; Xu *et al.*, 2004). Such pulses are common during dry seasons in a wide range of semi-arid ecosystems (Fierer & Schimel, 2003; Huxman *et al.*, 2004; Jarvis *et al.*, 2007) but uncertainty still exists about the origin of the labile carbon that is mineralized after these wetting events (Jarvis *et al.*, 2007). At the grassland, cumulative carbon losses via the pulses were found to be larger at exposed sites than at shaded sites (Xu *et al.*, 2004). We suggest that this difference between shaded and unshaded sites might partly be attributed to partial breakdown of the OM by solar irradiance before rain, making substrates more available to microbes at the unshaded sites. This hypothesis for asynchronous microbial facilitation also fits very well with the observation that the size of the CO_2 pulses tends to be proportional to the length of time since the last rainfall event (Jarvis *et al.*, 2007; Sponseller, 2007).

Potentially affected ecosystems

Photodegradation may be an important contributor to CO_2 loss in a wide range of ecosystems where SOM, litter and/or standing dead material are exposed to solar irradiance (Throop & Archer, 2009). Those affected might include arid and semi-arid ecosystems, barren peat areas in tundra, bare burnt areas, ecosystems that are sparsely vegetated like shrublands, savannas and other grasslands, agricultural sites after cultivation or harvest (especially when crop residues are left on the surface), deciduous forests after leaf fall, ecosystems during prolonged drought or ecosystems with a

naturally large amount of exposed standing dead material like peat bogs. The magnitude of photodegradation in these ecosystems is likely to be <34–66 g C m^{-2} yr^{-1} that we found at our peatland because the conditions will be less favorable for photodegradation. Most ecosystems have smaller amounts of accumulated exposed OM (especially arid and semi-arid ecosystems) or dead OM is only exposed to solar irradiance during part of the year (e.g. harvested cropland or ecosystems during seasonal drought like the Californian grassland). In some ecosystems, OM will be exposed to levels of incoming solar irradiance that are lower than in our study (e.g. exposed peat in tundra in boreal regions or deciduous forests where litter will only be exposed in winter).

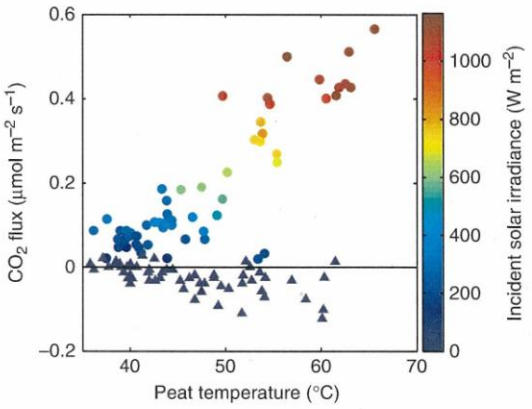

Fig. 4 CO_2 flux from air-dried peat measured in a container transparent to visible and UV light alternately exposed to solar irradiance (colored circles) and shaded (triangles).

Implications for measurements and modelling

There are several important implications of photodegradation for the current approaches to measurement and interpretation of CO_2 fluxes. Opaque chambers and soil CO_2 profiles are commonly used to measure CO_2 efflux. However, they may significantly underestimate actual CO_2 losses because they do not measure the irradiance-induced portion of the CO_2 flux. For example, at our sites, chamber and soil probe measurements underestimated the total CO_2 efflux by as much as 62% and 92% for the peatland and grassland, respectively, when the contribution of photodegradation to the total CO_2 flux was at its maximum. Also, for studies which aim to measure net ecosystem exchange of CO_2 of vegetated ecosystems using transparent chambers placed over plants, it is important that the chambers are transparent not only to photosynthetically active radiation, but also to radiation in the UV wavelengths. Otherwise, the photodegradation component of the CO_2 efflux might be underestimated, leading to overestimates of net CO_2 sequestration.

Additionally, in many ecosystem studies of CO_2 exchange using EC, models based on night-time measurements are used to estimate daytime respiration rates to enable partitioning of daytime NEE into photosynthesis and respiration (Falge *et al.*, 2002; Reichstein *et al.*, 2005). However, this approach does not take into account

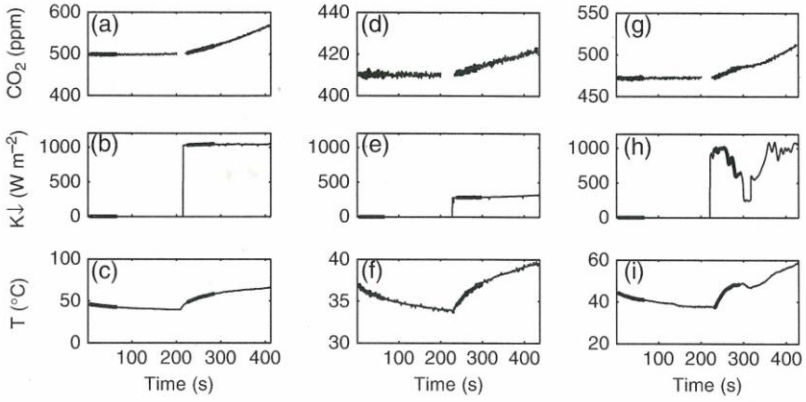

Fig. 5 Example data of the small scale container experiment. CO_2 molar fraction (a, d and g), incident solar irradiance (b, e and h) and peat temperature (c, f and i) during three sets of two consecutive runs: runs 8 and 9 (a, b and c), with CO_2 fluxes of −0.01 and 0.39 µmol m^{-2} s^{-1}, respectively; runs 80 and 81 (d, e and f) with CO_2 fluxes of 0.01 and 0.09 µmol m^{-2} s^{-1} respectively; runs 86 and 87 (g, h and i) with CO_2 fluxes 0 and 0.29 µmol m^{-2} s^{-1}, respectively. Individual runs were 200 s long. Bold lines indicate the CO_2 concentration data that were used for flux calculation (60 s) and the matching irradiance and temperature data. The container was shaded from the sun when irradiance (K↓) was 0 W m^{-2}. Please note that scales on *y*-axes differ between graphs of CO_2 concentration (top panels) and graphs of temperature (bottom panels).

photodegradation (a daytime-specific pathway of CO_2 loss) and consequently might underestimate both daytime total CO_2 losses and CO_2 uptake by photosynthesis.

Conclusions

We have demonstrated that solar irradiance contributes directly to ecosystem CO_2 losses through photodegradation of OM. Previously solar irradiance has been assumed to contribute to CO_2 losses only indirectly by regulating temperature, which in turn controls microbial respiration.

The grassland data showed that photodegradation can be responsible for a substantial portion of CO_2 losses in a natural ecosystem during the dry season. Because the ecosystems potentially affected by photodegradation comprise very large areas on a global scale [e.g. arid and semi-arid ecosystems cover ~30% of the Earth's land surface (Lal, 2004)], even small contributions from photodegradation to CO_2 fluxes could represent large fluxes of carbon when summed globally. These losses are currently unaccounted for by carbon cycling models.

Small-scale laboratory studies have started to elucidate how wavelength, litter species, litter density, irradiance intensity and moisture affect OM decomposition and CO_2 loss through photodegradation (e.g. Brandt *et al.*, 2009; Smith *et al.*, 2010), but it is essential to extend this work to natural field conditions and appropriate scales. Quantifying the role of irradiance-induced CO_2 losses in the field will be challenging; particularly problematic is separating CO_2 fluxes into photodegradation, biologically driven decomposition and photosynthesis in systems where water does not limit biological activity. Despite these challenges, it is crucial that we conduct further studies in a wide variety of ecosystems to increase our understanding of the importance and drivers of photodegradation. This knowledge is needed for gaining insight into the response of carbon cycling in terrestrial ecosystems to climate change (Austin & Vivanco, 2006) and for continued development of coupled carbon-climate models.

Acknowledgements

The New Zealand study was supported by the University of Waikato and Landcare Research Ltd (contract number C09X0705). S. R. was funded through a University of Waikato Doctoral Scholarship with additional funding from Landcare Research Ltd and Dairy NZ. We thank Environment Waikato for permission to conduct the study at Torehape peat mine and Gamman Mining for access to the peat mine and for delaying restoration activities; R. Gamman, P. Gamman and D. Bowers for general logistics; C. Burgess, C. McKinnon, M. Evans and C. Hosking helped maintain the EC system and many others assisted with chamber measurements. R. Littler conducted the statistical analyses. The California study was supported in part by the Office of Science (BER), U.S. Department of Energy, grant no. DE-FG02-03ER63638. We also thank Dr Siyan Ma, Dr Rodrigo Vargas, Dr Jianwu Tang and Mr Ted Hehn for assistance in the field and computation of the fluxes. We thank G. J. Steeneveld, G. P. Sparling, D. Whitehead, J. F. Bornman, J. E. Hunt, J. Laubach, M. U. F. Kirschbaum, J. Six and D. T. Rutledge for comments on earlier versions of the manuscript. The comments of the subject editor and two anonymous reviewers helped to substantially improve the manuscript.

References

Anesio AM, Tranvik LJ, Graneli W (1999) Production of inorganic carbon from aquatic macrophytes by solar radiation. *Ecology*, **80**, 1852–1859.

Austin AT, Vivanco L (2006) Plant litter decomposition in a semi-arid ecosystem controlled by photodegradation. *Nature*, **442**, 555–558.

Baldocchi D (2008) Breathing of the terrestrial biosphere: lessons learned from a global network of carbon dioxide flux measurement systems. *Australian Journal of Botany*, **56**, 1–26.

Baldocchi D, Tang JW, Xu LK (2006) How switches and lags in biophysical regulators affect spatial-temporal variation of soil respiration in an oak-grass savanna. *Journal of Geophysical Research-Biogeosciences*, **111**, doi: 10.1029/2005JG063.

Baldocchi DD (2003) Assessing the eddy covariance technique for evaluating carbon dioxide exchange rates of ecosystems: past, present and future. *Global Change Biology*, **9**, 479–492.

Baldocchi DD, Xu L, Kiang N (2004) How plant functional-type, weather, seasonal drought, and soil physical properties alter water and energy fluxes of an oak-grass savanna and an annual grassland. *Agricultural and Forest Meteorology*, **123**, 13–39.

Brandt LA, Bohnet C, King JY (2009) Photochemically induced carbon dioxide production as a mechanism for carbon loss from plant litter in arid ecosystems. *Journal of Geophysical Research*, **114**, doi: 10.1029/2008JG0772.

Brandt LA, King JY, Milchunas DG (2007) Effects of ultraviolet radiation on litter decomposition depend on precipitation and litter chemistry in a shortgrass steppe ecosystem. *Global Change Biology*, **13**, 2193–2205.

Day TA, Zhang ET, Ruhland CT (2007) Exposure to solar UV-B radiation accelerates mass and lignin loss of *Larrea tridentata* litter in the Sonoran Desert. *Plant Ecology*, **193**, 185–194.

Falge E, Baldocchi D, Tenhunen J *et al.* (2002) Seasonality of ecosystem respiration and gross primary production as derived from FLUXNET measurements. *Agricultural and Forest Meteorology*, **113**, 53–74.

Fierer N, Schimel JP (2003) A proposed mechanism for the pulse in carbon dioxide production commonly observed following the rapid rewetting of a dry soil. *Soil Science Society of America Journal*, **67**, 798–805.

Gallo ME, Porras-Alfaro A, Odenbach KJ, Sinsabaugh RL (2009) Photoacceleration of plant litter decomposition in an arid environment. *Soil Biology and Biochemistry*, **41**, 1433–1441.

Gallo ME, Sinsabaugh RL, Cabaniss SE (2006) The role of ultraviolet radiation in litter decomposition in arid ecosystems. *Applied Soil Ecology*, **34**, 82–91.

Gehrke C, Johanson U, Callaghan TV, Chadwick D, Robinson CH (1995) The impact of enhanced ultraviolet-B radiation on litter quality and decomposition processes in *Vaccinium* leaves from the subarctic. *Oikos*, **72**, 213–222.

Grace J, Rayment M (2000) Respiration in the balance. *Nature*, **404**, 819–820, doi: 810.1038/35009170.

Henry HAL, Brizgys K, Field CB (2008) Litter decomposition in a California annual grassland: interactions between photodegradation and litter layer thickness. *Ecosystems*, **11**, 545–554.

Huxman TE, Snyder KA, Tissue D *et al.* (2004) Precipitation pulses and carbon fluxes in semiarid and arid ecosystems. *Oecologia*, **141**, 254–268.

Janzen HH (2004) Carbon cycling in earth systems – a soil science perspective. *Agriculture, Ecosystems and Environment*, **104**, 399–417.

Jarvis P, Rey A, Petsikos C *et al.* (2007) Drying and wetting of Mediterranean soils stimulates decomposition and carbon dioxide emission: the 'Birch effect'. *Tree Physiology*, **27**, 929–940; doi: 910.1093/treephys/1027.1097.1929.

Lal R (2004) Carbon sequestration in dryland ecosystems. *Environmental Management*, **33**, 528–544.

Lloyd J, Taylor JA (1994) On the temperature dependence of soil respiration. *Functional Ecology*, **8**, 315–323.

Luo Y, Zhou X (2006) *Soil Respiration and the Environment*. Academic Press/Elsevier, San Diego, CA.

Ma S, Baldocchi DD, Xu L, Hehn T (2007) Inter-annual variability in carbon dioxide exchange of an oak/grass savanna and open grassland in California. *Agricultural and Forest Meteorology*, **147**, 157–171.

McMillen RT (1986) *A BASIC Program for EC in non-simple terrain*. NOAA Tech Memo ERL ARL-147.

Moody SA, Paul ND, Bjorn LO *et al.* (2001) The direct effects of UV-B radiation on *Betula pubescens* litter decomposing at four European field sites. *Plant Ecology*, **154**, 27–36.

Moore CJ (1986) Frequency response corrections for eddy correlation systems. *Boundary Layer Meteorology*, **37**, 17–35.

Newsham KK, McLeod AR, Roberts JD, Greemslade PD, Emmett BA (1997) Direct effects of elevated UV-B radiation on the decomposition of *Quercus robur* leaf litter. *Oikos*, **79**, 592–602.

Pancotto VA, Sala OE, Cabello M *et al.* (2003) Solar UV-B decreases decomposition in herbaceous plant litter in Tierra del Fuego, Argentina: potential role of an altered decomposer community. *Global Change Biology*, **9**, 1465–1474.

Reichstein M, Falge E, Baldocchi D *et al.* (2005) On the separation of net ecosystem exchange into assimilation and ecosystem respiration: review and improved algorithm. *Global Change Biology*, **11**, 1424–1439.

Rozema J, Tosserams M, Nelissen HJM, van Heerwaarden L, Broekman RA, Flierman N (1997) Stratospheric ozone reduction and ecosystem processes: enhanced UV-B radiation affects chemical quality and decomposition of leaves of the dune grassland species. *Calamagrostis epigeios*. *Plant Ecology*, **128**, 285–294.

Schipper LA, Clarkson BR, Vojvodic-Vukovic M, Webster R (2002) Restoring cut-over restiad peat bogs: a factorial experiment of nutrients, seed and cultivation. *Ecological Engineering*, **19**, 29–40.

Schotanus P, Nieuwstadt FTM, de Bruin HAR (1983) Temperature measurement with a sonic anemometer and its application to heat and moisture fluxes. *Boundary Layer Meteorology*, **26**, 81–90.

Schuepp PH, Leclerc MY, Macpherson JI, Desjardins RL (1990) Footprint prediction of scalar fluxes from analytical solutions of the diffusion equation. *Boundary Layer Meteorology*, **50**, 355–373.

Smith WK, Gao W, Steltzer H, Wallenstein MD, Tree R (2010) Moisture availability influences the effect of ultraviolet-B radiation on leaf litter decomposition. *Global Change Biology*, **16**, 484–495.

Sponseller RA (2007) Precipitation pulses and soil CO_2 flux in a Sonoran Desert ecosystem. *Global Change Biology*, **13**, 426–436.

Tang J, Baldocchi DD (2005) Spatial and temporal variation in soil respiration in an oak-grass savanna ecosystem in California and its partitioning into autotrophic and heterotrophic components. *Biogeochemistry*, **73**, 183–207.

Tang J, Baldocchi DD, Qi Y, Xu L (2003) Assessing soil CO_2 efflux using continuous measurements of CO_2 profiles in soils with small solid-state sensors. *Agricultural and Forest Meteorology*, **118**, 207–220.

Throop HL, Archer SR (2009) Resolving the dryland decomposition conundrum: some new perspectives on potential drivers. In: *Progress in Botany*, Vol. 70 (eds Lüttge U, Beyshchlag W, Büdel B, Francis D), pp. 171–194. Springer-Verlag, Berlin.

Vanderbilt KL, White CS, Hopkins O, Craig JA (2008) Aboveground decomposition in arid environments: results of a long-term study in central New Mexico. *Journal of Arid Environments*, **72**, 696–709.

Verhoef HA, Verspagen JMH, Zoomer HR (2000) Direct and indirect effects of ultraviolet-B radiation on soil biota, decomposition and nutrient fluxes in dune grassland soil systems. *Biology and Fertility of Soils*, **31**, 366–371.

Webb EK, Pearman GJ, Leuning R (1980) Correction of flux measurements for density effects due to heat and water vapour transfer. *Quarterly Journal of the Royal Meteorological Society*, **106**, 85–100.

Xu L, Baldocchi DD (2004) Seasonal variation in carbon dioxide exchange over a Mediterranean annual grassland in California. *Agricultural and Forest Meteorology*, **123**, 79–96.

Xu L, Baldocchi DD, Tang J (2004) How soil moisture, rain pulses, and growth alter the response of ecosystem respiration to temperature. *Global Biogeochemical Cycles*, **18**, doi: 10.1029/2004GB02281.

Zepp RG (2003) Solar ultraviolet radiation and aquatic carbon, nitrogen, sulfur and metals cycles. In: *UV Effects in Aquatic Organisms and Ecosystems* (eds Helbling EW, Zagarese H), pp. 137–183. Royal Society of Chemistry, Cambridge, UK.

Appendix B Timing error

B.1 Introduction

To assure reliable measurements of turbulent fluxes of water vapour (H_2O) and carbon dioxide (CO_2) from an eddy covariance (EC) system, it is necessary that signals from the gas analyser and sonic anemometer are synchronized (Aubinet et al., 2000; McDermitt, 2003; Wolf et al., 2008; Zeller et al., 2001). A common approach to synchronise the signals from the gas analyser and sonic anemometer is to find the delay (within a window allowed by the researcher) where the absolute correlation coefficient is optimal (e.g. Aubinet et al., 2000; Leuning and King, 1992; McMillen, 1988 and references therein). This approach is often applied when using closed path EC systems because of the (sometimes large) lag between sonic anemometer and gas analyser signals caused by the time it takes for air to travel through the tube from the sampling point close to the anemometer to the gas analyser. In contrast, this practice is not universally applied when using open path gas analysers because anemometer and gas analyser are co-located and there is no 'transport time' of air. The only processes that could lead to a-synchronous signals from sonic anemometer and gas analyser in this case are sensor separation and a difference in the processing time of the two sensors. Sensor separation and is normally accounted by frequency response corrections, for example those suggested by Moore (1986) or Massman (2000). The difference in processing time between the two sensors is constant with time (i.e. it is a fixed lag) and can be accounted for in the processing software (e.g. Haslwanter et al., 2008).

If the signals of the sonic anemometer and gas analyser are not properly synchronised and fluxes are calculated with a 'timing error', this causes a degradation of the correlation between the fluctuation in gas density and vertical wind speed, and leads to an underestimation of the measured flux (McDermitt, 2003; Wolf et al., 2008; Zeller et al., 2001).

In 2003, LI-COR discovered a timing error in the embedded software of the LI-7500 open path gas analyser and sent a notice to all users to upgrade to the new improved version of the software and to change the settings

(McDermitt, 2003). LI-COR's experiments indicated that the size of the underestimation of fluxes caused by this timing error was affected by wind speed and installation height, where largest errors were expected above a short crop at high wind speeds (McDermitt, 2003). The magnitude of the error was reported to be between 0 and 15% for CO_2 and H_2O fluxes (McDermitt, 2003).

Several other studies have examined the effect of errors in signal synchronisation on the calculated fluxes (summarised in Table B.1).

Table B.1Overview of studies on the effect of a timing error between signals of the gas analyser and sonic anemometer.

	Measurement height (m)	Measurement frequency (Hz)	Timing error (scans)	Underestimation of *LE* (%)	Underestimation of F_c (%)
(Zeller et al., 2001)	2.6	10	2	9 - 24	10 - 27
Application note LI-COR (McDermitt, 2003)	2 setups: 2.2 and 3.1 m above canopy	10	1	0 - 15	0 - 16
Mauder (2004)	2.4 m	20	2-3	7	33
Christen (2005)	5 setups between 2.4 and 31.7 m	20	1	0 - 2	0 - 3
Baker and Griffis (2005)	Varied throughout season	10	1.3	-	5 - 13
Wolf et al. (2008)	1 m above canopy	10	~1.5*	8	20

*Personal communication Adam Wolf.

Christen (2005) analysed the effect of the timing error using data obtained at several sites and found small underestimations (0 to 3%) for the CO_2 flux. The largest underestimates were found when instruments were mounted closer to the roughness elements. Baker and Griffis (2005) also found underestimations of both *LE* and F_c of between 5-13% when measuring over a corn-soybean field. Mauder (2004) showed one day of data for an experiment where instruments were mounted 2.4 m above a corn field, with a sampling frequency of 20 Hz. The timing error of 2-3 scans lead to an underestimation of 7% for *LE* and up to 33 % for F_c. Similarly large underestimation of fluxes were

measured by Wolf et al. (2008), who measured turbulent fluxes at 10 Hz 1.3 m above ground level, which was 1 m above a pristine grass-forb steppe. When correcting for the lag of approximately 1.5 scans (pers. comm. Adam Wolf) between anemometer and gas analyser signals, the CO_2 flux increased by 20%, whereas the effect on *LE* was much smaller with an 8% increase.

B.2 Timing error at the peatland

B.2.1 Aim

Our research group never received notification from LI-COR about the error in the embedded software of the LI-7500, and the peatland data presented in this thesis was collected with an LI-7500 gas analyser with the incorrect settings of the embedded software. This meant that the signals of the sonic anemometer and gas analyser were not properly synchronised before calculation of the fluxes of water vapour and CO_2. Recalculation of fluxes with the correct delays was not possible because high-frequency data were not available. In July 2007, after the current study at the peatland, the EC system was moved to a pasture site and upgraded to store high-frequency data. This section describes how the high frequency data at the pasture site were used to estimate the error in fluxes of water vapour (*LE*) and CO_2 (F_c) caused by the timing error at the peatland.

B.2.2 Methods: Estimation of effect of timing error

In short, the size of the bias in *LE* and *F*c at the peatland as a result of a timing error was estimated using the following approach:

- at the pasture site, fluxes were calculated with and without a simulated timing error
- empirical relationships were developed between the size of the underestimation of the flux caused by the timing error and relevant variables.
- the empirical relationships were applied to the peatland data to correct for the underestimation of the flux caused by the timing error.

These steps will be further explained below.

After the study at the peatland, the open path EC system was upgraded to store high frequency data before it was installed at a dairy farm in December 2007 for a different research project (Kuske, 2009; Mudge, 2009). This pasture site was situated approximately 50 km from the peatland site. Instruments were mounted at 2.85 m and the sampling frequency was increased to 20 Hz. At the peatland, measurements affected by the timing error had been made at both 1.5 m and 2.5 m height. Because measurement height was expected to influence the effect of a timing error (Christen, 2005; Mauder, 2004), the instruments at the pasture site were temporarily lowered from their normal measurement height of 2.85 m to 1.5 m for 22 days in June 2008 so that the effect of the timing error could be determined for both heights. For the analysis, the 20Hz high frequency data from the pasture site were sub-sampled to 10 Hz to match the sampling frequency at the peatland. The main remaining difference between the peatland site and the pasture site was the vegetation cover: the peatland was bare whereas there was short grass at the pasture site.

Covariances were calculated for the pasture site using an optimal delay determined by maximizing the absolute correlation coefficient between vertical wind speed and scalar concentration (Aubinet et al., 2000). Optimum delays were calculated separately for CO_2 and H_2O. The covariances were rotated using the classic 2D rotation (McMillen, 1986) , and corrected for the moisture effect on the sonic temperature (Schotanus et al., 1983) and for loss of frequency response (Moore, 1986). The WPL term was not added at this stage and these fluxes will be referred to as ‘before-WPL’ fluxes. In the same manner, two other sets of covariances were calculated for which the signals of vertical wind speed and scalar concentration were shifted by 1 and 2 scans respectively. These covariances were combined in a weighted average to give the covariance at a delay of 1.3 scans, because this was the number of scans that the signals were mis-aligned by during the measurements at the peatland (Box 1).

Box 1

To calculate turbulent fluxes correctly, the signals from the gas analyser and the sonic anemometer need to be synchronised. The processing time of the gas analyser however is longer than that of the sonic anemometer, resulting in an a-synchronous transfer of the signal to the datalogger that collects the data and calculates the fluxes. For this reason, the datalogger is programmed to delay the sonic anemometer signals so that it matches the time it takes for the gas analyser to process and transfer the measurements to the datalogger.

The documentation provided by LI-COR stated that the processing time of the LI-7500 was 230 ms (Table B.2, (McDermitt, 2003)), which equals 2.3 scans at 10 Hz To make this a round number, extra delay steps were added in the embedded software of the LI-7500 (11 steps of 6.579 each), to get a total delay time of 230 ms + 11 · 6.579 ms = 302 ms. The datalogger was therefore programmed to delay the sonic anemometer signals by 302 ms/100 ms scan^{-1} ≈ 3 scans.

Table B.2 Total system delay calculation. Total delay = delay time + (delay step · delay step increment). Data from McDermitt (2003).

	Delay time (ms)	Delay step (ms)	Delay step increment	Total delay (ms)	Number of scans (10 Hz)
Published	230	6.579	11	302*	3
Actual	88-147 (mean 117)	4.5	11	138-197 (mean 167)	± 1.7

However, the values reported in the documentation were found to be incorrect, with both the delay time and the delay step shorter than reported (Table B.2). This resulted in a total delay of approximately 167 ms, or 1.7 scans. The datalogger however was still set to delay the anemometer signals by 3 scans, introducing a timing error of approximately 3 – 1.7 = 1.3 scans.

Previous studies suggest that the size of the underestimation of the flux is affected by measurement height, the size of the flux itself (*LE* or F_c), wind speed, wind direction and sensor separation (Section B.1 and references therein). Stepwise regression was used to determine which of these variables were most strongly correlated to the underestimation of the flux. Because stringent filtering was already applied for wind direction at the peatland because of the limited fetch, wind direction was not considered in the development of the empirical relationships. Also, sensor separation was not included as a potential predictor because sensor separation was small (60 mm) and it was assumed that the effect of the sensor separation was already corrected for by the frequency response correction. Using the remaining potential drivers (size of the flux and wind speed

u), separate regressions were determined for the underestimation of the flux (= before-WPL flux with a timing error of 1.3 scans minus before-WPL flux without timing error) for both fluxes (LE and F_c) at both measurement heights (2.85 m and 1.5 m). Outliers for all regressions were removed using a 95% confidence interval.

To correct for the timing error at the peatland, the obtained regression equations were used to estimate the bias in the before-WPL *LE* and F_c separately for both measurement heights. It was assumed that the difference in height for the 'high instalment height' between pasture site and peatland (2.85 m and 2.5 m, respectively) would not affect the results and the regression equations based on data collected at 2.85 m at the pasture site were used to predict the underestimation of the fluxes obtained at 2.5 m at the peatland. These underestimations were added to the before-WPL fluxes to obtain an estimate of the correct before-WPL flux. For each estimate the WPL term was individually calculated and added to obtain the final flux.

B.2.3 Results and discussion

Effect of the timing error on *F*c and *LE* at the pasture site

Figure B.1 illustrates how asynchronous signals from the sonic anemometer and gas analyser caused underestimation of before-WPL fluxes of water vapour and CO_2 at the pasture site. Largest fluxes (most positive for *LE* and most negative for F_c) were calculated when the optimal delay was used, whereas introducing a delay of -2, -1, +1 or +2 scans led to an underestimation of the fluxes. The underestimation seemed linear with the number of scans delayed (i.e. the underestimation with a delay of 2 scans was twice as large as the underestimation with a delay of 1 scan), which justified the approach with the weighted average to obtain the underestimation of the flux at 1.3 scans.

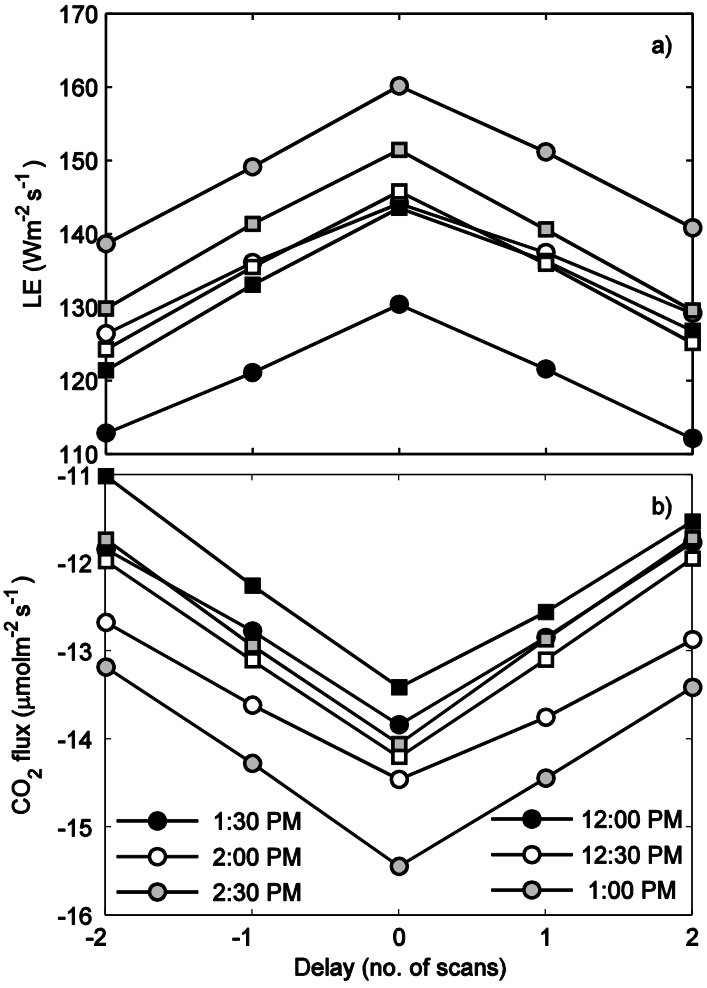

Figure B.1 Example of the effect of lack of synchronization of the signals from the sonic anemometer and the gas analyser on the size of the raw (before-WPL) fluxes of water vapour (a) and CO_2 (b). Data presented were collected at the pasture site during 6 half hours on 26 Feb 2008 with instruments mounted at 2.85 m.

Using stepwise regression, u^2 and *LE* were identified as significant predictors of the underestimation of the before-WPL *LE* caused by the timing error. For the CO_2 flux F_c, the best relationship (i.e. highest portion variance explained) was found using u, F_c and F_c^2. The regression parameters and R^2 values can be found in Table B.3 and the regressions are shown in Figure B.2. Regressions explained between 76% and 91% of the total variance.

Table B.3 Regression parameters for equations estimating the underestimation of the flux as a result of the timing error.

Flux	Measurement height	Regression parameters				R^2	*n*
		a	*b*	*c*			
LE	High	4.00	- 0.447	- 0.0665		0.83	851
	Low	2.95	- 0.731	- 0.132		0.89	75
		d	*e*	*f*	*g*		
F_c	High	-0.540	0.192	- 0.0756	$0.581 \cdot 10^{-3}$	0.77	859
	Low	-0.574	0.216	- 0.147	$3.89 \cdot 10^{-3}$	0.75	72

Regression equations $\Delta LE = a + b \cdot u^2 + c \cdot LE$ and $\Delta F_c = d + e \cdot u + f \cdot F_c + g \cdot F_c^2$ where ΔLE and ΔF_c are the underestimation in *LE* and F_c respectively. R^2 is the fraction of the variance that was explained by the total regression. The number of observations is given by *n*.

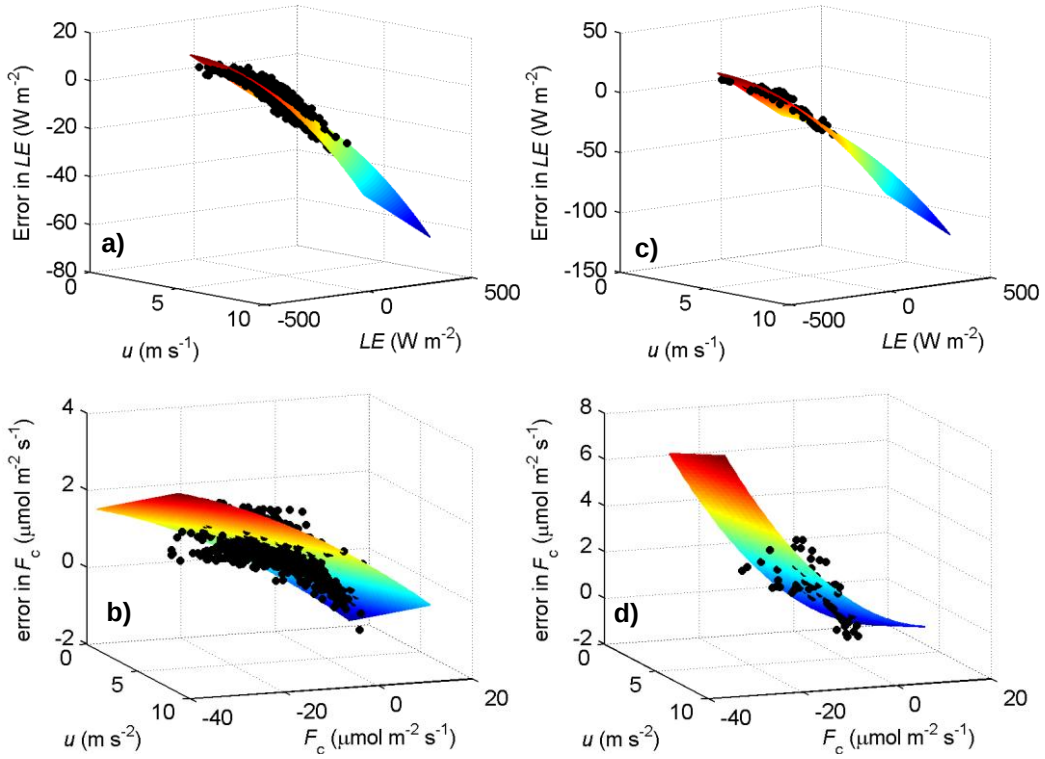

Figure B.2Regressions used to describe the error in the before-WPL flux of water vapour (a and c) and CO_2 (b and d) based on wind speed and the flux for high (a and b) and low (c and d) measurement heights at the pasture site. Points are the measured data and planes depict the regressions listed in Table B.3.

Effect of the timing error on *F*c and *LE* at the peatland

The regression equations based on the data from the pasture site were applied to the peatland data to obtain estimates of the underestimation of the before-WPL F_c and *LE* at the peatland.

Following Wolf et al. (2008), the effect of the timing error at the peatland was assessed by the slope of the regression of the flux affected by signal asynchrony (as dependent variable) vs. the flux corrected for the signal asynchrony (as independent variable; see Figure B.3 for an example).

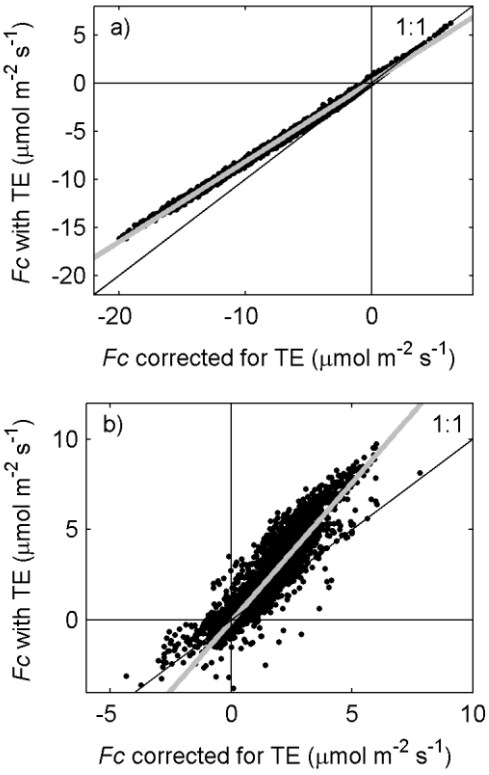

Figure B.3 Regression of F_c affected by the timing error on F_c corrected for the timing error (TE) before (a) and after (b) addition of the WPL term for peatland data obtained at the low measurement height. The black line indicates the 1:1 line, the grey line the regressions. Regression equations are listed in Figure B.4.

Before-WPL fluxes at the low measurement height were underestimated by approximately 15% and 16% for *LE* and F_c, respectively, as a result of signal asynchrony. At the higher measurement height, underestimations were smaller with 7% and 12% for *LE* and F_c respectively (Figure B.4). After-WPL *LE* was underestimated by approximately the same amount as the before-WPL *LE*: 14 %

and 7% for low and high measurement height, respectively (Table B.4), because of the relatively small size of the WPL term for *LE*. In contrast, when compared to the after-WPL flux, the underestimation of the CO_2 flux caused by the timing error resulted in a much larger discrepancy. The addition of the (often large) WPL term to the CO_2 fluxes often resulted in the change in the sign of the flux from negative (indicating apparent uptake by the peat surface) to positive (indicating loss of CO_2 from the peat surface; Figure B.4; see also Appendix D). Absolute values of the resulting positive after-WPL fluxes were smaller than those of the negative before-WPL fluxes. The smaller absolute value of the flux and the sign change meant that, when expressed as a ratio of the correct flux, F_c was on average *overestimated* by as much as 150 to 176 % for the high and low measurement height respectively as a result of the timing error (Table B.4 and Figure B.3).

Figure B.4 shows an example of the large effect of the timing error on the after-WPL daytime CO_2 fluxes during the summer of 2006.

Table B.4Regression parameters for equations like $LE_{TE} = a + b \cdot LE_{cor}$ where LE_{TE} is *LE* affected by the timing error, and LE_{cor} is *LE* corrected for the timing error. Intercept units are W m^{-2} for *LE* and µmol m^{-2} s^{-1} for F_c.

		Before WPL				After WPL			
Flux	Measurement height	Intercept	Slope	R^2	Ratio	Intercept	Slope	R^2	Ratio
LE	High	1.30	0.92	1.00	0.93	1.08	0.92	1.00	0.93
	Low	-2.6	0.86	1.00	0.85	-2.45	0.87	1.00	0.86
F_c	High	0.11	0.93	1.00	0.88	0.33	0.96	0.91	1.76
	Low	0.15	0.83	1.00	0.84	-0.08	1.53	0.89	1.5

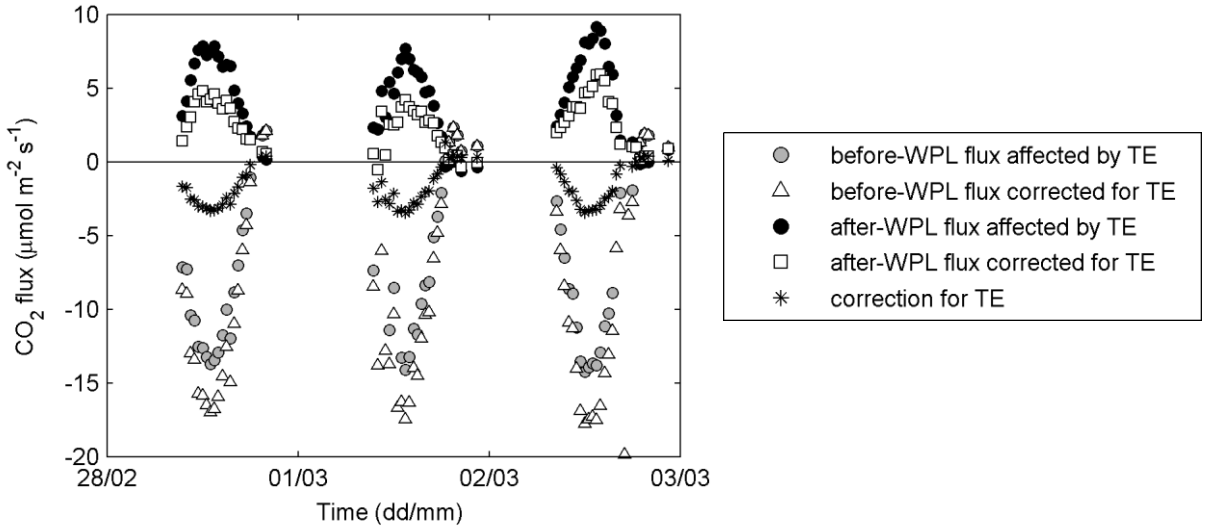

Figure B.4Example illustrating the effect of the timing error (TE) on before-WPL and after-WPL CO_2 fluxes at the peatland during late summer in 2006. Grey dots are the before-WPL fluxes affected by the timing error. Addition of the WPL term to these biased fluxes would result in large positive fluxes (black dots). Regression equations (based on the pasture-site data) applied to the before-WPL peatland fluxes (grey dots) results in before-WPL fluxes that are corrected for the bias caused by signal asynchrony (white triangles). The size of the bias caused by the timing error is shown as asterisks (*). Note how the bias shows a clear diurnal variation with largest bias during midday. Addition of the WPL term to the before-WPL fluxes corrected for the timing error (white triangles) results in the final fluxes (white squares).

The average underestimation of the before-WPL *LE* and F_c at the peatland (Table B.4) was within the range of underestimations caused by asynchronous signals reported by previous studies (Figure B.1 and Section B.1) but at the high end of the range found by LI-COR (McDermitt, 2003). The large size of the underestimation was probably due to the relatively low measurement height and high windspeeds at the peatland. Zeller et al., (2001) , Wolf et al. (2008) and Mauder (2004) reported even larger values for the underestimation of *LE* and F_c, but these studies reported on the underestimations of fluxes caused by larger timing errors (from 1.5 to 3 scans) than occurred at the peatland (1.3 scans). Similarly, the very small underestimations reported by Christen (2005) were possibly the result of the very small timing error (1 scan at 20 Hz) that was examined. The effect of measurement height on the underestimation (Christen, 2005; McDermitt, 2003) could most clearly be observed for *LE* at the peatland (decrease from 15% to 7% when moving from 1.5 to 2.5 m). Only at the high measurement height was the underestimation of *LE* smaller than that of F_c, similar to the findings by Mauder (2004) and Wolf et al. (2008). At the low

measurement height however, percentage underestimations were the same for *LE* and F_c, which was similar to the findings of McDermitt (2003), Christen (2005) and Zeller et al. (2001).

Effect of timing error on energy balance closure at the peatland

As an indicator of data quality, it is common to examine the degree to which the measured turbulent fluxes (sensible heat flux *H* + latent heat flux *LE*) can account for the available energy (net radiation R_n minus soil heat flux *G,* where *G* includes change of storage of heat in the soil) at the surface (Aubinet et al., 2000; Baldocchi, 2008a).

There are two common approaches to evaluate the energy balance closure. The first is the energy balance ratio (EBR, see Wilson et al., 2002), defined as

$$\mathrm{EBR} = \Sigma\left(H + LE\right)/\Sigma\left(R_n - G\right) \qquad \textbf{Equation B.1}$$

The second approach uses the slope of the linear regression, with R_n -*G* as independent variable and *H*+*LE* as the dependent variable, as an estimate of energy balance closure.

Before correcting for the underestimation of *LE* caused by signal asynchrony, energy balance closure was 84% (both EBR and the slope of the regression were 0.84, Figure B.5a). After correcting for the underestimation of *LE* caused by the timing error energy balance closure improved and the slope of the regression was 0.91 (EBR over the whole period was 0.92, Figure B.5b)

B.3 Summary

This appendix describes the effect of a timing error of 1.3 scans between the signals of the sonic anemometer and the gas analyser when sampling at 10 Hz at the peatland. Because high frequency data were not available for re-calculation of the fluxes with the correct delay, empirical correction equations based on high frequency data from a later installation of the same EC system at a different study site were used to quantify the effect of the timing error on fluxes

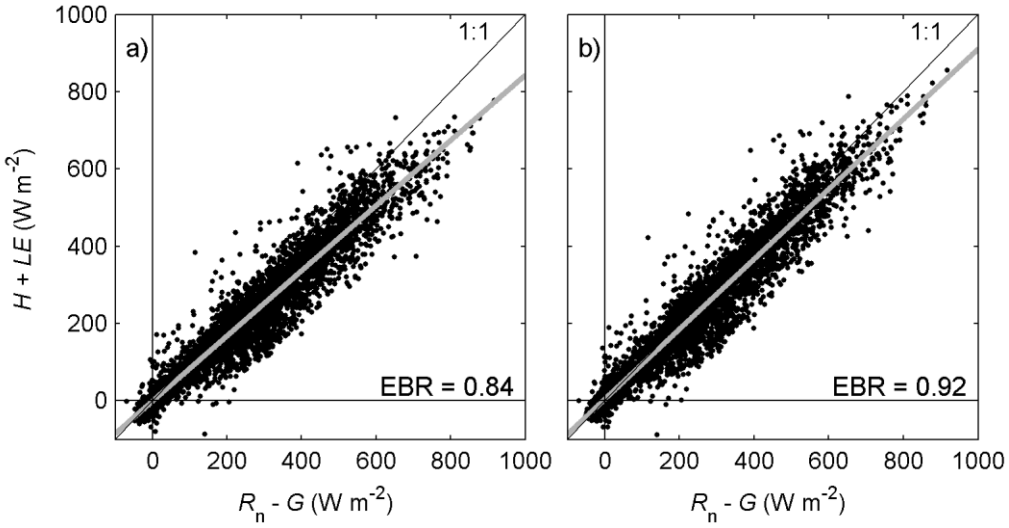

Figure B.5 Energy balance closure at the peatland for the low instalment height (1.5 m) before (a) and after (b) correcting for the underestimation of *LE* caused by signal asynchrony. Regression equations were $H + LE = -0.80 + 0.85 (R_n - G)$ before, and $H + LE = 4.85 + 0.911 \cdot (R_n - G)$ after correction.

of CO_2 and H_2O. The multiple regression equations described the underestimation of *LE* and F_c as a function of wind speed and the flux itself.

The calculated underestimations of the before-WPL *LE* and F_c ranged from 7% to 16% of the flux and showed some dependence on measurement height, mostly for *LE*. When compared to the final CO_2 flux (after additions of the WPL term), the timing error caused an overestimation of the positive F_c of 150% to 176% depending on measurement height. The correction of *LE* for the timing error improved the energy balance closure from 81% before correction to 92% after correction.

These results highlight the importance of synchronising the measurements from the sonic anemometer and gas analyser, not only when using a closed path EC system, but also for measurements made using an open path EC system.

Appendix C Estimates of UV irradiance at the peatland

The intensity of UV irradiance received at the Earth's surface is affected by seasonal changes in the distance between the sun and Earth, the solar zenith angle, the ozone amount in the atmosphere, cloud cover, aerosol loading of the atmosphere, altitude, and the albedo of the surface (Blumthaler and Webb, 2003; Bodeker and McKenzie, 1996; Madronich, 1993; McKenzie et al., 1999). After solar zenith angle, cloud cover is the most important influencing factor (Bodeker and McKenzie, 1996). However, cloud cover is also highly spatially and temporally variable (Madronich et al., 1998) and therefore not easily characterised.

UV irradiance is measured in New Zealand by the National Institute of Water and Atmospheric Research (NIWA) at five locations: Invercargill, Lauder, Leigh, Paraparaumu and Christchurch. For many other locations, NIWA makes available estimates of UV irradiance in the UV Atlas (Shiona et al., 2006). These estimates of UV irradiance are based on estimated clear-sky broadband irradiance (calculated from pressure, humidity and temperature using a radiative transfer model), estimated clear-sky UV irradiance (calculated from pressure and total column ozone using a radiative transfer model), and measured broadband irradiance (Shiona et al., 2006). To obtain estimates for the true UV irradiance, the calculated clear-sky UV irradiance is multiplied by a "cloud modifier function" (Bodeker and McKenzie, 1996) which uses the ratio of the measured broadband irradiance and the calculated clear-sky broadband irradiance to take into account the effect of clouds using:

$$\mathrm{UV}_{\mathrm{estimated}} = \mathrm{UV}_{\mathrm{clearsky}} \cdot A \cdot \left(K\downarrow_{\mathrm{meas}} / K\downarrow_{\mathrm{clearsky}} \right)^{p} \qquad \textbf{Equation C. 1}$$

where $\mathrm{UV}_{\mathrm{estimated}}$ is the estimated true (i.e. affected by clouds) UV irradiance, $\mathrm{UV}_{\mathrm{clearsky}}$ is the calculated clear-sky UV irradiance, $K\downarrow_{\mathrm{meas}}$ is the measured broadband irradiance, $K\downarrow_{\mathrm{clearsky}}$ is the calculated clear-sky broadband irradiance,

and *A* and *p* are coefficients that depend of the solar zenith angle (Bodeker and McKenzie, 1996; Shiona et al., 2006).

For the estimation of UV irradiance at the peatland at Torehape, data from the UV Atlas (Shiona et al., 2006) were used. The closest location to the peatland for which estimates were available for clear-sky UV irradiance was Paeroa (37.373°S, 175.684°E, 19.3 km from the peatland). Instead of assuming that levels of real (=cloud-affected) UV irradiance at the peatland were the same as those at Paeroa, estimates of UV irradiance levels for Paeroa were adjusted for local cloud conditions using radiation information obtained at the peatland.

Note that in this analysis the "broadband radiation" from NIWA was assumed to be the same as the "global radiation" or "shortwave incoming radiation" measured at Torehape. Both variables were measured with very similar instruments: a LI200 (LI-COR Inc., Lincoln, NE, USA) is commonly used for the NIWA network (NIWA, 2007) and was used by Bodeker and McKenzie (1996), vs. a SP Lite pyranometer (Kipp & Zonen, Delft, The Netherlands) that was used in the current study at the peatland. Both instruments measured the radiation between 400-1100 nm.

To obtain estimates of the real (=cloud-affected) UV irradiance levels at the peatland at Torehape, these data for Paeroa were used in the following manner (summarised in Figure C.1):

1. Calculated clear-sky broadband ($K\downarrow_{clearsky}$), UV irradiances ($UV_{clearsky}$), cloud-affected UV irradiance ($UV_{estimated}$) and measured broadband irradiance ($K\downarrow_{meas}$) were obtained for Paeroa from the UV Atlas. Hourly values from the NIWA database were interpolated to half-hourly values using linear interpolation.
2. Global irradiance ($K\downarrow_{meas}$) was measured at the peatland at Torehape. $K\downarrow_{clearsky}$ and $UV_{clearsky}$ at Torehape were assumed to be the same as at Paeroa.
3. Solar zenith angle (SZA) for each time step was calculated using a Matlab script sun_position (Roy, 2004) which is an implementation of the algorithms presented by Reda and Andreas (2003).

4. To determine the "cloud cover modifier function" (Bodeker and McKenzie, 1996), equations were fitted that described the relationship between clear-sky and measured UV and broadband irradiances using data from the Paeroa station from the UV Atlas. Equation C.1 was re-written to

$$\mathrm{UV}_{\mathrm{estimated}}/\mathrm{UV}_{\mathrm{clearsky}} = A \cdot \left(K\downarrow_{\mathrm{meas}}/K\downarrow_{\mathrm{clearsky}}\right)^{p} \qquad \textbf{Equation C.2}$$

Parameters A and p were fitted for different solar zenith angles (in bins of two degrees, see Figure C.2 for an example).

5. Assuming that the cloud modifier functions based on Paeroa could also be applied to Torehape, the fitted values of *A* and *p* were then used to estimated the real (cloud-affected) UV irradiation at Torehape using

$$\mathrm{UV}_{\mathrm{estimated\_at\_Torehape}} = \mathrm{UV}_{\mathrm{clearskly\_at\_Paeroa}} \cdot A \cdot \left(K\downarrow_{\mathrm{measured\_at\_Torehape}}/K\downarrow_{\mathrm{clearsky\_at\_Paeroa}}\right)^{p}$$

Equation C.3

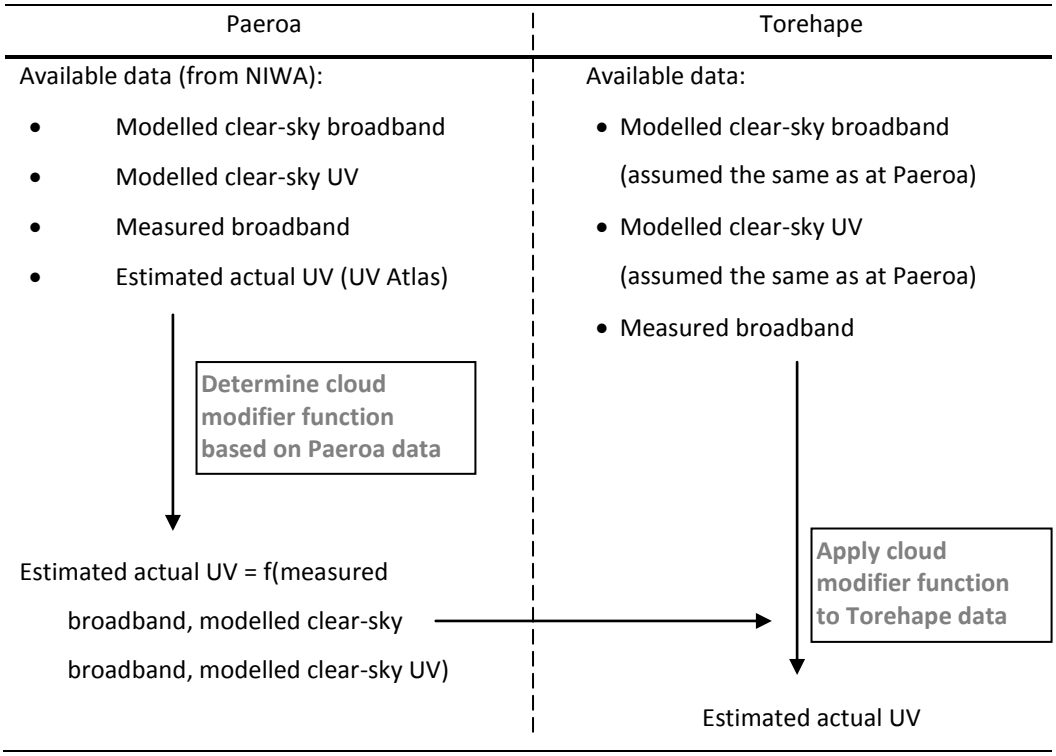

Figure C.1 Schematic showing the analysis steps followed to obtain estimates of 'cloud-affected' UV irradiance at the peatland.

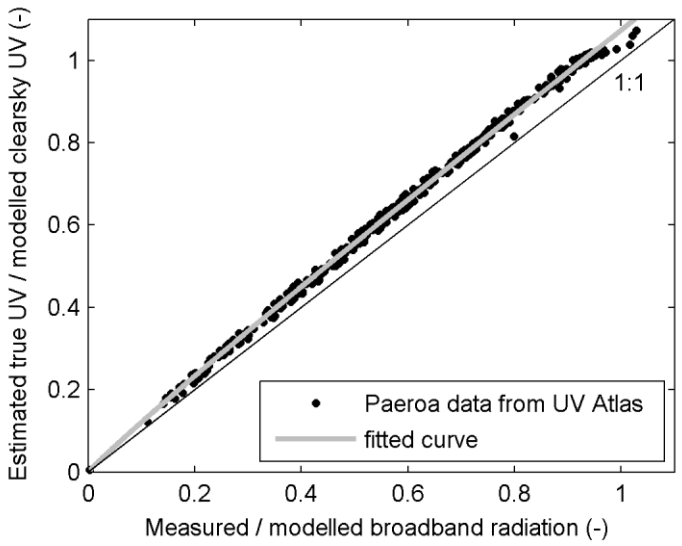

Figure C.2 Example graph of the empirical cloud cover modification function based on data for Paeroa determined for solar zenith angles between 32 and 34 degrees. Fitted function was Equation C.2 with A = 1.074 and P = 0.950 with an R^2 of 0.998.

Appendix D Density term

This appendix provides background information on the density (or WPL) term (Section D.1.1), the potential for error propagation through the WPL term algorithm (Section D.1.2) and a short discussion on field studies examining the WPL term (Section D.1.3). Two recently identified potential issues with the application of the density term for data collected using an open path eddy covariance system with spatially separate sensors are considered in Section D.1.4. The size of the density term at the study sites, the potential error propagation and the potential implications of the issues caused by sensor separation at the grassland are discussed in Section D.2.

D.1 Introduction

D.1.1 Background to the WPL term

When using the eddy covariance (EC) technique to determine the exchange of CO_2 between the Earth's surface and the atmosphere, it would be preferable to collect measurements of the mixing ratio of CO_2 in air (in µmol CO_2 / mol dry air) when determining the CO_2 flux, because it does not change (i.e. is conservative , see Kowalski and Serrano-Ortiz, 2007) when air expands or contracts as a result of changes in heat or water vapour content. However, an open path gas analyser is not able to measure mixing ratios. Instead, it determines the density of CO_2 in air (in kg m^{-3}), which is not only affected by the release or uptake of CO_2 at the surface-atmosphere interface, but also by changes in temperature and water vapour content of the air (i.e. it is non-conservative). This means that to calculate the real CO_2 flux arising from exchanges at the surface it is necessary to account separately for the changes in CO_2 density caused by exchanges of heat and water vapour at the surface (Webb et al., 1980). Webb, Pearman and Leuning (1980) were the first to formulate this so-called "density term" (also called Webb term, or WPL term), and addition of this term to the raw covariance is now a standard practice when calculating fluxes using eddy covariance data (Aubinet et al., 2000; The Ameriflux Workshop Team, 2003). Although recently there have been discussions about the exact

formulation and reasoning behind the equation for the density term (Kowalski, 2006; Kowalski and Serrano-Ortiz, 2007; Leuning, 2004; Leuning, 2007; Liu, 2006; Liu, 2005; Massman and Tuovinen, 2006; Paw et al., 2000), the original equation presented by Webb, Pearman and Leuning (1980) has been evaluated several times and has been found sound and applicable (Leuning, 2004; Leuning, 2007). This equation was re-written by Leuning (2004) as

$$F_c = \overline{w'c_c'} + \overline{c_c}\left[\frac{\overline{E}}{\overline{c}} + \frac{\overline{H}}{\overline{\rho c_p}\,\overline{T}}\right] \qquad \textbf{Equation D.1}$$

where w is the vertical wind speed (m s^{-1}), c_c is the molar density of CO_2 (mol m^{-3}), E is the flux of water vapour (mol m^{-2} s^{-1}), c is the molar density of moist air (mol m^{-3}), H is the sensible heat flux (W m^{-2}), ρ is the density of moist air (kg m^{-3}), c_p is the specific heat of air (J kg^{-1} K^{-1}) and T is the air temperature (K). Primes denote the deviations from the mean value and the overbar represents a time-average. Refer to Leuning (2004, p 129) for the relevant equations for H and E.

In Equation D.1, the second term on the right hand side is the density term. The equation shows that, among other things, the size of the density term depends on the sensible heat flux H, the water vapour flux E and the average CO_2 concentration. When H and LE (the latent heat flux in Wm^{-2}) are comparable in size (i.e. Bowen ratio $\beta = H/LE \approx 1$), contributions to the WPL term from H are approximately 5 times larger that that from LE (Webb et al., 1980). This means that the density term is largest under sunny conditions in summer (when available energy is high), over a dry surface with high sensible heat fluxes.

D.1.2 Potential error propagation

The calculation of WPL-corrected CO_2 fluxes measured using an open path EC system requires information on H and LE (see Eq. D.1). Potential errors in H and LE then propagate through the WPL algorithm to introduce errors in the CO_2 flux ("error propagation", Hollinger and Richardson, 2005; Liu et al., 2006; Serrano-Ortiz et al., 2008).

Errors in turbulent fluxes can be divided into random and systematic errors.

Random errors (for example those occurring as a result of footprint heterogeneity or instrument noise; Goulden et al., 1996; Hollinger and Richardson, 2005; Loescher et al., 2006; Moncrieff et al., 1996; Richardson et al., 2006b) cause flux data to appear noisy (Hollinger and Richardson, 2005). In general, absolute errors in *H* and *LE* increase as fluxes increase (Hollinger and Richardson, 2005) which means that the random uncertainty in the CO_2 flux is also largest when *H* (and to a lesser extent *LE*) is largest. However, when many half-hourly flux measurements are averaged, the uncertainty decreases and the precision increases (Baldocchi, 2003; Loescher et al., 2006).

Systematic errors can be caused by sensor separation, path length averaging, choice of averaging period and lack of sensor response (Goulden et al., 1996; Hollinger and Richardson, 2005; Loescher et al., 2006; Moncrieff et al., 1996; Richardson et al., 2006b). Whereas random errors do not cause a consistent under – or overestimation of CO_2 fluxes, systematic errors do. The two main phenomena that indicate that EC measurements are affected by systematic errors (Baldocchi, 2003) are the generally observed lack of energy balance closure (Aubinet et al., 2000; Baldocchi, 2008a; Twine et al., 2000; Wilson et al., 2002) and the incomplete measurements of nocturnal CO_2 exchange (Aubinet et al., 2005; Aubinet et al., 2000; Feigenwinter et al., 2004).

Systematic errors in *H* and *LE* can lead to systematic errors in the WPL-corrected CO_2 flux as errors propagate through the WPL algorithm. For example, under average conditions during the dry season of 2007 at the grassland site ($c_c \approx 14.1 \cdot 10^{-3}$ mol CO_2 m^{-3}, $\rho \approx 1.16$ kg m^{-3}, $c_p = 1000$ J kg^{-1} K^{-1} and $T \approx 294$ K), an error in the heat flux *H* of 100 Wm^{-2} would have resulted in an error in the WPL-corrected CO_2 flux of 4.13 µmol CO_2 m^{-2} s^{-1} (Equation D.1).

D.1.3 Field validation WPL term

Three studies have been reported in the literature where an open path EC system was used to measure CO_2 exchange above dry, un-vegetated surfaces under hot and dry conditions when the true CO_2 flux was small and the WPL term large (mostly caused by the large sensible heat fluxes). These studies are valuable because they test the robustness of the WPL term. In these studies, the

WPL correction satisfactorily removed the density effects which resulted in good agreement of the open path EC fluxes with the small fluxes measured with the Bowen Ratio technique (Leuning et al., 1982), chamber (Ham and Heilman, 2003) and a closed path EC system (Billesbach et al., 2004). In contrast to CO_2 fluxes measured using open path IRGA's, CO_2 fluxes measured using closed path IRGA's are not (or much less) affected by the density term, depending on the approach used to calculate the fluxes (Leuning, 2004; Leuning and Judd, 1996) and can therefore be used as a reference.

D.1.4 Sensor separation and the WPL term

The unavoidable spatial separation of the gas analyser and the sonic anemometer can lead to loss of covariance between the signals of the anemometer and gas analyser, and therefore to an underestimation of raw latent heat and CO_2 fluxes (Massman, 2004b; Moncrieff et al., 1996). This loss of flux increases with increasing distance between the two sensors, because the signals of the two sensors become less correlated with increasing distance (Baldocchi et al., 1988).

To correct for the loss of covariance caused by sensor separation frequency response corrections can be applied, for example the corrections proposed by Moore (1986) or Massman (2000).

Recent studies have demonstrated that sensor separation can contribute to both an under- and overestimation of the WPL term, therefore leading to an under- or overestimation of the resulting CO_2 flux. Both cases will be explained below and the potential relevance for the current study is discussed.

Sensor separation and potential underestimation of the WPL term and resulting CO_2 flux

Recently, a few studies have reported values of the CO_2 flux measured by an open path IRGA that are too negative, i.e. either an overestimation of CO_2 uptake or an underestimation of the CO_2 release by the surface (e.g. Burba et al., 2005a; Burba et al., 2005b; Hirata et al., 2007; Ono et al., 2007; Sottocornola and Kiely, 2010). For example, Ono et al. (2007) found unrealistic downward fluxes of

CO_2 above a surface with only a few active plants that were not confirmed by a co-located closed path EC system. Similarly, Hirata et al. (2007) reported negative open path EC fluxes measured over a snow-covered surface. The cause for this CO_2 flux that is too negative has been identified, and will be outlined below.

Ideally, the sensible heat flux *H* that is used for calculating the WPL term would be measured in the optical path of the open path IRGA. Instead, researchers use the *H* measured by the sonic anemometer (H_s), assuming that this *H* is the same as that at the optical path of the IRGA, despite the spatial separation between the instruments (Ono et al., 2007). Several researchers have examined whether this assumption is valid by also measuring the *H* in the optical path of the OP IRGA using fine wire thermocouples (H_{tc}) (e.g. Burba et al., 2008; Grelle and Burba, 2007; Ham and Heilman, 2003; Ono et al., 2007). Although some studies found no large discrepancies between H_s and H_{tc} (Ham and Heilman, 2003; Ono et al., 2007), some have identified that H_{tc} is larger than H_s. The cause of this difference was additional heat emitted from the IRGA, either from absorbed radiation or the internal heat source (Burba et al., 2008; Grelle and Burba, 2007). In this case the use of H_s for calculation of the density term has been found to cause underestimation of the WPL term.

Recent studies have found that this underestimation of the WPL term can indeed be resolved by using H_{tc} instead of H_s for the WPL term (Burba et al., 2008; Grelle and Burba, 2007). Alternatively, previously collected open path EC data can be satisfactorily corrected using an additional density correction for the surface heating of the IRGA (Burba et al., 2006; Burba et al., 2008; Grelle and Burba, 2007).

However, the size of this extra correction seems to depend on the weather conditions (e.g. unrealistic uptake has mostly been observed under cold conditions, (Hirata et al, 2007 and references therein)) and is not applicable under all conditions or for all ecosystems (e.g. Sottocornola and Kiely, 2010; Wohlfahrt et al., 2008).

Sensor separation and potential overestimation of corrected CO_2 flux

A recent study has reported values of the CO_2 flux measured by an open path IRGA that were too positive. Kondo and Tsukamoto (2008) measured the CO_2 flux above a parking lot, where the CO_2 flux was expected to be negligible, but the WPL term was large and an overestimation of the CO_2 efflux from the parking lot was observed. The cause for this overestimation of the CO_2 flux was identified, and will be outlined below.

Spectral analysis of the high frequency data showed that spatial separation of the anemometer and the gas analyser lead to an underestimation of the raw CO_2 flux caused by loss of covariance. The heat flux, unlike the flux of CO_2 and water vapour, was not affected by sensor separation, because it is measured by the sonic anemometer alone. This means that the WPL term, which depends mostly on this heat flux, also was not affected (much) by sensor separation. After adding the density term to the raw CO_2 flux this lead to an overestimation of the CO_2 efflux from the tarmac (Kondo and Tsukamoto, 2008).

The importance of correcting all covariances for lack of frequency response before calculating the WPL term had been outlined before (Massman, 2004a). However, one could imagine that if not properly corrected for, loss of covariance caused by sensor separation could lead to a corrected CO_2 flux that is too positive (i.e. either an underestimation of a negative CO_2 flux or an overestimation of a positive flux).

D.2 WPL term at the peatland and grassland

D.2.1 Size of the WPL term

The size of the WPL term calculated for CO_2 fluxes in this study varied between -3.5 and 25 µmol CO_2 m^{-2} s^{-1} at the peatland and between -4 and 20 µmol CO_2 m^{-2} s^{-1} at the grassland (Figure D.1). Often the WPL term was relatively small; for example, for 50% of the fluxes the WPL term was smaller than 3.0 and 3.8 µmol CO_2 m^{-2} s^{-1} at the peatland and grassland respectively (Figure D.2).

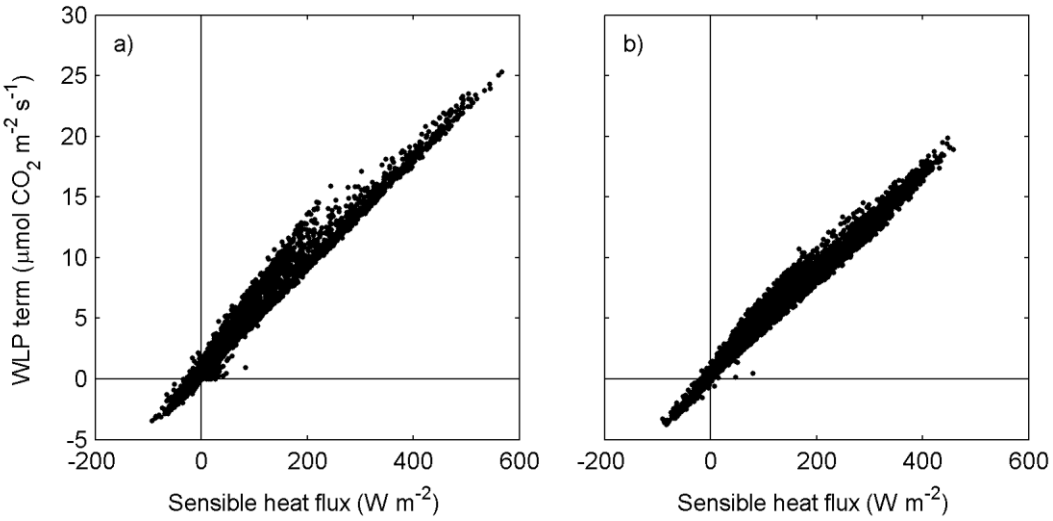

Figure D.1 Size of WPL term for the a) peatland for June 2005 to May 2007 and b) grassland for the 2007 dry seasons.

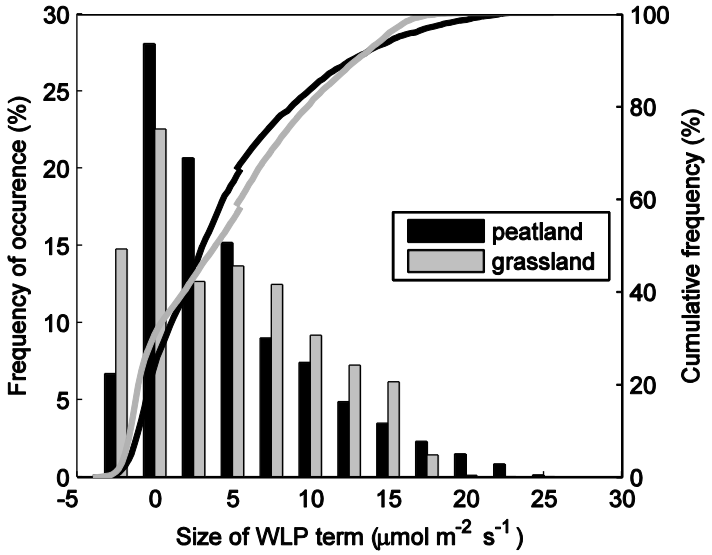

Figure D.2 Frequency distribution (bars) and cumulative frequency distribution (lines) of the WPL term for the peatland between June 2005 and May 2007 (black) and grassland for the 207 dry season (grey).

However, at both the peatland and the grassland hot and dry conditions were encountered during summer, and in those instances it was not uncommon that the size of the density term was much larger than the absolute value of the measured raw flux itself (Figure D.3). In these cases, addition of the density term changed the sign of the CO_2 flux from negative (apparent uptake by the surface) to positive (release from the surface; see for example Figure D.3).

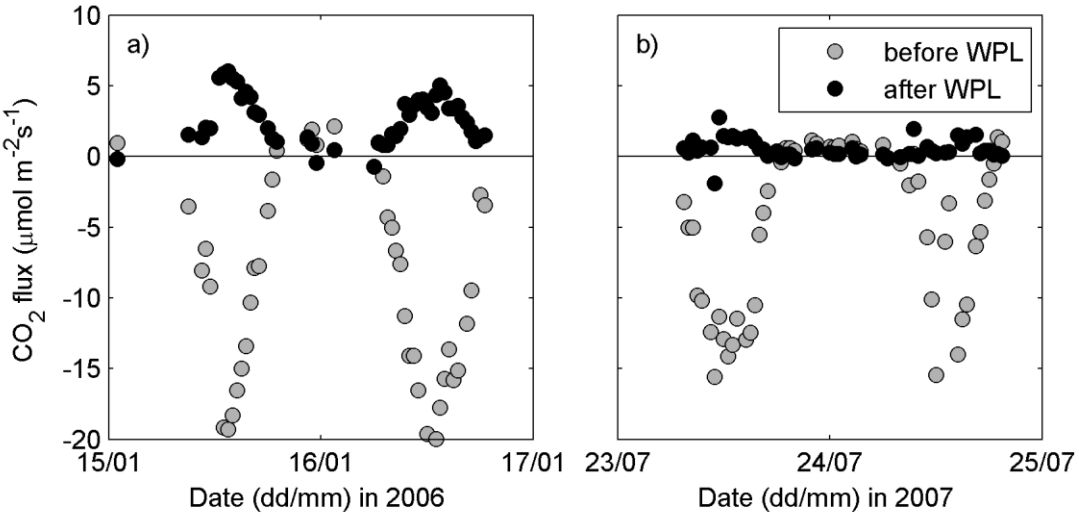

Figure D.3Example of the large WPL term in summer for (a) the peatland and (b) the grassland. Raw fluxes before applying the WPL term (grey circles) are negative during the day, denoting apparent uptake of CO_2 at the surface. After addition of the WPL term (black circles), fluxes are positive, indicating losses of CO_2 from the surface.

D.2.2 Potential error propagation tested at the peatland

Aim

At both the peatland and the grassland, daytime fluxes measured using open path EC systems were larger (more positive) than those measured using a chamber (at the peatland) or soil CO_2 probes (at the grassland, see Section 4.3.1), especially under high levels of solar irradiance. These observations are used as one line of evidence for photodegradation. To test whether this discrepancy in fluxes obtained by different methods was not partly the result of systematic overestimation of the EC flux caused by potential error propagation of systematic errors in *H*, *LE* or the raw CO_2 flux through the WPL algorithm, case studies of error propagation based on the peatland data will be presented below. The peatland was chosen because the WPL term and resulting positive fluxes were largest at that site.

Methods

The method of Liu et al. (2006) and Serrano-Ortiz et al. (2008) was used to illustrate the potential effect of errors in *H*, *LE* and before-WPL CO_2 flux on the corrected (after-WPL) CO_2 fluxes. The before-WPL CO_2 flux ($\overline{w'\rho_c'}$) will be referred to as "raw", even though this flux has been rotated (McMillen, 1986), and corrected for the moisture effect on the sonic temperature (Schotanus et al., 1983) and for lack of frequency response (Moore, 1986). The term 'corrected CO_2 flux' will be used for the CO_2 fluxes after addition of the WPL term (F_c).

Liu et al. (2006) formulated an equation that described relative errors in the CO_2 flux ($\delta F_c / F_c$) as a function of errors in the raw flux of CO_2 ($\omega_c = \delta\overline{w'\rho_c'}/\overline{w'\rho_c'}$), water vapour ($\omega_v = \delta\overline{w'\rho_v'}/\overline{w'\rho_v'}$) and sensible heat ($\omega_T = \delta\overline{w'T'}/\overline{w'T'}$) where ρ_c, ρ_v are the densities of CO_2 and water vapour (in kg m^{-3}) respectively. Serrano-Ortiz et al. (2008) found that relative errors in the mean CO_2 concentration ($\omega_{\rho_c} = \delta\overline{\rho_c}/\overline{\rho_c}$) could also have a large effect on the size of the resulting WPL term, however, in the current study ω_{ρ_c} was set to 0 for all cases. Simultaneous measurement of the mean CO_2 concentration by the LI-7500 and a reference sensor (LI-6262, LI-COR Inc., Lincoln, NE, USA) for 2 months during the study showed reasonably good agreement (data not shown), thereby providing evidence that the mean CO_2 concentration was measured correctly by the LI-7500. Contrary to Liu et al. (2006) and Serrano-Ortiz et al. (2008) who calculated relative errors (i.e. errors as a percentage of the total flux, $\delta F_c / F_c$), absolute errors in corrected CO_2 flux were calculated for the current case studies (δF_c). This approach was chosen because relative errors can be deceptive, especially when CO_2 fluxes are very small and almost zero.

Seven case studies are presented to show the potential impact of systematic errors in *H*, *LE* and $\overline{w'\rho_c'}$ on the size of F_c (summarised in Table D.1).

Table D.1 Summary of case studies used to illustrate the effect of error propagation.

	ω_c	ω_v	ω_T	Description	Resulting error in F_c*
Case 1	-0.08	-0.08	-0.08	Average lack of EBC attributed to *H* and *LE*	– (small)
Case 2	-0.18	-0.18	0	Lack of EBC fully attributed to *LE*	+ (large)
Case 3	0	0	-0.14	Lack of EBC fully attributed to *H*	– (large)
Case 4	-0.30	-0.30	-0.30	Large lack of EBC attributed to *H* and *LE*	– (medium)
Case 5	0	0	+0.20	Large overestimation of raw *H*	+ (large)
Case 6	0	+0.40	0	Very large overestimation of raw *LE*	+ (small)
Case 7	-0.20	0	0	Large overestimation of raw CO_2 flux	+ (large)

EBC = Energy balance closure, negative error depict instances where that the errors ω_c, ω_v, *and* ω_T lead to more negative estimates for F_c compared to the 'real flux'.

* see also Figure D.5 for the impact of the errors ω_c, ω_v, *and* ω_T on F_c.

Examination of the energy balance is a common method for assessing data quality in eddy covariance studies (Aubinet et al., 2000; Baldocchi, 2008a), whereby large difference between the measured incoming and outgoing fluxes may indicate errors in the measurements of the turbulent fluxes (see e.g. Aubinet et al., 2000; Culf et al., 2004; Foken et al., 2004 for other possible causes of lack of energy balance closure). The first four cases presented below assess the effects of underestimation of *H* and *LE* on the resulting CO_2 flux. For all cases, errors in measurement of net radiation and the soil heat flux were assumed to be zero. The energy balance was evaluated using two approaches. The first used the energy balance ratio (EBR, see Wilson et al., 2002), defined as

$$\mathrm{EBR} = \Sigma\left(H + LE\right)/\Sigma\left(R_n - G\right) \qquad \textbf{Equation D. 2}$$

where R_n is the net radiation and *G* the soil heat flux*,* which includes change of storage of heat in the soil. The second approach used a linear regression with R_n - *G* as the independent variable and *H* + *LE* as the dependent variable. The slope of this regression was used as a second estimate of energy balance closure. The mean of the two estimates for closure was used in the formulation of the case studies. The energy balance results described below are shown in Figure D.4 and summarised in Table D.2. Case studies for the error propagation analyses are summarised in Table D.1.

The EBR over the whole study period from June 2005 until May 2007 was found to be 0.93 (Figure D.4), whereas the regression approach resulted in a

slope of 0.91. This means that at the peatland, the average lack of energy balance closure was between 9 and 7%. In case 1, it was assumed that both sensible and latent heat fluxes were underestimated by about 8% (ω_T and ω_v = -0.08). The raw CO_2 fluxes were assumed to be underestimated by the same amount (ω_c = -0.08). For case 2, the assumption was made that the lack of energy balance closure could be fully attributed to an underestimation of *LE*. Because $\Sigma(LE)/\Sigma(R_n - H - G) = 0.88$, and the slope of the regression of $R_n - H - G$ vs. *LE* was 0.77, ω_v (and by extension also ω_c) was set to -0.18 (= 1 – (0.88+0.77)/2). Case 3 illustrated the case whereby the lack of energy balance closure was assumed to be caused by underestimation of *H* alone. Because $\Sigma(H)/\Sigma(R_n - H - G) = 0.85$, and the slope of the regression of $R_n - LE - G$ vs. *H* was 0.88, ω_T was set to -0.14. As an additional illustration of the effect of lack of energy balance closure on the resulting CO_2 flux, case 4 was included which shows the effect of a larger lack of energy balance closure of 30%, which occurs in some studies (Twine et al., 2000; Wilson et al., 2002), which was assumed to be caused by underestimations of both *H* and *LE* (and by extension, F_c).

Table D.2 Linear regression results for energy balance closure in cases 1, 2 and 3. *n* is the number of half-hourly data points, R^2 is the portion of variance explained by the regression. "Ratio of sum" depicts the ratio of cumulative sums of the dependent and independent variable: Ratio of sums = Σ (dependent variable) / Σ (independent variable).

case	Description	Independent variable	Dependent variable	*n*	Intercept	Slope	R^2	Ratio of sum
Case 1	Average lack of EBC attributed to *H* and *LE*	$R_n - G$	$H + LE$	3855	7.7	0.91	0.96	0.93
Case 2	Lack of EBC fully attributed to *LE*	$R_n - H - G$	*LE*	3853	17	0.77	0.91	0.88
Case 3	Lack of EBC fully attributed to *H*	$R_n - LE - G$	*H*	3869	-2.1	0.88	0.91	0.85

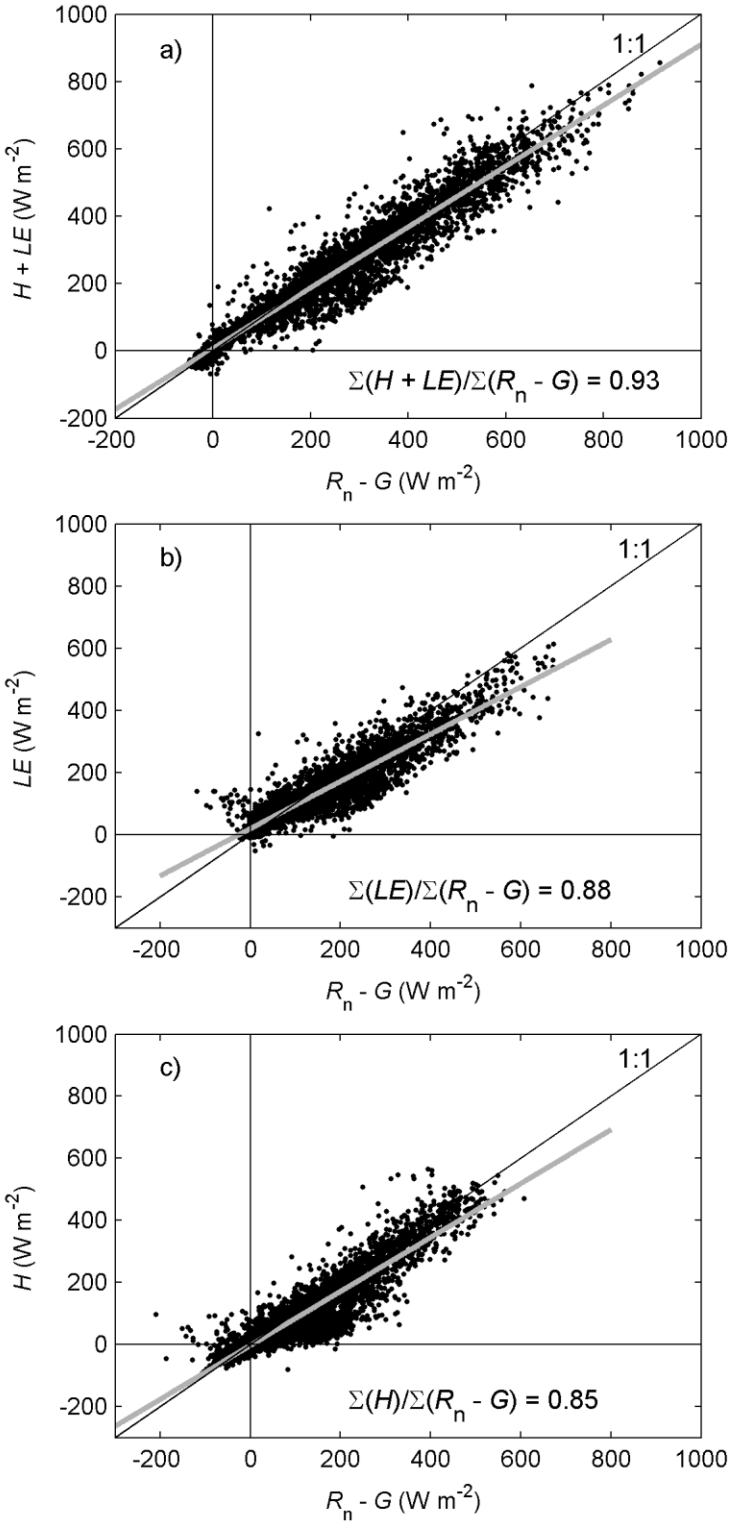

Figure D.4 Linear regression results for energy balance closure in cases 1, 2 and 3. See also Tables D.1 and D.2.

At the peatland, comparison of daytime EC data with night-time EC data and chamber data suggested that WPL-corrected fluxes of CO_2 during the day were larger (more positive) than would be expected if resulting from biological activity alone (Section 4.3.1). Cases 5, 6 and 7 were purely hypothetical and were included to aid identification of potential scenarios of errors in *H*, *LE* and $\overline{w'\rho_c'}$ that might have been responsible for the potential overestimation of the *Fc*. The cases reflected unlikely scenarios of large overestimation of the sensible heat flux (case 5, ω_T = 0.20, ω_c =0, ω_v =0) or latent heat flux (case 6, ω_v = 0.40, ω_T =0, ω_c =0), or a large underestimation of the raw CO_2 flux (but not *LE* and *H*; case 7, ω_c = -0.20, ω_T =0, ω_v =0).

Results

Following the analysis approach presented by Liu et al. (2006) and Serrano-Ortiz et al. (2008), the average absolute error in CO_2 flux (δF_c) was calculated over the whole study period based on day-time peatland flux data for the cases introduced above. Results are presented as a function of sensible heat flux in (Figure D.5), where negative values for the error indicated that the errors ω_c, ω_v, *and* ω_T led to estimates for F_c that were less than the 'real flux' (values too negative or "further from zero" for photosynthesis and too small for respiration). Positive values indicated that the errors ω_c, ω_v, *and* ω_T led to values for F_c that are too large compared to the real flux (i.e. too large for respiration or too positive or "too close to zero" for photosynthesis).

Assumptions made in cases 1, 3 and 4 led to underestimation of the corrected CO_2 flux (Figure D.5 and Table D.1); in other words, daytime F_c was smaller than the "real" flux. Lack of energy balance closure (as indicated by EBR < 1) when assumed to be caused by underestimation of both *H* and *LE* (and by extension underestimation of $\overline{w'\rho_c'}$ was also assumed) resulted in underestimation of F_c of at most -0.44 and -1.7 µmol CO_2 m^{-2} s^{-1} for cases 1 and 4 respectively. Larger underestimation of F_c was the result of the large 14% underestimation of *H*, when errors in *LE* and $\overline{w'\rho_c'}$ were assumed zero (case 3, maximum underestimation of F_c at large *H* -3.3 µmol CO_2 m^{-2} s^{-1}).

Assumptions made in the remaining cases (cases 2, 5, 6 and 7) led to an overestimation of CO_2 fluxes. The very large overestimation of *LE* (40%) assumed in case 6 resulted in a relatively small overestimation of F_c. This overestimation was largest (up to 0.70 µmol CO_2 m^{-2} s^{-1}) at low to intermediate levels of *H* (0 < *H* < 250 W m^{-2}), because *LE*, and therefore the absolute error in *LE*, was largest in those instances (data not shown).

Large overestimation of the corrected CO_2 flux was the result of either underestimation of $\overline{w'\rho_c'}$ with a matching or zero underestimation of *LE* combined with zero error in *H* (case 2 and 7), or overestimation of *H* with errors in *LE* and $\overline{w'\rho_c'}$ assumed zero (case 5). The largest overestimation of *Fc* at high *H* was 4.7 µmol CO_2 m^{-2} s^{-1} when *H* was assumed to be overestimated by 20% (case 7), and 3.8 µmol CO_2 m^{-2} s^{-1} when $\overline{w'\rho_c'}$ was assumed to be underestimated by 20%.

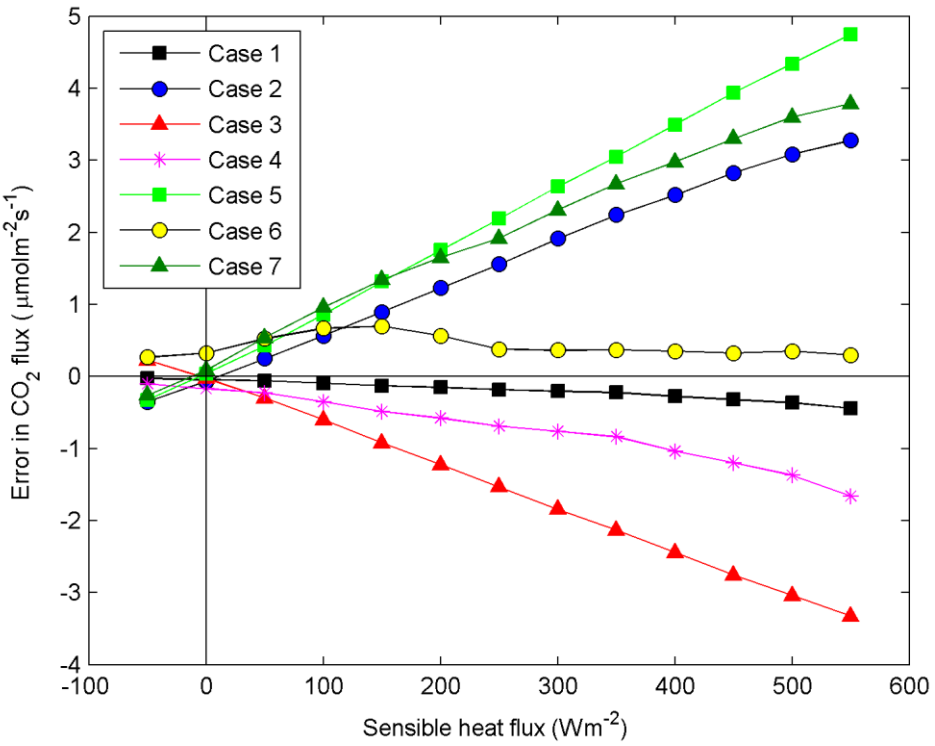

Figure D.5 Average error estimates for the corrected CO_2 flux caused by errors in sensible and latent heat flux and raw CO_2 flux. Cases are summarised in Table D.1. Negative values for the error indicate that the errors $\overline{\omega_c}$, $\overline{\omega_v}$, $\overline{\omega_T}$ led to estimates for F_c that are less than the 'real flux'. Positive values indicate that the errors $\overline{\omega_c}$, $\overline{\omega_v}$, $\overline{\omega_T}$ lead to estimates for F_c that are greater than the 'real flux'.

Keeping the pattern of Figure D.1 in mind, Figure D.6 shows the mean diurnal patterns of F_c and the error in F_c as a result of systematic errors in *H*, *LE* or $\overline{w'\rho_c'}$ for two summer months.

Calculated WPL-corrected EC fluxes without additional assumed errors in *H*, *LE* or $\overline{w'\rho_c'}$ (black dots) showed a clear diurnal variation with larger values during the day compared to the night. This difference between day and night-time EC fluxes was not measured to the same extent by the chamber (e.g. Figure 4.1) and forms part of the evidence for photodegradation presented in Chapter 4. To investigate whether any of the presented scenarios of systematic errors could potentially erroneously have caused a similar apparent diurnal variation the mean diurnal variation of the calculated errors was plotted alongside the fluxes.

For all seven cases errors were small during the night (Figure D.6). However, during the day errors propagated through the WPL algorithm were large in some cases. At midday, when *H* was large, assumptions made in cases 3 and 4 led to an underestimation in the CO_2 emissions and cases 1 and 6 caused very small errors in the CO_2 flux. Cases 2, 5 and 7 lead to considerable overestimation of F_c and the diurnal variation of these errors in F_c resembled the diurnal variation in the flux itself (Figure D.6).

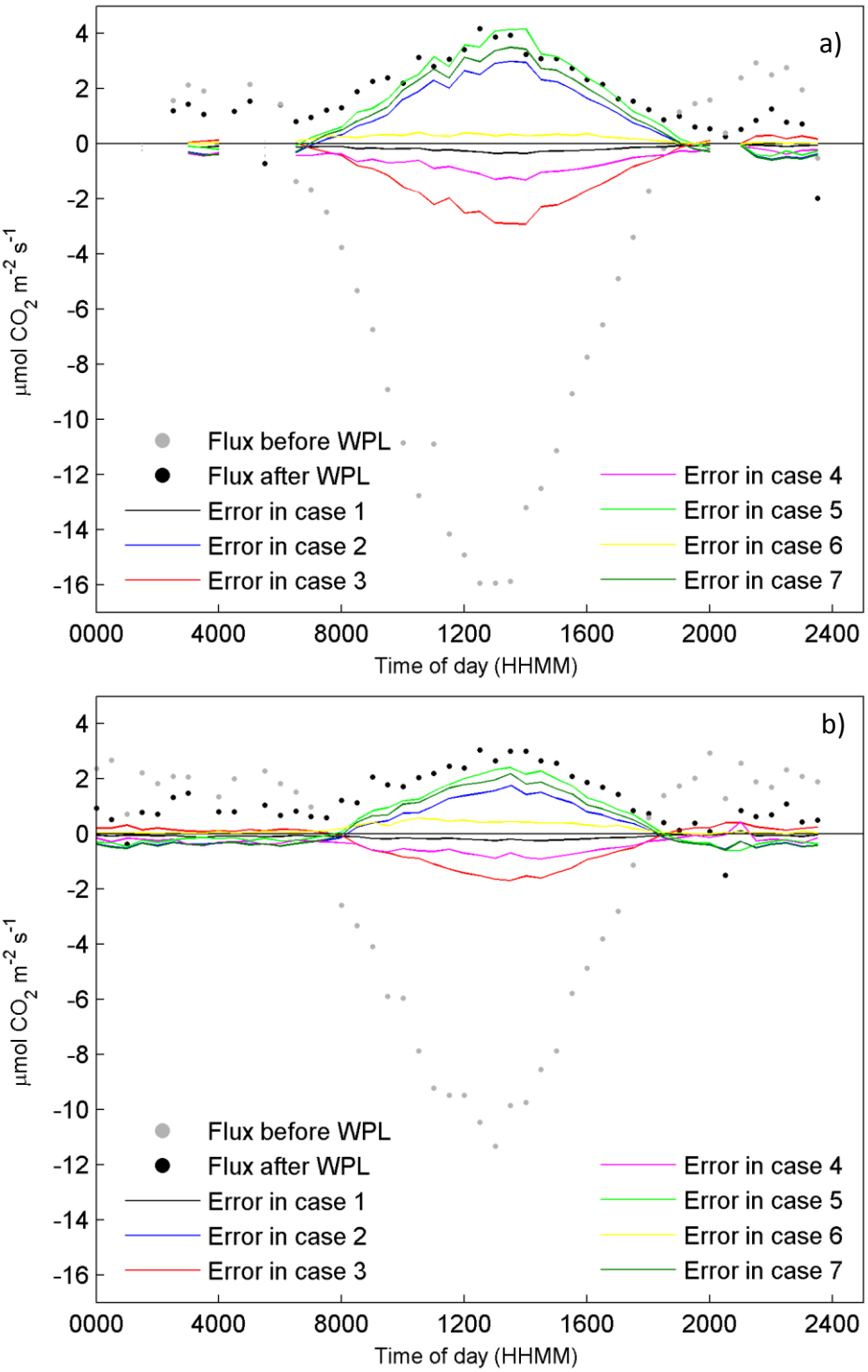

Figure D.6 Implications of potential systematic errors in *H*, *LE* and $\overline{w'\rho_c'}$ on corrected CO_2 fluxes calculated for monthly mean diurnal values for a) January 2006 and b) March 2006. Note that whereas the dots represent the raw (grey) and corrected (black) CO_2 fluxes, the lines represent only the error in the flux for the different scenario's, without the flux itself. Large gaps in the night-time data in January are caused by loss of battery power to the instruments. See Table D.1 for a summary of the cases.

Discussion

The most likely scenarios were case 1 and 3, where the observed (case 1) or imagined (case 3) lack of energy balance closure were assumed to be the result of the underestimation of both *H* and *LE* (and where $\overline{w'\rho_c'}$ was assumed to be underestimated by the same amount). These assumptions resulted in a small underestimation of F_c during the day. Scenarios like these can therefore not be responsible for the observed diurnal variation of F_c with larger fluxes during the day.

The assumption that only *H* was underestimated (case 3) lead to large underestimation of F_c, yet this scenario is unlikely. The sensible heat flux is measured using only one instrument which makes the measurement relatively straightforward in contrast to the measurements of *LE* and F_c, which require two instruments that are spatially separated. Measurement of *LE* and F_c are therefore more error-prone than the measurement of *H* and it is therefore unlikely that only *H* would be underestimated.

Case 6 illustrates that errors in *LE* have only a small effect on the resulting CO_2 flux (Webb et al., 1980). The very large overestimation of *LE* (40%) assumed in case 6 resulted in a small overestimation of F_c which was not large enough to explain the diurnal pattern observed in F_c (Figure D.6). Also, overestimation of turbulent fluxes (*H* or *LE*) as assumed in case 6 are unlikely, because this would lead to energy balance closure of more than 100%, which is generally not observed (Aubinet et al., 2000; Baldocchi, 2008a). For example, in the study by Wilson (2002), energy balance closure for 50 site-years from 22 sites (determined as the slope of the regression of $H + LE$ on $Rn - G$) was found to vary between 0.53 and 0.99, with none of the sites reporting energy balance closure of more than 100%.

There were two scenarios (represented by three cases) that could potentially be responsible for the large positive CO_2 fluxes measured during the day at the peatland during summer: i) the overestimation of *H* without overestimation of $\overline{w'\rho_c'}$ (case 5) and ii) the underestimation of the $\overline{w'\rho_c'}$ without a matching underestimation of *H,* and with or without a matching

underestimation of *LE* (case 2 and 7). However, both scenarios are not very likely.

Overestimation of *H* (case 5) is not likely for the same reason overestimation of *LE* is not likely (see case 6). In comparison, the scenario with underestimation of $\overline{w'\rho_c'}$ without matching underestimation of *H* (cases 2 and 5) is more likely. As discussed previously (Section D.1.4), sensor separation can lead to underestimation of the raw CO_2 flux without affecting *H*, leading to overestimation of the corrected CO_2 flux if not properly corrected for (e.g. Kondo and Tsukamoto, 2008). At the peatland however, sensor separation was minimal (60 mm), and data were corrected for loss of covariance caused by sensor separation (McMillen, 1986) before addition of the WPL term (Massman, 2004a). Night-time EC measurements also showed good agreement with chamber measurements made at the same time (Figure 4.1). Therefore, it is unlikely that large overestimation of $\overline{w'\rho_c'}$ of the order of 20% would have occurred at the peatland.

In summary, these case studies show that the discrepancy in fluxes obtained by EC and chamber during the day at the peatland (Figure 4.1) and the diurnal variation of EC fluxes with larger fluxes during the day (Figure D.6) were not likely the result of systematic overestimation of the EC flux caused by potential error propagation of systematic errors in *H*, *LE* or the raw CO_2 flux through the WPL algorithm. The two scenarios leading to large overestimation of F_c (overestimation of *H* or underestimation of $\overline{w'\rho_c'}$) were unlikely to have occurred at the peatland.

D.2.3 Effect of sensor separation tested at the grassland

Aim and methods

At the grassland, a test was performed to determine whether the positive fluxes measured were not partly the result of overestimation of the CO_2 flux caused by sensor separation. A thermocouple was installed very close to the optical path of the gas analyser so that the heat flux could be measured twice: once using the temperature measured by the sonic anemometer (H_s), and once

by using the temperature measured by the thermocouple (H_{tc}). By measuring in the sensor path of the gas analyser one would expect the H_{tc} to be smaller than H_s if lack of covariance due to sensor separation was an issue. Alternatively, if sensor heating was occurring, H_{tc} (corrected for sensor separation) would be expected to be larger than H_s.

Results and discussion

The results of this comparison during part of the dry season of 2007 are presented in the figures below. H_{tc} was slightly greater than H_s (Figure D.7). The discrepancy between the two H's was on average 4.3 Wm^{-2} (paired t-test, P <0.001), and was largest at high values of the sensible heat flux. The discrepancy was at most 14 Wm^{-2} (at $H \approx 400$ W m^{-2}, see regression equation in caption of Figure D.7).

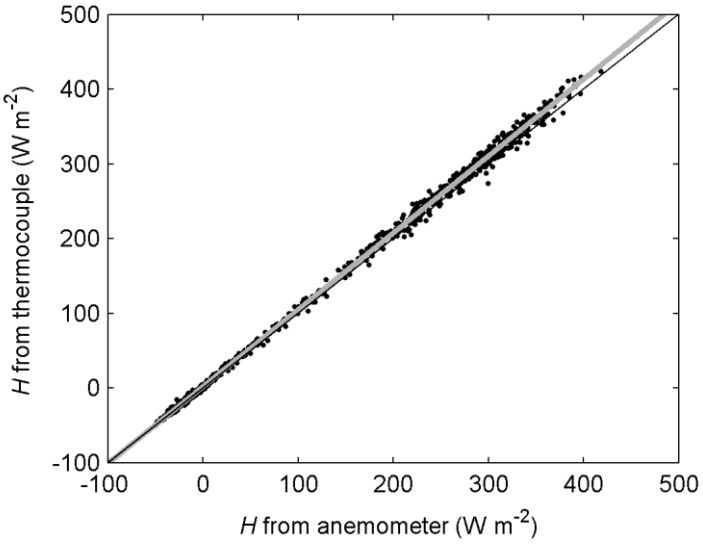

Figure D.7 Comparison between the sensible heat fluxes measured using the temperature measured with the sonic anemometer (H_{tc}) and with a thermocouple close the IRGA path (H_{tc}). The grey line is the linear regression (y =1.65 + 1.03x, adjusted R^2 = 1.00). The black line is the 1:1 line.

The higher values of H_{tc} compared to H_s meant that corrected CO_2 fluxes were more positive when using H_{tc} for the WPL term instead of H_s. However, the difference in H and CO_2 fluxes was small. The linear regression indicates that maximum discrepancy between two F_c's occurred at high values for the CO_2 flux and was at most 0.6 µmol m^{-2} s^{-1} (at $F_c \approx 3$ µmol m^{-2} s^{-1}, see regression equation

in caption of Figure D.8). However, the average discrepancy between the two F_c's was lower (0.30 µmol m^{-2} s^{-1}, paired t-test, $P < 0.001$).

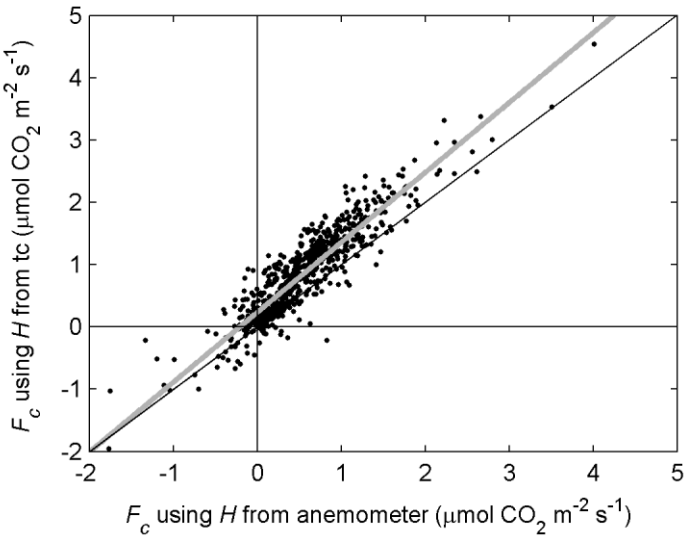

Figure D.8 Comparison between the CO_2 fluxes after addition of the WPL term using the two *H*'s compared in Figure D.7 as input for the WPL term. The grey line is the linear regression (y = 0.24 + 1.12x, adjusted R^2 = 0.84). The black line is the 1:1 line.

These results suggest that sensor separation might have led to an underestimation of at most 20% of the corrected CO_2 fluxes at the grassland. This potential underestimation, although possibly important when integrated over long periods of flux measurements, does not alter the main conclusion of Chapter 4; namely that photodegradation contributed substantially to the total CO_2 fluxes at the grassland site.

A similar test with an additional measurement of *H* at the gas analyser's optical path was not performed at the peatland site. However, the effect is expected to be very small, because the sensor separation was on average only 60 mm, compared to an approximate sensor separation of 200 mm at the grassland (pers. comm. Dennis Baldocchi). Also, data were first corrected for loss of covariance before calculation of the WPL term, as suggested by Massman (2004a). These factors make it very unlikely that the CO_2 fluxes above the peat were an artefact of the sensor setup.

Appendix E Negative CO_2 fluxes observed in the container

E.1 Background and aim

Results obtained using the container described in Section 3.4 were used to verify the field results that indicated that solar irradiation, by itself, could cause CO_2 production from peat. In the container, air dried peat was used to minimise the microbial respiration. Peat was alternately exposed to and shaded from sunlight to study the irradiance-induced CO_2 flux. During the shade runs CO_2 fluxes were expected to be around zero. However, small negative fluxes were observed (Figure 5.12a).

Even though the fluxes were generally small compared to the fluxes measured during the sun runs (Figure 5.12a) the fact that negative fluxes were observed during the dark runs could cast doubt on the reliability of the methodology used to measure irradiance-induced fluxes. It is especially important to determine the reliability of the sun run measurements, on which the conclusions of Chapter 5 are based.

E.2 Methods

To investigate the negative fluxes observed during the shade runs, data collected for Experiment A (peat substrate) were examined in detail. Runs during this experiment were either 140 seconds or 200 seconds long. For the analysis presented below, runs were divided into subruns of 40 seconds duration, starting from second 7 (Figure E.1). The so-called deadband of 6 seconds was taken to allow for travel time of gas between the container and the gas analyser. Data from three consecutive subruns (i.e. using the first 6+3*40 = 126 seconds of each run) were used for the analysis. Data of the remainder of the runs (14 seconds for the 2.20 minute runs, and 72 seconds for the 3.20 minute runs) were not used. For the 3 consecutive subruns per run, CO_2 fluxes and mean container temperatures were calculated. Also, the change in container temperature over the sun run was calculated using:

Change in *T* = average temperature over the last 5 seconds of the subrun minus the average temperature over the first 5 seconds of the subrun.

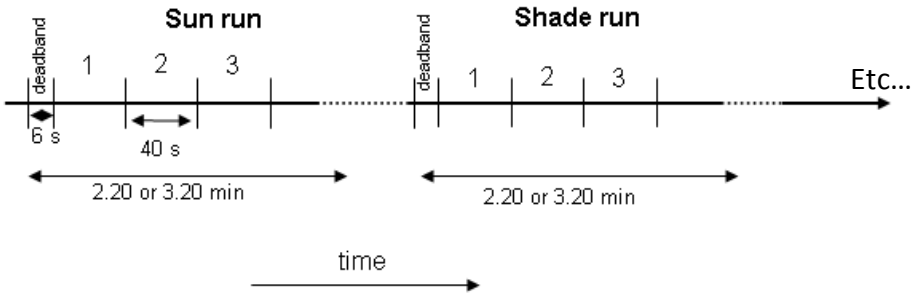

Figure E.1 Schematic indicating how individual runs (of 2.20 minutes or 3.20 minutes) were subdivided into 3 subruns of 40 seconds.

E.3 Results

Data from the subruns showed a general increase in temperature during the sun subruns (Figure E.2a), caused by absorption of solar irradiance. Average CO_2 fluxes during the sun subruns appeared not to vary between subruns (Figure E.2b).

During the shade runs, the container temperature generally decreased from subrun 1 to 3 (Figure E.2a), because of shading after being exposed to the sun. This decrease in temperature was accompanied with a small increase in the negative CO_2 fluxes (Figure E.2b), i.e. fluxes were closer to zero at the end of a shade run (during subrun 3) compared to the beginning of a shade run (subrun 1). This means that the most negative fluxes were observed during the beginning of a run (i.e. shade subrun 1; Figure E.2b).

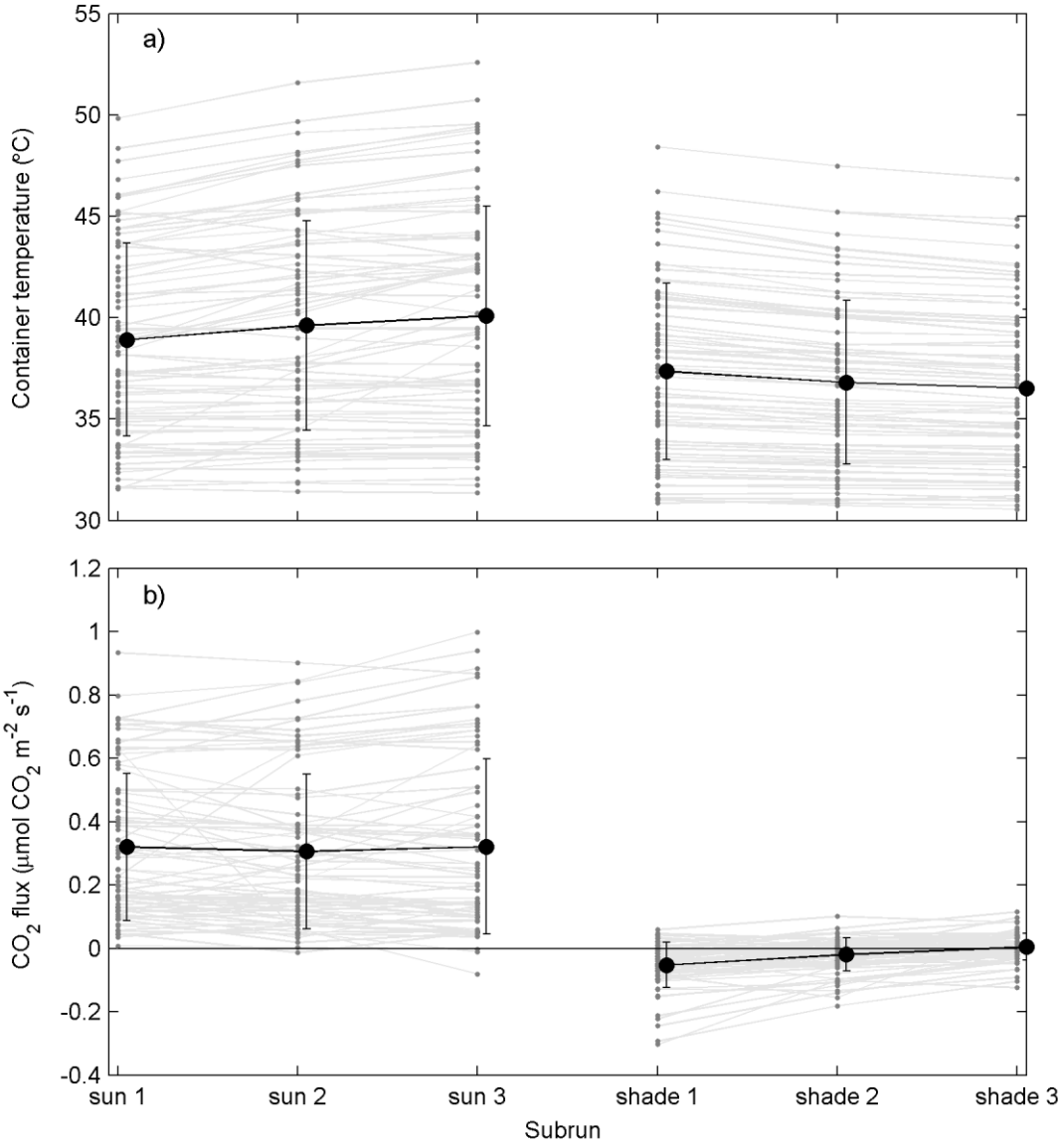

Figure E.2 Average mean temperature (panel a) and CO_2 flux (panel b) calculated for three 40-second subruns per run of Experiment A. Error bars depict standard deviations.

Fluxes of CO_2 during the shade subruns showed a trend with average subrun temperature, whereby the most negative fluxes were observed at the highest temperatures (-0.053 µmol CO_2 m^{-2} s^{-1} during subrun 1, Figure E.3c). Similarly, CO_2 fluxes observed during the shade subruns also seemed correlated with the *change in temperature* during the subrun (Figure E.3d). The subruns during which most cooling occurred displayed the most negative CO_2 fluxes (Figure E.3d).

Because the mean fluxes during the sun subruns did not vary between subruns 1-3 (mean fluxes between 0.31-0.32 µmol CO_2 m^{-2} s^{-1}), no trend was observed with container temperature (Figure E.3a) and change in container temperature (Figure E.3b).

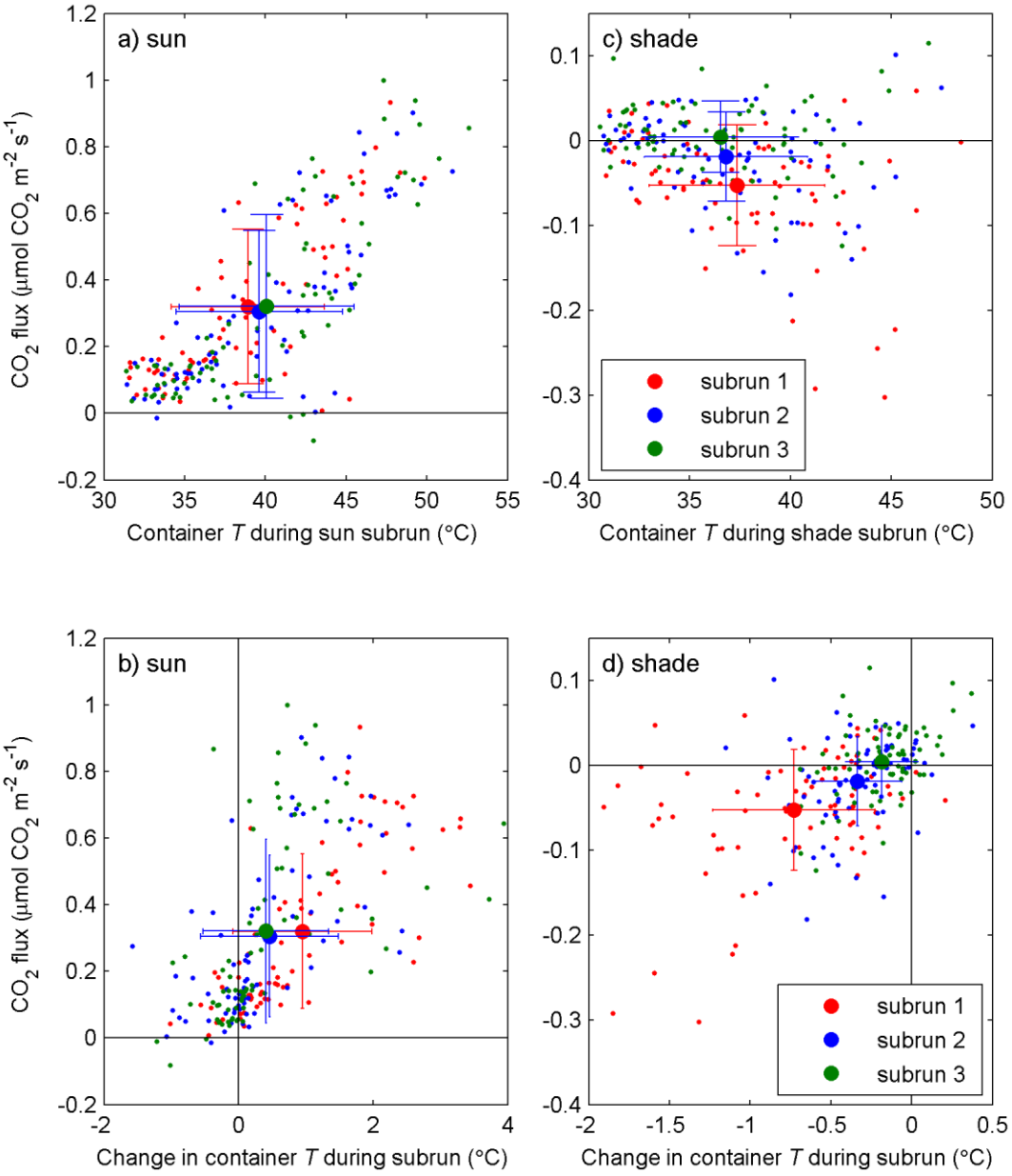

Figure E.3Relationship between the air temperature in the container and CO_2 flux measured during subruns of the sun and shade runs of Experiment A. Relationship between the change in air temperature in the container during the subrun and CO_2 flux measured during subruns of the sun and shade runs of Experiment A. Error bars depict standard deviations.

E.4 Discussion

E.4.1 Shade runs

Fluxes during the shade runs seemed to increase with time during the run (i.e. fluxes were closer to zero near the end of a run) and appeared to be correlated with the container temperature and the change in container temperature during the run. At present, it is not known what causes this behaviour.

It is possible that these small negative fluxes caused by adsorption of CO_2 to the plastic in the tubing at higher temperatures, even though test runs confirmed that the container materials did not emit or take up CO_2 by exposing the empty container to solar irradiance (Section 3.4.9). However, the temperature in the container was generally higher when peat was present compared to the empty container because the peat was still warm after absorbing solar irradiance in the sun run preceding the shade runs. Also, the CO_2 concentration in the container during the runs when peat was present were generally higher (between ~380 – ~1000 ppm) than during the runs when the container was empty (~380 ppm).

Alternatively, CO_2 might have adsorbed onto the peat particles themselves. Typically, adsorption of CO_2 onto porous media is temperature mediated, with higher adsorption rates at lower temperatures (Parsons et al., 2004), and this could (partly) explain the more negative fluxes during runs (Figure 5.12) or subruns (Figure E.3c) at higher temperatures.
Possibly, temperature changes could have affected the amount of water in the liquid phase (through evaporation and condensation) and the solubility of CO_2 in water (Wiebe and Gaddy (1940) and references in Duan and Sun (2003)), which might have resulted in observed CO_2 fluxes. If temperature was indeed the only factor affecting the adsorption or changes in solubility, this would mean that shaded and exposed measurements made at the same temperature were still comparable.

Alternatively, negative fluxes may not have been caused by adhesion of CO_2 and/or not controlled by temperature itself. Possibly, the *change* in

temperature during the subrun was the main factor driving the negative fluxes (Figure E.3d). If this was the case, the negative fluxes might have been an artefact of the gas analyser measurements, and its' inability to deal with changing temperatures during the measurement period. At this stage of the research, the mechanism through which non-stationary temperature conditions could lead to apparent fluxes remains unclear, and will be the topic of further research.

E.4.2 Sun runs

During the sun runs, photodegradation of the peat by solar irradiance led to CO_2 losses from the peat. Under higher irradiance intensity, more CO_2 was formed (Figure 5.11). Because high irradiance levels were accompanied by larger temperature increases, fluxes were also correlated with temperature (Figure E.3a), and change in temperature (Figure E.3b). Even though temperature changes were larger in subrun 1 compared to subruns 2 and 3, fluxes did not – on average – show a trend with time within the runs, i.e. average fluxes did not seem to vary from subrun 1 to 3.

So even though desorption of CO_2 caused by rising temperature (Parsons et al., 2004), changes in CO_2 solubility in water and possible measurement artefacts caused by the non-stationary conditions might have affected the resulting CO_2 flux during the sun runs, it is clear that the CO_2 flux resulting from these processes was of minimal importance compared to the irradiance-induced CO_2 production.

E.4.3 Length of run chosen for analysis

For the analysis of the results from the container experiment presented in Chapter 5, runs of 60 seconds were used. This run length was chosen as a compromise between long and short runs.

Long (2-3 minute) runs have the advantage that many 1-second data points contribute to the regression calculation, making the CO_2 flux estimate robust. One of the disadvantages of long runs is that temperature and radiation conditions are likely to vary throughout the run (for example caused by clouds

passing by), the effect of which would be averaged out. Also, long runs would allow the temperature to rise considerably, leading to less overlap in mean temperature between sun and shade runs.

On the other hand, short (20-40 seconds) runs have the advantage of more constant temperature and irradiance conditions throughout the run, but flux calculations rely on regressions with fewer points, possibly making the flux estimates less robust.

Runs of 60 seconds were chosen for the main analyses of Chapter 5 as a compromise between long and short runs and their corresponding advantages and disadvantages. Although the analysis of data from the shade runs suggested that data from the beginning of the runs might less reliable than data from later in the runs (Figure E.3c and d), this did not seem to affect the sun runs (Figure E.3a and b). Because sun runs were more important for the analysis, and because overlap in temperature between sun and shade runs was important for direct comparability, 60-second runs obtained at the beginning of the full (140 or 200 second) runs were used for analyses of Chapter 5.

E.4.4 Further work

- In the current setup, the effect of increasing temperature could not be de-coupled from exposure to irradiance. If the substrate could be heated up in the absence of solar irradiance, a clearer picture could be painted of the effect of the temperature increases during a run.
- A study into the effect of temperature and changes in temperature using a inert substrate in the container like dark glass beads, which would heat up and cool down similar to peat, but would not contain water and would provide less surface area for CO_2 to adsorb to.

E.5 Conclusion

Negative fluxes observed during the shade runs correlated with container temperature and change in container temperature. The mechanisms which caused the decrease in CO_2 concentration are unclear, but it might have been adsorption of CO_2 to tubing, container or the peat itself or changes in solubility of

CO_2 in water (with evaporation and condensation of the minor amount of remaining water determining how much water was in the liquid phase). Alternatively, the observed negative fluxes might not have reflected real fluxes, but instead might have been caused by the gas analyser's inability to measure fluxes reliably under non-stationary temperature conditions.

The same processes might have affected the CO_2 flux measurement during the sun runs. However, CO_2 fluxes measured during the sun run were much greater than the negative fluxes observed during the shade runs, and assuming that the size of the possible non-irradiance induced CO_2 flux would be the same during the sun and shade runs, the mean error would be small.

In the analyses contained in Chapter 5, runs of 60 seconds were used, which would coincide with the first plus half of the second subrun of the analysis in this appendix. The estimated mean error for the 60 second run would be approximately 13% (-0.042 µmol CO_2 m^{-2} s^{-1} /0.31 µmol CO_2 m^{-2} s^{-1}, based on weighted averages of average flux from subrun 1 and 2), which was considered tolerable.

Appendix F Spatial representativeness of CO_2 efflux measurements

F.1 Background and aim

Spatial heterogeneity of soil CO_2 efflux as determined by chambers is often found to be large (Drewitt et al., 2002; Khomik et al., 2006; Luo and Zhou, 2006; Rayment and Jarvis, 2000).

For this reason, when using chambers to determine the CO_2 efflux, it is desirable to measure fluxes continuously at a range of sites randomly located across the area of interest. However, resource constraints prevented this in the current study. Instead of continuous measurements at multiple locations, continuous measurements were made at only one location, supplemented with repeated spatial measurements throughout the year, as recommended by Savage and Davidson (2003).

The analysis presented in Chapter 6 is based on data collected by the long-term chamber at only one location at the peatland. It is not the main purpose of this appendix to characterise the spatial variation of the CO_2 efflux in detail, but rather to determine whether the CO_2 flux measurements of the long-term chamber were not dissimilar to spatial measurements of CO_2 efflux across the peatland. For this purpose, measurements obtained using the long-term and survey chambers are compared.

F.2 Methods

F.2.1 Survey chamber measurements

At the peatland, measurements of CO_2 efflux from the peat were made using both a long-term chamber at one location and survey measurements across the peat lane. The survey chamber (LI8100 -102, collars 100 mm) was used to make spatial measurements of the CO_2 flux at 20 collars, the positions of which were randomly chosen across the 40 m by 900 m lane within which the EC system was sited (Figure F.1).

Soil temperature measurements were made adjacent to each collar at a depth of 30 mm using 8100-201 soil temperature probe connected to the LI-8100. Adjacent to each of the 20 survey collars, a dipwell was installed so that the depth to the water table could be determined at time of measurements using a water level indicator (Dipper-T, Heron Instruments Inc., Ontario, Canada). Measurements were only made during the daytime, generally between 9 am and 5 pm. Each individual measurement was between 2 and 3 minutes long, depending on the magnitude of the flux: in summer, when CO_2 fluxes were greater, shorter measurement periods sufficed. Three measurements were made of the CO_2 flux at each collar of which the average value was used. It often took ~ 5.5 hours to collect all the measurements.

A description of the automated long-term chamber can be found in Section 3.3.2.

Measurements of the depth to water table (DWT) next to at least 10 collars were available for 33 days between Dec 2005 and July 2008. On 27 of those days, automated measurements for DWT were also available.

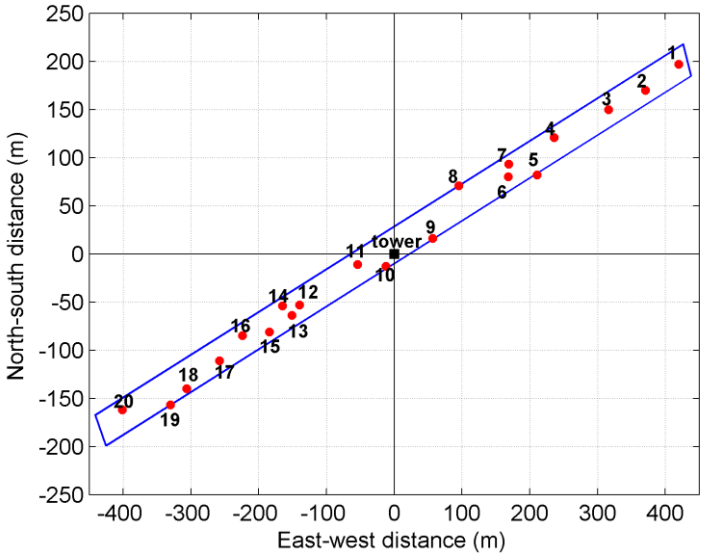

Figure F.1 Map of the positions of the 20 collars used for spatial chamber readings of CO_2 flux.

F.2.2 Analysis

The coefficients of variation of the depth to water table (DWT) and CO_2 flux were used to quantify spatial variability and calculated by:

$$CV = (\text{standard deviation} / \text{mean}) \cdot 100\% \qquad \textbf{Equation F. 1}$$

The CV's were calculated for every day separately.

To compare the CO_2 flux responses measured by the long-term and survey chambers to changes in temperature and DWT, only daytime data collected between 9 am and 5 pm were taken into account, because survey measurements were generally made between these times. Daily averages of survey chamber readings were based on measurements made from at least 10 collars (but were in most instances averages of all 20 collars). Daily averages of long-term chamber readings were based on all available measurements between 9 am and 5 pm. Because only a single gas analyser was available, long-term and survey measurements were not available for the same times.

F.3 Results and discussion

Time series of peat depth to water table, peat temperature and CO_2 flux are shown in Figure F.2. This graph allows for comparison of the measurements collected at the location of the long-term chamber (in grey) and the spatial measurements collected across the peatland.

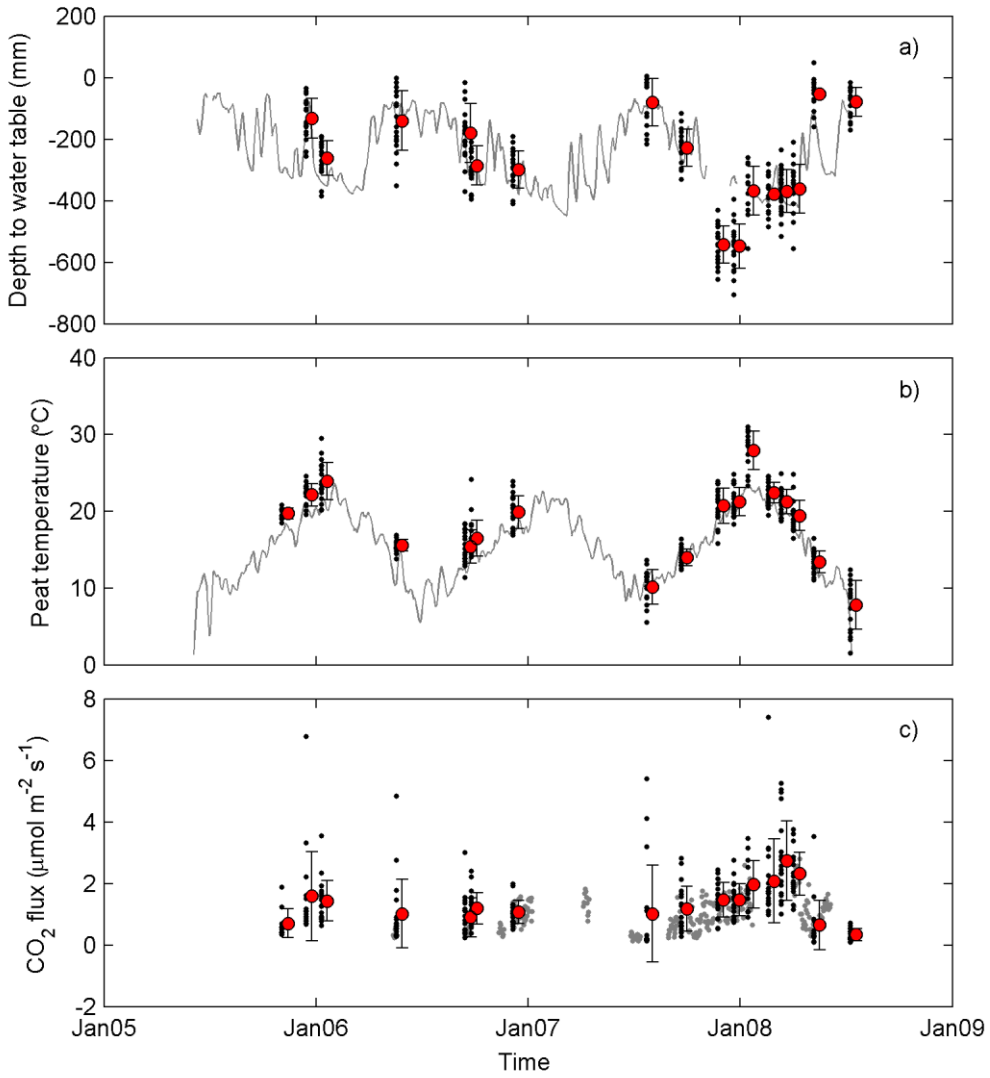

Figure F.2 (a) Depth to water table, (b) peat temperature and (c) CO_2 efflux between June 2005 and July 2008. DWT, peat temperature and CO_2 fluxes measured at each of the 20 collars across the peat lane are shown as black dots, with values averaged across all sites for that day in red. Error bars are 1 standard deviation. The dots indicating the averages have been offset slightly to avoid overlap of the error bars with the spatial data. Daytime averaged values measured at the location of the long-term chamber are shown in grey. Note that in panel b), peat temperature at 50 mm depth as measured near the location of the long-term chamber is shown in grey, whereas the temperature adjacent to the spatial collars was measured at 30 mm depth.

F.3.1 Depth to water table

Spatial variability of DWT measured at 20 dipwells across the peatland was large, with a CV averaged over all 33 days of 60% (Figure F.2a). The CV was largest under conditions of shallow water table depths (data not shown), but this was mostly caused by smaller mean value of the DWT in the denominator of Equation F.1, rather than by smaller standard deviations under those conditions.

The range in measured DWT over all collars did not appear to depend on the value of DWT (Figure F.3).

On the days that survey chamber measurements were made, comparison was possible between the automated measurement of the water table depth adjacent to the eddy covariance tower (and close to the long-term chamber) and the spatial average of the depth to water table (DWT) measured next to the 20 collars within the peat lane. In general, DWT measured near the long-term chamber correlated well with the spatial average (Figures F.2a and F.3); the correlation coefficient was 0.97), although the depth to the water table was about 15% deeper near the EC tower compared to the spatial average (Figure F.3). Maximum discrepancy between the measurements near the tower and the spatial average was approximately 60 mm when the water table was relatively deep (~400mm; Figure F.3).

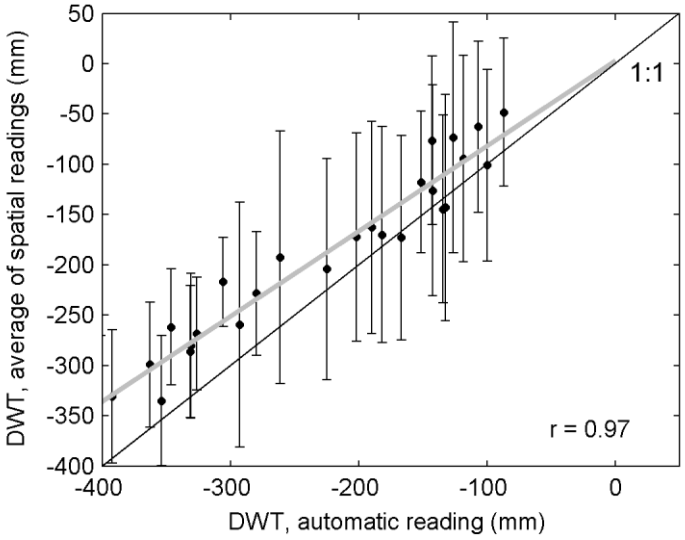

Figure F.3 Relationship between automated reading of depth to water table near the long-term chamber and the average of (up to) 20 manual readings collected next to the collars used for spatial chamber readings. Error bars indicate one standard deviation. The regression equation was y = 0.85x + 2.65 (R^2 = 0.94) and is indicated by the grey line. r denotes the correlation coefficient.

F.3.2 Peat temperature

Peat temperature measured adjacent to the 20 collars across the peatland was much less variable than DWT, with an average CV of 12% (Figure F.2b).

Peat temperature at -50 mm depth measured near the long-term chamber (used here because measurements at -30 mm were not available) showed very good agreement with the spatial average of the -30 mm peat temperature measured adjacent to the collars on days that spatial sampling was undertaken, with a correlation coefficient of 0.98 (Figures F.2b and F.4).

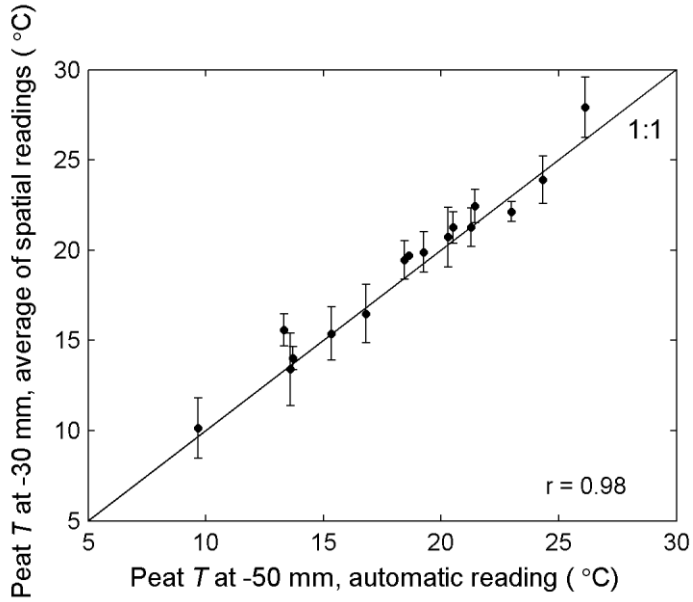

Figure F.4 Relationship between automated reading of peat temperature at -50 mm depth near the long-term chamber and the average of 20 manual readings collected next to the collars used for spatial chamber readings. Error bars indicate one standard deviation. r denotes the correlation coefficient.

F.3.3 CO_2 flux

Spatial variability of the CO_2 flux measured using the survey chamber was large, with an average CV of 65% (Figure F.2c). This is at the high end of the CV's reported in other studies measuring soil respiration (Loescher et al., 2006; Luo and Zhou, 2006), but not uncommon (for example, Rayment and Jarvis (2002) found a CV of 87% for respiration measured throughout a boreal forest on a peaty soil).

Direct comparison of fluxes obtained by survey and long-term chambers was not possible because measurements were never made simultaneously using both chambers.

To determine whether trends of the spatially averaged CO_2 flux obtained using the survey chamber with temperature and water table were similar to the trends obtained using the long-term chamber, daily daytime-averaged CO_2 fluxes from both chambers were regressed against peat temperature and DWT.

Figure F.5 shows the linear regressions of CO_2 flux on peat temperature and DWT and the linear regression of ln(CO_2 flux) on peat temperature and DWT (which is similar to an exponential fit of CO_2 flux on peat temperature and DWT as used in Chapter 6; Figure 6.5 a and c) for data collected using both the survey and the long-term chamber.

In general, patterns with temperature and DWT observed using the survey data resembled the patterns displayed by the long-term data: CO_2 fluxes generally increased with increasing peat temperature and with lowering water table (Figure F.5a and c). Wide confidence intervals were found for the regressions based on the survey chamber data, caused by the relatively low number of data points and large scatter. As a consequence, the regressions based on survey data largely overlapped with the regressions based on long-term data. The main difference between the fluxes from survey and long-term chambers seemed to be the (generally) somewhat greater values of CO_2 fluxes obtained using the survey chamber compared to those obtained by the long-term chamber (Figures F.2.c and F5).

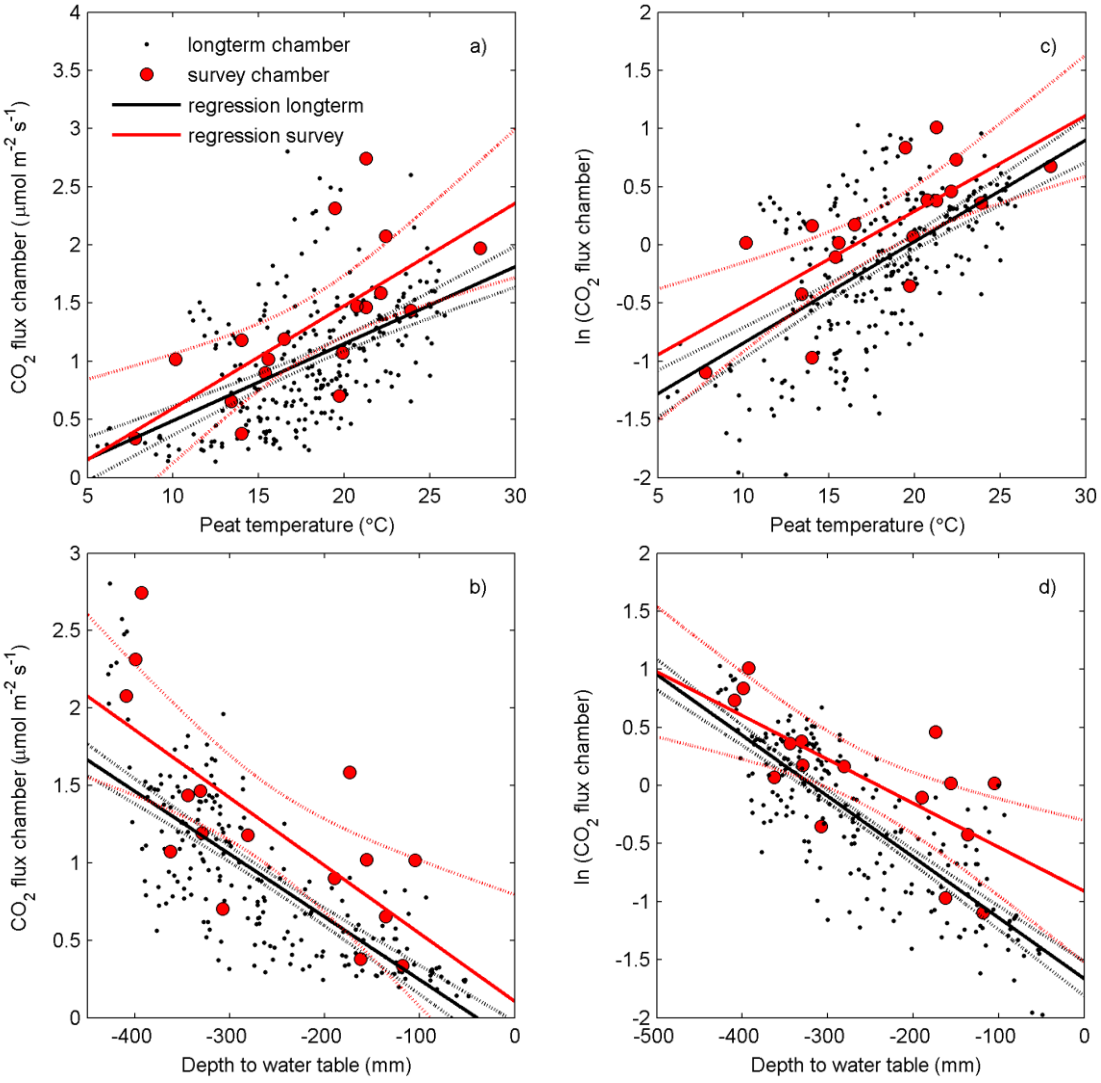

Figure F.5 Daily averaged CO_2 flux as a function of (a) peat temperature at 30 mm and (b) depth to water table for both the survey and the long-term chambers. Natural logarithms of daily averaged CO_2 flux as a function of (c) peat temperature at 30 mm and (d) depth to water table for both the survey and the long-term chambers. Lines depict linear regressions, with dashed lines indicating the 95% confidence intervals of the fits.

F.4 Conclusion

Spatial variability of both depth to water table and CO_2 flux were great, as indicated by the high values of calculated CV's.

Nevertheless, observed patterns with temperature and water table depth were similar between CO_2 fluxes obtained using long-term and survey chambers. In general, daily averaged CO_2 fluxes from the survey chamber were somewhat greater than values obtained by averaging long-term chamber measurements.

It was concluded that measurements obtained using the long-term chamber were suitable for determining patterns between controlling factors and CO_2 flux, but not necessarily suitable for estimating the absolute magnitude of the CO_2 flux.

This is the approach taken in Chapter 6, where the focus is on the controls of the CO_2 flux from the peatland rather than the absolute magnitude of the flux. To obtain the magnitude of biological CO_2 fluxes across the peatland would require additional automated chambers collecting flux data simultaneously, modelling of night-time eddy covariance measurements or an approach that separates daytime eddy covariance CO_2 fluxes into biological respiration and photodegradation. This topic would benefit from extra research but is beyond the scope of this thesis.